

THESIS FOR THE DEGREE OF DOCTOR OF PHILOSOPHY

**Secondary emissions from concrete floors with
bonded flooring materials**

- effects of alkaline hydrolysis and stored decomposition products

ANDERS SJÖBERG

Department of Building Materials
CHALMERS UNIVERSITY OF TECHNOLOGY
Göteborg, Sweden 2001

Secondary emissions from concrete floors with bonded flooring materials
- effects of alkaline hydrolysis and stored decomposition products

ANDERS SJÖBERG

ISBN 91-7291-031-3

© ANDERS SJÖBERG, 2001.

Doktorsavhandlingar vid Chalmers Tekniska Högskola

Ny serie nr 1715

ISSN 0346-718X

Publication P-01:2

ISSN 1104-893X

Department of Building Materials

Chalmers University of Technology

SE-412 96 Göteborg

Sweden

Tel.: +46 (0)31 772 1000

Cover:

The source of secondary emissions, a moisture damaged floor construction
with stored decomposition products. Drawn by Bo Olsson.

Translated by L J Gruber BSc(Eng) CEng MICE MStructE

Wasastadens bokbinderi

Göteborg, Sweden 2001

Secondary emissions from concrete floors with bonded flooring materials
- effects of alkaline hydrolysis and stored decomposition products

ANDERS SJÖBERG
Department of Building Materials
Chalmers University of Technology

Abstract

It has been demonstrated before that the presence of VOC lowers the quality of indoor air. There are also several indications that certain organic compounds in indoor air (OCIA) can give rise to sick building syndrome (SBS). This thesis investigates and describes one of the most important sources of elevated concentrations of VOC in indoor air in the Nordic building stock. This source, foundation and floor constructions damaged by moisture, has often been identified in conjunction with SBS investigations and has been given remedial treatment with good results.

By studying ca 100 test specimens in different experiments and evaluating measurements which included monitoring relative humidity (RH) in the construction, as well as almost 300 samples of emissions, chemical decomposition of flooring adhesive has been established as the source of secondary emission products. In this thesis, the causative relationship is summarised in a model which is based on an understanding of the physical transport processes and reactions, as well as material properties which can be measured by non-accelerated methods.

By evaluating the results of measurements and through parametric studies in the model, the critical parameters for decomposition of the adhesive and secondary emission to indoor air have been identified and quantified. The moisture content of concrete, its pH value and the method of bonding are some of the factors that govern decomposition of the adhesive. The rate of secondary emission to indoor air is governed, inter alia, by the rate of decomposition, the resistance of the flooring to the flow of decomposition products, and the storage capacity of the concrete for decomposition products.

The storage capacity of concrete for decomposition products is a critical factor for future emissions from the floor, since up to one half of the decomposition products can be transported downwards and stored in the concrete. The organic compounds stored in the concrete (OCIC) can, if conditions change, be emitted to the indoor air over a long period. It is therefore important, for instance during a renovation project, to make a careful note of the total quantity and penetration depth of OCIC in concrete.

Keywords: Adhesive, building materials, concrete, decomposition products, floorings, IAQ, moisture, OCIC, secondary emission, VOC.

Foreword

This doctoral thesis is the final report on the third phase of the project "Durability and service life of flooring materials on concrete – the influence of the substrate". The project has been financed by the Swedish Council for Building Research (BFR) and the Swedish Building Industry Development Fund (SBUF).

The work has been carried out at the Department of Building Materials, Chalmers University of Technology, with professor Lars-Olof Nilsson as my principal supervisor. Helene Wengholt Johnsson, NCC-Teknik, Göteborg, has acted as assistant supervisor and also represented the contractors' views concerning the issues raised during the work.

I wish first of all to thank my supervisors for their support and valuable advice during the course of the work. I also wish to thank my colleagues at the Department and all others who have generously given their time to help me and explain things that I did not know. The fact that I do not mention them by name does not mean that I have forgotten their kindness.

I wish to express my special thanks to tekn. Dr. Olle Ramnäs, Department of Chemical Environmental Science, Chalmers. Olle has given me invaluable help, both as a teacher as regards measurement of VOC, and as a mentor in connection with other issues in chemistry.

Finally, I wish to thank Anders Kumlin at AK-konsult Indoor Air AB and all other SBS investigators who helped me understand the relevance of various issues. Without the long discussions that we had, I would probably have become tied up in academic details of little importance for the work outside the walls of the university.

In view of the scope of the work, in writing the report I tried to bear in mind the words of advice that I received from a very wise man here at Chalmers:

*So tell me quick and tell me true
- or else I have no time for you!*

*Not how this study came to be
- but what its news can do for me.*

*And if it is not meant for me
- please tell me fast so I may flee!*

Göteborg, April 2001

Anders Sjöberg

1	INTRODUCTION	1
1.1	Background	1
1.2	Previous studies	2
1.3	Object	9
1.4	Limitations	9
1.5	Hypothesis	10
1.6	Arrangement	11
2	MATERIALS AND METHODS OF MEASUREMENT	14
2.1	Materials	14
2.1.1	Concrete	15
2.1.2	Screeds	19
2.1.3	Adhesives	21
2.1.4	Floorings	25
2.1.5	pH solution	28
2.2	Test specimens	28
2.2.1	PF1 (plate)	29
2.2.2	PF2 (cup)	30
2.2.3	PF3 (pot)	30
2.2.4	PF4 (bucket)	31
2.3	Measuring methods	32
2.3.1	Distribution of moisture in concrete	33
2.3.2	Organic compounds in concrete (OCIC)	36
2.3.3	Emission from the surface	41
3	EXPERIMENTS ON FLOORING AND ADHESIVE IN COMBINATION	43
3.1	Test specimens	43
3.2	Method of measurement and results	45
3.3	Evaluation of results	46
3.3.1	Description of general emission process	46
3.3.2	Measured emission process	47
3.3.3	Mass balance of OH ⁻ and decomposition products	49
3.3.4	The significance of the quantity of adhesive	51
3.3.5	Mass balance for different quantities of adhesive – 5, 10 and 15 g	53
3.3.6	Critical pH for decomposition of adhesive	55
3.3.7	The importance of the choice of materials	57
4	MEASUREMENTS OF THE TRANSPORT OF ORGANIC COMPOUNDS IN MATERIALS	59
4.1	The resistance R_{fc} of the flooring	59
4.1.1	Test specimens	59
4.1.2	Sampling	60
4.1.3	Results	60
4.1.4	Evaluation	61
4.2	Diffusion coefficient δ_{OC} for butanol in concrete	62
4.2.1	The test specimen	62
4.2.2	Measurement	62
4.2.3	Results	63
4.2.4	Evaluation of δ_{OC} for butanol	64
4.2.5	Theoretical evaluation of δ_{OC} for ethylhexanol	65
4.3	Determination of effective diffusion coefficient D_{eff}	66
4.3.1	Test specimen	66
4.3.2	Sampling	66

4.3.3.	Results	68
4.3.4	Evaluation of D_{eff}	68
4.4	Field measurements of effective diffusion coefficient D_{eff}	71
4.4.1	Floor No 1 – ca 1 year old emission damage	72
4.4.2	Floor No 2 – ca 3.5 year old emission damage	73
4.4.3	Floor No 3 – ca 6 year old emission damage	74
5	STUDIES OF THE SIGNIFICANCE OF MOISTURE STATUS FOR EMISSION	76
5.1	Measurement of RH at the concrete surface	76
5.1.1	Test specimens	76
5.1.2	Moisture measurement	76
5.1.3	Results	77
5.1.4	Evaluation	80
5.2	Evaporation of moisture of adhesive	81
5.2.1	Test specimens	82
5.2.2	Weighing	82
5.2.3	Results	82
5.2.4	Evaluation	83
5.3	Influence of method of application and type of adhesive	84
5.3.1	Test specimens	84
5.3.2	Moisture and emission measurements	85
5.3.3	Results	85
5.3.4	Evaluation	87
5.4	The influence of screed	90
5.4.1	Test specimens	90
5.4.2	Moisture and emission measurements	91
5.4.3	Results	91
5.4.4	Evaluation	93
5.5	Influence of time during which the concrete surface dries before the flooring is bonded	95
5.5.1	Test specimens	95
5.5.2	Moisture and emission measurements	95
5.5.3	Results	96
5.5.4	Evaluation	97
5.6	Discussion of moisture distribution, moisture of adhesive and elevated EF, and conclusions	99
6	QUALITATIVE MODEL	101
6.1	General	101
6.2	Concrete of high w/c ratio, ca 0.7	102
6.3	Self-desiccating concrete	104
6.4	Self-desiccating concrete with screed	106
7	QUANTITATIVE MODEL	108
7.1	Quantity of OC produced in the reaction	108
7.2	Concentration of OC in concrete	111
7.3	Transport of OC in concrete	114
7.4	Transport of OC through the floor covering	119
7.5	Moisture fixation in concrete	120
7.6	Moisture transport in concrete	122
7.7	Moisture of adhesive	124
7.8	Moisture transport through the floor covering	124

7.9	Numerical solution	125
8	QUANTIFYING THE PARAMETERS IN THE MODEL	126
8.1	Evaluation of the storage capacity of concrete for butanol	126
8.1.1	Theoretical evaluation	126
8.1.2	Evaluation from measured data	127
8.1.3	Appraisal of the evaluation	128
8.2	Evaluation of q_R for butanol from experiments	131
8.2.1	Quantity of OC emitted from the sample through the flooring	131
8.2.2	Quantity of OC stored in the concrete	133
8.2.3	Quantity of OC produced in the reaction	134
8.2.4	Mass balance	136
8.3	Discussion	137
9	COMPARISON OF MEASUREMENTS AND CALCULATIONS WITH THE MODEL	138
9.1	Material data for the calculations	138
9.1.1	Material data for the transport and fixation of moisture	138
9.1.2	Material data for the transport, formation and fixation of butanol	141
9.2	Adsorption of moisture of adhesive	142
9.2.1	Calculation of experiment No 1, 300 g moisture of adhesive per m ² of concrete C1, w/c ratio 0.32.	142
9.2.2	Calculation of experiment No 2, 90 g moisture of adhesive per m ² of concrete C3, w/c ratio 0.42.	143
9.2.3	Calculation of experiment No 3, 230 g moisture of adhesive per m ² of concrete C4, w/c ratio 0.66.	145
9.2.4	Discussion, adsorption of moisture of adhesive	146
9.3	Comparison with earlier measurements.	147
9.3.1	Moisture curve	147
9.3.2	Emission from the surface	148
9.3.3	OCIC	150
9.3.4	Discussion, previous measurements	150
9.4	Comparison with new measurements	152
9.4.1	PVC flooring	152
9.4.2	Linoleum flooring	153
9.4.3	Loose laid flooring	155
9.4.4	Discussion	155
10	PARAMETRIC STUDY WITH THE MODEL	157
10.1	Highest possible moisture status at the surface	157
10.1.1	Discussion, highest moisture status	159
10.2	Emission of butanol from the surface	160
10.2.1	The influence of $q_{R,max}$	160
10.2.2	Influence of RH for floor constructions with PVC flooring	161
10.2.3	Influence of RH for floor constructions with linoleum flooring	163
10.2.4	Discussion, emission from the surface	164
10.3	Transport and fixation of butanol in concrete	165
10.3.1	The influence of different assumption regarding binding	165
10.3.2	Influence of RH for PVC flooring	167
10.3.3	Influence of RH for linoleum flooring	168
10.3.4	Discussion, transport and fixation of OCIC	170
10.4	Residual OCIC after exposure to the air	170
10.4.1	Discussion, residual OCIC after exposure to the air	173

11	DISCUSSION AND CONCLUSIONS	174
11.1	Attainment of the objects	174
11.2	The hypothesis	174
11.3	The calculation model	175
11.4	The assumption regarding fixation	176
11.5	Maximum quantity of OC which is formed	176
11.6	Emission of VOC from the surface	177
11.7	OCIC stored in the concrete	177
11.8	Practical application of concentrations in the concrete	178
11.9	Conclusions	181
12	FUTURE RESEARCH AND DEVELOPMENT	182
13	REFERENCES	184
APPENDIX1	UNCERTAINTY IN MEASURING RH WITH ELECTRICAL INSTRUMENTS	
APPENDIX2	UNCERTAINTY IN MEASURING ORGANIC COMPOUNDS	
APPENDIX3	VAPOUR CONTENT AT SATURATION FOR SOME OC	
APPENDIX4	RESULTS FROM ALL CALCULATIONS	

Glossary

Abbreviations

AT	Applying technique of adhesive
DT	Drying time of concrete surface before the flooring is laid
FLEC	Field and Laboratory Emission Cell
OC	Organic Compound
OCIC	Organic Compounds In Concrete
OT	"Open time" of adhesive (drying time)
SBS	Sick Building Syndrome
VOC	Volatile Organic Compound

Symbols & units

C_0	$\text{kg/m}^3_{\text{air}}$	background concentration of OC
C_1	$\text{kg/m}^3_{\text{air}}$	concentration of OC (low)
C_2	$\text{kg/m}^3_{\text{air}}$	concentration of OC (high)
C_{air}	$\text{kg/m}^3_{\text{air}}$	concentration of OC in air
C_{sat}	$\text{kg/m}^3_{\text{air}}$	saturation concentration of OC
C_w	$\text{kg/m}^3_{\text{water}}$	concentration of OC in water
CEM	$\text{kg/m}^3_{\text{concrete}}$	cement content
C_{bound}	$\text{kg/m}^3_{\text{mtrl}}$	total content of OC bounded per volume of material
C_c	$\text{kg/m}^3_{\text{mtrl}}$	content of OC bound to cell walls per volume of material
C_m	$\text{kg/m}^3_{\text{mtrl}}$	content of OC bound to structural matrix per volume of material
C_{air}	$\text{kg/m}^3_{\text{mtrl}}$	content of OC in air pores per volume of material
C_s	$\text{kg/m}^3_{\text{mtrl}}$	content of OC in the surface, per volume of material
C_{tot}	$\text{kg/m}^3_{\text{mtrl}}$	total content of OC per volume of material
C_w	$\text{kg/m}^3_{\text{mtrl}}$	content of OC dissolved in pore liquid per volume of material
δ_{OC}	m^2/s	diffusion coefficient for OC in gas phase
δ_v	m^2/s	diffusion coefficient for water vapour transport
d	m	thickness of concrete structure
D_{eff}	m^2/s	effective diffusion coefficient for OC
D_{OC}	m^2/s	diffusion coefficient for OC in gas phase
D_w	m^2/s	diffusion coefficient for total water transport
D'_w	m^2/s	diffusion coefficient for liquid water transport
EF	$\mu\text{g}/(\text{m}^3 \cdot \text{h})$	emission factor
g_s	$\text{kg}/(\text{m}^2 \cdot \text{s})$	moisture flow (capillary transport), pore liquid pressure as driving potential
g_v	$\text{kg}/(\text{m}^2 \cdot \text{s})$	moisture flow, vapour as driving potential
g_w	$\text{kg}/(\text{m}^2 \cdot \text{s})$	total moisture flow
G	kg/m^2	absorbed / emitted amount of moisture
k_p	kg/m	water permeability
M	g/mol	molecular weight
ρ	$\text{m}^3_{\text{pore}}/\text{m}^3_{\text{mtrl}}$	porosity
ρ_a	$\text{m}^3_{\text{air}}/\text{m}^3_{\text{mtrl}}$	available porosity
P_w	Pa	pore water pressure

Q	kg/m^2	absorbed / emitted / produced amount of OC
q_{air}	$\text{kg}/(\text{m}^2 \cdot \text{s})$	OC flow via diffusion in gas phase
q_m	$\text{kg}/(\text{m}^2 \cdot \text{s})$	OC flow via diffusion in the structural matrix
q_{mw}	$\text{kg}/(\text{m}^2 \cdot \text{s})$	OC flow, via transport in mass transport of water, of OC dissolved in water
q_R	$\text{kg}/(\text{m}^2 \cdot \text{s})$	produced amount of OC per time
q_{tot}	$\text{kg}/(\text{m}^2 \cdot \text{s})$	total flow of OC
q_w	$\text{kg}/(\text{m}^2 \cdot \text{s})$	OC flow via diffusion of OC in water
R_{fc}	s/m	flow resistance of floor covering to OC
RH	%	relative humidity
RH_{act}	%	actual relative humidity
RH_{crit}	%	critical relative humidity
S	$\text{kg}/\text{m}^3_{\text{water}}$	solubility of OC in water
t	s	time
t_1	s	first time
t_2	s	second time
v	$\text{kg}/\text{m}^3_{\text{air}}$	vapour content
v_{sat}	$\text{kg}/\text{m}^3_{\text{air}}$	saturation vapour content
V_a	m^3	available pore volume
V_{mtrl}	m^3	total pore volume of the material
V_p	m^3	pore volume
w	$\text{kg}/\text{m}^3_{\text{mtrl}}$	water content
w_{ad}	$\text{kg}/\text{m}^3_{\text{mtrl}}$	water content in wet adhesive
w_n	$\text{kg}/\text{m}^3_{\text{mtrl}}$	chemically bound water
w_{max}	$\text{kg}/\text{m}^3_{\text{mtrl}}$	maximal water content
w/c	–	water cement ratio
x	m	length / thickness
Z_{fc}	s/m	flow resistance of floor covering to vapour
Z_{ad}	s/m	flow resistance of a film of adhesive to vapour
ρ_w	kg/m^3	density of water
η	Ns/m^2	dynamic viscosity

1 Introduction

1.1 Background

In recent years, the term "sick building syndrome" has been used with increasing frequency. It relates to people who feel unwell when they are in certain buildings. The symptoms may be headache, dryness of the mucous membranes and fatigue. It is difficult to give a medical explanation for these complaints, but it is easy to draw the conclusion that it is something in these buildings which affects these people.

Medical research has not as yet been able to pinpoint any single factors in the indoor environment or the building that gives rise to these adverse health effects. However, there are a lot of indications that it is certain Organic Compounds in Indoor Air (OCIA) which can affect people in a way that we do not understand, Andersson et al (2001). But at present it is impossible to determine which compounds or combination of compounds cause illhealth in our buildings. The precautionary principle is often applied instead. This implies that the concentration of OCIA and their sources must be kept to a minimum. In this way there are fewer compounds, and at lower concentrations, which people in the building are exposed to.

This study examines one of the sources of OCIA. The source studied are the secondary emissions of Volatile Organic Compounds (VOC) from combinations of PVC or linoleum floorings bonded to a subfloor of concrete. This construction sometimes gives rise to sensory problems such as a strange smell. But purely technical problems such as inadequate bonding and blisters in the flooring may also occur. We do not know with certainty whether people are adversely affected by the VOC emitted from these constructions, but there are a lot of indications that health problems occur in buildings with secondary emissions from the floor. At least we do know that VOC decreases the Indoor Air Quality (IAQ), Salthammer (1999).

The definition of primary and secondary emissions is given by Salthammer et al (2000):

Primary emission product: The physical release of compounds which are present in a new product.

Secondary emission product: Compound produced by a chemical reaction in the material or in the indoor environment.

1.2 Previous studies

Several Nordic studies were previously made to describe emission from floor combinations comprising PVC floorings bonded to concrete. In Wengholt Johnsson (1995) a summary is given of the important studies performed prior to 1995.

Up to that time, investigations had largely concentrated on measuring emissions from the surface. It was mainly the measurements of the primary emissions from the floorings which was of interest. Some studies had however concentrated on measuring the emission from the entire floor system with or without an intermediate layer. These intermediate layers consist of a moisture or alkali barrier or a screed between the concrete and the bonded flooring.

This report therefore lists only the most important investigations and reports which were published during the period 1995-2000 and deal with alkaline hydrolysis of floorings. Apart from the reports which have been listed, a number of minor projects have also been carried out, as well as degree projects undertaken mainly at the technical universities in Sweden.

Some of the studies described below investigate the underlying causes, while others broaden the combinations to comprise more components such as screeds and different types of floorings. The list of previous studies also includes reports in which the state of knowledge at the time of publication was compiled and evaluated.

Chemical emissions from floor systems – the effect of different grades of concrete and moisture loads

Wengholt Johnsson (1995) studied the emission from 19 test specimens. These specimens consisted of material combinations of "normal" structural concrete (w/c ratio = 0.66) or self-desiccating concrete (w/c ratio = 0.42) which had been cast in stainless steel pots of 200 mm diameter. The concrete was allowed to dry to different moisture levels before the flooring was bonded to the specimens. Some test specimens contained a layer of screed between the concrete and flooring.

The study showed that high emissions of butanol and 2-ethylhexanol occurred when the flooring was bonded to normal concrete of 95% RH at the characteristic depth, i.e. the depth which has a moisture level corresponding to that which the whole concrete will attain when the moisture content has equalised after the flooring had been bonded. High emissions also occurred when the flooring was bonded to a self-desiccating concrete with 85% RH at the characteristic depth. Emission was low or not detectable when the flooring had been bonded to test specimens of self-desiccating concrete, coated with a screed, and to test specimens of normal structural concrete with RH less than, or equal to, 91%.

The study also investigated the primary emission (VOC, including of formaldehyde) from concrete with different admixtures and from screeds with and without admixtures. The primary emission from the concretes was low. The screed with a melamine based admixture emitted high quantities of VOCs inclusive of formaldehyde, one to a few weeks after casting. The screed without admixtures also emitted high quantities of VOC apart from formaldehyde.

In some floor systems an analysis was also made of the alkali content in concrete and screed. Measurements showed an elevated content in the surface of the concrete. The content of potassium oxide was several times higher in the uppermost 2 mm of the concrete surface and 2 mm in the concrete precisely below the screed. The content in the screed was lower than the basic level in the concrete.

Emission of chemicals from floor adhesive on concrete - the effect of different moisture and alkali barriers

Fritsche (1996) studied the emission from 11 different test specimens. The specimens consisted of adhesive and possibly a barrier layer on ordinary structural concrete (w/c ratio = 0.66) or self-desiccating concrete (w/c ratio = 0.42), cast in stainless steel pots of 200 mm diameter. No flooring was applied in order to reduce the time from applying the adhesive to measurement. The barrier layer consisted of different kinds of screed and of mineral and organic "alkali barriers". In the measurements, activated carbon was used as the adsorbent instead of TENAX TA which is most common in this type of measurement. However, comparative measurements showed good agreement between these adsorbents.

The study demonstrated that emission from the test specimens was lower when a barrier layer was used. The emission from the test specimen was lower with the adhesive on self-desiccating concrete than on ordinary structural concrete. Measurements of primary emission from the adhesive directly from the tin showed that, even in the undegraded state, the adhesive emits butanol and ethylhexanol. These alcohols usually occur as decomposition products from alkaline hydrolysis of adhesives and floorings.

Flooring materials on different types of moist concrete floor - overview and comments on investigations into chemical decomposition and emission

Gustafsson (1996) presented and compiled five Swedish laboratory studies in which, as a common factor, the test specimens consisted of concrete coated with different combinations of screed, latex adhesive and PVC flooring. In all cases, ordinary structural concrete and self-desiccating concrete had been cast in stainless steel pots. PVC flooring was bonded to the concrete after it had dried to different moisture levels.

Gustafsson (1996) describes that all five studies show the following:

- Application of flooring to a moist substrate, primarily concrete, involves the risk of chemical decomposition of adhesive layer and flooring.
- A substrate of high RH generally increases the risk of elevated and altered emission.
- A substrate of low-alkali screed generally gives rise to lower emission from the floor construction than similar specimens of only concrete. This difference is most pronounced at high moisture levels.
- Emission mainly consists of decomposition products from the floor adhesive.

Gustafsson (1996) writes that the results of the studies also show the composition of the adhesive to be significant for the compounds that are emitted. The high emission levels measured in some of the studies can be partly explained by the technique used in applying the adhesive and the quantity applied.

Chemical emission from floor systems of PVC flooring bonded to self-desiccating concrete - the influence of adhesive application technique, drying process and types of cement, adhesive and flooring

Fritsche et al (1997) studied the emission from 10 different test specimens consisting of PVC flooring, latex adhesive and self-desiccating concrete (w/c ratio = 0.42). The drying time, i.e. the time over which the concrete was exposed to air before adhesive was applied, varied. The flooring was bonded using different application methods and different drying times. Tests were also made in which the concrete was based on sulphate resisting cement of low alkali content.

The study showed that emission was highest in "wet bonding", when the flooring is laid down immediately after the adhesive has been spread on the concrete. Emission was least when a pressure sensitive adhesive was used, when the flooring was laid down in the wet adhesive and was immediately removed. The adhesive was then allowed to dry until it was just tacky before the flooring was finally pressed down onto the concrete. Test specimens with a long drying time and low alkali cement also produced low emissions.

The conclusions of the study are that the following recommendations can be given to reduce the risk of high secondary emission:

- To ensure that the flooring does not absorb moisture from the adhesive, lay it loose.
- On a sub-floor of self-desiccating concrete which has dried out sufficiently, level the surface with a screed. A screed based on aluminate cement has a low alkali content and it also has moisture capacity to distribute the moisture from the adhesive.
- Wait for a long time after applying the adhesive in order to prevent absorption of moisture from the adhesive. Compared with the first two recommendations, this is a less reliable method.

Concrete for healthy floors - moisture design, choice of materials and production

The Swedish Concrete Association report (1997) can be seen as a summary of the state of knowledge in 1997. The main part of the report discusses the problem of surface material combinations and moisture in concrete floors. It gives definitions and practical advice in choosing the grade of concrete and surface materials. One section of the report also deals with production aspects. Appendices deal with issues such as indoor environment and emissions. There is a description of chemical compounds in indoor air and the influence of concrete in combination with other materials. There is also a discussion of constructional aspects, moisture design, moisture and emission measurement, and reference buildings.

Concrete in buildings - evaluation of its impact on indoor environment and health

Blom (1998) studied the emission from 152 test specimens. These test specimens comprised flooring, adhesives, different barrier layers and seven different grades of concrete. The study used two different PVC floorings and four different adhesives, one of which was an experimental

adhesive of low emission values. This adhesive was called CascoProff Solid when it was later marketed in 1998. Four different screeds and two moisture barriers were used as barrier layers. The moisture barriers were based on water glass and epoxy respectively. The concrete grades had different water/cement ratios and different amounts of admixture. W/c ratio varied from 0.74 (ordinary structural concrete) to 0.39 (self-desiccating concrete).

The study claimed that the adhesives which are used commercially can cause smells in the room air during the first six months, and what is emitted to a high degree from the system is butanol,

2-ethylhexanol and 2-(2-butoxyethoxy)ethanol. These VOCs are generated by decomposition of the adhesive. A rise in the temperature of the floor, for instance from heating cables, accelerates decomposition of the adhesive. The report also showed that emission can be reduced by using

- New, low emission types of adhesive
- Screed without admixtures.

Long term effects of alkaline decomposition of floors

Alexandersson (1998) studied the emission from 20 different test specimens 2-3 years after the flooring had been bonded. The first measurements on test specimens after about six months are presented in Alexandersson (1996). Test specimens consisted of PVC, polyolefin and linoleum floorings, latex adhesive, screed and concrete.

Four PVC floorings, one polyolefin flooring and two linoleum floorings were studied in the investigation. These seven floorings were combined with seven latex adhesives and two concrete grades (w/c ratio 0.5 and 0.7).

The investigation showed that

- In all cases, the screed impeded decomposition of the floorings. This meant that emission from floor systems with a screed was consistently low.
- Emission from floor systems with linoleum and polyolefin floorings was low.
- The choice of material influenced the extent of emission. For instance, emission increased by several orders of magnitude when a different adhesive was used in an otherwise identical floor construction.
- Butanol and 2-ethylhexanol have different time scales. Butanol dominated in measurements after six months, while in measurements after two years 2-ethylhexanol dominated.

Transport processes and reactions in concrete floors with floorings - the influence of various factors on emissions from floor constructions

Sjöberg (1998a) studied four essential parameters governing emissions from floor structures. These were surface moisture, alkali distribution, organic compounds in concrete (OCIC) and emission of VOC from the surface. The report describes a qualitative model based on a physical understanding of transport processes and reactions. This qualitative model is also described in Chapter 6 of this report.

Chapters 2, 3, 5 and 6 of this report have been taken more or less directly from Sjöberg (1998a). Apart from these sections, Sjöberg (1998) also contains measurements of alkali distribution and carbonation, and a somewhat more comprehensive discussion of the results of measurements.

Floorings on a concrete subfloor - field measurements of drying times and emissions at Gärdsrået, Umeå

Wengholt Johnsson (1998) describes a field project in which moisture and emission measurements were used to evaluate the function of different floor constructions. The measurements comprised drying processes in concrete slabs laid directly on the ground and in intermediate concrete floors, and emissions from these floors both when the building was relatively new, and more than two years after the floorings had been laid.

The floor constructions comprised in the study consisted of "normal" structural and self-desiccating concrete. Half the floors were coated with screed based on aluminate cement, and the flooring was either a PVC flooring bonded with a conventional adhesive, or a polyolefin flooring bonded with a solvent-free adhesive.

The investigation showed that

- A concrete floor with a screed based on aluminate cement gave the lowest emission regardless of the type of concrete.
- Decomposition commences quickly after the flooring is laid, but slows down over time.
- It was mainly butanol and 2-ethylhexanol that was emitted.
- The lowest emissions were generally measured two years after the flooring had been laid.
- After two years the moisture in the concrete had also largely dried out.

Alkalinity measurements on screed exposed to incremental alkalinity

Björk et al (1999) studied the alkali buffering capacity of screed. The test specimens used were boxes of stiff thermosetting plastics measuring 56 x 36 cm which were filled with 20 cm structural concrete (w/c ratio = 0.55). After the concrete had been conditioned to 95%, 90% and 80% RH respectively, 10 mm screed of three different kinds was cast on the surface. PVC flooring was bonded with a latex adhesive after 1 week. Alkalinity was measured at three different levels in the screed and in the concrete, 1, 6 and 12 months after the flooring had been laid. Comparative test series were performed as a reference

on screed cast in Petri dishes. Sampling was performed in two ways, pore pressing of pieces and collection of drillings from drill holes. The analysis was performed with a pH electrode and titration of hydrochloric acid with a methyl orange indicator which changes colour around pH = 3,5. Measurement of sodium and potassium ions was performed with flame ionisation spectroscopy.

The study showed that

- Over 12 months, the screeds studied do not permit alkaline moisture to be transported from the concrete to the area below the flooring.
- The RH of the concrete at the characteristic depth at the time the screed is applied has no critical significance for alkali migration.
- Carbonation before the flooring is laid reduces alkalinity in the screed.
- Whether drying occurs from both sides or from one side only has no appreciable effect on alkali migration from the concrete to the screed.
- Titration with methyl orange as an indicator is not a good method for measuring alkalinity in pore water squeezed from samples of screed since it does not correctly detect carbonation.

Alkaline decomposition of floor components

Björk et al (1999) have degraded 20 common components of floorings and floor adhesives. The components investigated were e.g. plasticiser in PVC, five different polymer dispersions, primer, tackiness indicator, PVC polymer and thickener. The components were laid directly on an alkaline bed consisting of a mixture of aluminium oxide and sodium hydroxide in a test tube. The bed consisted of aluminium oxide and had been prepared with sodium hydroxide so that the pH value was either 11 or 13. Moisture content in the bed was kept constant by placing small containers of salt solutions in the test tubes. Moisture levels in the test tubes were 75, 95 or 100% RH. A total of 120 combinations were analysed.

In the test tubes with 75 and 100% RH, analysis of VOC in the air in the test tube was performed after approximately 5 months. Owing to functional problems with the analytical equipment, test tubes with 95% RH were analysed after about 10 months. The sampling and analysis method was tested on some specimens for sampling with SPME (solid phase microextraction) and subsequent analysis with GC-MS. Sampling with SPME was laborious and the method was therefore changed. Sampling was performed on all specimens with automatic headspace injector and subsequent analysis with GC-MS.

The investigation showed that

- The moisture and alkali levels affect decomposition of some components such as polymer dispersions in adhesive and some plasticisers in PVC flooring.
- Some components exhibit highly variable resistance to moisture/alkaline decomposition. Large variation among the product groups.
- For several of the components, an increase in alkalinity caused a large increase in decomposition products, in spite of the fact that relative humidity was kept at a level which was low in the context. This occurred

for e.g. a polymer dispersion and for some plasticisers, although not for all.

Moisture and emission conditions in conjunction with bonding PVC and linoleum floorings to concrete

Sjöberg & Wengholt Johnsson (1999) studied the quantity of moisture of adhesive as well as adsorption and evaporation in conjunction with bonding. This is also described in Section 5.2 of this report.

Emission measurements were also made on the surfaces of 21 test specimens. These had been dried for different periods and then bonded in different ways. This is also described in Section 5.5 in this report.

Industry standard: Measurement of emission properties of composite floor constructions

GBR (1999) has published a standard for the Swedish flooring industry which makes it possible to test the emission properties of composite floor constructions.

When the properties of a specific product are to be tested, it is incorporated in a floor construction whose other components, i.e. reference products, are well defined. A reference specimen comprising only the reference products is made at the same time. The test specimen and the reference specimen are made and handled as identically as possible.

The emission from the surface of both specimens is measured 26 weeks after the flooring had been bonded. The result is expressed as the ratio of the TVOC emission of the test construction to that of the reference construction. The result reflects both the primary emission of the test construction and secondary emissions caused by e.g. alkaline decomposition.

1.3 Object

The object of this study has been to enhance knowledge of the interaction in combinations of floor materials which include concrete. The reason that concrete has been chosen is that it creates an aggressive environment which affects the durability of many other materials.

If possible, a model capable of predicting the reduction in the service life of materials in floor constructions should be developed. On the basis of this model, a method to prevent the reduction in the service life of (polymeric) materials in combination with concrete should then be formulated. The term reduction in service life implies that function, after already a short time, can no longer be maintained.

The model should be based on an understanding of the physical processes in the floor combination. It should be a whole life model in order to predict the function of the material combinations over their entire service lives. The model should be based on material properties which can be measured on new materials.

Methods for non-accelerated measurement of these properties should also be developed in the project.

It should also be possible to use the model in acquiring knowledge of how to prevent or limit the emission of VOC from the building to indoor air, in both the long and short term.

1.4 Limitations

The study is limited to treatment of a selection of Nordic floor material combinations and the effects that arise owing to actions on the floorings from below. It is the service life of the floorings, and not that of the complete floor system, which is studied.

It is mainly the concentrations of different compounds in the construction and the mass balance in connection with transport processes and chemical reactions that are studied.

The project is limited to examination of a limited sample of common floorings on subfloors of some common types of concrete. Different types of PVC flooring and linoleum flooring have been used as floorings. These floorings are laid loose or bonded to the substrate. A limited selection of latex adhesives have been used. In some cases an intermediate layer, a screed, has also been placed between the flooring and the concrete.

In the analysis of secondary emission products, only two of these have been studied. These two are good indicators of the decomposition of acrylate copolymers in the adhesive.

- One VOC is butyl alcohol. It is called 1-butanol or n-butanol, but for the sake of simplicity it is referred to as butanol or BuOH in the report.
- The other is ethylhexyl alcohol. It is called 2-ethylhexyl alcohol or 2-ethyl-1-hexanol, but is referred to in the report as ethylhexanol or EtHx.

1.5 Hypothesis

The hypothesis used in elucidating the interaction in the floor construction is based on more or less accepted theories concerning materials and on experiences from previous projects.

The model is based on the migration of certain significant compounds in the materials owing to differences in concentration. These compounds may move within the material and often also between the different materials. Water vapour and VOC can even leave the material system by evaporating from the surface.

According to the hypothesis, certain substances in the subfloor can affect the flooring. Examples of such substances are the hydroxide ions (OH^-) in Fig. 1. Under certain conditions, these substances can move and migrate upwards through the subfloor. One of the requirements for this to occur is that the relative humidity (RH) in the material should exceed a critical value, since it is assumed that transport occurs in the aqueous phase. The conditions governing migration vary over time.

The quantity of the substance that migrates upwards is governed by the transport properties of this substance in the subfloor material, by the gradients that arise in the subfloor, and by the density of the floor materials. An intermediate material such as a screed or an alkali barrier can prevent or facilitate continued migration of the substance, depending on the transport properties of this material.

At the bottom of the flooring the substance may react with some component of the adhesive or the flooring. The substance is then consumed, which creates a further gradient, facilitating further migration from below. The reaction changes the flooring and produces OC which, in turn, migrate further up through the flooring and affect its properties. Some VOCs can reach the surface, vaporise and escape into the ambient air. Other parts of the VOCs can migrate down into the concrete and remain there for a long time.

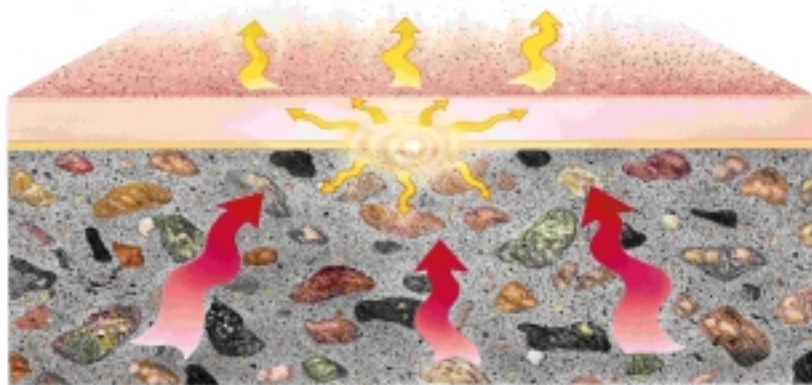


Fig. 1.1 Certain substances in concrete (OH^-) react with the flooring under special conditions. The reaction products, Organic Compounds (OC), can either migrate through the flooring and reach the surface where they evaporate, or migrate down into the concrete where they remain for a long time.

1.6 Arrangement

Chapter 1, Introduction

This gives an introduction to the research area and a summary of studies and reports made in this area.

The object and limitations of the study are described. The hypothesis underlying the study is also discussed. It is set out as an initial qualitative model of the interaction in the material. The model is developed in Chapters 6 and 7.

Chapter 2, Materials and methods of measurement

The materials selected for the study are described. Four to seven materials were chosen from each selected material group. These groups are concrete, screed, floor adhesive and flooring. The six moulds used in the study are also described.

The instruments and methods of measurement used are then described. The investigations in the study are based on measurement of three parameters: surface moisture, concentration of organic compounds in concrete (OCIC) and the emission factor (EF) from material surfaces.

Chapter 3, Experiments on flooring and adhesives in combination

This chapter describes a multifactor test on flooring, adhesive and alkaline solution. The aim of the investigation is to elucidate the relationships which govern alkaline hydrolysis of floor adhesive. Studies are made of the significance of the quantity of adhesive, critical RH (RH_{crit}) for the adhesive, and general emission processes.

This investigation has previously been described in Sjöberg (1998a). The results of this investigation are presented and discussed.

Chapter 4, Measurements of the transport of organic compounds in materials

This chapter describes investigations of the transport of butanol and ethylhexanol in concrete and through floorings. The experiments are made both by different types of cup tests and by measuring and evaluating the penetration profiles of butanol and ethylhexanol into concrete.

The resistance of floorings to the transport of OC, and the diffusion coefficient for OC in concrete, are measured. The results of the investigation are presented and discussed.

Chapter 5, Studies of the significance of moisture status for emission

Investigations of the influence of moisture of adhesives are described. A description is first given of experiments in which absorption and evaporation of moisture of adhesive are studied, followed by a description of experiments in which variations in emission from floor systems are studied. The effect of water from adhesives has been varied in various ways in these floor systems.

This investigation has been previously described in Sjöberg (1998a). The results of this investigation are presented and discussed.

Chapter 6, Qualitative model

A qualitative model of the interaction between the materials is described in this chapter. The model comprises moisture in concrete, alkali, reaction products, VOC upwards and OCIC downwards. The most important properties of the materials are examined and discussed.

The different transport processes in the system and the reactions between the substances in the materials are described for three typical cases of a PVC flooring bonded to substrates of

- normal structural concrete
- self-desiccating concrete
- self-desiccating concrete, with screed.

Chapter 7, Quantitative model

The relationships set out in the qualitative model are developed and described mathematically. Accepted explanatory models for the fixation and transport of moisture are incorporated into the quantitative model.

Terms, relationships and equations which form the basis for the fixation, transport and emission of VOC are introduced and explained. In many respects this is very similar to corresponding explanatory models for moisture.

Chapter 8, Quantifying the parameters in the model

In this chapter some of the parameters set out in Chapter 7, which have not been measured before, are quantified. Quantification is based on measurements in this study and is performed for parameters whose values have not been given in the literature. These parameters are

- storage capacity of butanol in concrete
- maximum rate of formation of butanol

Chapter 9, Comparison of measurements and calculations with the model

Comparisons between calculations with the model and measured results are set out here. Comparisons are first made between the increase in moisture level in concrete in conjunction with bonding the flooring. Comparisons are then made with OCIC measured in the concrete, and finally with the emission of VOC from the surface in a number of cases.

Chapter 10, Parametric study with the model

In this chapter, the model is used to study the effect of different parameters. To start with, an analysis is made for a number of cases of the maximum acceptable moisture level in the surface after bonding.

A study is then made of the measured emission from the surface and the quantities of OCIC for different maximum rates of formation, binding capacity and moisture status when different types of flooring are laid.

Chapter 11, Discussion and conclusions

This chapter contains an overall discussion of this area. Conclusions are drawn on the basis of the study. Suggestions about how to transfer the results into practice are given.

Chapter 12, Further research and development

Further areas of research are proposed in this chapter.

2 Materials and methods of measurement

2.1 Materials

Since the object of the study was to study the interaction between materials, great emphasis was placed on selecting a few interesting materials. Four to seven materials have been chosen from each of the material groups concrete, screed, floor adhesive and flooring. The materials for the study have been chosen because they have interesting properties different from those of the other materials in the material group.

Four different concrete mixes have been used. The ones chosen have largely the same constituents but have different compositions so that the hardened concretes have different properties.

Seven screeds have been used in the study. Two of these are gypsum based and five aluminate cement based. Two of the cement based screeds are rapid hardening compounds.

Four floor adhesives of different compositions have been studied. All are latex adhesives.

Four different types of floorings have been used. These are homogeneous PVC flooring, heterogeneous PVC flooring, PVC flooring for loose laying, and linoleum flooring.

The product names of the materials used are given so that the readers may themselves evaluate the material properties not referred to in the report. These names have been given since the study does not compare individual materials but examines the material combination.

The different materials are described in greater detail in the following subsections.

2.1.1 Concrete

Materials

The main difference between the four concrete mixes was the water/cement ratio, i.e. the cement content, and hydraulic binders and admixtures; see Table 2.1. In some of the mixtures, for instance, silica fume (amorphous SiO_2) has been added.

Table 2.1 Concrete mix specifications, all materials in kg/m^3 .

Designation	C1	C2	C3	C4
w/c ratio	0.315	0.39	0.42	0.66
Cement	462	425	380	290
Water	146	166	160	191
Sand (0-8 mm)	813	783	916	980
Stones (8-12 mm)	39	805	924	899
Stones (12-16 mm)	761	-	-	-
Filler Baskarp No 7	81	-	-	-
Silica fume (dry)	-	21	21	-
Air entraining admixture Cementa 16L	0.05	-	-	-
Superplasticiser Mighty	-	8	-	-
Superplasticiser Cementa 92M	5.00	3.76	3.76	-

The three types of concrete selected for the study all contain standard portland cement from Skövde, but in different proportions. In one experiment standard portland cement was replaced by sulphate resistant low alkali Portland cement (SRPC) from Degerhamn in order to reduce the alkali content. By varying the water/cement ratio, concretes of different properties were obtained. For instance, a concrete with a low w/c ratio is more alkaline than one with a high w/c ratio, provided that they are based on the same type of cement. The one with low w/c ratio is also more impervious to e.g. moisture than the one with high w/c ratio. The reason is that the former has a finer pore system. To put it simply, where there is mixing water initially, there will be pores when the water "disappears". A concrete with a low w/c ratio has a little less mixing water but a lot more cement. It therefore has a small and finer pore system. The consequence of this is that moisture transport takes place at different rates in concretes with different w/c ratios.

In a structural context, a concrete of low w/c ratio is referred to as concrete free from construction water or as self-desiccating concrete. This nomenclature has been chosen because such a concrete contains no harmful construction water which must be removed by drying. Almost all the water which is added during mixing such a concrete is used up during hydration (curing). What remains is strongly bound physically in the pore system. The mixing proportions between cement and water (w/c ratio) which confer these properties depend on the type of cement. For instance, for Degerhamn cement a lower w/c ratio, more cement in proportion to water, is needed than for standard portland cement. This is due to the chemical composition of the cement but also its fineness. Sulphate resisting cement is ground to "coarser" fractions than standard portland cement. Atlassi et al (1991) showed that for standard

portland cement the limit for the w/c ratio was around 0.40 if the RH in concrete was to be brought down to 85% at 28 days, while with sulphate resisting cement the w/c ratio had to be 0.25 for the same result to be achieved.

One of the reasons that silica fume is used is to enhance self desiccation; see Fig. 2.1. Silica fume is finer than cement and this affects the pore structure in the hardened concrete, so that it is finer and more impervious because it has fewer and smaller capillary pores. Since the bulk of moisture transport in concrete takes place in capillary pores, this gives rise to lower moisture transport under otherwise identical conditions. The sorption isotherm in Fig. 2.2 shows how the size distribution of concrete pores is changed by silica fume. There is a relationship between relative humidity and pore size, which is, briefly, that at a low RH only pores of small diameter are filled, while the large pores are not filled until RH is high.

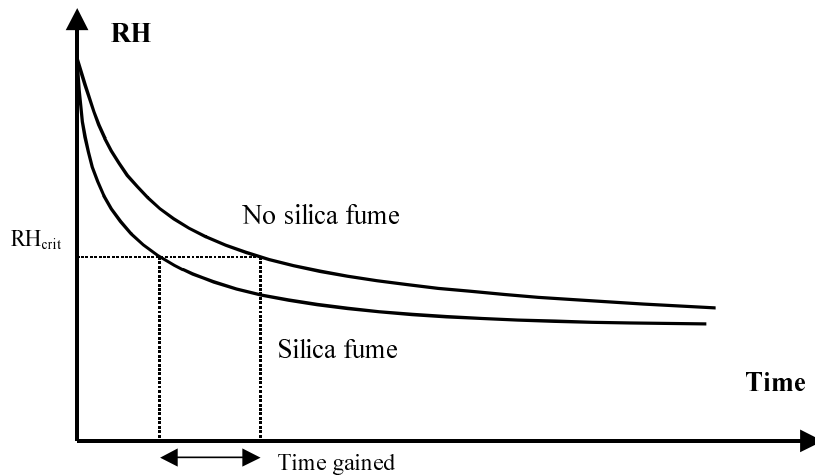


Fig. 2.1 Effect of silica fume on self desiccation of concrete. Diagrammatic.

Fig. 2.2 is to be read so that, for a certain RH (e.g. 70%), concrete with silica fume can contain more moisture than concrete with no silica fume. The reason is that concrete with silica fume has a higher proportion of pores of a diameter that can be filled at that moisture level.

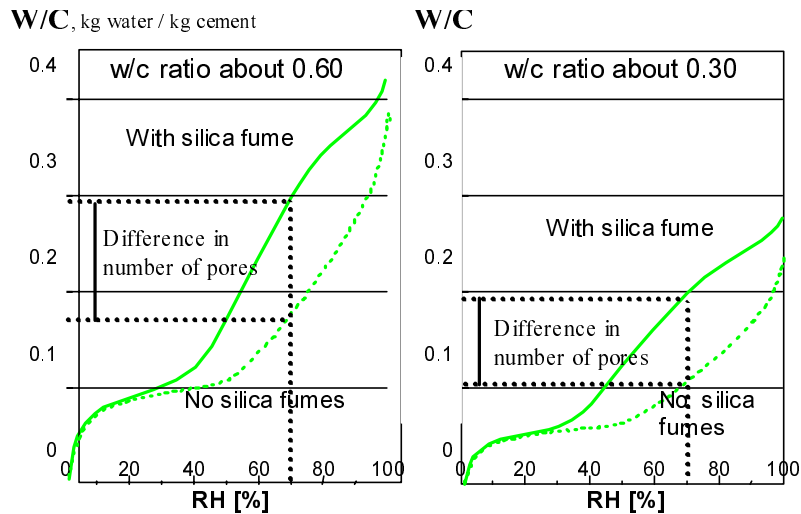


Fig. 2.2 Effect of silica fume on sorption curve (moisture isotherm). Diagrammatic figure from Atlassi (1995).

Mixing

When concrete was made, sand, cement and silica if any were mixed dry for a minute or two. Crushed rock, half the water and admixtures were then added. Finally the remaining water was added and the concrete was mixed for about four minutes. The admixtures were mixed with a little water before being added to the mix.

Concrete was mixed in a 20 l paddle mixer of the type Tecnotest T650 with stepless speed regulation between about 60 and 150 rpm. It is somewhat similar to a dough mixer in catering. The constituents were weighed with a Mettler PM34 weighing machine; this had two weighing ranges, a low one up to 4.000 kg with a resolution of 0.1 g and measurement uncertainty of about ± 0.2 g, and a high range up to 32.000 kg where the resolution was 1 g and the measurement uncertainty ± 0.6 g.

Casting

The casting procedure was the same for all types of test specimens used in the study. The test mould was first partly filled and the concrete compacted by placing it on a vibrating table. The mould was then filled almost completely and again vibrated. The mould was then completely filled, vibrated and the surface struck off with a trowel. The moulds were covered with building plastic and any measuring tubes mounted in the mould were closed with rubber plugs to exclude ambient air. There was no noticeable water separation.

During final vibration of the buckets small "craters" formed above the shallowest tubes. The craters were filled with a little concrete without coarse aggregate which was struck off with a trowel.

After casting the specimens were covered with closely fitting plastic and cured in a climatically stable room. During this period self desiccation occurred in concrete of low w/c ratio. The plastic was removed some time before application of adhesive and the concrete was allowed to dry. In the report, the drying

period between removal of the plastic and bonding of the flooring is referred to as DT (drying time).

In some investigations, PF3 (the pot) which is described in Section 2.2 was turned upside down on a steel plate after being completely filled. Final vibration thus occurred upside down. It was also stored upside down on the steel plate for 24 hours before being turned the right way. The aim was to achieve a smooth surface on to which the flooring could be bonded. This process produced a "mirror" surface which is unlike the rough concrete surface obtained in a real casting process. The surface was filled with paste, and only one or two pores appeared.

The method of smoothing the surface was changed for later investigations with PF3 (the pot) and the investigations in which PF4 (the bucket), Section 2.2, was used. Instead of turning them upside down, the surface was smoothed once more some hours after casting. This method produced a surface more similar to that achieved in casting under real conditions. This procedure demanded a lot of experience and skill to give the test specimen a surface that was smooth enough for the FLEC measurements after the flooring was bonded on.

The day after casting the building plastic was taken off and the moulds that were upside down were turned the right way up. The surface was covered with a vapourtight material to prevent premature drying. In the investigation d1, the pots were covered with two layers of aluminium foil. On the remaining test specimens polyolefin foil (gladpack) was used instead, the change being made to prevent the risk of alkaline reactions with the aluminium. The specimens were stored in a climatically stable room during the curing process and subsequent tests. This room had a temperature of +20°C and 50% relative humidity.

2.1.2 Screeds

Materials

Screeds are used to level up concrete floors when the surface of the concrete is not smooth enough for the flooring to be laid. Screeds are of the self levelling filler type.

Screeds consist of a binder, filler and admixture. The binder is usually cement or gypsum based. Examples of filler are dry sand or crushed dolomite. Admixtures may be superplasticisers or various polymers.

In the study seven different screeds were used. Five had aluminate cement as binder and the other two were gypsum based. Of the five cement based ones, two were rapid drying. Details of the screeds are given in Tables 2.2 and 2.3.

Table 2.2 Screeds S1 – S4. Data given by manufacturers.

Designation	S1	S2	S3	S4
Name	ABS 147	Universal	Ventonit	ABS 154
Supplier	Optiroc	Stråbruken	Optiroc	Optiroc
Type	Normal	Normal	Normal	Rapid
Binder	Aluminate cement	Aluminate cement	Aluminate cement	Aluminate cement
pH	11	-	-	11
Layer thickness (mm)	2-30	5-30	2-30	2-30
Walkable (hours)	1-3	2-6		-
Flooring applied after (days)	7-21	7-42	7-21	0.5-1

Table 2.3 Screeds S5 – S7. Data given by manufacturers.

Designation	S5	S6	S7
Name	Rapid	AE 20	Soluflex
Supplier	Stråbruken	Knauf D.	Strängbtg.
Type	Rapid	Gypsum	Gypsum
Binder	Aluminate cement	Anhydrite	Synthetic anhydrite
Approx. pH	-	-	Low alkali
Layer thickness (mm)	2-30	-	>20
Walkable (hours)	1-2	21-24	24
Flooring applied after (days)	0.7	21-49	14*

* at 25 mm thickness and optimum drying

Casting

The screeds were delivered in the dry, i.e. they were ready mixed, with water to be added prior to mixing. Weighing of the dry material and water, and mixing, were carried out using the same equipment as for mixing the concrete, Subsection 2.1.1.

The screeds were mixed and cast in largely the same way for all types. The differences were in the quantity of water and mixing time, as well as layer thickness, where the manufacturers gave different instructions. The dry material was first weighed and mixed dry for a few minutes, after which about half the water was added and mixing continued for a few minutes longer. The remaining water was then slowly poured into the mix, and the whole was mixed for a few more minutes according to the manufacturer's instructions.

Before the screed was applied a primer was spread on the test specimens. The specimens were then allowed to "dry" for some time before the screed was mixed and poured on the specimen. All this was in accordance with the instructions of the manufacturer concerned.

After completion the test specimens were immediately put into a climatically stable room where they were stored during the curing process and subsequent tests. The room had a temperature of +20°C and 50% relative humidity.

2.1.3 Adhesives

Materials

Nordic floor adhesives now contain no solvent in the traditional sense. The binder is instead dissolved in a solvent (plasticiser) of high boiling point. Small droplets of this solution are dispersed in a liquid phase. This type of adhesive is often referred to as a latex adhesive. When the adhesive dries, the liquid phase evaporates first, the droplets of the binder then coalesce, and finally the solvent evaporates; see Fig. 2.3. Evaporation of the solvent is the primary emission of the adhesive.

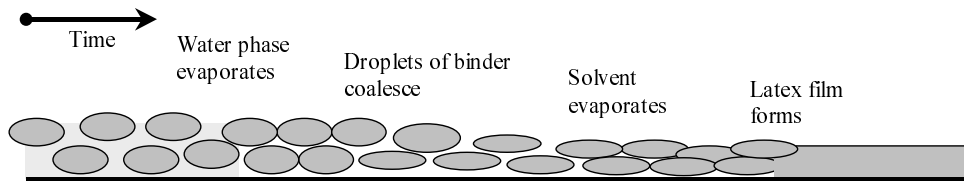


Fig. 2.3 Diagrammatic illustration of the drying process in a latex (acrylate) adhesive. Based on Björk (1996).

There is a risk that, in moist alkaline environments, adhesives with binders based on acrylate copolymers of 2-ethylhexylacrylate and butylacrylate will be hydrolysed. On hydrolysis the alcohols ethylhexanol and butanol are formed. This type of emission is referred to in the report as secondary emission.

All adhesives used in this study were latex adhesives. Four different types were used, Bona Futurum, Casco Proff, Bona wet area adhesive, and Evonor 2001; see Table 2.4. The adhesives were acquired through a flooring wholesaler. Tins were stored in a cool dark room.

Table 2.4. Types of adhesive used in the study. Data given by manufacturers.

Designation	A1	A2	A3	A4
Name	Futurum	Casco Proff	Wet area adhesive	Evonor 2001
Manufacturer	Bona	Casco	Bona	Bostik
Solvent	Water	Water	Water	Water
Copolymers	Acrylate, Acetate	Acrylate, Acetate	Acetate	Acrylate
pH	8.5	7.8	6.5-7.5	7-8
Density (kg/m ³)	1250	1300	1400	1270
Dry content (%)	68	70	67	-

% indicates percentage of the weight of cement

Bona Futurum (A1) is a latex adhesive which is, according to the manufacturer, well suited for bonding homogeneous vinyl floorings with or without a backing of glass fibre or mineral wool and textile floorings with or without a backing of foam. The composition of the adhesive is set out in Table 2.5.

Table 2.5. Bona Futurum (A1).

Compound	CAS No*	Content %	Hazard symbol	Risk phrase**
Acrylic copolymer		-		
Ethylenevinyl acetate copolymer		-		
Polyester resin		5-10		
Chloromethylisothiazolinone	26172-55-4	<15 ppm	Xi	43

* Chemical Abstracts Services Registry Number

** International Health and Environmental Classification

According to the manufacturer, Casco Proff 3448 (A2) can be used for many types of floor and wall materials and also on absorbent substrates such as concrete. The composition of the adhesive is set out in Table 2.6.

Table 2.6. Casco Proff (A2).

Compound	CAS No*	Content %	Hazard symbol	Risk phrase
Acrylic copolymer		10-30		
Butyldiglycol acetate	124-17-4	1-5	V	R-321
Inert filler		>30		
Pine resin		5-10		
Water	7732-18-5	10-30		
Vinylacetate copolymer		10-30		

Bona Wet Area Adhesive (A3) is not based on 2-ethylhexylacrylate. It was therefore not likely that it emitted ethylhexanol on hydrolysis. The composition of the adhesive is set out in Table 2.7.

Table 2.7. Bona Wet Area Adhesive (A3).

Compound	CAS No*	Content %	Hazard symbol	Risk phrase
Ethenevinyl acetate copolymer		-		
Polyvinyl acetate dispersion		-		
Methyl-1H-besimidazole-2-yl carbamate	10605-21-8	<0.02		
Chloromethylisothiazolinone	26172-55-4	<15 ppm	Xi	43

Evonor 2001 (A4) had high primary emissions when it was used in the beginning of the work. The manufacturer changed the specification, but use of the adhesive was discontinued in the later parts of this work. The composition of the adhesive is set out in Table 2.8.

Table 2.8. Evonor 2001 (A4).

Compound	CAS No*	Content %	Hazard symbol	Risk phrase
Acrylic dispersion		-		
Thickener		-		
Dolomite		-		
Wood rosin		-		
Stabiliser		-		
Di-n-butylphthalate	84-74-2	1-5		
N-paraffin	64771-72-8	1-5		

Methods of applying adhesive

Three different methods of applying the adhesive were used in the study, single spread bonding with the flooring laid into the wet adhesive, bonding with pressure sensitive adhesive and bonding with contact adhesive. In most tests, the adhesive was applied to the concrete only, and the open time was so short that the adhesive was still wet to the touch when the flooring was pressed down. The "open time" is the period during which the adhesive is allowed to "dry", from the time it is spread on the substrate to the time when the flooring is laid. In one test the effect of different bonding methods was studied. The methods are summarised in Table 2.9. The bonding methods are described in greater detail in Fritsche et al (1997).

The adhesive was applied to the concrete with a brush in order that spread should be even and the quantity of adhesive could be controlled. A sufficient quantity of adhesive was first poured into a plastic mug. The weights of the plastic mug together with the adhesive and brush were determined with a weighing-machine, Mettler PM 480 with a resolution of 0.001 g. The exact quantity of adhesive was then spread on the floor. The weight of the applied adhesive was recorded by weighing the mug together with the adhesive and brush and calculating the reduction in weight.

Table 2.9. Summary of bonding methods according to Schrewehus (1997).

	Single spread bonding		Double spread bonding*	
Application technique (AT)	Wet adhesive	Press.sensitive adhesive	Wet adhesive	Contact adhesive
Designation	AT1	AT2	AT3	AT4
Open time (OT)	0 – 15 min	from 45 min	0 min	ca 30 min
Consistence on mounting	Adhesive wet to touch	Like a tape	Adhesive wet to touch	Like a tape
Remarks	High final strength	On non-absorb. material	High final strength	Immediate high strength

* The flooring is laid into the wet adhesive, removed and allowed to dry during the open time before final mounting

In single spread bonding the adhesive is spread on one of the surfaces, while in double spread bonding it is spread on both surfaces. The boundary between laying the flooring into the wet adhesive and bonding with a pressure sensitive adhesive is rather indistinct, and sometimes it is possible to use open times that are longer than those applied when the flooring is laid into the wet adhesive, and shorter than those when a pressure sensitive adhesive is used. These cases are referred to as "late wet laying" or "early bonding with pressure sensitive adhesive". Generally speaking, in late wet laying the adhesive is still wet to the touch, while in early bonding with a pressure sensitive adhesive there is no such wetness.

2.1.4 Floorings

Floorings consist of binder, filler, possibly a carrier, and in many cases admixtures. Natural or synthetic polymers are usually employed as binders. Linoleum is an example of natural polymers. Synthetic polymers are plastics, e.g. PVC (polyvinylchloride) and Polyolefin. Filler is added to give the material bulk and to some extent to give the flooring desired properties. Examples of filler are wood flour or stone flour. Admixtures are plasticisers, stabilisers, process aids and similar. Aesthetic properties are altered by adding pigment or including a printed layer in the flooring.

Four different types of floorings were used in the study. These types were homogeneous PVC flooring (Smaragd Aqua), heterogeneous PVC flooring (Novilon Scandinavia), linoleum flooring (Marmoleum Real) and loose laid PVC flooring (Tarkett Stabil). The properties of the floorings are set out in Table 2.10.

Table 2.10 Types of flooring: Data according to manufacturers.

Designation	F1	F2	F3	F4
Name	Smaragd Aqua	Novilon Scandinavia	Marmoleum Real	Stabil
Manufacturer	Forbo-Forshaga	Forbo-Forshaga	Forbo-Forshaga	Tarkett
Binder	PVC	PVC	Linseed oil and resin	PVC
Plasticiser	DOP	DOP, BBP, DIOA	-	DOP, BBP
Filler	Dolomite	-	Wood flour, limestone flour	Aluminium silicate
Backing	PVC	PVC foam	Jute fabric	Polyester
Thickness (mm)	2.0	2.4	2.0	3.0
Weight (kg/m ²)	2.8	1.75	2.2	2.3
Vapour resistance (s/m)	2.0·10 ⁶	0.5·10 ⁶	0.3·10 ⁶	-

The floorings were obtained through a flooring wholesaler or directly from the manufacturer. It is estimated that no flooring was more than 1 year old and that no flooring had been exposed to UV light or to (cleaning) chemicals.

F1, homogeneous PVC flooring (Smaragd Aqua), Fig. 2.4. This is a 1.5 mm thick PVC flooring intended for use in wet areas. The flooring is made up of a wear layer of transparent polyurethane-reinforced PVC and a base coat of filled PVC. Smaragd Aqua contained about 54% by weight PVC, 19% by weight dioctylphthalate (DOP) plasticiser and about 23% by weight filler, dolomite. Stabilisers, pigment and other components together made up less than 5% by weight.

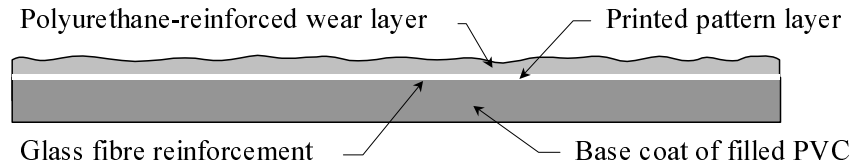


Fig. 2.4. Structure of homogeneous PVC flooring.

F2, heterogeneous PVC flooring (Novilon Scandinavia). It is 2.4 mm thick and made up of several layers as shown in Fig. 2.5. The surface consists of transparent polyurethane-reinforced plasticised PVC. The backing consists of mineral fibre reinforced PVC foam. Novilon Scandinavia contained about 53% by weight PVC, 27% by weight plasticisers of types butylbenzylphthalate (BBP), dioctylphthalate (DOP) and dioc tyladipate (DIOA). The flooring had no filler but contained about 15% by weight carrier (latex impregnated nonwoven mineral fibre). Stabilisers, pigment and other additives together made up less than 6% by weight.

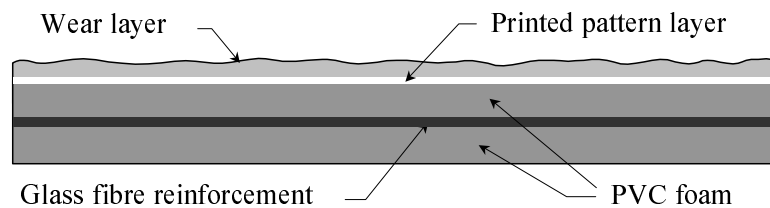


Fig. 2.5. Structure of heterogeneous PVC flooring.

F3, linoleum flooring (Marmoleum Real), Fig. 2.6. It is 2.0 mm thick and consists of about 28% by weight binders, an oxidised and polymerised mixture of dried natural vegetable oils and resins. The filler consisted of wood flour (29% by weight) and limestone flour (26% by weight). The backing of jute fabric made up about 10% by weight. Pigment and other components together made up less than 7% by weight.

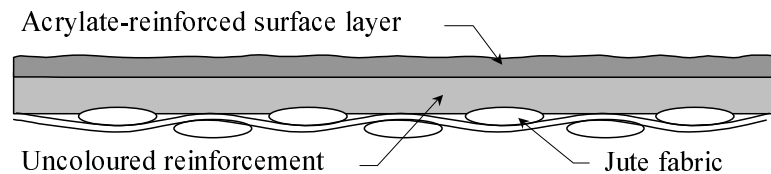


Fig. 2.6. Structure of linoleum flooring.

F4, PVC flooring for loose laying (Tarkett Stabil). It is 3.0 mm thick and made up of layers as shown in Fig. 2.7. The surface consist of a polyurethane-reinforced wear layer. The backing consists of compacted polyester fibre. Novilon Scandinavia contained about 54% by weight PVC, 17% by weight dioctylphthalate (DOP) and 9% by weight butylbenzylphthalate (BBP) plasticiser. The flooring contained 5.2% by weight aluminium silicate as filler. The glass fibre reinforcement and surface layer made up about 5.4% by weight. Stabilisers, pigment and other components together made up less than 10% by weight.

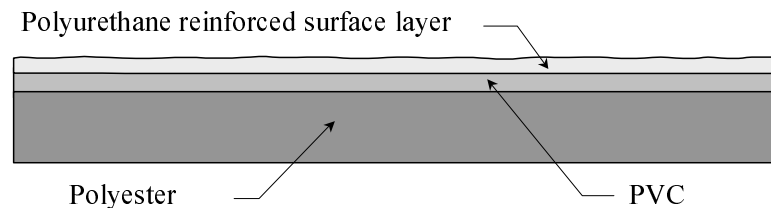


Fig. 2.7. Structure of PVC flooring for loose laying.

2.1.5 pH solution

Using pH solutions, the floorings could be exposed to a specific alkaline environment in PF1 (plate). The solutions used in the study have definite pH values which are at the same level as the pH in cement based materials.

Three different solutions were used in the study; see Table 2.11. Two were pH solutions of make Titrisol. They had a pH of 11 to represent a low-alkali screed and 13 to represent concrete. P1 (pH 11) had high buffer capacity and maintained a stable pH value even if some action (alkaline hydrolysis) occurred. P2 (pH 13) did not have such buffer capacity, and the pH level of the solution decreased as the hydroxide ions were consumed in the reaction.

The third solution (P3) had about the same pH value as P2. In contrast to the others which had been bought ready mixed, P3 was mixed in the laboratory. The mix specification for P3 was initially produced to correspond to the liquid obtained when pore water was pressed out of concrete. The concrete pressed was based on standard cement from Degerhamn and had a w/c ratio of 0.5. It has not been possible to find a reference to the original analysis of the liquid or to pore pressing.

Table 2.11 pH solutions of definite pH value. Composition and "make" of the liquids.

Designation	P1	P2	P3
pH	11	13	13,05*
Type	Titrisol	Titrisol	Concrete
NaOH [M]	$91 \cdot 10^{-3}$	$100 \cdot 10^{-3}$	$28 \cdot 10^{-3}$
KCl [M]	$48 \cdot 10^{-3}$	$50 \cdot 10^{-3}$	
H ₃ BO ₃ [M]	$94 \cdot 10^{-3}$		
KOH [M]			$83 \cdot 10^{-3}$
CaSO ₄ ·2H ₂ O [M]			$40 \cdot 10^{-6}$

* similar to pH value of concrete

2.2 Test specimens

The test specimens in the study were made as simple as possible but nevertheless representative of the constructions met with in reality, partly because many of the measurements were of a pilot study character, and partly because complex specimens are difficult to recreate if the tests are to be repeated, for instance with some other material. The test moulds are referred to in the report as PF1-4, but are in most cases described by the name they were given during laboratory work.

2.2.1 PF1 (plate)

The plate was made from a circular sheet of stainless acid resistant steel (SS2333, \varnothing 250 mm, t 20 mm). In the middle of the plate a hollow was made by turning (\varnothing 165 mm, d 10 mm); see Fig. 2.8. Two holes were drilled through the side of the plate. The holes were threaded, one was fitted with a level tube and the other was plugged with a screw. These holes are used to add pH solution during sample preparation.

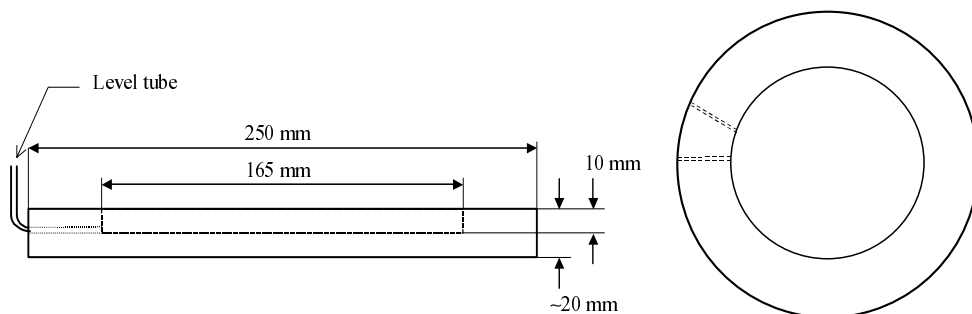


Fig. 2.8. Diagram of PF1 (plate), made for use with FLEC.

The flooring to be tested was fixed to the top of the plate with a clamping ring; see Fig. 2.9. The hollow was filled with pH solution through the hole in the side, and the liquid level was checked with the level tube.

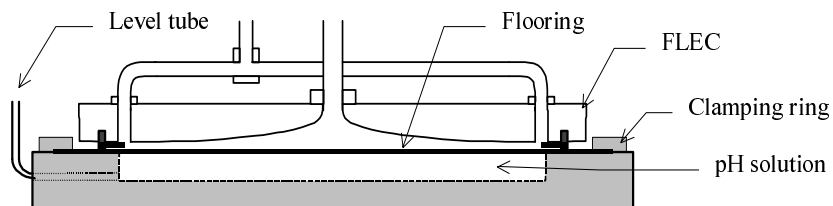


Fig. 2.9. Equipment for decomposition of flooring, FLEC and newly constructed bottom part (PF1).

2.2.2 PF2 (cup)

The mould used for cup tests was a crystallisation dish with a straight edge and without a spout. The cup was made of duran glass, with inside height of 50 mm and internal diameter of ca 90 mm; see Fig. 2.10.

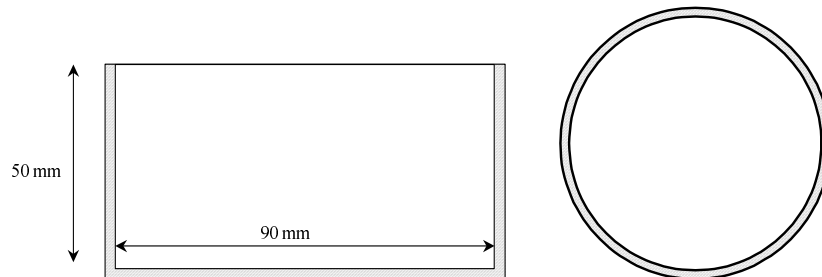


Fig. 2.10. Diagrammatic sketch of PF2 (cup).

2.2.3 PF3 (pot)

The mould was a circular "pot" of stainless steel. This pot was press formed in one piece and drying from one side only was thus secured; see Fig. 2.11. The diameter of the mould was 200 mm and its height 100 mm. 40 mm from the top of the pot a horizontal metal tube was mounted for measurements of RH. This tube had an inside diameter of 7 mm to fit the RH probes. Prior to casting, the end of the tube inside the mould was sealed with a microporous tape and the other was stopped with a rubber plug. The depth of 40 mm from the top was chosen in view of the recommendations for RH measurements in RBK (1999). The moisture level at 40% of the thickness of the concrete slab, in drying from one side only, was approximately the same as the moisture level obtained when the moisture level has been redistributed after the flooring had been laid.

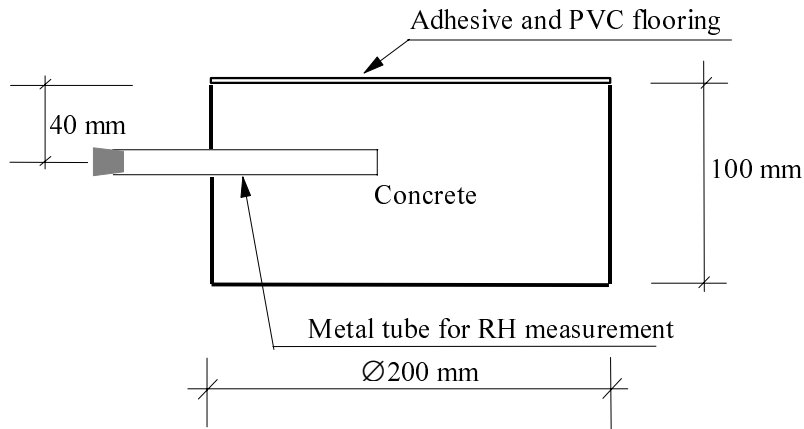


Fig. 2.11. Cross section of PF3 (pot).

Stainless steel has no primary emissions but can in certain circumstances act as a sink, at least according to Afshari (2000). It is supposed to be possible for OC (organic compounds) to be adsorbed onto the surface of the steel and stay there, but this effect was considered to be negligible in the study.

2.2.4 PF4 (bucket)

The mould was a cylindrical container of polythene, with the walls and bottom moulded in one piece. Its diameter was 205 mm, its height 200 mm, and its volume ca 6.6 l. The bottom of the bucket was reinforced from the outside with a 5 mm thick plate of PVC in order to brace the measuring tubes which were mounted through the bottom; see Fig. 2.12. In view of its origin, this mould for concrete was given the working name bucket.

The measuring tubes in which RH probes were placed during measurements were made of PVC tubes (electrical conduits) of an inside diameter to fit the RH probes. The tubes were mounted so that their openings inside the mould were at different levels. The first bucket used had six different levels, 2, 7, 11, 19, 39 and 79 mm, measured from the finished concrete surface. Other buckets had four levels, 2, 7, 15 and 30 mm.

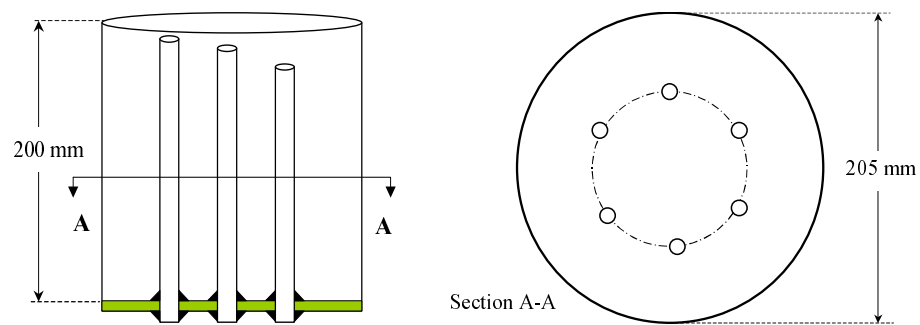


Fig. 2.12. Diagram of mould PF4 (bucket).

In order to stop concrete running into the tubes during casting, the tube openings were sealed with a microporous tape.

2.3 Measuring methods

In the study, a number of quantities were measured in different situations. The measuring methods employed were well proven ones. In some cases the methods were developed further so that a quantity or property may be measured in a way that had not been done before. Development or deviation from the original method was at no time so great that the quality of the results was jeopardised. Results were assessed by using common sense and asking experts, and by noting the reasonableness of the results.

- RH levels in the concrete were measured with RH probes which were either inserted into cast-in measuring tubes or inserted into test tubes into which pieces of sample had been put.

At the beginning of this project an investigation was made to find which measuring methods were suitable for measuring the emission of VOCs from building materials. The measuring methods chosen comprise two stages. Sampling is first performed in which the VOCs are collected and concentrated on an adsorbent, and analysis is then performed with gas chromatography.

- VOCs were sampled in two ways, with a modified headspace procedure for the VOCs that had migrated down into the concrete, and with FLEC (Field and Laboratory Emission Cell) for emission from surfaces. The adsorbent used was TENAX TA.
- Subsequent analysis was performed with GC (gas chromatography) and FID (flame ionisation detector); MS (mass spectrometry) was sometimes used instead of FID.

These measuring methods are described in detail in the following sections.

2.3.1 Distribution of moisture in concrete

Measuring instruments

Moisture in a material can be described in different ways. One usual way is to express moisture level as RH (relative humidity). RH denotes the ratio of the vapour content in air that is in equilibrium with the material, to the maximum vapour content of the air at the same temperature. RH in concrete was measured with RH probes which were inserted either into measuring tubes or into test tubes into which pieces of sample had been put.

Two different equipments were used to measure moisture levels in concrete samples. These were capacitive RH probes with associated instrumentation for data storage and presentation of measured values. The sensor in these probes consisted of a thin polymer film whose capacity altered when RH in the ambient air changed. The two RH probes, their measuring uncertainties etc are described in detail below.

1. For measuring single values, RH probe HMP 36 and hand instrument HMI 31, made by Vaisala OY, Finland, were mainly used. These measuring instruments were calibrated on several occasions during the period of measurement using saturated salt solutions in accordance with ASTM (1985). The uncertainty in measurement quoted for the probe by the manufacturer is as follows: $\pm 2\%$ in the range 0-90% RH and $\pm 3\%$ RH in the range 90-100%, and $\pm 0.3^\circ\text{C}$ in the range -40 to $+60^\circ\text{C}$. No uncertainty is quoted for the hand instrument.
2. In cases where RH was to be logged over a prolonged period, RH probe HMP 44 from Vaisala OY, together with datalogger Mitec AT40, was used. These measuring instruments were calibrated at the time of measurement using saturated salt solutions in accordance with ASTM (1985). The uncertainty in measurement quoted for the probe by the manufacturer is as follows: $\pm 2\%$ RH in the range 0-90% RH and $\pm 3\%$ RH in the range 90-100% RH. The total uncertainty of the datalogger is quoted as $0.20\% \pm 2$ mV at full scale. The logger was set up so that 1 V is approximately equal to 1% RH; the range of measurement was -3 to 120 V.

Measuring method

Three different methods were used for measuring moisture in concrete. These methods have been well established for a long time and have been gradually developed at the Department of Building Materials, Chalmers, and no special reference is therefore given.

1. The first method was used to measure single RH values in test specimens through cast-in measuring tubes. In these test specimens measuring tubes had been installed in the side of the container; see Fig. 2.13. The tubes were sealed with a microporous tape at the end inside the concrete and with a rubber plug at the end in ambient air. At equilibrium, the RH of the air inside the tube was the same as that in the concrete. When a measurement was to be made, the rubber plug was removed and the RH probe was inserted into the tube. The probe was sealed against the ambient air with a rubber expansion ring. When the RH probe was inserted, conditions in the tube were changed since air is

forced out when the probe is inserted. The instrument was read when the probe was in equilibrium with the RH of the concrete. Measurement took about 24 hours, and in some cases longer. The values obtained were then converted into RH with reference to calibration curves. The probe HMP 36 and the hand instrument HMI 31 from Vaisala OY were used for this method.

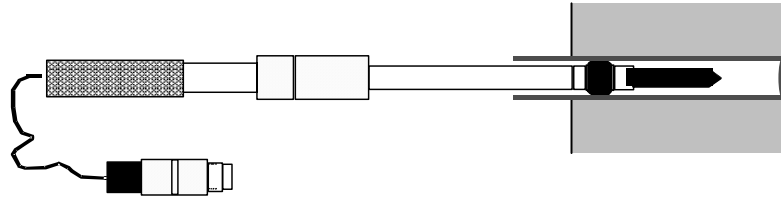


Fig. 2.13 Diagrammatic arrangement of RH probe inside measuring tube.

2. The second method was a development of the first one. The difference was that the RH probe remained inside the measuring tube over a prolonged period, and readings were made continuously during the whole period. By leaving the probe in the measuring tube, the effects that contributed to the total uncertainty in measurement were reduced. For instance, the significance of the moisture capacity of the probe was reduced. It takes about 4 mg moisture to moisten the probe so that it attains equilibrium during a normal moisture measurement. According to Sjöberg (1998b,c), this gives rise to an error of ca 2% RH which is reduced by one half every five days. The drill hole also had greater temperature stability, which was an advantage when the probe was left in place.

The measuring tubes were mounted through the bottom of the container and were sealed with a microporous tape at the end inside the concrete and with a rubber plug at the end in the ambient air. When measurements began, the rubber plugs were removed, the RH probes were inserted into the tubes and left there for some weeks while readings were continuously made. The readings were adjusted with reference to calibration curves. In the initial experiments the probe HMP 36 and hand instrument HMI 31 were used, but in most measurements probe HMP 44 and the datalogger Mitec AT40 were employed.

3. The third method was used to measure the RH on pieces removed from the concrete and placed in test tubes. In this method, samples were taken from the concrete at several levels so that a moisture profile may be determined. The test specimens were broken up with a hammer and chisel, and pieces from each level were quickly taken and placed in test tubes which were sealed with rubber plugs. It was essential for breaking up and placing of samples in the test tubes to be done quickly so that no moisture would be lost from the samples. The next day RH probes were inserted into the test tubes; see Fig. 2.14. The measuring instrument was read when the RH probe was in equilibrium with the RH in the concrete. Measurement usually took about 24 hours, and sometimes longer. The values obtained were then converted into RH with reference to calibration curves. For this method, probe HMP 36 and hand instrument HMI 31 were used.

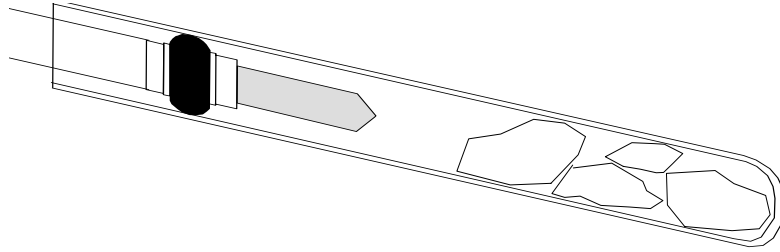


Fig. 2.14. Pieces of concrete and RH probe in a test tube.

Measurement uncertainty

The measurement uncertainty for the three methods described in Subsection 2.3.1 is estimated on the basis of our own measurements and data in the literature.

Calculation of uncertainty is described in Appendix No 1 which is based on Sjöberg (1998b,c). The standardised measurement uncertainty for electrical RH instruments was between ± 1.6 and $\pm 3.2\%$ RH, see Table 2.12.

Table 2.12 Standard measurement uncertainty in measurements with electrical RH instruments.

W/c ratio	Method 1	Method 2	Method 3
0.4	± 3.2	± 1.7	± 2.0
0.7	± 2.8	± 1.6	± 2.0

2.3.2 Organic compounds in concrete (OCIC)

Sampling equipment

OCIC were measured in two stages. The first stage was sampling using a "headspace" technique in which VOC were collected and concentrated on an adsorbent. This was followed by analysis by gas chromatography (GC-FID).

The first step in the headspace technique was sample preparation. The sample was divided into fragments of about 1 cm using the same equipment and technique as in taking samples for moisture measurements in a test tube, Subsection 2.3.1. The pieces were then placed in a 250 ml glass bottle with a wide neck ($\text{\O}_{\text{int}} = 30 \text{ mm}$); Fig. 2.15. The cover of the bottle had an internal teflon gasket to ensure that no VOC were emitted or taken up through the cover. In the cover there were stainless steel fittings for tubes; these enabled controlled replacement of air in the bottle at the time of sampling. Sampling was performed when the VOC in the concrete attained equilibrium with the air in the bottle.

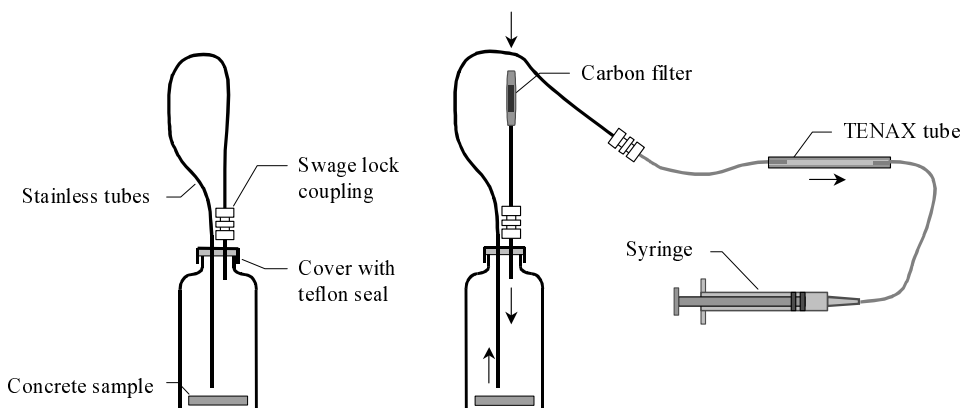


Fig. 2.15. Bottle during conditioning and sampling.

During sampling a 20 ml plastic syringe was used to draw the correct volume of air through the TENAX tube.

In sampling for analysis of VOCs, a filled glass tube (TENAX tube) was used as adsorbent; see Fig. 2.16. The length of this tube was 155 mm and its inside diameter 3.2 mm. Inside the tube there was ca 0.15 g TENAX TA, mesh 20-35, between two wads of glass fibre wool. The tubes had a crimp at each end, so that a teflon tube ($\text{\O}_{\text{ext}} = 1.8 \text{ mm}$) which was threaded into the tube was a close fit against the glass.

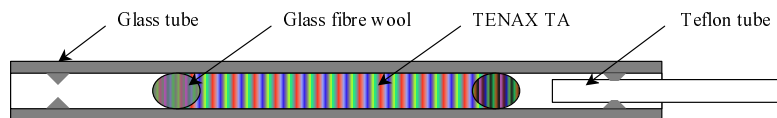


Fig. 2.16. TENAX tube, glass tube with 0.15 g TENAX TA.

Sampling method

The method used to measure OCIC was a modified headspace technique. In this technique, air which is in equilibrium with the sample in a closed volume is analysed.

Concrete cores for the experiment were drilled out of the test specimens with a core drill that produced a core of 25 mm diameter. Cores were "sliced" and placed immediately into bottles which were sealed and marked. In the first experiments the cores were cut using an abrasive water jet. Equipment for this was available at the Department of Production Engineering, Chalmers. The water jet produced a fine cut surface, but there was a risk that certain VOCs next to the cut may be washed away. In later experiments the core was broken up with a chisel. This did not provide the same opportunity to determine the sizes of the sample pieces since the cleavage surface could not be predicted. The method with the chisel was quicker and less expensive than the water jet method.

The bottles with the concrete pieces were conditioned in different ways, with the period and temperature of conditioning varied.

Prior to sampling, a hose fitting for the TENAX tube was screwed on to the swage lock coupling on the bottle; see Fig. 2.15. A carbon tube was fixed to the tube that draws air into the bottle during sampling, to clean the air and ensure that VOCs in the room air do not have an effect in subsequent analyses. A 20 ml plastic syringe was used to draw the correct volume of air through the TENAX tube. The volume of air that was drawn through the TENAX tube was varied but was mostly 10 ml. The different tubes and the syringe were in most cases connected with teflon hoses, using swage lock type couplings or silicon hose.

Analytical equipment

The VOCs adsorbed in the TENAX tube were analysed with a Varian 3350 gas chromatograph. For quantifying the concentration the GC was fitted with a flame ionisation detector (FID). To identify the peaks in the chromatogram, mass spectrometry (MS) was used.

The GC at the Department of Building Materials, Chalmers, had been modified to enable thermal desorption of VOCs in the TENAX tube to be performed. The modification was carried out in collaboration with dr Olle Ramnäs at the Department of Chemical Environmental Science, Chalmers. The desorption chamber of stainless steel is housed in an insulated aluminium cylinder to ensure good temperature stability. See Fig. 2.17. The carrier gas is also preheated in the aluminium cylinder. The temperature in the cylinder is regulated by means of an integral heating unit controlled by the GC.

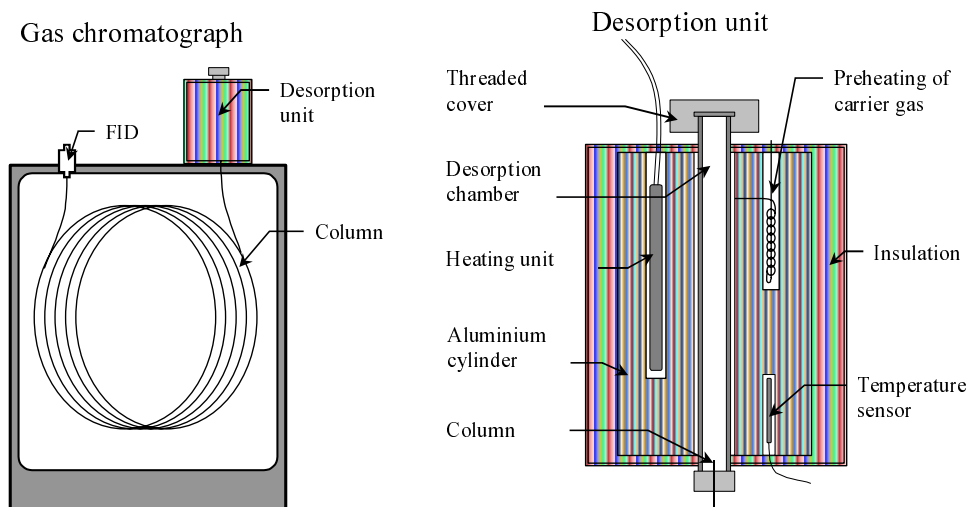


Fig. 2.17. General arrangement of GC-FID with details of the in-house designed injector unit for thermal desorption of the TENAX tube.

The GC was fitted with a 60 m long polar column of 0.25 μm phase. The temperature limits of the column were -60°C to $325/350^{\circ}\text{C}$.

Hydrogen gas (H_2) was used both as carrier gas and as fuel gas for the flame ionisation detector.

Method of analysis

The method used for analysis of the VOCs that had concentrated on the adsorber tube was based on gas chromatography. The adsorber was desorbed thermally, and VOCs were detected using flame ionisation and in some cases mass spectroscopy.

During thermal desorption, the adsorbed VOCs are driven off from the adsorber and transported by the carrier gas to the stationary phase of the column. During the desorption phase which takes about ten minutes, the column is kept refrigerated so that the VOCs condense and increase in concentration at the beginning of the column. After the desorption phase the temperature in the column is raised according to a predetermined scheme; see Fig. 2.18. When the temperature in the column increases, the VOCs begin to move through the column. During this movement the VOCs are separated because they are retained to different degrees in the stationary phase of the column. There is a constant voltage across the flame in the FID. When the VOCs pass through as organic hydrocarbon radicals, electrical conduction increases and a higher current is produced. The variation in current is plotted as a function of time in a chromatogram.

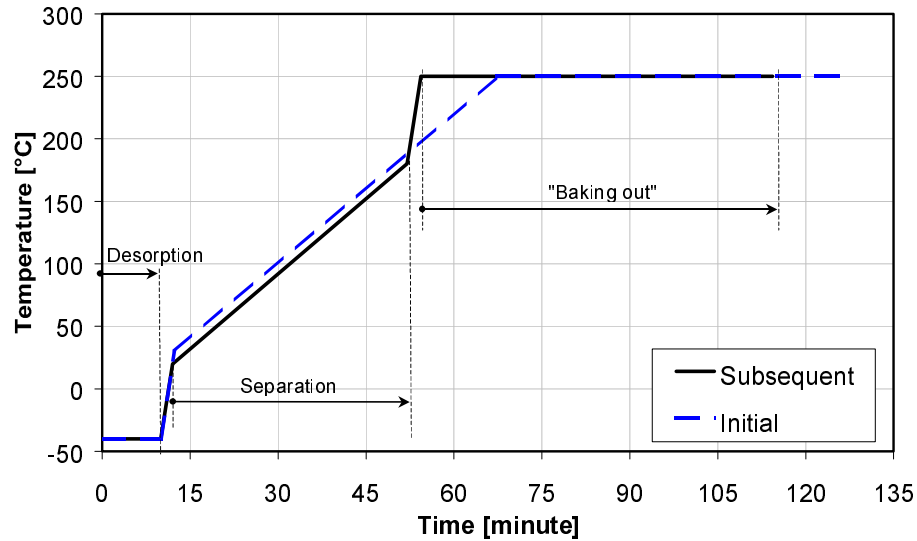


Fig. 2.18. Temperature program for the column during analysis.

The temperature in the desorption oven was kept constant at 230°C during the whole analysis and the pressure of the carrier gas (H_2) was kept constant at ca 15 psi. During the desorption phase the carrier gas swept the desorbed VOCs into the column. During the desorption phase a semi-automatic cryo-equipment was used to keep the column at $-40^\circ C$ by means of liquid nitrogen (N_2). The desorption phase took ten minutes. The temperature in the column was then raised according to a fixed program in which the initial temperature gradient was $+30^\circ C/minute$ until the temperature reached $+20^\circ C$. When this temperature was reached, the separation phase began. During the separation phase the temperature was increased at $+4^\circ C/minute$ until it reached $+180^\circ C$. Finally, the temperature gradient was again increased to $+30^\circ C/minute$ until it reached $+250^\circ C$ where it was maintained constant for 60 minutes so that the column was baked out, i.e. there was time for all "late eluting hydrocarbons" to emerge. See Fig. 2.18.

Some of the previous analyses were made using a different temperature program. After the program had been altered, it was easier to separate out the most volatile hydrocarbons. In the original temperature program the temperature was held at $-40^\circ C$ for ten minutes and was then raised at $+30^\circ C/minute$ to $30^\circ C$. The temperature was then raised at $+4^\circ C/minute$ until it reached $+250^\circ C$ where it was maintained constant for 60 minutes.

The results from the flame ionisation detector were presented in the form of a chromatogram, with the retention time along the x axis and the relative peaks of the FID along the y axis. Each peak in the chromatogram represents a organic compound with a specific retention time. With reference to the sampling volume for the analysed TENAX tube and the integrated area below the peaks, the total concentration or the concentration of the individual VOCs could be calculated. Contents are calculated with reference to the sampling volume for each tube, and the content of VOCs is given as toluene equivalents. An example of a chromatogram is shown in Fig. 2.19.

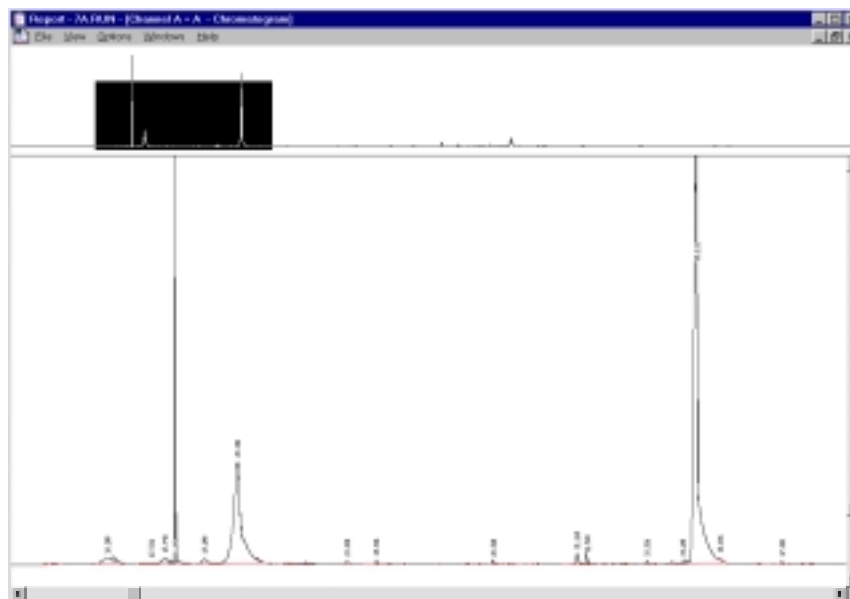


Fig. 2.19. Chromatogram where the first peak, after about 20 minutes, is butanol and the second (highest) peak, after about 35 minutes, is ethylhexanol.

The method is also briefly described in Wengholt Johnsson (1995).

TENAX tubes in the first measurement series were analysed with GC-FID by dr Olle Ramnäs at the Department of Chemical Environmental Engineering, Chalmers. Most of the analyses have however been performed at the Department of Building Materials, Chalmers. The method and the equipment were broadly the same. The differences were small and do not affect the results.

Some analyses were made with GC-MS to identify individual VOCs. These analyses were mainly made by dr Olle Ramnäs at the Department of Chemical Environmental Engineering, Chalmers.

Measurement uncertainty

In this limited study, it was not possible to exactly determine the standardised measurement uncertainty in measuring OCIC. The total measurement uncertainty was however judged to be about the same as in sampling VOC with FLEC; see Appendix No 2.

The total standardised measurement uncertainty for the method was assessed at $< \pm 20\%$.

2.3.3 Emission from the surface

Sampling equipment

Emission from material surfaces was measured in two stages. Sampling was first performed with a special measuring chamber in which the VOCs were captured, extracted and concentrated on an adsorber. This was followed by analysis with GC-FID.

The measuring chamber used in the work was a FLEC (Field and Laboratory Emission Cell). It may be likened to a cover that is put directly on the material surface to be measured; see Fig. 2.20. Pure air (<0.1 ppm hydrocarbons) from a gas cylinder is moistened and forced in through a gap around the sides of the measuring cell. The air flows over the surface of the material and out through a tube in the centre. Some of this air is then passed through a TENAX tube and the VOCs are adsorbed. The measuring cell and its capacity are described in detail by Wolkoff et al (1991) and Nordtest (1995). The active surface of the measuring cell has the area 0.0177 m^2 and its volume is $35 \cdot 10^{-6} \text{ m}^3$.

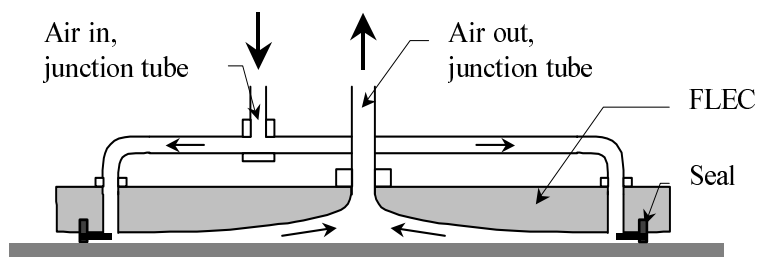


Fig. 2.20. Diagrammatic cross section of FLEC.

The air that was forced into the measuring cell was first purified through a carbon tube and then moistened to 50% RH by passing some of it through a gas washing bottle. The arrangement for moistening the air is described in detail in Wengholt Johnsson (1995). A TENAX tube and an SKC PCXR8 air pump were connected to the FLEC outlet.

The air pump delivered constant flow over a certain period. The measurement uncertainty in the flow was judged to be $\pm 4\%$. Measurement uncertainty in timing was given in the product sheet as $\pm 0.05\%$.

Sampling method

The specimens were conditioned for 24 hours prior to sampling. However, at the beginning of the study samples were taken after only 4 hours of conditioning. During conditioning the FLEC lay on the material surface with a constant air flow of 100 ml/min.

At the time of sampling a TENAX tube was attached to the FLEC outlet with a teflon tube; see Fig. 2.21. The tube that has a much smaller diameter than the outlet tube was inserted into this. The pump was coupled to the TENAX tube

and delivered 25 ml/min for four minutes. The sampling procedure is also described in Wengholt Johnsson (1995).

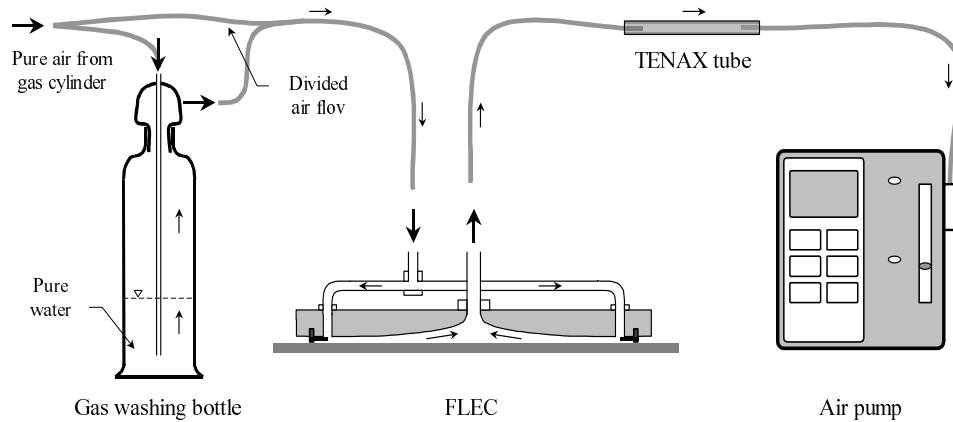


Fig. 2.21. Arrangement for sampling with FLEC. Pure air from a gas cylinder is moistened and passed through the FLEC. 100 ml of air is drawn through the TENAX tube for subsequent analysis in GC-FID.

The equipment for analysis of the contents of the TENAX tube was a gas chromatograph (GC) with a flame ionisation detector (FID). This equipment and the method of analysis are described in Subsection 2.3.2.

Measurement uncertainty

In this limited study, it was not possible to determine the standardised measurement uncertainty in measuring the emission from the test specimens. The total measurement uncertainty is however estimated in Appendix No 2.

The total standardised uncertainty for this method is judged to be $<\pm 20\%$.

3 Experiments on flooring and adhesive in combination

This chapter describes a multifactor experiment which was started early in the work on the thesis. In the beginning, the intention of the experiment was merely to show whether it was the flooring or the adhesive that gave rise to decomposition products. The first experiment therefore consisted of only two specimens, one with flooring and adhesive, and one without adhesive (only flooring). On the basis of the results of this first experiment, new hypotheses and theories were put forward. Two months after the first experiment, eight new experiments were started, and two months later on, another six. These experiments form the basis for the continued work and the interpretation of the processes in this area which is set out in the qualitative model in Chapter 6.

3.1 Test specimens

In the investigation, different floorings and adhesives were exposed to alkaline solutions with pH values of 11 and 13. The aim was to study the interaction between adhesive and flooring without the need to use moist concrete as the substrate. Owing to the fact that concrete had been replaced by an alkaline solution, the properties of the flooring such as alkali resistance could be studied. After the test specimens had been made and conditioned, the emissions were measured on several occasions by sampling with FLEC and TENAX tube and subsequent analysis with GC-FID. The experimental setup is given in Table 3.1 in the form of deviations from the reference system. The reference system is made up of the test specimen "plate" (P1) with a homogeneous PVC flooring (F1), 10g of latex adhesive (A1) and a pH solution (P3) with a pH value of ca 13.

Table 3.1. Summary of the most important differences in the test specimens in the investigation in relation to the "basic" setup (2a&b), which is: flooring F1 – 10g adhesive A1 – OT 15 minutes – liquid P3, pH value ca 13.

Experiment	Start 1996	Special property of test specimen in experiment		
		pH solution	Flooring	Adhesive
d1.00	22/4	No solution	Steel	A1
d1.01	22/4	No solution	F1	A1
d1.02	28/10	No solution	F2 (heterogen. PVC)	A1
d1.03	28/10	No solution	F3 (linoleum flooring)	A1
d1.1a	22/4	P3	F1	No adhesive
d1.1b	28/6	P3	F1	No adhesive
d1.2a	22/4	P3, Ref.sample	F1	A1
d1.2b	28/6	P3, Ref.sample	F1	A1
d1.3a	28/6	P3	F1	A1, on fabric
d1.3b	28/6	P3	F1	A1, on fabric
d1.4a	28/6	P3	F1	A3 (Wet area adh.)

d1.4b	28/6	P3	F1	A3 (Wet area adh.)
d1.5	28/6	P1 (pH 11)	F1	A1
d1.6	28/6	P2 (pH 13)	F1	A1
d1.7a	28/10	P3	F1	A1 (5 g)
d1.7b	28/10	P3	F1	A1 (10 g)
d1.7c	28/10	P3	F1	A1 (15 g)
d1.8a	28/10	P3	F3 (linoleum flooring)	A1
d1.8b	28/10		F3 (linoleum flooring)	A2 (Casco Proff)
d1.9	28/10		F2 (heterogen. PVC)	

Floorings of three different types were cut to size and small holes were punched in them for the clamping ring. Adhesive was then spread on the back of the flooring. Some experiments were however performed without adhesive; see Table 3.1. In experiments d1.3a and b, the adhesive was spread on a glass fibre fabric. When the adhesive was applied in experiments d1.2 – d1.6, a notched spreader was used which gave ca 10 g adhesive on the spread surface, and the adhesive layer was then evened out with a brush before the flooring was applied to the test specimen. In experiments d1.7a – d1.9, the adhesive was weighed and applied with a brush according to the method described in Subsection 2.1.3. The open time after application of the adhesive was about 15 minutes before the flooring was fixed to the test specimen; see Fig. 3.1. When the flooring had been fixed to the plate with the clamping ring, alkaline solution was added through the holes in the side. These holes were then closed with screws.

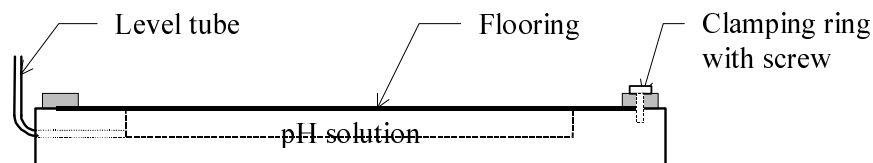


Fig. 3.1. Test specimens used in the investigation.

3.2 Method of measurement and results

After approximately four weeks, the first emission measurements were made on the samples. Measurements were made at slightly varying intervals for the different samples. On some of the samples, the first measurement was made about 32 weeks after application of the adhesive. Sampling was performed according to the method described in Subsection 2.3.3 with FLEC and TENAX tube. The subsequent analysis on the TENAX tube was performed with GC-FID.

The results in the form of the emission factor EF from the flooring are set out in Fig. 3.2 and 3.3.

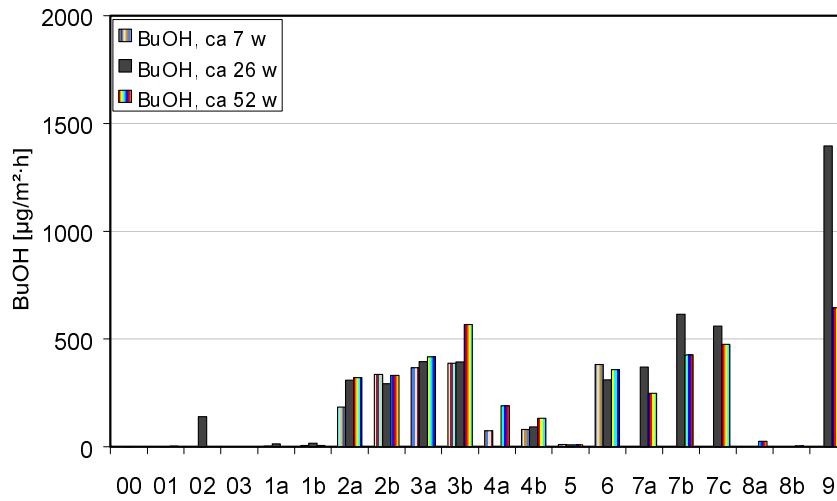


Fig. 3.2. Comparison of emission of butanol from 20 flooring + adhesive systems which had been exposed to alkaline solutions.

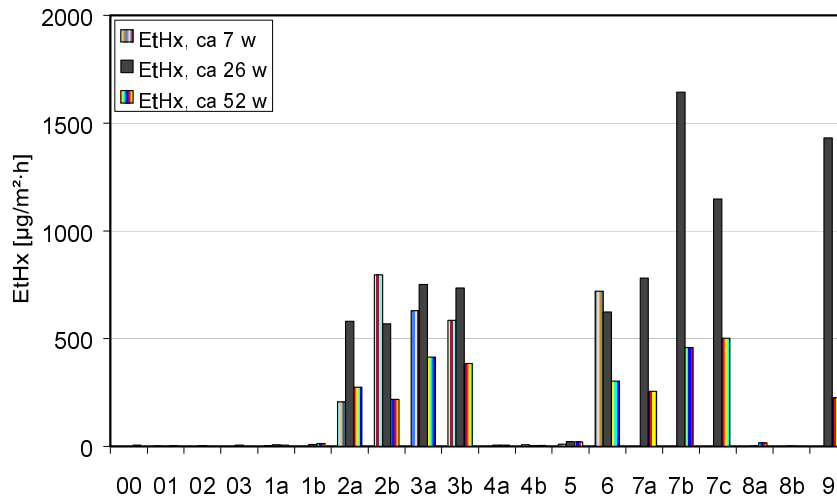


Fig. 3.3. Comparison of emission of ethylhexanol from 20 flooring + adhesive systems which had been exposed to alkaline solutions.

3.3 Evaluation of results

3.3.1 Description of general emission process

It is a common feature of all samples studied in this investigation that their emission processes can be described in a similar way. The process can be roughly divided into three phases, as shown in Fig. 3.4. These phases may vary in length and a phase has at times been so short that it was "missing". Examples of the causes of this variation may be the extent of decomposition, the impermeability of the flooring and the condition of the substrate. The phases are characterised as follows:

1. During an introductory starting phase, emission from the surface increases with time. The reason may be that the decomposition products formed need some time to penetrate through the flooring. The time this takes may depend on the intensity of decomposition and the impermeability of the flooring.
2. During phase 2, emission is approximately constant the whole time. Its magnitude may depend on the intensity of decomposition and the impermeability of the flooring. The length of the phase may depend on the extent of decomposition and the condition of the substrate. Conditions in the substrate are presumably critical for the length of the decomposition process.
3. During phase 3, emission from the surface decreases. The reason may be that decomposition has decreased or ceased. What is emitted from the surface are presumably VOCs left over from the earlier decomposition. The length of this phase may depend on the impermeability of the flooring and the condition of the substrate.

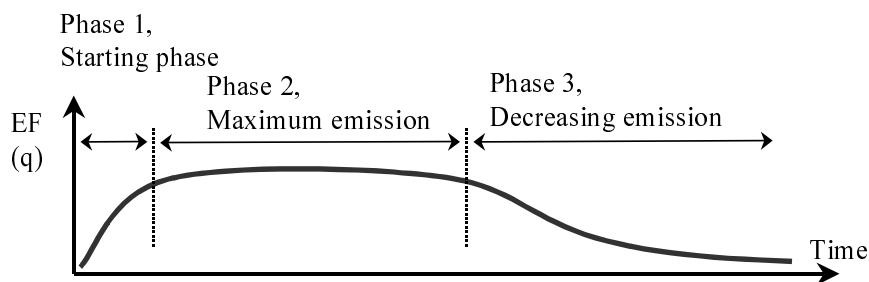


Fig. 3.4. The three phases of the emission process in alkaline decomposition of adhesive in floor constructions.

3.3.2 Measured emission process

The emission process in sample d1.2a was observed by FLEC measurements at frequent intervals. The aim of these frequent measurements was to describe the process and to study the way emission increased, gradually decreased and finally ceased.

By plotting the results from the reference samples d1.2a and b together with the results from samples d1.3 a and b, a mean curve for the emission process can be estimated; see Fig. 3.5 and 3.6.

In samples d1.3a and b the adhesive was applied to fabric, separate from the flooring. This difference from the reference sample did not give rise to any noticeable difference in the measurement results. This indicates that the adhesive degrades in the same way in all four samples, presumably without any significant interaction with the flooring. It must however be said that the adhesive is dissolved to a certain extent by the solution and makes this cloudy. It is probable that the adhesive which has been dissolved in the alkaline solution may have come into contact with the flooring.

By inserting a trend curve into Fig. 3.5 and 3.6, the different phases can be identified; see Fig. 3.4. However, only two phases could be identified in each figure.

According to the trend curve in Fig. 3.5, phase 2 for butanol had not ended after more than 1.5 year. One theory is based on butanol being highly water soluble. Extensive decomposition of the adhesive may have taken place and the butanol formed dissolved in the alkaline solution. Owing to the fact that butanol may be emitted from the liquid phase, a constant difference in concentration, and therefore a constant flow (emission), was maintained across the flooring.

According to the trend curve in Fig. 3.6, phase 2 does not exist for ethylhexanol. The basis for one possible explanation is that ethylhexanol has little water solubility. Extensive decomposition of the adhesive may have taken place, and since only a small quantity of ethylhexanol could be dissolved in the liquid, the result was a high concentration in the gas phase below the flooring. The concentration below the flooring decreases monotonically as the ethylhexanol evaporates. Owing to this decreasing concentration difference across the flooring, the flow (emission) decreases.

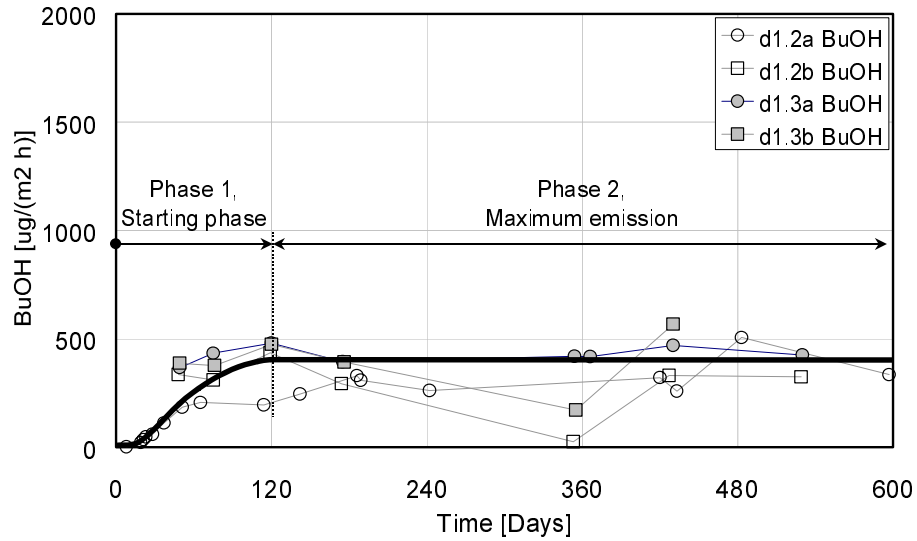


Fig. 3.5. Mean curve for butanol when ca 10 g of adhesive is exposed to alkaline solution below a homogeneous PVC flooring. The mean curve is produced by averaging the trend curves of four measurement series.

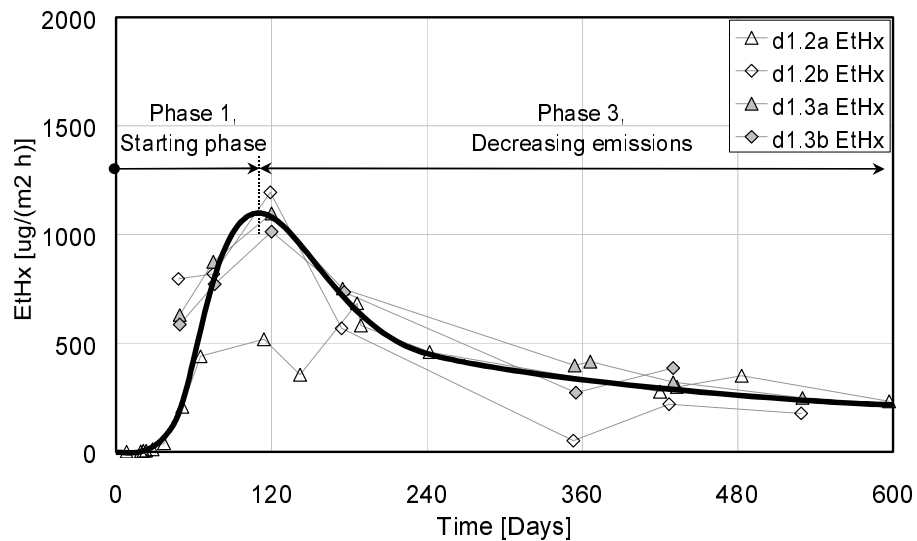


Fig. 3.6. Mean curve for ethylhexanol when ca 10 g of adhesive is exposed to alkaline solution below a homogeneous PVC flooring. The mean curve is produced by averaging the trend curves of four measurement series.

3.3.3 Mass balance of OH⁻ and decomposition products

With the help of a mass balance, the quantities of consumed and created compounds can be estimated. By calculating the critical components in the system, a plausibility assessment can be made.

The copolymers in the adhesive are the critical components which are consumed. The emissions from the test specimen and any decomposition products dissolved in the solution are the compounds created.

The mass balance for experiments d1.2 and d1.3 is summarised in Table 3.2. The bar "manufactured VOCs" states, briefly, that according to the assumption below, the adhesive is enough for the production of ca 1.65 g decomposition products.

The column "consumed VOCs" states, briefly, that 0.24 g has been emitted from the sample. The remaining VOCs produced in the reaction may be dissolved in the alkaline solution up to 16.71 g.

Table 3.2. Mass balance for the critical components in experiments d1.2 and d1.3 (g). The volume of the pH solution is 0.214 litre and the area covered by the adhesive is 0.0214 m².

Compound	"Manufactured" VOCs (+)	"Consumed" VOCs (-)	
	Quantity of adhesive	Dissolved in water	Area in figure
BuOH	0.8	6.5	0.11
EtHx	0.8	0.21	0.13
Total	ca 1.65	16.71	0.24

Quantity of adhesive

The supplier of the adhesive used in the experiments states in the product information that it consists of 10 – 30% copolymers. In a telephone conversation, a chemist states that the acrylate dispersion is a 55% aqueous solution and makes up ca 30% by weight of the adhesive. This means that ca 16.5% by weight of the adhesive consists of copolymers that can be hydrolysed.

It is a reasonable assumption that the acrylate copolymer consists of 50% butylacrylate and 50% 2-ethylacrylate. It may at times also contain some other acrylate, but for the sake of simplicity this is ignored. Let us assume that all copolymers can be broken down into butanol and ethylhexanol without any residues. This is perhaps unlikely, but it yields the maximum quantity of decomposition products. This reasoning implies that, as a maximum, 10 g of adhesive would decompose into ca 0.8 g butanol and 0.8 g ethylhexanol.

Dissolved in liquid

There is no pore system into which the VOCs can migrate down into, but there is a liquid in which they can dissolve. According to CRC (2000), a butanol solution contains 77 g/litre of water, and an ethylhexanol solution 1 g/litre of water. Since the hollow in the plate contains approximately 214 g water, 16.5 g butanol and 0.21 ethylhexanol can dissolve in this.

Total quantity of VOCs emitted through the flooring

The total quantity of VOCs that was emitted through the flooring can be calculated by integrating emission over time. This method is shown in detail in Section 8.2.

In the case of butanol, the integral represented by the area below the mean curve in Fig. 3.5 is equal to 5.3 (g/m²). Multiplication by the area of the plate ($21 \cdot 10^{-3}$ m²) gives that the total quantity of emitted butanol is 0.11 g.

In the case of ethylhexanol, the integral represented by the area below the mean curve in Fig. 3.6 is equal to 6.3 (g/m²). Multiplication by the area of the plate ($21 \cdot 10^{-3}$ m²) gives that the total quantity of emitted ethylhexanol is 0.13 g.

Mass balance

According to the assumptions, ca 0.8 g butanol has been formed and 0.11 g has been emitted through the surface. The remaining 0.69 g may be found dissolved in the flooring and in the pH solution.

According to the assumptions, ca 0.8 g ethylhexanol has also been formed. 0.13 g has been emitted through the surface and 0.02 g may have been dissolved in the pH solution, but where has the remaining 0.65 g disappeared?

Perhaps it was never formed at all. The reason may be that 2-ethylhexanol is not broken down completely, or that the assumption regarding the proportions of the copolymers is not correct.

3.3.4 The significance of the quantity of adhesive

The aim of the comparison made here is to highlight the importance of the adhesive for the emission from the test specimens. Emission was measured from seven experiments in which the same adhesive, flooring and alkaline solution were used. In experiments 7a, b and c there are no measurements in week 7.

In the first three experiments which are shown in Fig. 3.7 and 3.8, different quantities of adhesive were used in otherwise identical test specimens. The quantities in experiments d1.7a, b and c are 5, 10 and 15 g respectively. The measurements show that the least emission occurs in the experiment with the least adhesive, but that emissions from the other two experiments are about equal.

If we look at the whole measurement series for butanol which is set out in Fig. 3.9, it is clear that emission is greater from the experiment with 15 g than with 10 g. The whole measurement series for ethylhexanol is set out in Fig. 3.10, and it is seen that the emission process is about the same in both experiments.

In experiments d1.2a and 2b, about 10 g adhesive was used. These are the reference samples of the experiment. In experiments d1.3a and 3b, about 10 g adhesive was spread on a braided glass fibre fabric below the flooring. This procedure had no influence on emission.

If we look at the whole measurement series, we can conclude from the results for butanol in Fig. 3.7 that emission has the same magnitude and sequence in all four experiments. The same also applies for ethylhexanol. The emission for ethylhexanol over the whole measurement series is set out in Fig. 3.8. Variations in the results in the figures may be due to measurement uncertainties and random variations rather than to the systematic effects of the studied parameters.

When some other plates with the same adhesive and flooring were dismantled, it was noted that the adhesive had dissolved in the pH solution. One layer of adhesive was however still left on the back of the flooring. The consistency of the pH solution had changed and was white and milky, instead of clear and transparent as in the beginning.

The possible conclusions that can be drawn from this comparison are as follows:

- The quantity of applied adhesive influences emission during highly alkaline decomposition of the material combination concerned.
- Emission volume is the same irrespective of whether or not the adhesive has direct contact with the flooring during alkaline decomposition.

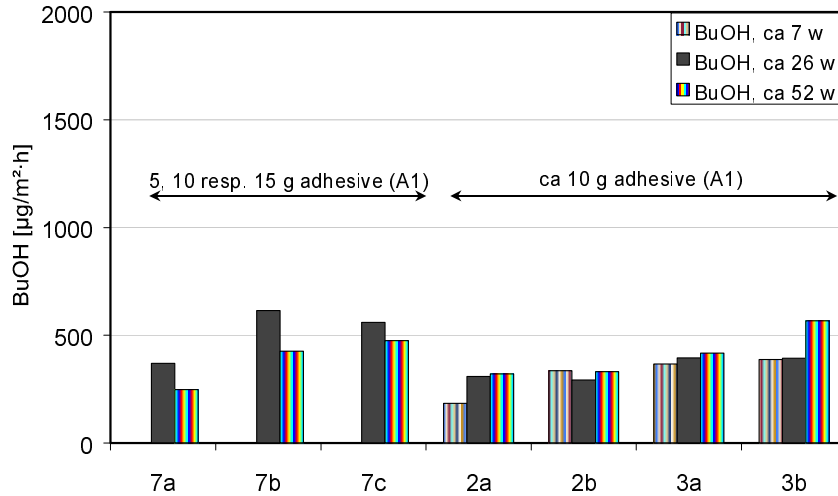


Fig. 3.7. Comparison of emission of butanol when the quantity of adhesive and the way the adhesive is applied vary. d1. 7a, 7b and 7c are made with 5, 10 and 15 g of adhesive on the flooring respectively. d1. 2a and 2b have about 10 g of adhesive on the flooring, d1. 3a and 3b have about 10 g adhesive on a woven glass fibre fabric below the flooring. All combinations of adhesive and flooring were exposed to an alkaline solution of pH 13.

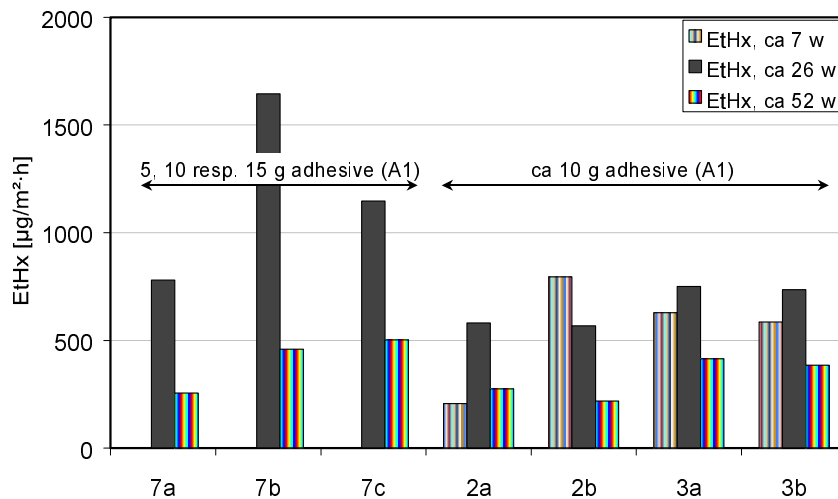


Fig. 3.8. Comparison of emission of ethylhexanol when the quantity of adhesive and the way the adhesive is applied vary. Explanation of the bars is given in fig 3.7.

3.3.5 Mass balance for different quantities of adhesive – 5, 10 and 15 g

A comparison is made here between three experiments with different quantities of adhesive but with otherwise identical conditions. The comparison is made by setting up a mass balance for important components in these three experiments, d1.7a, b and c.

The mass balance for the copolymer which is probably critical for emissions from the system is shown in Table 3.3. The initial values before any decomposition has taken place are as follows:

The copolymer which is available for decomposition is calculated in the same way as in Subsection 3.3.3. Let us assume that 16% of the adhesive is acrylate copolymer. From a quantity of 5 g adhesive, $(5 \cdot 0.16 =)$ 0.8 g VOCs can be formed on complete decomposition. Analogously, the corresponding quantities for 10 and 15 g adhesive will be 1.6 and 2.4 g.

Table 3.3. Records for VOCs in experiments d1.7a, b and c. The quantities (g) are based on an area of 0.0214 m² and 0.214 litre liquid.

	d1.7a	d1.7b	d1.7c
	Polymer	Polymer	Polymer
	$\cdot 10^{-3}$ (g)	$\cdot 10^{-3}$ (g)	$\cdot 10^{-3}$ (g)
Initially	800	1600	2400
Area _{BuOH}	-79	-121	-143
Area _{ETHx}	-125	-214	-214
"missing"	596	1265	2043

The VOCs emitted from the surface can be calculated in the way discussed in Subsection 3.3.3. Since there are no measured values for phase 1 and the values that are available relate only to six months, the emission process is estimated. This estimate is based both on the measured values obtained in these experiments and the shape of the mean curve which was determined for the emission process in four other experiments earlier in this chapter.

The chain line curves in Fig. 3.9 and 3.10 are the mean curves for the investigation. The full curves represent the emission process during the period measurements were made, and the dotted curves represent an estimate of the emission process with reference to the shape of the mean curve.

The mass balance could not be completed. A number of polymers are "missing" in the table. The explanation may be that they had not been decomposed or that the decomposition products are dissolved in the liquid. Since the emission has not finished, there is still a considerable concentration of VOCs below and inside the flooring.

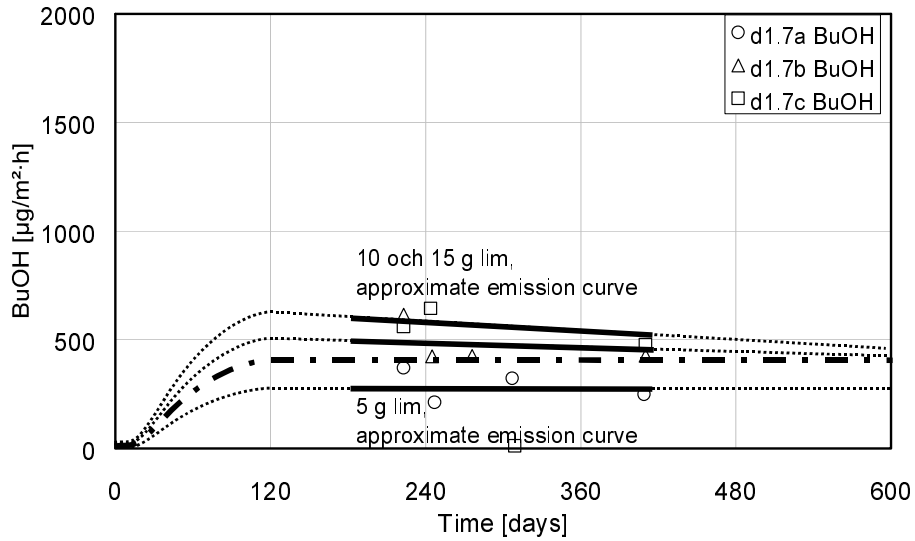


Fig. 3.9. Possible emission process for butanol when 5, 10 and 15 g of adhesive are exposed to alkaline solution below a homogeneous PVC flooring.

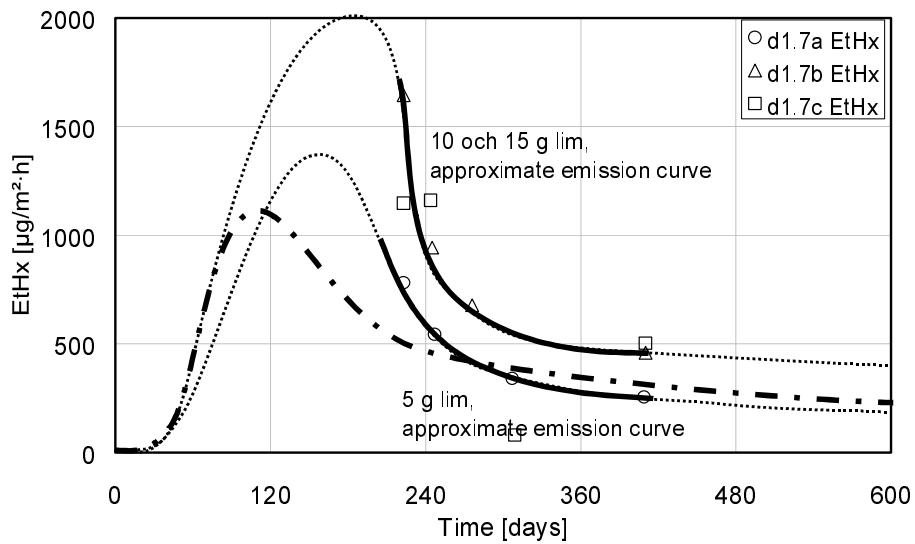


Fig. 3.10. Possible emission process for ethylhexanol when 5, 10 and 15 g of adhesive are exposed to alkaline solution below a homogeneous PVC flooring.

3.3.6 Critical pH for decomposition of adhesive

The aim of the comparison made here is to show whether it is the adhesive that is degraded and whether the critical pH value is between 11 and 13. The emission from seven experiments is compared; these have been divided into two groups, those with low and high emission.

The bars at the left of Fig. 3.11 and 3.12 represent low emission, they show little or no signs of decomposition. The first experiment d1.01 is measured on a homogeneous PVC flooring. The flooring is laid loose on a steel plate and has not been exposed to chemicals or sunlight. Experiments d1.1a and 1b are parallel samples which consist of the same type of flooring as that exposed to the pH solution of pH 13 without adhesive. Experiment d1.5 consists of the same type of flooring and a latex adhesive which is exposed to a pH solution of pH 11. During the whole measurement period, emission from all these experiments is low, the explanation for which is that no decomposition has taken place.

The bars to the right of the figures represent high emission from the test specimens as a result of extensive decomposition of the adhesive. Experiment d1.6 consists of the same flooring and adhesive as those in d1.5 although they have been exposed to a Titrisol solution of pH 13. Experiments d1.2a and 2b are parallel samples which consist of the same type of flooring and adhesive, but exposed to an alkaline solution of pH = ca 13.

A comparison of the emission from the twin samples d1.1a and 1b with the twin samples d1.2a and 2b shows that no decomposition appears to take place in the experiment if the test specimen contains no adhesive. We must also bear in mind that approximately 16% of the adhesive consists of a copolymer which can be degraded into butanol and ethylhexanol. The conclusion that can be drawn from these results is that it is the adhesive which is degraded.

By comparing experiment 5 with the twin samples d1.2a and 2b, it is found that the composition of the alkaline solution is of less significance. It does not appear critical what counterions to OH^- are present in the liquid; it is only the pH level of the liquid that is critical.

The above statement, that it is the pH level which is most important for decomposition, can be confirmed by comparing experiments d1.5 and d1.6. The only difference between the test specimens in these experiments is the pH value of the pH solution. At pH 11 (d1.5) the emission is low, while at pH 13 (d1.6) it is high. There may also be a critical pH value for decomposition that is situated somewhere between 11 and 13. This appears plausible if we bear in mind that the pH scale is logarithmic, i.e. the concentration of OH^- at pH 13 is one hundred times that at pH 11.

The possible conclusions that can be drawn from this comparison are as follows:

- It is the adhesive, and not the flooring, which is degraded in this material combination.
- The critical pH may be situated between 11 and 13.

- Systems from which some critical component such as the (copolymer in the) adhesive or the hydroxide ions have been removed yield low emission.

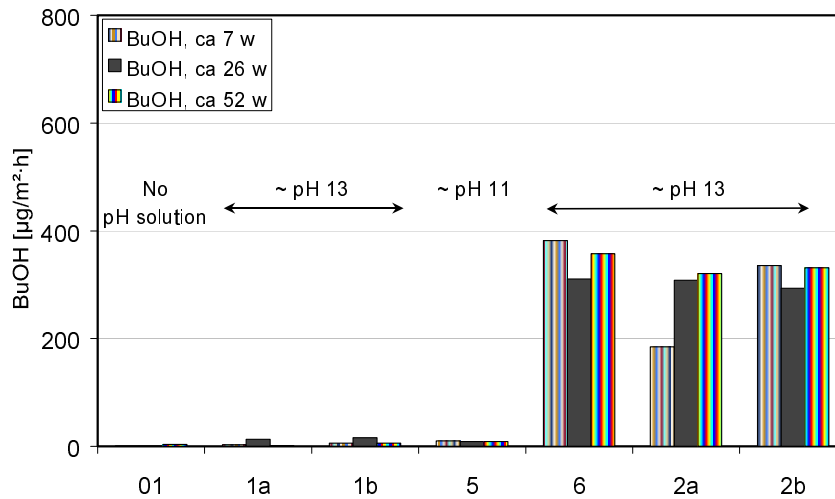


Fig. 3.11. Emission of butanol from floor systems of different pH values. Flooring on plate (01), flooring without adhesive on pH 13 (1a and 1b), flooring with adhesive on pH 11 (5), flooring with adhesive on pH 13 (6) and flooring with adhesive on ca pH 13 (2a and 2b).

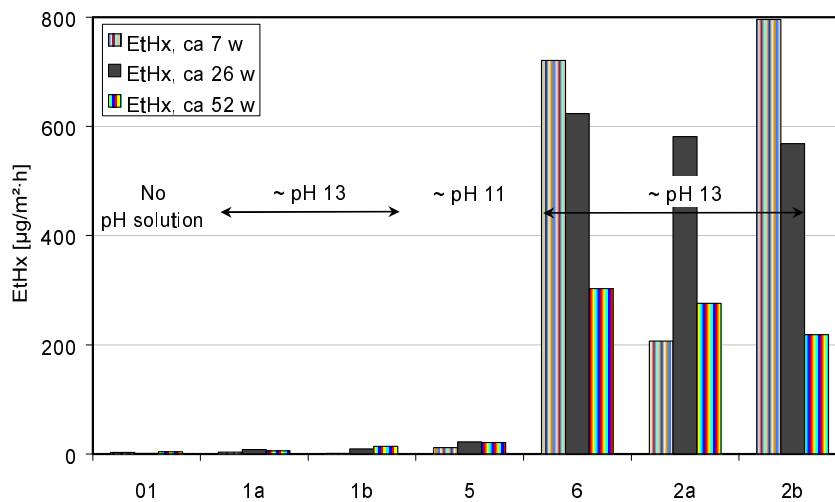


Fig. 3.12. Emission of ethylhexanol from floor systems of different pH values. Explanation of the bars is given in fig 3.11.

3.3.7 The importance of the choice of materials

The comparisons made here demonstrate the importance of the choice of materials for emission from the test specimens. Emission has been measured in seven experiments where three adhesives and three floorings were combined in different ways. In experiments 8a and b, and 9, there are no measurements for week 7.

In the first four experiments plotted in Fig. 3.13 and 3.14 the same adhesive was used together with different floorings. The combination of flooring and adhesive was exposed to alkaline solution of approximately pH 13. In the first experiment (8a) a linoleum flooring was used. In experiments d1.2a and 2b which are twin samples and the reference in this investigation, a homogeneous PVC flooring was used. In experiment d1.9 a heterogeneous PVC flooring was used.

The emission measurements reveal large differences in the emission of both butanol and ethylhexanol in these experiments. The test specimens in the experiments were treated in the same way. They consist of the same adhesive which was exposed to the same pH solution, so it would be reasonable to expect that decomposition of the adhesive would be the same in all four experiments. One explanation may be that the floorings have different degrees of impermeability to decomposition products.

The possible reason for the apparent impermeability of the linoleum flooring to VOCs in comparison with that of the PVC floorings is that the VOCs perhaps "dissolve" in the PVC flooring and are therefore transported in a way that is not possible in the linoleum flooring.

Experiment d1.2a has a somewhat lower emission than d1.2b although they are twin samples in which all materials are identical. The differences are presumably due to the uncertainty of the method. By comparing the differences in measurement results in Fig. 3.4 and 3.5, the uncertainty in the measurements can be estimated.

Experiment d1.8b comprises a linoleum flooring with a different adhesive but with the binder similar to that in the reference adhesive. Emission in this material combination is also low, just as in d1.8a in which a linoleum flooring was also used.

Experiments d1.4a and 4b were made on twin samples in which an adhesive with the binder not based on 2-ethylacrylate was used together with a homogeneous PVC flooring. Since the adhesive does not have the acrylate copolymer which gives rise to ethylhexanol, this VOC cannot be formed during decomposition. Only small emissions were measured in these experiments. The emission of ethylhexanol is of the same order as the primary emission of the flooring.

The conclusions that can possibly be drawn from this comparison are as follows:

- The choice of adhesive influences emission in alkaline decomposition, since the quantities of decomposition products are different.
- The choice of flooring influences emission in alkaline decomposition because different floorings have different degrees of impermeability to decomposition products.

- Material combinations comprising linoleum flooring give rise to small emissions in alkaline decomposition of the adhesive because the linoleum flooring is "apparently" more impermeable to the decomposition products of the adhesive.

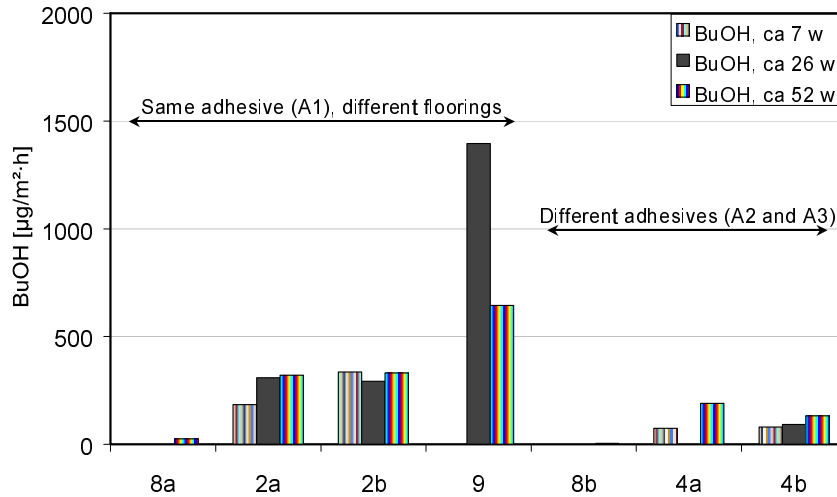


Fig. 3.13. According to the investigation, emission of butanol depends on the way three different adhesives and three floorings are combined. Bar 8a represents linoleum flooring and adhesive, 2a and 2b a homogeneous PVC flooring with the same adhesive, 9 a heterogeneous PVC flooring with the same adhesive. 8b represents a linoleum flooring with a different adhesive, and 4a and 4b a homogeneous PVC flooring with a different adhesive.

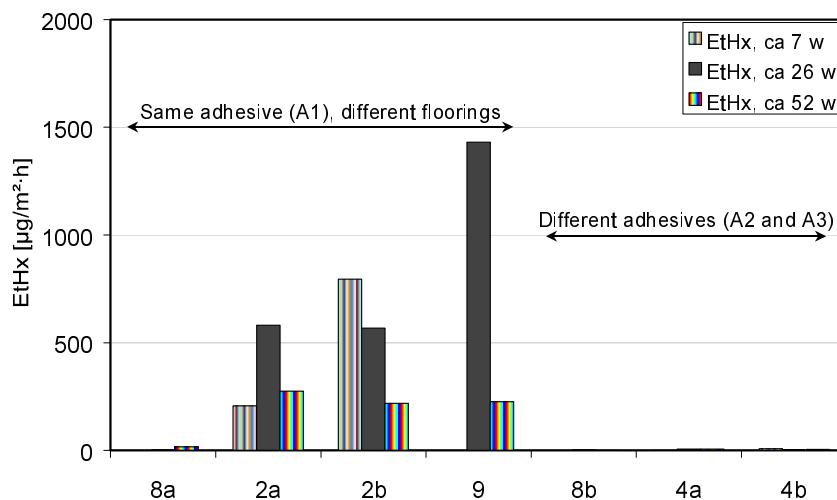


Fig. 3.14. According to the investigation, emission of ethylhexanol depends on the way three different adhesives and three floorings are combined. Explanation of the bars is given in fig 3.13.

4 Measurements of the Transport of Organic Compounds in Materials

OC which are formed below the flooring during alkaline hydrolysis of flooring adhesive can migrate into surrounding materials. They may migrate upwards through the flooring and escape into the room air, and they may also migrate down into the concrete and be stored there for a long time.

In this chapter, a study is made of the transport of butanol and ethylhexanol inside concrete and through floorings.

4.1 The resistance R_{fc} of the flooring

In this investigation, the resistance to transmission of butanol and ethylhexanol was measured in two floorings. This experiment may be likened to a cup experiment in which the underside of the flooring was exposed to known concentrations of butanol and ethylhexanol. The flow through the floorings was measured with a FLEC (Field and Laboratory Emission Cell), and the transmission resistance of the floorings to butanol and ethylhexanol was evaluated.

The investigation was made in two series. At first, only PVC floorings were studied in four different experiments. A year or two later eight new experiments were started, four with newly made PVC floorings of the same type in order to verify earlier results, and four with linoleum floorings.

4.1.1 Test specimens

The floorings were cut to size and fixed to the plate which is described in Subsection 2.2.1. The hollow in the plate for pH solution was then filled with butanol or ethylhexanol through the hole for the level tube; see Fig. 4.1. One test specimen with butanol (No 2) and one with ethylhexanol (No 8) were completely filled so that the liquid was in contact with the flooring. The other test specimens with their appropriate liquids were about half filled so that an air gap was left between the liquid and the flooring. The air in the gap was at saturation concentration.

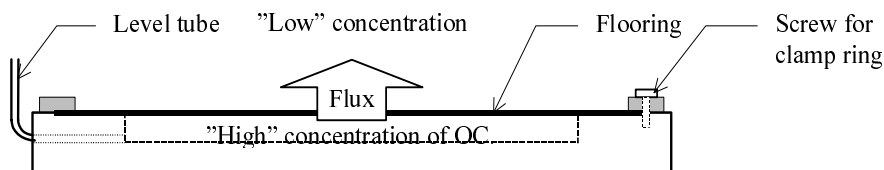


Fig. 4.1. Test specimen where a flooring can be stretched over a space with VOCs in liquid phase. The flux of VOCs through the flooring is measured with a FLEC.

4.1.2 Sampling

The first emission measurement on the first samples (Nos 1, 2, 7 and 8) was made after about 24 weeks. Measurements were then repeated at approximately ten week intervals for about one year. Sampling was performed using a FLEC and a TENAX tube. Subsequent analysis of the TENAX tube was performed with GC-FID, according to the method described in Subsection 2.3.3.

Emission measurements on the other eight specimens were made at monthly intervals for about six months.

4.1.3 Results

The results of the measurements exhibited large variations. The estimated results for butanol and ethylhexanol are set out in Tables 4.1 and 4.2. They are given as both emission factor EF [$\mu\text{g}/(\text{m}^2\cdot\text{h})$] and flow q [$\text{kg}/(\text{m}^2\cdot\text{s})$]. EF is the most common way of presenting the results of measurements with FLEC, while q is based on SI units and is probably a more correct way of describing the results of measurements.

The method of measurement needs development to yield more reliable results. It may be better to measure the flow by determining weight loss than by using FLEC.

*Table 4.1. Flow of butanol through PVC and linoleum floorings when the difference in vapour pressure is the maximum. Nos 1-4 are identical except for *. Nos 5-6 are identical. Flow is measured with FLEC.*

Experi- ment	EF _{BuOH} [$\mu\text{g}/(\text{m}^2\cdot\text{h})$]	q _{BuOH} [$\text{kg}/(\text{m}^2\cdot\text{s})$]	R _{fc} - PVC $\cdot 10^3$ [s/m]	R _{fc} - linoleum $\cdot 10^3$ [s/m]
1	13 000	$3.6\cdot 10^{-9}$	4 800	–
2*	16 000	$4.5\cdot 10^{-9}$	3 800	–
3	15 000	$4.3\cdot 10^{-9}$	4 000	–
4	22 000	$6.2\cdot 10^{-9}$	2 700	–
5	19 000	$5.3\cdot 10^{-9}$	–	3 200
6	24 000	$6.5\cdot 10^{-9}$	–	2 600

* Exposure of underside of flooring to VOC in liquid phase, others to saturated gasphase.

*Table 4.2. Flow of ethylhexanol through PVC and linoleum floorings when the difference in vapour pressure is the maximum. Nos 7-10 are identical except for *. Nos 11-12 are identical. Flow is measured with FLEC.*

Experi- ment	EF _{ETHX} [$\mu\text{g}/(\text{m}^2\cdot\text{h})$]	Q _{ETHX} [$\text{kg}/(\text{m}^2\cdot\text{s})$]	R _{fc} - PVC $\cdot 10^3$ [s/m]	R _{fc} - linoleum $\cdot 10^3$ [s/m]
7	10 000	$2.8\cdot 10^{-9}$	250	–
8*	7 000	$1.9\cdot 10^{-9}$	360	–
9	5 000	$1.5\cdot 10^{-9}$	480	–
10	4 000	$1.1\cdot 10^{-9}$	630	–
11	27 000	$7.5\cdot 10^{-9}$	–	90
12	29 000	$7.9\cdot 10^{-9}$	–	90

4.1.4 Evaluation

It is assumed that the driving force for transport is the endeavour of the system to establish concentration equilibrium. A simplified calculation of the VOC flux can be made if it is assumed that there is only one resistance without storage capacity between two different concentrations. Flux is then determined by the difference in concentration but also by the transmission resistance of the flooring; see Fig. 4.2. The flux from the flooring is expressed in terms of either q in SI units or the emission factor (EF). EF is the most common quantity in measurements with FLEC.

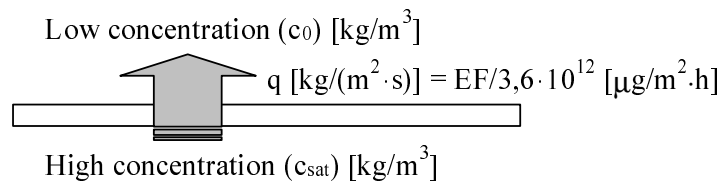


Fig. 4.2. The flux q endeavours to equalise the differences in concentration on the two sides of the flooring. The storage capacity of the flooring is ignored.

The results of measurements in the investigation can be used to evaluate the resistance of the flooring to the transport of OC. The calculation is based on Fick's first law which is described in detail in Section 7.4.

The equation for Fick's first law can be rewritten so as to be better suited for the case with saturation concentration below a flooring in a ventilated room, as shown in Equation 7.40. In comparison with the saturation concentration below the flooring (c_{sat}), at 20°C, the concentration in the room (c_0) is negligible. The equation then has the form

$$q_{\text{air}} = \frac{(c_{\text{sat}} - c_0)}{R_{f1}} \quad \left[\text{kg}/(\text{m}^2 \cdot \text{s}) \right] \quad (4.1)$$

According to Appendix No 3, the saturation vapour content (c_{sat}) for butanol at room temperature (20°C) is $17 \cdot 10^{-3}$ and the corresponding value for ethylhexanol is $0.7 \cdot 10^{-3}$ (kg/m^3). For calculation of the transmission resistance (R_{fc}) of the flooring, the simplified equation 4.1 is used. These parameters and the results of the investigation, as well as the transmission resistance of the flooring to butanol and ethylhexanol, calculated according to Equation 4.1, are set out in Table 4.3.

Table 4.3. Summary of measurement results, the parameters used and the calculated mean values of the transmission resistance of PVC and linoleum flooring to butanol and ethylhexanol.

Unit	Butanol		Ethylhexanol	
	PVC	Linoleum	PVC	Linoleum
EF $\mu\text{g}/(\text{m}^2 \cdot \text{h})$	16 700	21 200	6 600	27 800
q $10^{-9} \text{ kg}/(\text{m}^2 \cdot \text{s})$	3.56	5.89	1.83	7.72
c_m $10^{-3} \text{ kg}/\text{m}^3$	17	17	0,7	0,7
R_{fc} $10^3 \text{ s}/\text{m}$	3 700	2 900	380	90

4.2 Diffusion coefficient δ_{oc} for butanol in concrete

In this investigation, transport of butanol through concrete was studied with the cup method. The aim was to evaluate the diffusion coefficient δ_{oc} for butanol in the gas phase in dry concrete.

4.2.1 The test specimen

The cup (PF2) used in this investigation is described in Subsection 2.2.2. A round slice of concrete cut from a cylinder, which had in turn been drilled out of a larger concrete cube with a core drill, was fixed to the top of the cup. The concrete used in this study was ordinary structural concrete (C4) described in Subsection 2.1.1. Before the cube was drilled, it was conditioned in a laboratory environment. The diameter of the slice of concrete was 95 mm and its thickness 20 mm.

The cup was filled with butanol so that it was ca 5 mm above the bottom; see Fig. 4.3. The concrete slice was carefully fixed to the cup with butyl based "Platon" sealing compound. A layer of aluminium tape, which is completely vapourtight, was carefully placed around the outside of the sealing compound.

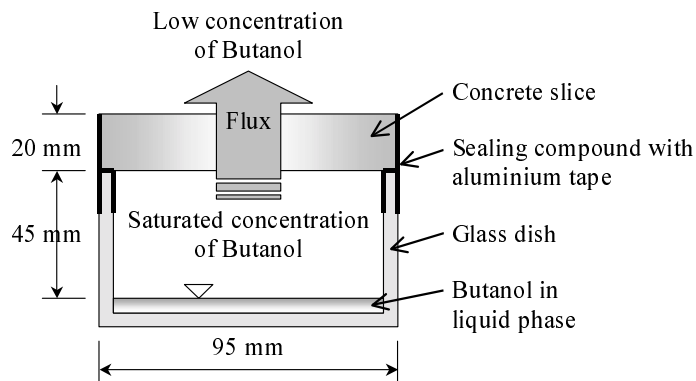


Fig. 4.3. General arrangement of cup experiment. During the experiment the cup containing butanol was placed in a controlled climate room at 20°C and 65% RH.

Four cups with butanol were prepared for the study. During the whole measurement, these cups were placed in a controlled climate room at constant 20°C and 65% RH.

4.2.2 Measurement

Flow through the slice of concrete was measured by determining the weight loss through repeated weighing of the test specimen. In the beginning of the measurement series, the cups were weighed in the controlled climate room at intervals of about one week, and at the end of the series at intervals of about two weeks. The weighing machine used was a Mettler PM 4000 with a resolution of 0.01 g. Over the measurement range the reproducibility of the weighing machine is ± 0.01 g.

4.2.3 Results

The results in the form of the weight loss of the cups are set out in Table 4.4 and Fig. 4.4.

Table 4.4. Summary of results, loss in weight due to emission of butanol in cup experiments with 20 mm thick concrete slices.

Time [hours]	Weight loss [g]			
	1	2	3	4
21	0.00	0.00	0.00	0.00
167	0.14	0.16	0.16	0.12
332	0.21	0.27	0.25	0.20
499	0.44	0.48	0.49	0.44
671	0.51	0.58	0.63	0.57
940	0.81	0.84	0.95	0.93
1125	1.06	1.07	1.23	1.24
1363	1.39	1.36	1.60	1.64
1651	1.83	1.74	2.07	2.14
2039	2.54	2.35	2.80	2.95
2349	3.14	2.85	3.41	3.60
2685	3.82	3.43	4.08	4.32
3021	4.55	4.06	4.80	5.10

The weight loss per unit time which is represented by the slope of the curves in Fig. 4.4 increases slightly over time. It normally takes a very long time before the flow becomes steady. Steady flow has not really been reached in the experiment.

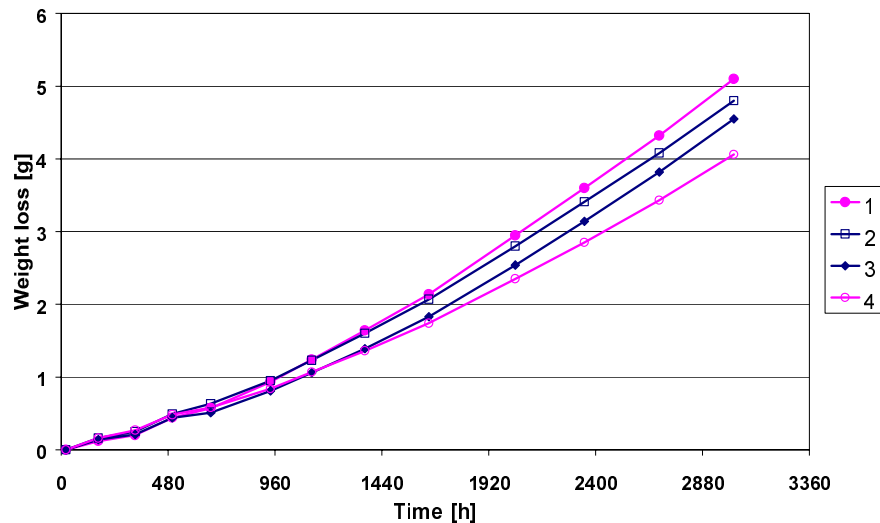


Fig. 4.4. Weight loss in cup with butanol due to diffusion through 2 cm thick slice of concrete. Constant climate, 20°C and 65% RH.

4.2.4. Evaluation of δ_{OC} for butanol

The diffusion coefficient δ_{OC} was evaluated from the last two measurement results which were 336 hours apart. A regression curve is usually employed in evaluating a measurement series, but in this case the last two measurements yield the best results since steady flow has probably not yet been attained. Equation 4.2 is used for evaluation.

$$q_{air} = \delta_{OC} \cdot \frac{\Delta c_{air}}{\Delta x} \quad [kg/(m^2 \cdot s)] \quad (4.2)$$

The flow q_{air} is obtained from the weight loss between the last two measurements, set out in Table 4.4. Δx is the thickness of the concrete slice, Δc_{air} the difference in concentration between the vapour phase butanol in the cup and in the room. The air in the cup is assumed to be saturated with butanol, and the concentration of butanol in the room air is assumed to be equal to zero.

According to Appendix No 3, the saturation concentration of butanol at a room temperature of 20°C is equal to $17 \cdot 10^{-3} \text{ kg/m}^3$.

The conditions and results for the four cups in the investigation are set out in Table 4.5.

Table 4.5. Summary of measurement results, parameters and calculated diffusion coefficients δ_{OC} for butanol in dry concrete.

Designation		Sample			
Quantity	Unit	1	2	3	4
Δweight	[g]	0.73	0.63	0.72	0.78
Δtime	[hours]	336			
Δx	[10^{-3} m]	20			
area	[10^{-3} m^2]	7.09			
q_m	[$10^{-9} \text{ kg/m}^2/\text{s}$]	85.2	73.5	84.0	91.0
c_{sat}	[10^{-3} kg/m^3]	17			
δ_{OC}	[$10^{-9} \text{ m}^2/\text{s}$]	94.6	81.6	93.3	101.1

According to the experiment, the mean value of δ_{OC} is $92.7 \cdot 10^{-9} \text{ m}^2/\text{s}$. The spread in the results shows that the experiment has a standardised uncertainty of $\pm 8.1 \cdot 10^{-9} \text{ m}^2/\text{s}$, i.e. $\pm 8.7\%$.

These values for butanol appear reasonable since studies by Meinighaus (2000a) show that the diffusion coefficient for octane is ca $100 \cdot 10^{-9}$ and for ethyl acetate ca $50 \cdot 10^{-9}$ in "solid concrete".

It is very probable that the diffusion coefficient is highly moisture dependent. During the experiment, the slice of concrete was much drier than what is normal in a concrete floor where alkaline decomposition occurs or has occurred. The humidity in the controlled room where the samples were kept was 65% RH. It is even probable that parts of the concrete slice were drier still since the alcohol used in the cups is hygroscopic. In such a case the implication is that the cups had adsorbed moisture and the actual weight loss due to emission of butanol is greater than that measured.

Earlier studies by Tuutti (1982) show how the diffusion coefficient of oxygen (O_2) changes when the moisture level in concrete changes. It decreases by three orders of magnitude from a value of $ca\ 20 \cdot 10^{-8}$ (m^2/s) at an RH of a few per cent to $0.02 \cdot 10^{-8}$ (m^2/s) at $ca\ 100\%$ RH; see Fig. 4.5. It is likely that the same phenomenon can occur in concrete for every VOC that has properties similar to those of O_2 .

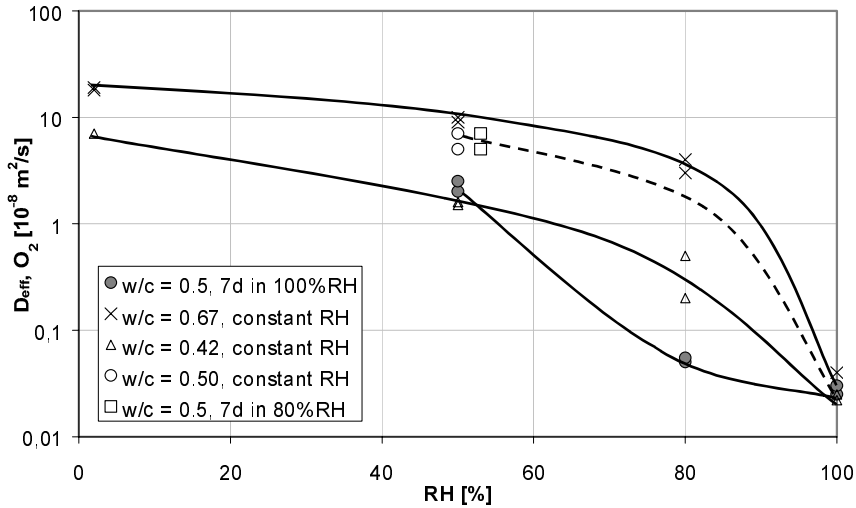


Fig. 4.5. Diffusion coefficient for oxygen, O_2 , as a function of the moisture level in concrete; values from Tuutti (1982).

4.2.5. Theoretical evaluation of δ_{oc} for ethylhexanol

According to an investigation by Nilsson & Luping (1992), the diffusion coefficients of different gases can be compared. The differences in the diffusion coefficients of different gases can be calculated with reference to their molecular weights. "According to the kinetic theory of gases, the diffusivity in materials is inversely proportional to the square root of the molecular weight M ".

For the concrete concerned at the prevailing RH, the value of δ_{oc} for ethylhexanol is set out in Table 4.6.

Table 4.6. Assumptions and results in the investigation of δ_{oc} .

Designation	Unit	Sample	
Quantity		BuOH	EtHx
M	[g/mol]	74	130
Measured δ_{oc} at $ca\ 65\%RH$	[m^2/s]	$92.7 \cdot 10^{-9}$	–
Calculated δ_{oc} (from BuOH)	[m^2/s]		$69.9 \cdot 10^{-9}$

4.3 Determination of effective diffusion coefficient

D_{eff}

In this investigation measurements were made of the quantities of butanol and ethylhexanol that had penetrated into an old test specimen which had been subject to alkaline hydrolysis. The aim of the investigation was to evaluate the effective diffusion coefficient D_{eff} which is a measure of the apparent diffusion capacity of the compound in a material.

4.3.1 Test specimen

This investigation was performed to study the penetration of OC into concrete when the adhesive had been hydrolysed. The test specimen used was cast in conjunction with an earlier study described in Wengholt Johnsson (1995). In the original study this test specimen was designated NSt2. This specimen was selected because in the original study it had large emissions.

The test specimen is identical to those used in this study, described as PF3 (pot) in Subsection 2.2.3. The concrete was an ordinary structural concrete, designated material C4 in Subsection 2.1.1. The adhesive used was a latex adhesive designated adhesive A4 in Subsection 2.1.3. The method of bonding was AT1, laying of the flooring in the wet adhesive with an open time of only a minute or two. The flooring was a homogeneous PVC flooring described as F1 in Subsection 2.1.4. Casting and application of adhesive in Wengholt Johnsson (1995) is the same as the methods described in Chapter 2, without any appreciable deviations.

4.3.2 Sampling

OC in concrete was measured in two stages, followed by analysis. The first stage was extraction of samples from the concrete at different depths and conditioning of these in a sample container. In the second stage sampling was performed in the sample container using the headspace technique in which the OC was captured and concentrated on an adsorbent. This was followed by analysis by gas chromatography (GC-FID).

A core of 25 mm diameter was drilled from the test specimen; see Fig. 4.6. Drilling was carried out without a coolant to prevent OC at the surface of the core from being washed away. Immediately after the core had been extracted, it was wrapped in aluminium foil to prevent emission of OC. The core was then cut at different levels by an abrasive water jet and the pieces were placed into bottles with a specially designed cover, as described in Subsection 2.3.2.

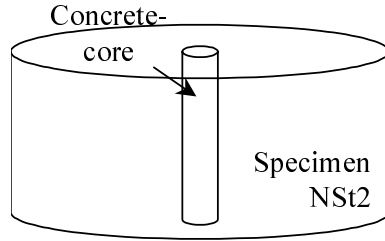


Fig. 4.6. The concrete core analysed in this investigation was taken from test specimen NSt2 from the investigation in Wengholt Johnsson (1995).

In later studies the core was split into "slices" using a hammer and chisel. This does not provide the same opportunity for determining the sizes of the test pieces since the cleavage surface cannot be predicted. This change in method is nevertheless considered to be for the better since it is quicker and less costly than the water jet method.

The mean depths from the surface to the pieces of the core are shown in Fig. 4.7.

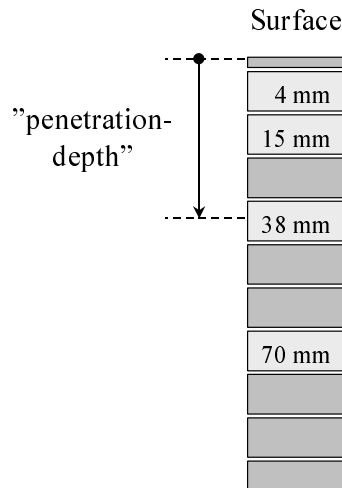


Fig. 4.7. The core was sliced into layers using abrasive water jetting. The mean depth of each slice is given.

The sampling method and the equipment used to measure concentration are based on the headspace technique and concentration on a TENAX tube. Subsequent analysis was performed by GC-FID; see Subsection 2.3.2.

4.3.3. Results

The results in the form of free concentrations of butanol and ethylhexanol per m³ of air are set out in Table 4.7.

Table 4.7. Summary of the concentrations of free OC at different depths in the concrete.

Depth [10 ⁻³ m]	Butanol [kg/m ³ _{air}]	Etylhexanol [kg/m ³ _{air}]
0	43.80·10 ^{-6*}	30.95·10 ^{-6*}
4	38.48·10 ⁻⁶	23.70·10 ⁻⁶
15	24.97·10 ⁻⁶	8.31·10 ⁻⁶
38	7.03·10 ⁻⁶	0.19·10 ⁻⁶
70	0	0.12·10 ⁻⁶

* according to evaluation of D_{eff} by fitting a curve to the error function solution of Fick's second law

4.3.4 Evaluation of D_{eff}

The results of the investigation of OC in the concrete below the flooring show that OC from decomposition of the adhesive had penetrated deep into the concrete. According to Crank (1975), the effective diffusion coefficient D_{eff} can be evaluated with reference to Fick's second law. For such an evaluation it is necessary to know the penetration profile for a specific compound which has formed during incremental changes in a semi-infinite medium.

With the simplification that the surface concentration c_{su} in the test specimen had changed in stages from the initial value 0 to a constant value which then remained unchanged during the whole period, the fundamental incremental change requirement is satisfied. In view of the fact that the concentration at the bottom of the test specimen, 100 mm from the surface, is very low, depth may be considered infinite in this respect.

Fick's second law can then be solved with Equation 4.3 according to Crank (1975); this is the complement to the "error function".

$$c(x, t) = c_s \cdot \left[1 - \operatorname{erf} \left(\frac{x}{2 \cdot \sqrt{D_{\text{eff}} \cdot t}} \right) \right] \quad \left[\text{kg} / \text{m}^3_{\text{air}} \right] \quad (4.3)$$

In Fig. 4.8, the complement to the error function has been calculated for a number of different combinations of D_{eff}·t where t is the time during which the surface concentration was high after the incremental change.

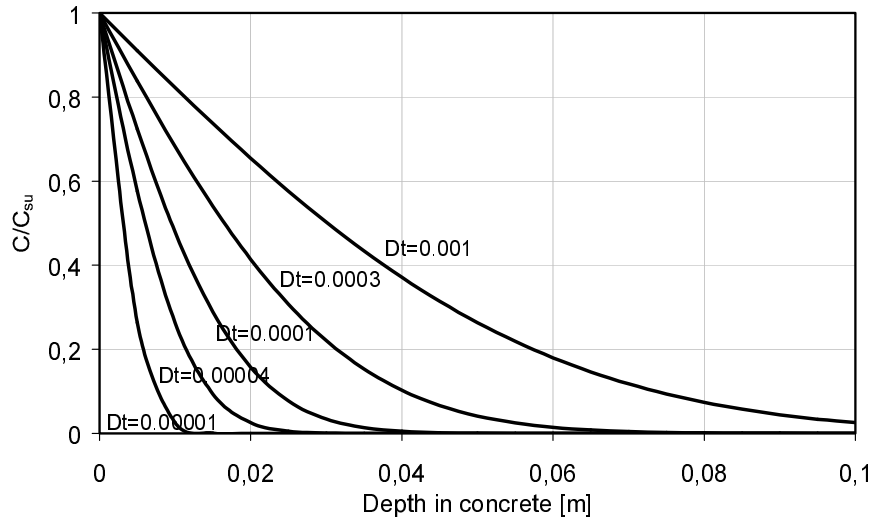


Fig. 4.8. Solution of Fick's second law with the complement to the error function. The figures along the curves are the values of $D_{eff} \cdot t$; see Equation 4.3.

In test specimen NSt2 which was investigated in this experiment there had been high surface concentration of OC for about 2 years. By fitting the measurement results in Table 4.7 to the curves in Fig. 4.8, the values of c_{su} and D_{eff} can be evaluated.

The best fit to the measured values for butanol is plotted in Fig. 4.9. Curve fitting was performed by the method of least squares for differences in concentration at the different depths. Curve fitting for the results for ethylhexanol is shown in Fig. 4.10.

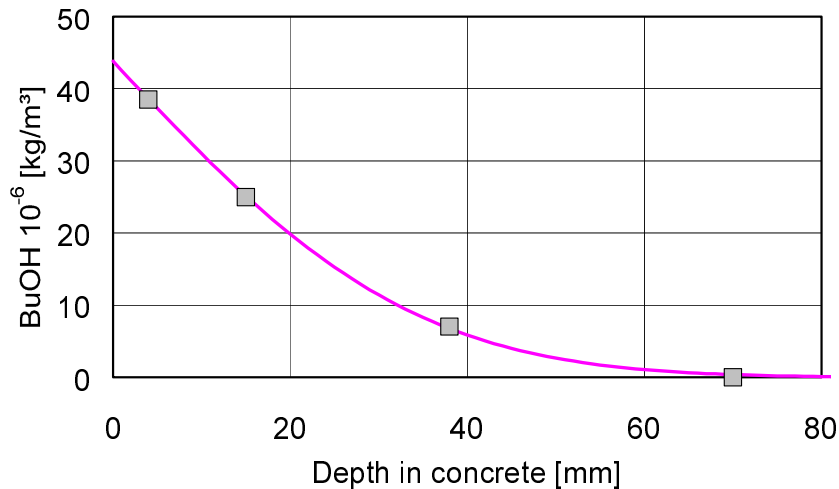


Fig. 4.9. Distribution of butanol in concrete from experiment c1.2 and the best fit of the error function by the method of least squares. $c_{su} = 43.9 \cdot 10^6 kg/m^3$, and $D_{eff} = 5.80 \cdot 10^{-12} m^2/s$.

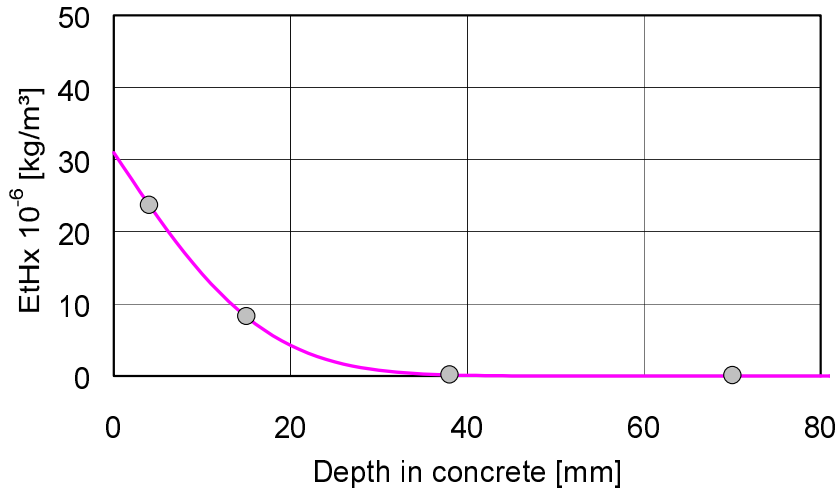


Fig. 4.10. Distribution of ethylhexanol in concrete from experiment c1.2 and the best fit of the error function by the method of least squares. $c_{su} = 30.9 \cdot 10^{-6} \text{ kg/m}^3$, and $D_{\text{eff}} = 1.48 \cdot 10^{-12} \text{ m}^2/\text{s}$.

Surface concentration (c_{su}) for butanol was higher than for ethylhexanol, $43.8 \cdot 10^{-6}$ as against $30.9 \cdot 10^{-6} \text{ kg/m}^3$. This, in combination with the fact that butanol has the greater penetration depth, means that D_{eff} is different for the different decomposition products. The effective diffusion coefficient D_{eff} is $5.80 \cdot 10^{-12} \text{ (m}^2/\text{s)}$ for butanol and $1.48 \cdot 10^{-12}$ for ethylhexanol.

If the assumption regarding incremental change is not correct, the surface concentration (c_{su}) which has been calculated may be seen as an effective mean value. The test specimen was approximately two years old when the core was drilled out. The concentration below the flooring may have changed during these two years. The concrete may have dried out through the flooring, so that the reaction and thus the production of OC had ceased.

The diffusion coefficient (D_{eff}) which has been evaluated may also be a mean value for variable moisture conditions. The rate of penetration of OC down into the concrete has probably been affected by the redistribution and drying of moisture in the concrete.

4.4 Field measurements of effective diffusion coefficient D_{eff}

In order to verify the laboratory measurements of OC which has penetrated into the concrete, four field measurements were carried out. Sampling with the TENAX tube and analysis with GC-FID were performed in the same way as in the laboratory measurements. The floors selected all had PVC flooring bonded to concrete and exhibited signs of alkaline hydrolysis of the adhesive.

Sampling was carried out by experienced research engineers from two investigation consultancies in Stockholm.

Sampling in floor No 3 was performed by research engineer Aime Must of BARAB and the analysis by tekn.dr. Jan Kristiansson of Chemik Lab AB. The conditioning procedure was different from that used at Chalmers. During conditioning of the headspace, elevated temperature and RH were used. It was not possible to evaluate the maximum concentration below the flooring at room temperature. The difference is not considered to have affected the results.

Sampling at the other three floors was performed by different employees of AK-konsult Indoor Air AB. Subsequent conditioning of the test pieces in the "bottle" and analysis of the TENAX tube with GC-FID were carried out at the Department of Building Materials, Chalmers University of Technology.

The results of analysis in the form of penetration profiles for butanol and ethylhexanol from the four floors are set out in Fig. 4.11 – 4.18. The plots which are shown in outline in Fig. 4.12, 4.14, 4.17 and 4.18 were considered to be unreasonable. This may be due to faulty handling or leakage during sampling or the subsequent conditioning and analysis. These measurement results are presumably erroneous, and they were therefore not used in evaluating c_{su} and D_{eff} .

The results of the investigations are summarised in Table 4.8.

Table 4.8. Summary of concentrations of OC below the flooring, c_{su} , and the effective diffusion coefficient, D_{eff} , which were measured in the field on damaged floors and on the test specimen in Section 4.3. W/c ratio in all samples ca 0.7, with the exception of sample No 1 where it is ca 0.5.

Floor	Age of damage [years]	Butanol		Ethylhexanol	
		c_{su} [10^{-6} kg/m ³]	D_{eff} [10^{-12} m ² /s]	c_{su} [10^{-6} kg/m ³]	D_{eff} [10^{-12} m ² /s]
1*	1	10.0	16	5.8	19
2	3.5	49	4.1	3.3	3.6
3	6	–	4.9	–	6.1
4	10	2	5.2	0.9	8.4
Lab	2	43.9	5.8	30.9	1.5

* Concrete with w/c ratio = 0.5.

Note that in floor No 2 the difference between c_{su} for butanol and ethylhexanol is large, while in other floors it is small. There is not enough information available regarding the floors for these differences to be explained. It is likely that factors such as moisture level, the impermeability of the floorings and the concrete grade are important.

4.4.1 Floor No 1 – ca 1 year old emission damage

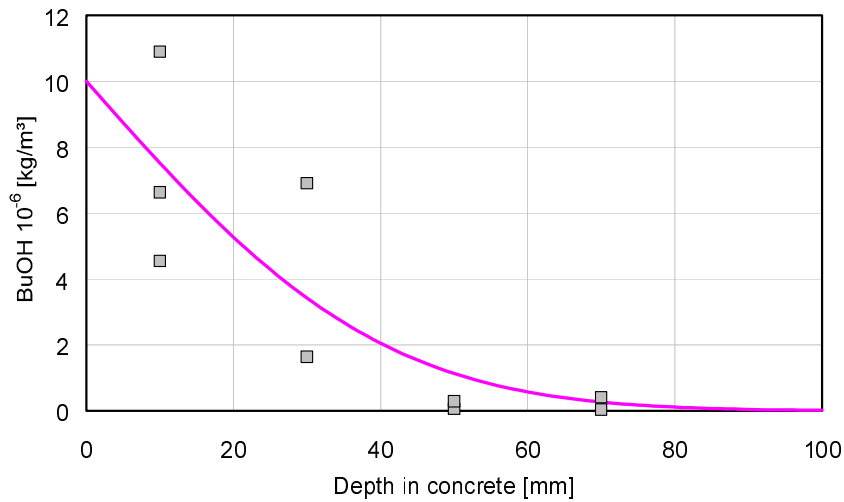


Fig. 4.11. Distribution of butanol in concrete from field measurements on ca 1 year old damage. The curve is the best fit to the error function with the method of least squares. $C_s = 10.0 \cdot 10^{-3} \text{ g/m}^3$, $D = 16 \cdot 10^{-12} \text{ m}^2/\text{s}$.

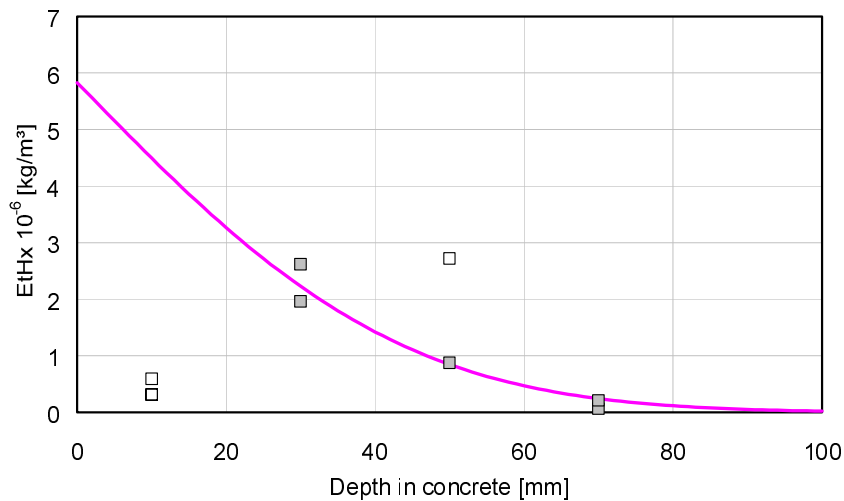


Fig. 4.12. Distribution of ethylhexanol in concrete from field measurements on ca 1 year old damage. The curve is the best fit to the error function with the method of least squares. $C_s = 5.8 \cdot 10^{-3} \text{ g/m}^3$, $D = 19 \cdot 10^{-12} \text{ m}^2/\text{s}$.

4.4.2 Floor No 2 – ca 3.5 year old emission damage

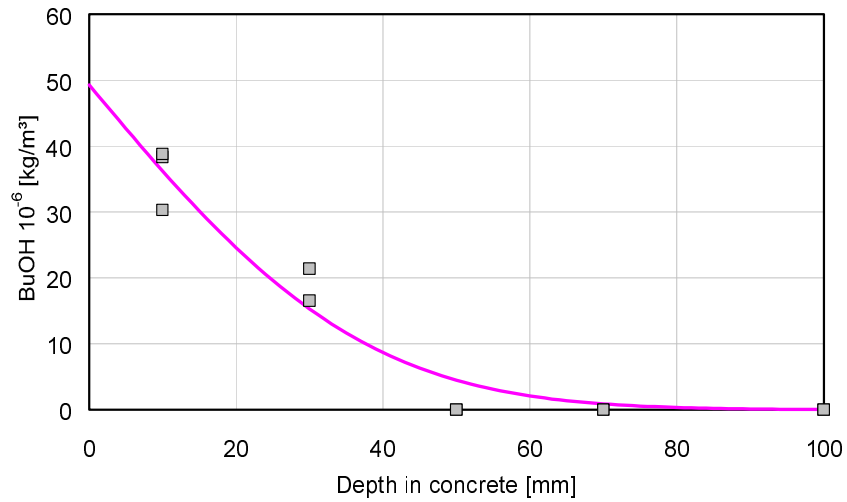


Fig. 4.13. Distribution of butanol in concrete from field measurements on ca 3.5 year old damage. The curve is the best fit to the error function with the method of least squares. $C_s = 49.0 \cdot 10^{-3} \text{ g/m}^3$, $D = 4.1 \cdot 10^{-12} \text{ m}^2/\text{s}$.

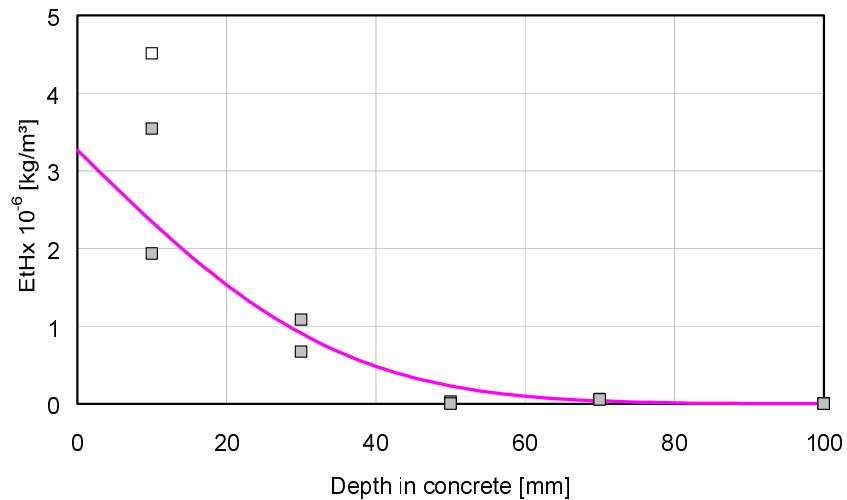


Fig. 4.14. Distribution of ethylhexanol in concrete from field measurements on ca 3.5 year old damage. The curve is the best fit to the error function with the method of least squares. $C_s = 3.3 \cdot 10^{-3} \text{ g/m}^3$, $D = 3.6 \cdot 10^{-12} \text{ m}^2/\text{s}$.

4.4.3 Floor No 3 – ca 6 year old emission damage

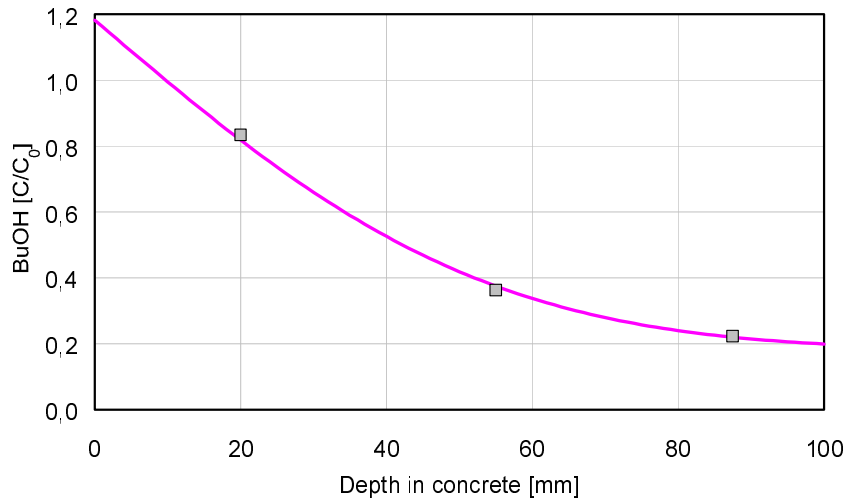


Fig. 4.15. Distribution of butanol in concrete from field measurements on ca 6 year old damage. The curve is the best fit to the error function with the method of least squares. $D = 4.86 \cdot 10^{-12} \text{ m}^2/\text{s}$. And background of 0.2.

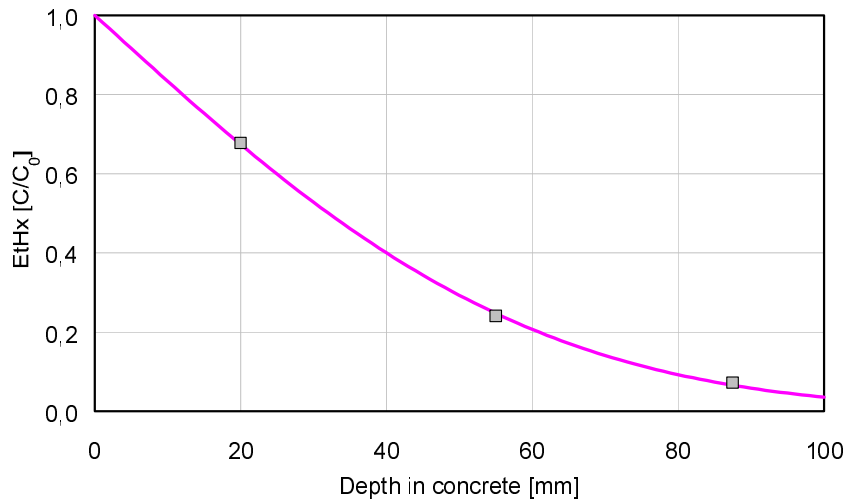


Fig. 4.16. Distribution of ethylhexanol in concrete from field measurements on ca 6 year old damage. The curve is the best fit to the error function with the method of least squares. $D = 6.13 \cdot 10^{-12} \text{ m}^2/\text{s}$.

4.4.4 Floor No 4 – ca 10 year old emission damage

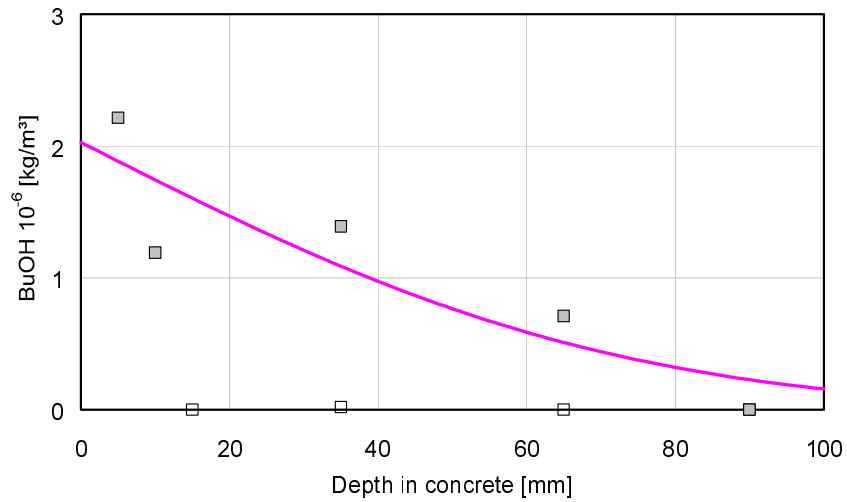


Fig. 4.17. Distribution of butanol in concrete from field measurements on ca 10 year old damage. The curve is the best fit to the error function with the method of least squares. $C_s = 2 \cdot 10^{-3} \text{ g/m}^3$, $D = 5.2 \cdot 10^{-12} \text{ m}^2/\text{s}$.

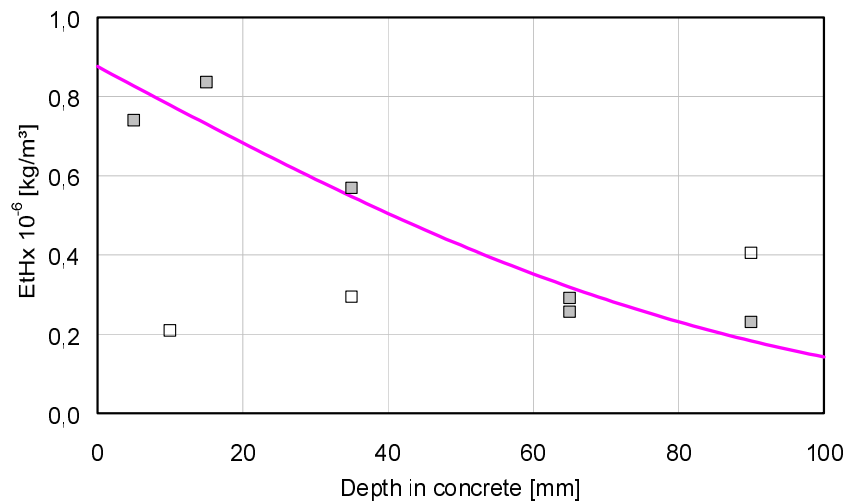


Fig. 4.18. Distribution of ethylhexanol in concrete from field measurements on ca 10 year old damage. The curve is the best fit to the error function with the method of least squares. $C_s = 0.9 \cdot 10^{-3} \text{ g/m}^3$, $D = 8.4 \cdot 10^{-12} \text{ m}^2/\text{s}$.

5 Studies of the significance of moisture status for emission

When impermeable floorings are bonded directly to concrete floors, alkaline hydrolysis of the adhesive can take place. The moisture level in the concrete exerts an influence on this process. In this chapter, a description is given of five investigations of the moisture status of concrete and the influence of the moisture status on the emission factor EF.

A description is first given of an investigation of the absorption of moisture from the adhesive at the surface of the concrete, followed by an investigation of the quantity of moisture of adhesive that evaporates in conjunction with different methods of applying the adhesive. Finally, there is an account of three investigations of emission from test specimens in which various parameters associated with moisture of adhesive and other surface moisture were varied.

5.1 Measurement of RH at the concrete surface

The method used in the study to measure moisture of adhesive is originally described in Sjöberg (1997). It is a development of a method that was originally employed in studying the moisture status of the surface layer of concrete when screeds are applied; Nilsson (1984).

5.1.1 Test specimens

The test specimens, materials and the procedure applied in production are described in Chapter 2. The test specimen used was the "bucket" (PF4) which was cast with different concrete grades, C1, C3 and C4, and the flooring F1 which was bonded with adhesive A2. The method of applying the adhesive was AT1, with an open time of only a minute or two.

5.1.2 Moisture measurement

A day or two before the adhesive was applied, the RH probes were mounted in the measuring tubes of the test specimens. The rubber plug was removed and the RH probe was placed in the measuring tube where it was sealed with an inflatable rubber ring to prevent ingress of ambient air. When the RH probe was mounted, conditions in the tube were changed since air is forced out when the probe is inserted. When the measured values stabilised after the probes had reached equilibrium at the depths concerned, the flooring was bonded to the concrete.

Measurements in experiment No 2 were made with the hand instrument as described in Method No 1 in Subsection 2.3.1. In the other experiments the temperature and RH were logged every 5 minutes according to Method No 2. The values obtained were converted into RH with reference to the calibration curves for each measuring probe.

5.1.3 Results

The results from the three measurement series are presented as RH at 20°C. The measurements were made at 20°C, and therefore no corrections were necessary. Any correction of RH measured at a temperature other than 20°C can be made according to Nilsson (1987).

Experiment No 1, application of 300 g/m² moisture of adhesive to concrete C1

When the flooring was bonded to concrete C1, 33 g of adhesive was applied to the test specimen. This is equivalent to ca 300 g of moisture of adhesive per m² of concrete surface. A litre of adhesive is normally sufficient for 5 m² of floor surface, which corresponds to 80 g moisture of adhesive per m².

RH probe HMP 44 and the datalogger were used for the measurement. After the probes had been mounted, the temperature and RH were automatically logged every 5 minutes. This is described in detail as Method No 2 in Subsection 2.3.1.

The values for the whole measurement sequence for RH are plotted in Fig. 5.1.

The temperature measurement shows a stable temperature of 20°C during the measurement period. The results are described in detail in Sjöberg (1998a).

The measuring tubes for the four RH probes were located at depths of 11, 17, 19 and 34 mm in this test specimen.

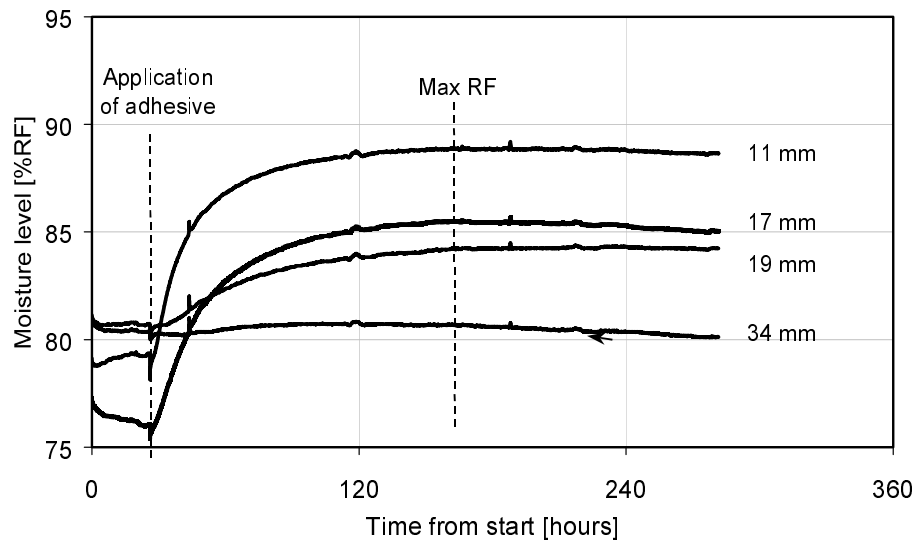


Fig. 5.1. Change in moisture level at different depths after a PVC flooring was bonded to concrete C1 of w/c ratio = 0.32. The moisture of adhesive introduced is ca 300 g/m².

Experiment No 2, application of 90 g/m² moisture of adhesive to concrete C3

When the flooring was bonded to concrete C3, 10 g of adhesive was applied to the test specimen. This is equivalent to ca 90 g of moisture of adhesive per m² of concrete surface.

RH probe HMP 36 and hand instrument HMI 31 were used for the measurement. After the probes had been mounted, readings were taken manually several times per day. This is described in detail as Method No 2 in Subsection 2.3.1.

The values for the whole measurement sequence for RH are plotted in Fig. 5.2.

The temperature measurement shows a stable temperature of 20°C during the measurement period. The results are described in detail in Sjöberg (1998a).

The measuring tubes for the six RH probes were located at depths of 3, 8, 13, 21, 41 and 84 mm in this test specimen.

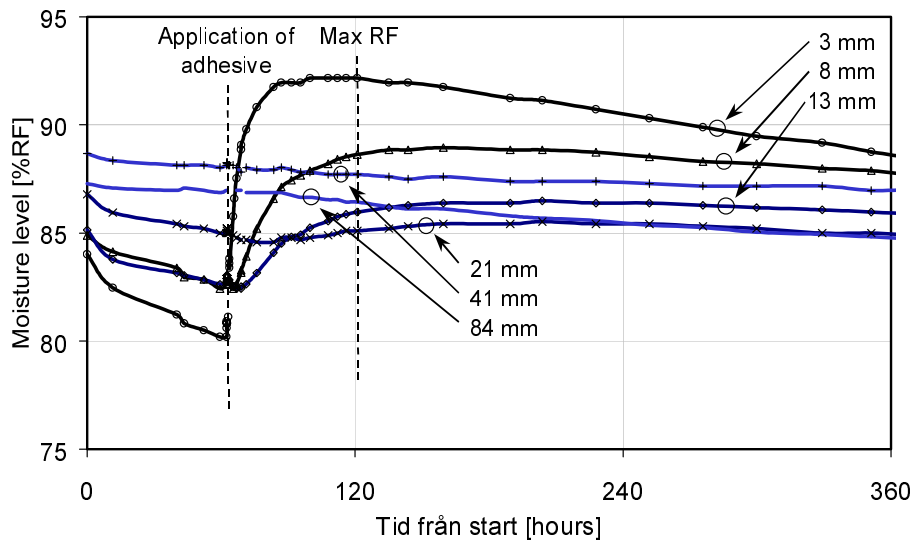


Fig. 5.2. Change in moisture level at different depths after a PVC flooring was bonded to concrete C3 of w/c ratio = 0.42. The moisture of adhesive introduced is ca 90 g/m².

Experiment No 3, application of 230 g/m² moisture of adhesive to concrete C4

When the flooring was bonded to concrete C4, 25 g of adhesive was applied to the test specimen. This is equivalent to ca 230 g of moisture of adhesive per m² of concrete surface.

RH probe HMP 44 and the datalogger were used for the measurement. After the probes had been mounted, the temperature and RH were logged automatically every 5 minutes. This is described in detail as Method No 2 in Subsection 2.3.1.

The values for the whole measurement sequence for RH are plotted in Fig. 5.3.

The temperature measurement shows a stable temperature of 20°C during the measurement period. The results are described in detail in Sjöberg (1998a).

The measuring tubes for the four RH probes were located at depths of 5, 10, 18 and 34 mm in this test specimen.

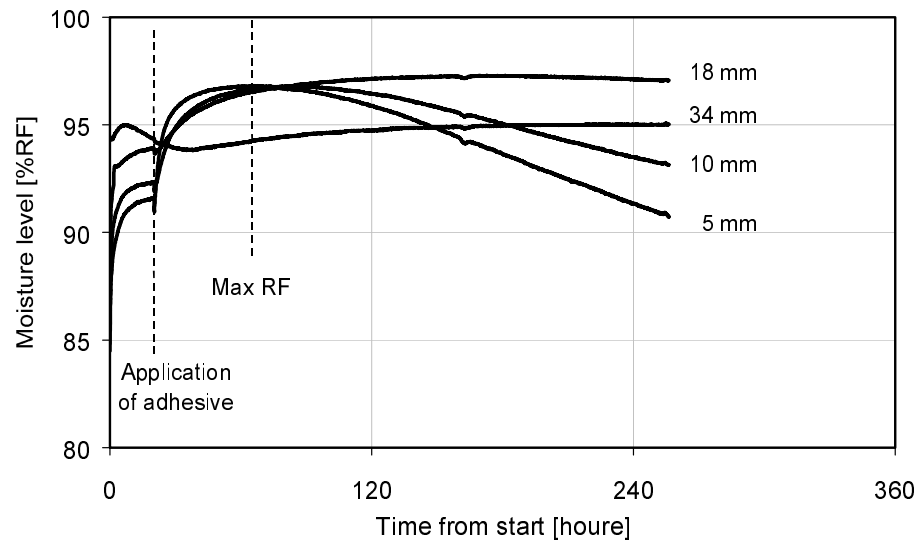


Fig. 5.3. Change in moisture level at different depths after a PVC flooring was bonded to concrete C4 of w/c ratio = 0.66. The moisture of adhesive introduced is ca 230 g/m².

5.1.4 Evaluation

When the RH measurements were evaluated, the total quantity of moisture that had penetrated was calculated and compared with the applied quantity.

The quantity of moisture of adhesive that had penetrated into the concrete can be determined by calculations based on the increase in moisture level. By integrating the increase in RH over the penetration depth and multiplying this by the moisture capacity, the quantity of moisture that had penetrated can be determined using Equation 5.1. This method is described in detail in Sjöberg (1998a).

$$\Delta W_{tot} = \frac{\partial w}{\partial \phi} \cdot \int_0^L \Delta RH \cdot dx \quad \left[\text{kg} / \text{m}^3_{\text{concr}} \right] \quad (5.1)$$

The total increase in the moisture content of concrete is equal to the moisture capacity of the concrete multiplied by an integral. The integral is equal to the sum of the change in RH at every depth. In other words, the integral is equal to the area between the different RH profiles, as shown in Fig. 5.4.

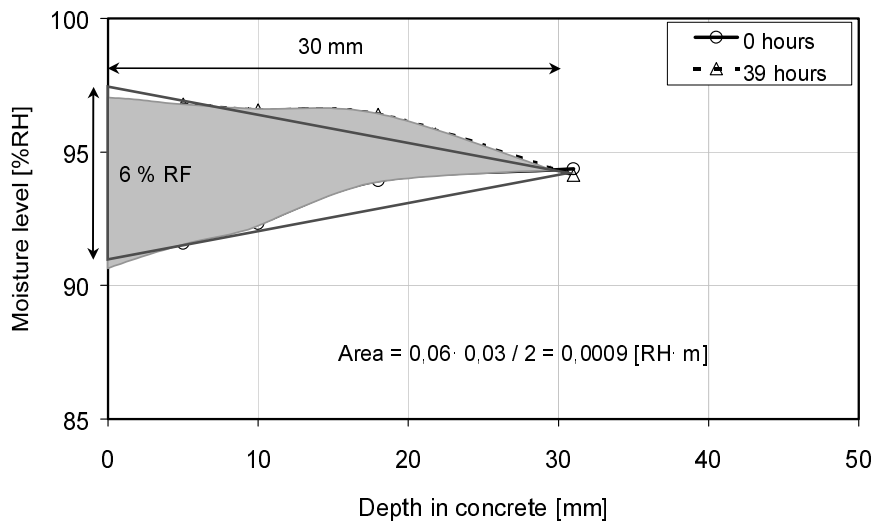


Fig. 5.4. Calculation of the size of the area for the experiment with w/c ratio = 0.66 in order to determine the total quantity of moisture that had penetrated into the concrete.

The quantities of moisture which had been introduced into the concrete in the investigation are set out in Table 5.1. The summary also contains the total quantity of moisture (w_{tot}) that had penetrated during all the experiments, calculated as shown in Fig. 5.4.

Table 5.1. Applied moisture of adhesive and total measured quantity of moisture (w_{tot}) which had penetrated.

Experiment W/C ratio	Moisture of adhesive [10^{-3} kg/m ²]	Area [10^{-3} RH·m]	RH level [%]	dw/dRH [kg/m ²]	w_{tot} [10^{-3} kg/m ²]
0.32	300	0.47	80-95	>360	>170
0.42	91	0.26	80-95	360	94
0.66	230	0.90	92-97	300	270

As seen in Table 5.1, some of the moisture of adhesive was not recovered as the total quantity of moisture (w_{tot}) that had penetrated; see also Fig. 5.5. The reason that moisture is "missing" in the experiment on C1 (w/c 0.32) may be that the moisture capacity used in evaluation was too small, or that the estimated area in the diagram underestimates the moisture content of the concrete outside the outermost plot. It is also possible that a large proportion of the moisture is still contained in the adhesive.

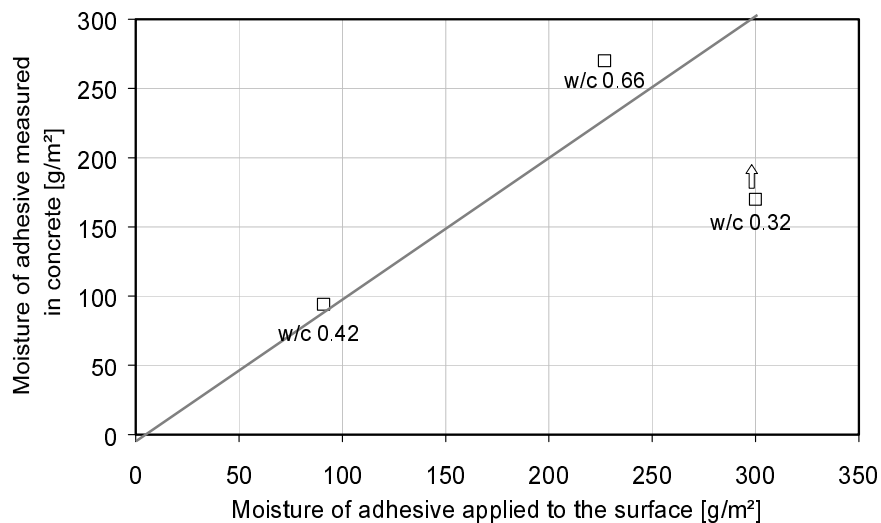


Fig. 5.5. Relationship between applied and measured moisture of adhesive in the experiment.

5.2 Evaporation of moisture of adhesive

When a flooring is bonded to a substrate, the open time (OT) is an important parameter. The term refers to the period during which the adhesive is allowed to "dry", from the time it is spread on the substrate to the time when the flooring is laid. During the open time there is an opportunity for the moisture of adhesive to evaporate into the room air. If the substrate is absorbent, some of the moisture of adhesive will also be redistributed in this.

In this investigation, the weight loss due to evaporation of moisture from a film of adhesive over a period of one hour was measured and evaluated. This investigation was originally published in Sjöberg & Wengholt Johnsson (1999).

5.2.1 Test specimens

In this investigation, the test specimens in two experiments were a steel plate to represent a non-absorbent substrate, and in another two a piece of plasterboard to represent an absorbent substrate. The investigation was performed in a laboratory at ca 20°C and 50% RH.

5.2.2 Weighing

The plate or board was placed in a weighing machine and its weight was noted. About 30 g of adhesive was then uniformly applied (ca 5 m²/l) to it. The new weight including the adhesive was noted. Readings were then made at frequent intervals for an hour.

5.2.3 Results

The results in the form of moisture of adhesive that had evaporated during an open time of one hour are plotted in Fig. 5.6. When 100% of the moisture of adhesive had evaporated, all water in the adhesive, i.e. ca 30% of the total weight of adhesive, had gone.

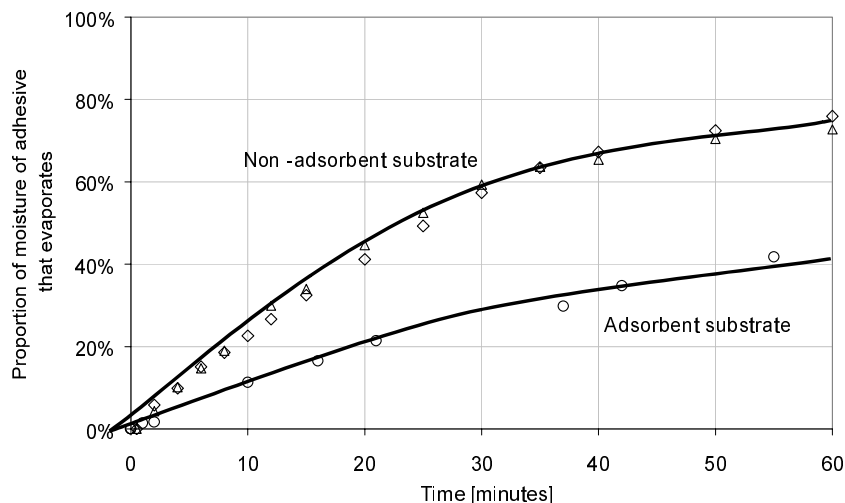


Fig. 5.6. Proportion of moisture of adhesive that evaporates during the first hour on different types of substrate. Sjöberg & Wengholt Johnsson (1999).

5.2.4 Evaluation

The quantity of moisture remaining in the adhesive which can be absorbed into the substrate can be calculated from Fig. 5.6. The quantities of moisture that remain after different waiting times when the adhesive is applied to an absorbent substrate are set out in Table 5.2. The original moisture content of the adhesive (kg/m^3) can be calculated from the manufacturer's data concerning the density and solids content of the adhesive.

Similar calculations of the remaining quantities of moisture on a non-absorbent substrate are set out in Table 5.3.

Table 5.2 Absorbent substrate. Remaining quantities of moisture of adhesive for 5 m²/l of adhesive (4 m²/l in brackets) after different open times (in minutes). The original quantity of water can be calculated as density x (1 – solids content (%)).

OT minute	%	Remaining quantity of moisture [10-3 kg/m ²]				
		300	350	400	450	500
0	100	60 (75)	70 (88)	80 (100)	90 (113)	100 (125)
2	98	59 (73)	68 (86)	78 (98)	88 (110)	98 (125)
5	94	57 (71)	66 (83)	75 (94)	85 (107)	94 (118)
10	89	53 (67)	62 (78)	71 (89)	80 (101)	89 (111)
15	84	50 (63)	59 (74)	67 (84)	76 (95)	84 (105)
30	72	43 (54)	51 (64)	58 (72)	65 (82)	72 (90)
45	64	39 (48)	45 (56)	51 (64)	58 (73)	64 (80)
60	59	35 (44)	41 (52)	47 (59)	53 (66)	59 (73)
120	46	28 (34)	32 (40)	37 (46)	41 (52)	46 (57)

Table 5.3 Non-absorbent substrate. Remaining quantities of moisture of adhesive for 5 m²/l of adhesive (4 m²/l in brackets) after different open times (in minutes). The original quantity of water can be calculated as density x (1 – solids content (%)).

OT minute	%	Remaining quantity of moisture [10-3 kg/m ²]				
		300	350	400	450	500
0	100	60 (75)	70 (88)	80 (100)	90 (113)	100 (125)
2	95	57 (71)	66 (84)	76 (95)	85 (107)	95 (119)
5	88	53 (66)	61 (77)	70 (88)	79 (99)	88 (109)
10	77	46 (58)	54 (68)	62 (77)	70 (87)	77 (97)
15	67	40 (50)	47 (59)	53 (67)	60 (75)	67 (83)
30	42	25 (31)	29 (37)	33 (42)	37 (47)	42 (52)
45	31	19 (23)	22 (27)	25 (31)	28 (35)	31 (39)
60	26	15 (19)	18 (23)	21 (26)	23 (29)	26 (32)
120	18	11 (14)	13 (16)	15 (18)	16 (21)	18 (23)

5.3 Influence of method of application and type of adhesive

The aim of this investigation which was originally published in Fritsche et al (1997) was to make a detailed study of how emission from a flooring on a substrate of self-desiccating concrete is affected by different conditions. Examples of such conditions are method of application and type of adhesive, type of cement and drying process.

5.3.1 Test specimens

Nine test specimens PF3 were cast with concrete C3 as described in Subsection 2.1.1. These test specimens were turned upside down prior to final vibration during casting. The next day the moulds were turned the right way up and the stainless steel plates were removed from the surfaces. The surfaces were now covered with two layers of aluminium foil to prevent premature drying of the surface. One test specimen, however, was not covered with foil but was allowed to dry directly. The test specimens were stored in a controlled climate room (+20°C, 50% RH) until the time the floorings were laid. The aluminium foil was removed 28 days after casting, and two days later the flooring was bonded. In most cases a homogeneous PVC flooring and a latex adhesive were used; see Table 5.4, Experimental setup.

In experiments d2.01 and d2.02 the floorings were laid loose on the concrete. The floorings were of different types and makes, and were kept in place with a steel ring.

Samples d2.1 and d2.2 were made with the same materials, open times and bonding method as in Wengholt Johnsson (1995). The open time during application of the adhesive was ca 15 minutes before the flooring was fixed to the concrete surface. In experiment d2.3 a "solventless" adhesive was used. The method of applying the adhesive was varied in experiments d2.4 – 6; in experiment d2.4 the adhesive was applied by single spread, to the flooring instead of the concrete. In experiment d2.5 the flooring was bonded by contact adhesive, i.e. the flooring was laid directly into the wet adhesive, immediately withdrawn and finally laid on the concrete when the adhesive on both the flooring and concrete had dried to a tacky state. The flooring in experiment d2.6 was laid in the wet adhesive, i.e. the flooring was laid directly into the wet adhesive without any open time.

The concrete surface of the sample in experiment d2.7 was not covered with aluminium foil but the concrete was allowed to dry directly. In experiment d2.8 the aluminium foil was removed 14 days after casting. The flooring was bonded in these experiments in the same way as in the reference samples, 30 and 16 days respectively after drying commenced. The only difference between d2.1 and d2.2 (reference samples) and experiment d2.9 was that in the latter experiment sulphate resisting low alkali cement was used instead of standard cement. This was done to study the effect of lower alkali content in the concrete.

5.3.2 *Moisture and emission measurements*

The moisture status of the test specimens was measured several times during the curing period. When the adhesive was applied the moisture level was approximately 84% RH in all test specimens with the exception of d2.9 which had a moisture level of 94% RH; see Table 5.5 and Fig. 5.7. The moisture level was also measured one week after the adhesive had been applied and once more about 20 weeks later. RH measurements were made with RH probes which were inserted into measuring tubes at a depth of 4 cm in the test specimen, one day before a reading was made. The method is described in Subsection 2.3.1.

Emissions from the test specimens were measured on two occasions. The first was about 7 weeks, and the second about 26 weeks, after the flooring had been laid. Sampling was performed by the method described in Subsection 2.3.3, with FLEC and TENAX tube. The subsequent analysis of the TENAX tube was performed with GC-FID at the Department of Chemical Environmental Science, Chalmers University of Technology.

5.3.3 *Results*

The results in the form of the emission factor EF, 7 and 26 weeks after the flooring had been laid, are set out in Table 5.4. The results from all the RH measurements in the investigation are set out in Table 5.5 and in Fig. 5.7.

Table 5.4 Experimental setup and the results of investigation d2.

Experiment	.01	.02	.1	.2	.3	.4	.5	.6	.7	.8	.9
Bonding method	–	–	1	1	1	1 [♥]	4	1 [▲]	1	1	1
Open time	–	–	15	15	15	15	60	0	15	15	15
Flooring	F1	F1	F1	F1	F1	F1	F1	F1	F1	F1	F1
Adhesive	–	–	A4	A4	A1	A4	A4	A4	A4	A4	A4
Concrete	C3	C3	C3	C3	C3	C3	C3	C3	C3 [*]	C3 [*]	C3 [♣]
Designation	VIa	VIb	I	Ie	II	IIIa	IIIb	IIIc	IVa	IVb	V
BtOH 7w	< 2	4	17	203	395	371	7	1941	12	23	26
BtOH 26w	< 2	< 2	8	32	20	55	24	280	9	16	21
EtHx 7w	< 2	9	28	5	134	83	18	326	38	39	16
EtHx 26w	7	5	15	44	100	72	19	315	4	19	32

♥ Adhesive on flooring
 ▲ Flooring laid into wet adhesive
 ♦ Drying for 2 and 4 weeks respectively
 ♣ Sulphate resisting low alkali cement

Table 5.5 RH in test specimens at 40% of the depth at different times after casting. Investigation d2.

Experiment	8 days	15 days	24 days	30 days*	37 days	169 days
d2.1	84	83	83	84	83	77
d2.2	—	—	—	—	—	—
d2.3	—	—	—	—	—	—
d2.4	—	—	—	—	—	—
d2.5	—	—	—	—	—	—
d2.6	85	83	83	83	83	79
d2.7	83	82	83	82	82	76
d2.8	83	83	83	83	82	76
d2.9	99	96	96	94	92	82

* Bonding of PVC flooring

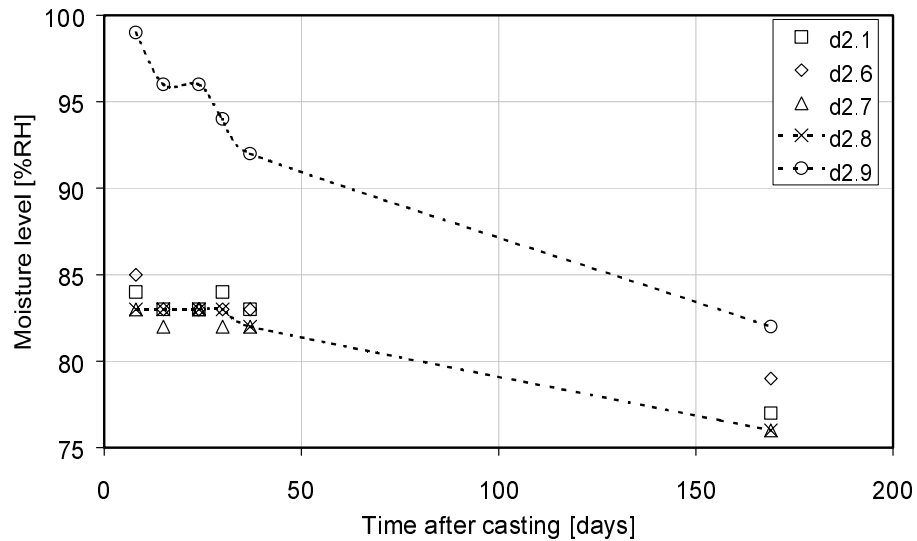


Fig. 5.7 RH in test specimens at 40% of the depth at different times after casting. Investigation d2.

5.3.4 Evaluation

Influence of drying of concrete surface and type of cement

When EF from test specimens that were allowed to dry for 2 and 4 weeks (d2.7 and d2.8 respectively) and from the reference samples (d2.1 and d.2.2) is compared, no major difference can be seen apart from one single value for butanol at 7 weeks from experiment d2.2. This reading may be erroneous since the values in the twin sample d2.1 are not equally high. Nor did a different cement type, with a lower alkali content, change emission appreciably (d2.9).

The reason that there is no difference may be that the moisture level at the time the adhesive was applied was too low, about 84% for all test specimens with the exception of d2.9 in which the moisture level according to Table 5.5 was 94%. The rapid drying may be due to self desiccation of the concrete. The reason that elevated emissions were not measured from d2.9 in spite of the high moisture level may be that this sample had a different cement, or that moisture leaked out between the flooring and the steel mould before it was redistributed and gave rise to alkaline hydrolysis of the flooring adhesive.

Emissions when the flooring is loose laid

The comparisons made here show that the loose laid floorings were not affected by the concrete. Two different types of PVC floorings were laid loose, and the values of EF have been compared with their primary emissions in Fig. 5.8.

The flooring in experiment d2.01 is a homogeneous PVC flooring (M1) intended for bonding. The EF measured shows that it emits only a small proportion of what is quoted as primary emission; see Fig. 5.8.

The flooring in experiment d2.02 is a heterogeneous PVC flooring (M4) with a backing of compressed polyester fibre, intended for loose laying. The polyester fibres on the back resemble felt. Emission measurements show that this flooring also emits only a small proportion of what is quoted as primary emission.

Since EF from the loose laid floorings is low, even lower than the values of primary emission quoted by the manufacturers, it may be assumed that in these floorings there had been no decomposition. The reason that EF is low in the investigation may be that the manufacturers measure primary emission 4 and 26 weeks after manufacture. The floorings used in the investigation were older, and primary emission may have ceased even though they had been packed in several layers of aluminium foil since manufacture.

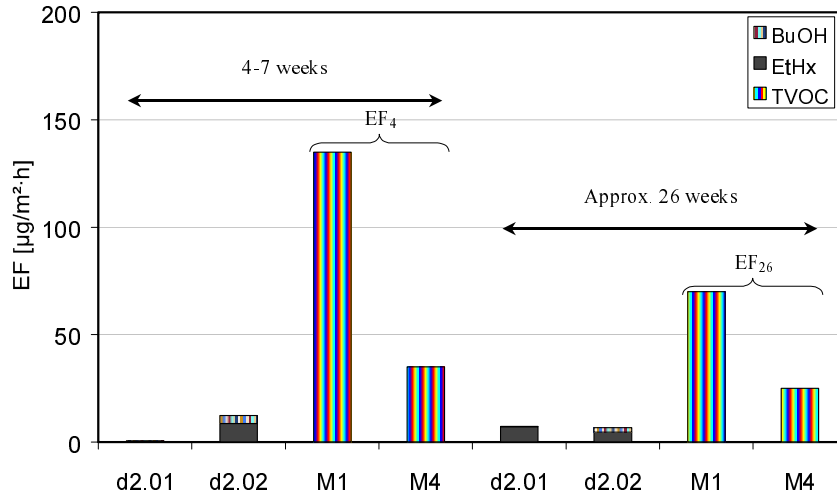


Fig. 5.8 Emissions from loose laid floorings after 7 and 26 weeks and values of primary emission quoted by the manufacturers. EF_4 and EF_{26} denote primary emissions from the floorings 4 and 26 weeks after manufacture. d2.01 is flooring M1, and d2.02 is flooring M4.

Influence of method of application and type of adhesive

The comparison made here shows the significance for emission from the finished floor system of the method used to apply the adhesive, and the significance of the type of adhesive. The comparison is made for EF from seven of the experiments in the investigation.

The bars at the left of Fig. 5.9 and 5.10 show high EF from the test specimens. In experiment d2.6 the flooring was laid into the wet adhesive on the test specimen, and this may explain the high EF. According to Fig. 5.6, only a small proportion of the moisture of adhesive could evaporate before the flooring was laid down.

In the next experiment (d2.4) the adhesive was applied to the flooring, and the open time was ca 15 minutes. In this experiment also, the emission was higher than in the references (see below). The reason may be that there is no opportunity for the moisture of adhesive to be absorbed into and to be redistributed inside the concrete during the open time. According to Fig. 5.6, approx. 35% of the moisture of adhesive had however evaporated after 15 minutes on a non-absorbent substrate, and only about half as much on an absorbent substrate.

The twin samples in experiments d2.2 and d2.1 may be regarded as references in this investigation. Compared with the loose laid flooring, decomposition has occurred in these samples also. The high value of butanol at the first measurement on d2.2 may be due to an erroneous reading.

In experiment d2.5 the flooring was laid by pressure sensitive bonding as described in Subsection 2.1.3. Emission from these test specimens is low. According to Fig. 5.6, 40% of the moisture of adhesive may have evaporated before the flooring was laid.

The loose laid flooring in experiment d2.1 had low primary emissions.

The bars at the right of Fig. 5.9 and 5.10 are from an experiment with a different adhesive (A1) which is based on broadly the same polymers as the reference adhesive (A4). Conditions were otherwise the same as in the references d2.2 and d2.1, but EF was higher. The difference demonstrates that apparently similar materials may give rise to different values of EF.

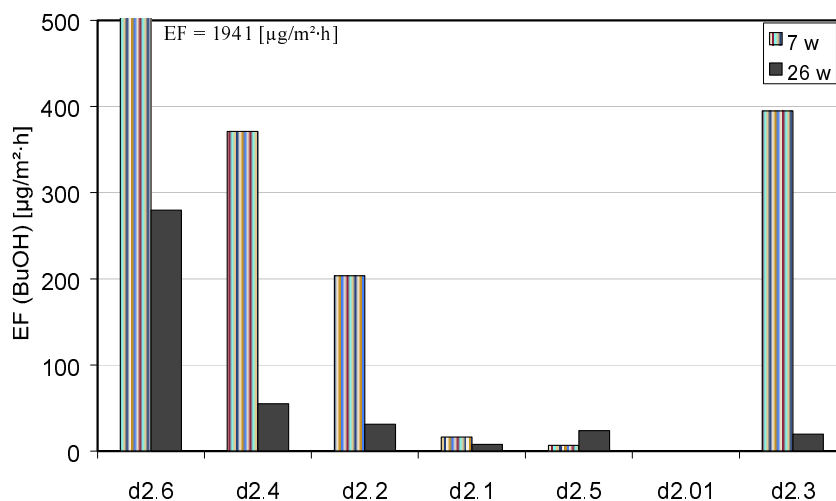


Fig. 5.9 Comparison of emissions of butanol from floor systems bonded by different methods. Flooring laid into wet adhesive (d2.6), adhesive spread on flooring (d2.4), adhesive spread on concrete (d2.2 and d2.1), pressure sensitive bonding (d2.5) and loose laying (d2.01). Finally, d2.3 was bonded to the concrete with a different adhesive (L1).

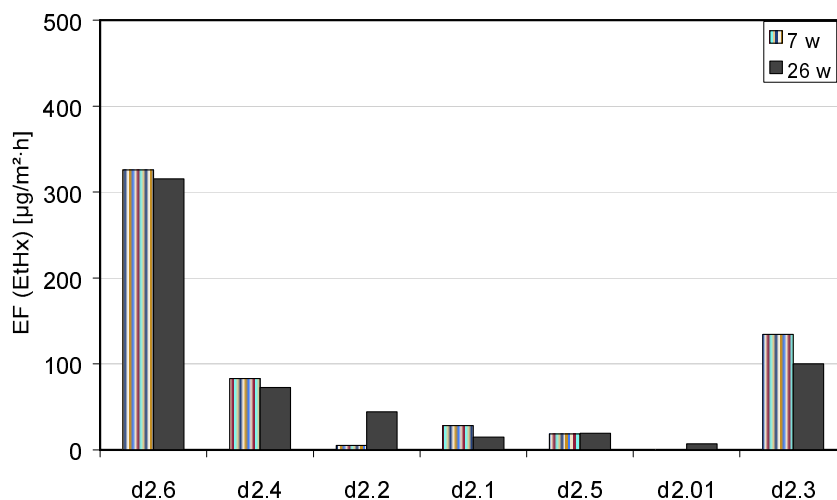


Fig. 5.10 Comparison of emissions of ethylhexanol from floor systems bonded by different methods. Explanation of the bars is given in fig 5.9.

5.4 The influence of screed

In this investigation, a comparison was made of emissions when PVC floorings were bonded to test specimens with seven different kinds of screed. Previous investigations by Wengholt Johnsson (1995) showed that a screed had a favourable effect when PVC floorings were bonded to self-desiccating concrete (low w/c ratio).

5.4.1 Test specimens

Eight test specimens PF3 (pot) were cast with concrete C3 as described in Subsection 2.1.1. A space was left between the surface of the concrete and the top of the mould to accommodate the thickness of the layer of screed to be spread later on. The test specimen for experiment d3.0 which had no screed was turned upside down on a steel plate and vibrated. The next day it was turned the right way up and covered with plastic. The other test specimens were covered with close fitting plastic directly after casting. Test specimens were stored in a controlled climate room up to the time when emission measurements were made.

After the test specimens had cured for seven days under a close fitting plastic, the screed was spread on all samples except d3.3 and the one (d3.0) without screed. RH at this time had dropped to below 90%, see Table 5.7 and Fig. 5.11 and 5.12. This moisture level was the highest recommended by the suppliers for spreading the screeds. The screeds were delivered ready mixed, only water had to be added. After water had been added, the screeds were mixed in a paddle mixer and spread as described in Subsection 2.1.2. The screed for test specimen d3.3 was spread on a separate occasion.

The seven screeds studied were of three types. The first three (d3.1 – d3.3) were normal screeds based on aluminat cement; see Subsection 2.1.2. Two (d3.4, d3.5) were rapid hardening screeds based on aluminat cement, and the last two (d3.6, d3.7) were gypsum based screeds. The experimental setup and the results are set out in Tables 5.6. The experiment and the results are also described in Konieczny (1997).

The floorings were bonded one day after the rapid hardening screeds had been spread. On the normal hardening screeds the floorings were bonded 7 days after spreading, and on the gypsum based screeds after 14 days. These were the shortest drying times recommended for the screeds concerned. The floorings on all test specimens were laid into the wet adhesive in the same way, with 10 minutes' open time before the flooring was pressed down. PVC floorings and adhesives were the same for all test specimens. The method of applying the adhesive is described in Subsection 2.1.3.

5.4.2 Moisture and emission measurements

The moisture status of the test specimens was measured several times during the curing period. The first measurement was made at the time the screeds were spread, ca 1 week after the concrete had been cast. Measurements were then repeated 2, 3 and 14 weeks after casting. RH measurements were made using RH probes which were inserted into measuring tubes 4 cm below the tops of the test specimens, inclusive of screed if any, one day before a reading was made. The measuring method (No 1) is described in Subsection 2.3.1.

Emissions from the test specimens were measured on five occasions, 14, 26, 36, 40 and 44 weeks after the floorings had been laid. Sampling was performed with FLEC and TENAX tube and the subsequent analysis with GC-FID, as described in Subsection 2.3.3.

5.4.3 Results

The results in the form of the emission factor EF, 14 – 44 weeks after the floorings had been laid, are set out in Table 5.6. The results of all RH measurements in the investigation are set out in Table 5.7 and in Fig. 5.11 and 5.12.

Table 5.6 Experimental setup and the results of investigation d3.

Experiment	d3.00	d3.01	d3.0	d3.1	d3.2	d3.3	d3.4	d3.5	d3.6	d3.7
Screed	–	–	–	S1	S2	S3	S4	S5	S6	S7
t [mm]	–	–	–	5	5	5	5	5	20	20
Σ Time [days]	–	–	8	7+7	7+7	7+7	7+1	7+1	7+14	7+14
Flooring	Steel	F1	F1	F1	F1	F1	F1	F1	F1	F1
Adhesive	–	–	A2	A2	A2	A2	A2	A2	A2	A2
Concrete	–	–	C3	C3	C3	C3	C3	C3	C3	C3
Designation	Steel	Flooring	A	G	F	H	D	E	C	B
B 14 w	< 2	6	141	16	9	12	< 2	< 2	7	12
B 26 w	< 2	< 2	77	2	15	7	< 2	8	20	7
B 36 w	< 2	< 2	40	4	3	< 2	< 2	5	5	< 2
B 40 w	< 2	< 2	28	5	< 2	< 2	50	< 2	< 2	5
B 44 w	< 2	< 2	24	< 2	< 2	< 2	3	< 2	< 2	< 2
E 14 w	< 2	4	150	9	17	14	< 2	< 2	12	8
E 26 w	< 2	< 2	193	10	17	18	4	15	13	24
E 36 w	8	5	139	29	26	22	144	29	34	26
E 40 w	< 2	< 2	154	143	95	93	159	39	35	42
E 44 w	6	< 2	89	12	< 2	8	7	8	8	12

Table 5.7 RH in test specimens at 40% of the depth at different times after casting. Investigation d.3.

Experiment	7 days	8 days	14 days	21 days	95 days
d3.0	89.2	89.1**	87.0	86.1	86.5
d3.1	88.1*	87.3	86.3**	85.3	83.3
d3.2	87.2*	85.9	84.1**	82.7	84.9
d3.3	90.1	89.3	87.6*	87.2**	84.9
d3.4	87.5*	86.9**	85.1	84.3	85.3
d3.5	88.0*	87.5**	86.0	85.8	87.0
d3.6	86.2*	87.2	86.6	77.8**	80.0
d3.7	85.5*	86.4	86.7	78.4**	82.0

* Spreading of screed
 ** Bonding of PVC flooring

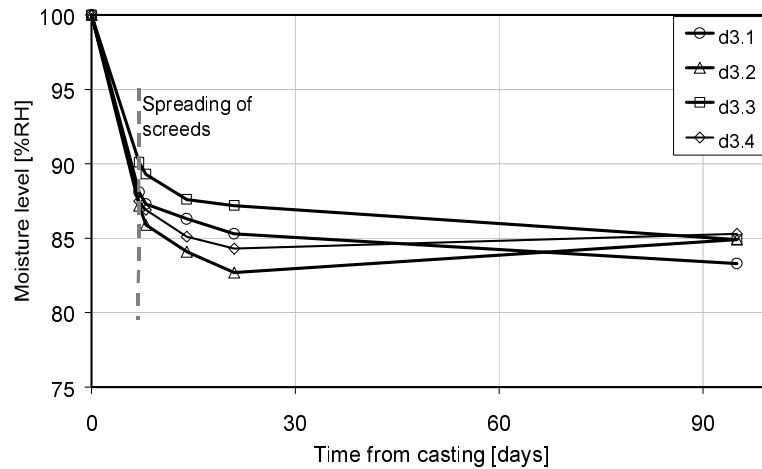


Fig. 5.11 RH in test specimens at 40% of the depth at different times after casting. Investigations d3.1 – d3.4.

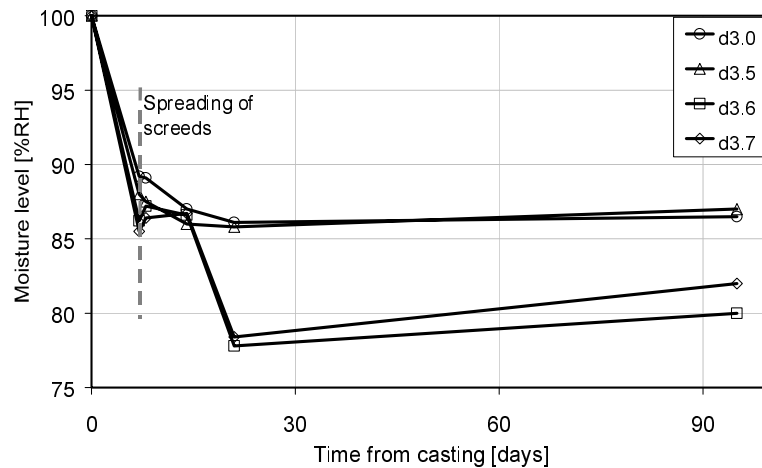


Fig. 5.12 RH in test specimens at 40% of the depth at different times after casting. Investigations d3.0 and d3.5 – d3.7.

5.4.4 Evaluation

Influence of type of screed

This comparison was made to find if the type of screed that is used on self-desiccating concrete has any critical significance.

EF from the experiment with concrete C3 without screed is shown at the extreme left in Fig. 5.13 and 5.14. The value of EF in this experiment is the highest in this investigation. The result is so high that it may be due to secondary emissions caused by alkaline hydrolysis of the adhesive, which also agrees with the results in Wengholt Johnsson (1995).

The other seven experiments, with screed, all have a low EF at the first two emission measurements plotted in Fig. 5.13 and 5.14. However, the value of EF measured after 40 weeks is high, which may be due to external disturbance of the measurement and analysis procedure.

It is remarkable that the moisture level in the concrete drops to ca 86-90% RH after 7 days. After three weeks, the moisture level in most experiments is around 85% RH. After this the level does not drop appreciably, apart from samples d3.6 and d3.7 on which a gypsum based screed had been spread. The rapid drying down to 85% RH may be due to self desiccation of concrete C3.

The reason that the decrease in moisture level ceases may be that an impermeable flooring which prevents drying from the surface has been bonded to the samples. The reason that the moisture level rises between 21 and 95 for experiments d3.0, .2, .4, .6 and .7 may be that the moisture in the test specimen is redistributed. Any moisture from the bottom of the test specimen may be transported up to the level at which measurement is made, or moisture in the screed may be transported down to this level.

One failing in the investigation is that all the cement based screeds were based on aluminate cement. Aluminate based screeds are low alkaline, with pH around 11.

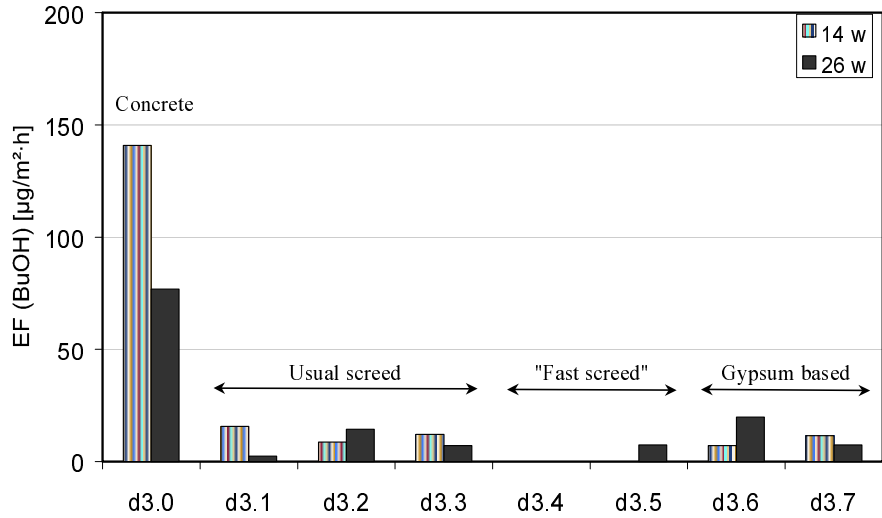


Fig. 5.13 Comparison of emission of butanol from test specimens with homogeneous PVC flooring bonded to different types of screed. In experiment d3.0 the flooring was however bonded directly to the concrete.

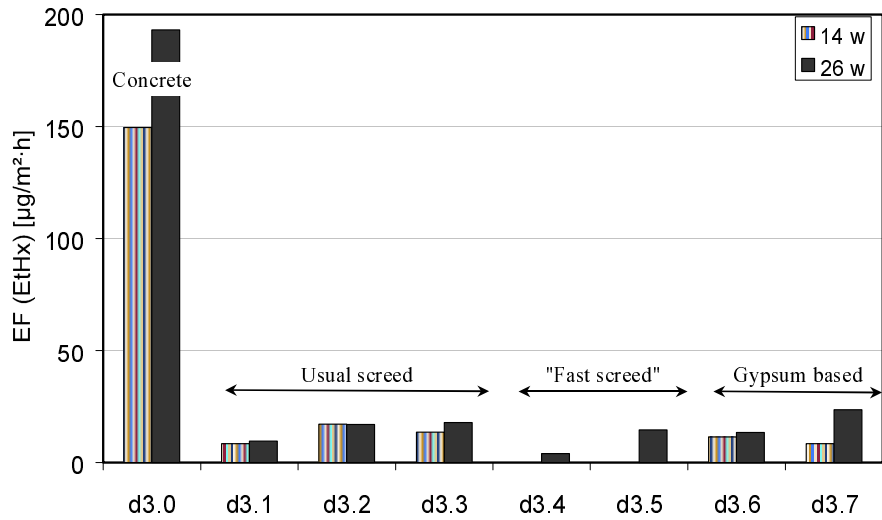


Fig. 5.14 Comparison of emission of ethylhexanol from test specimens with homogeneous PVC flooring bonded to different types of screed. In experiment d3.0 the flooring was however bonded directly to the concrete.

5.5 Influence of time during which the concrete surface dries before the flooring is bonded

The moisture properties of the concrete layer below the adhesive and flooring are significant for the rate of emission. In the above investigation d2 which is also described in Fritsche et al (1997), it was found that the open time after application of adhesive to concrete of low w/c ratio was an important parameter.

In this investigation emission from floorings with different concrete substrates and open times was measured. In some cases the period of exposure to air, from removal of the plastic to application of the adhesive, was varied.

5.5.1 Test specimens

For this investigation, 21 test specimens PF3 (pot) according to the description in Subsection 2.3.3 were cast. Of these, 13 were concrete C2 and the remaining 8 concrete C4; see Tables 5.7 – 5.9. Directly after casting, the test specimens were turned upside down on a steel plate and vibrated. The next day they were turned the right way up and covered with plastic. They were then stored in a controlled climate room (20°C, 50% RH), covered with plastic, for 25 days. The plastic foil was removed and after 5 days PVC floorings were bonded to the concrete samples. The quantity of adhesive applied, 15 g, was the same for all samples. The floorings were laid into the wet adhesive with open times of 2 or 10 minutes. See Subsection 2.1.3 for description of the methods of applying the adhesive. Some samples dried without plastic for 20 instead of 5 days.

The samples on which screed was to be spread were not turned but were stored covered for 25 days, and ca 5 mm screed was spread after another 5 days. The flooring was bonded to the substrate 7 days after the screed had been spread.

A different experiment, d4.1 with a linoleum flooring, was included in the investigation. The aim of this was to have a pilot experiment for a possible later investigation of EF from bonded linoleum floorings.

5.5.2 Moisture and emission measurements

The results of RH measurements of surface moisture in test specimens made from the same concrete, which had dried under the same conditions for the same time, are set out in Table 5.6. Measurements of surface moisture were made on samples extracted at depths of 0-5 mm by method No 3 described in Subsection 2.3.1. A complete description of the RH measurements and all results are given in Sjöberg & Wengholt Johnsson (1999).

Measurements of EF were made approximately 10 and 26 weeks after the flooring had been laid. Sampling was performed with FLEC and TENAX tube, followed by analysis with GC-FID according to the method described in Subsection 2.3.3.

5.5.3 Results

The results in the form of RH at the concrete surface are set out in Table 5.8 for the two concrete types and drying times.

The experimental setup and emission factors EF, 10 and 26 weeks after the flooring had been laid, are set out in Tables 5.9 – 5.11 and in Fig. 5.15 and 5.16.

Table 5.8 Moisture at concrete surface (0-5 mm) when impermeable flooring is laid.

Experiment	Surface moisture [%RH]	
	C2	C4
Drying for 5 days	71.8	81.3
Drying for 20 days	66.9	78.5

Table 5.9 Experimental setup and the results of investigation d2.

Experiment	4.00	d4.1	d4.2	d4.3	d4.4	d4.5	d4.6	d4.7
Open time [min]	–	2	5	5	10	2	2	2
Drying [days]	–	5	5	5	5	5	5	20
Screed	–	–	–	–	–	–	–	–
Flooring	Steel	F3	F1	F1	F1	F1	F1	F1
Adhesive	–	A2	A2	A2	A2	A2	A2	A2
Concrete	–	C2	C2	C2	C2	C2	C2	C2
Designation	00	EB2	EB1	EB3	EB4	EB5	EB6	EB7
EF BuOH 10 w	< 2	3	899	1254	786	1612	1673	20
EF BuOH 26 w	< 2	2	322	294	266	678	577	152
EF EtHx 10 w	< 2	1	540	895	618	720	813	17
EF EtHx 26 w	< 2	210	726	765	641	1016	876	178

Table 5.10 Experimental setup and the results of investigation d2.

Experiment	d4.8	d4.9	4.10	4.11	4.12	4.13	4.14	4.15
Open time [min]	10	2	2	2	15	25	10	10
Drying [days]	20	5	5+7	5+7	5+7	5+7	5	5
Screed	–	–	S2	S2	S2	S2	–	–
Flooring	F1	F1	F1	F1	F1	F1	F1	F1
Adhesive	A2	A2	A2	A2	A2	A2	A2	A2
Concrete	C2	C2	C2	C2	C2	C2	C4	C4
Designation	EB8	EB9	EBA1	EBA2	EBA3	EBA4	ET1	ET2
EF BuOH 10 w	80	1285	27	20	17	0	1383	1319
EF BuOH 26 w	69	579	9	5	1	3	731	590
EF EtHx 10 w	59	780	26	25	31	21	663	730
EF EtHx 26 w	114	1059	26	17	17	17	1303	1177

Table 5.11 Experimental setup and the results of investigation d2.

Experiment	4.16	4.17	d4.17	d4.19	d4.20	d4.21
Open time [min]	2	2	2	2	15	25
Drying [days]	5	5	5+7	5+7	5+7	5+7
Screed	–	–	S2	S2	S2	S2
Flooring	F1	M1	M1	M1	M1	M1
Adhesive	L2	L2	L2	L2	L2	L2
Concrete	C4	C4	C4	C4	C4	C4
Designation	ET3	ET4	ETA1	ETA2	ETA3	ETA4
EF BuOH 10 w	1986	1411	1	18	12	7
EF BuOH 26 w	723	563	7	6	1	4
EF EtHx 10 w	1121	973	4	32	30	25
EF EtHx 26 w	1505	1232	26	13	20	16

5.5.4 Evaluation

Influence of linoleum flooring

EF from experiment d4.1 with linoleum flooring can be compared with experiments d4.5 and d4.6 which have PVC flooring but are in all other respects similar. In all measurements, EF for the linoleum flooring is lower than those for PVC flooring.

On both occasions, the measured values for butanol are low for d4.1. The measured value for ethylhexanol is low at the first measurement but increases at the second. This is usual for EF for ethylhexanol in this investigation when a high EF has been measured.

Influence of different open times

On comparing experiments which are otherwise similar, the significance of open time can be studied. When open times of 2 and 5 minutes are compared for concrete C2, no clear differences in EF can be discerned. This may be because the difference in the remaining quantity of moisture of adhesive is not so great that it has an appreciable effect; according to Table 5.3, the difference is only 7%.

Nor do the results in comparisons of EF from corresponding experiments with concrete C4, in which the open time varied between 2 and 10 minutes, show any clear differences. According to Table 5.2, in this case the difference in the remaining quantity of moisture of adhesive is 5%.

Influence of time during which the concrete surface dries before the flooring is bonded

By grouping the bars for EF in Fig. 5.15 and 5.16, the effect of drying time can be judged. For all concretes, the bars at the left, EF after 5 days' drying time, are generally higher than the bars at the right. In other words, in all tests EF is high after 5 days' drying time, irrespective of concrete, but low for concrete C2 after 20 days of drying. The reason may be that the concrete surface is drier and copes with moisture increment from the adhesive; see Table 5.8. Generally, however, concrete may be drier in these experiments because of the longer drying period.

In experiments where screed was laid on the concrete, EF is low irrespective of the concrete. The explanation may be that the screed dries rapidly and copes with moisture increment from the adhesive.

Another explanation may be that alkaline hydrolysis does not occur when the surface had dried for 20 days, and/or when a screed is used because its pH value is low. After drying for 20 days, the concrete surface may react with atmospheric carbon dioxide, i.e. carbonation takes place. This lowers the pH value from ca 13 to below 9. According to the manufacturer, the pH value of screed is lower than 11.

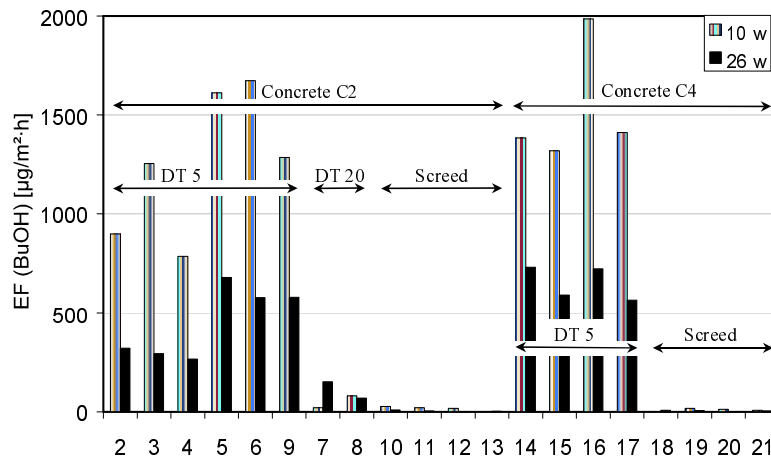


Fig. 5.15 Influence of the period during which the concrete surface dries before adhesive is applied, and of the use of screed, on emission of butanol. Experiments were made on two concrete types with ca 90% RH when the PVC flooring was bonded. Experiments Nos 2-21 refer to d4.x. Experiments d4.00 and d4.1 have been omitted.

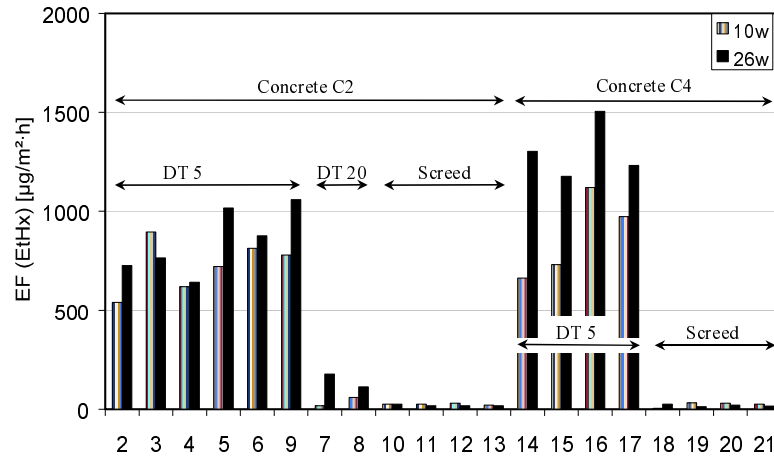


Fig. 5.16 Influence of the period during which the concrete surface dries before adhesive is applied, and of the use of screed, on emission of ethylhexanol. Explanation of the bars is given in fig 5.15.

5.6 Discussion of moisture distribution, moisture of adhesive and elevated EF, and conclusions

A moisture increment on the top of the concrete can temporarily increase the moisture level at the surface. If an impermeable layer such as a PVC flooring is laid on the concrete immediately after the moisture increment, moisture redistribution can take place only downwards into the concrete. This may take one to several weeks.

If the moisture increment is considerable in proportion to the available moisture capacity of the concrete surface, there may be an appreciable increase in RH. This increase in RH may cause hydrolysis of the flooring materials, primarily the adhesive since this is in direct contact with the concrete. This reaction forms decomposition products which can migrate upwards through the flooring and escape from the top surface. At this surface, elevated EF values can be measured for a long time.

For otherwise similar conditions, this increase in RH at the surface may be greatest when moisture is added to impervious concrete. Such concrete in most cases has less available moisture capacity than normal concretes of higher w/c ratios. Depending on the moisture capacity and moisture transport properties of the concrete, a similar moisture increment can give rise to different increases in RH. See Fig. 5.17.

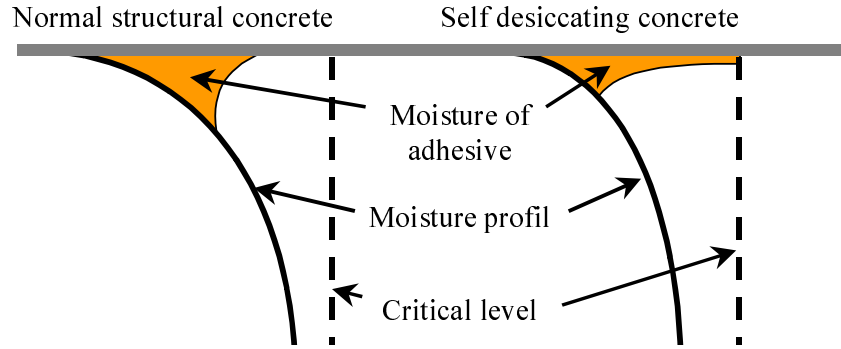


Fig. 5.17 RH profile (%) before application of adhesive and moisture increment due to moisture of adhesive. Fritsche et al (1997).

The open time between application of the adhesive and laying of the flooring can affect EF from the floor construction. A large proportion of the moisture of adhesive may evaporate during the open time if it is sufficiently long. The effect of a long open time on a concrete of low w/c ratio may be twice that on a concrete of high w/c ratio.

Drying of the concrete surface can reduce EF from the floor construction. A possible explanation for this is that alkaline hydrolysis of floorings does not occur if the concrete had dried for a sufficiently long period. The reason may be that in such a case the concrete can cope with the moisture increment from the adhesive without the critical moisture level being exceeded. Another reason might be that the pH value of the concrete surface decreases owing to carbonation, reaction with atmospheric carbon dioxide, during the drying period.

A screed can have a positive effect in preventing elevated values of EF. According to experiments made in this study, the different types of screed appear to have a similar effect. An explanation for this favourable effect may be that alkaline hydrolysis of the flooring is prevented by the screed. The reason may be that the screed dries rapidly and can cope with the moisture increment from the adhesive. Another reason may be that the screed reduces the pH value in contact with the flooring to ca 11; the pH value of concrete is 13 or higher.

6 Qualitative model

6.1 General

The model discussed in the introductory chapter has been verified by measurements in a large number of experiments in this study. Relationships and properties which may have a critical influence on EF from the floor construction and OCIC have been determined. The qualitative model in the form of a block diagram is shown in Fig. 6.1.

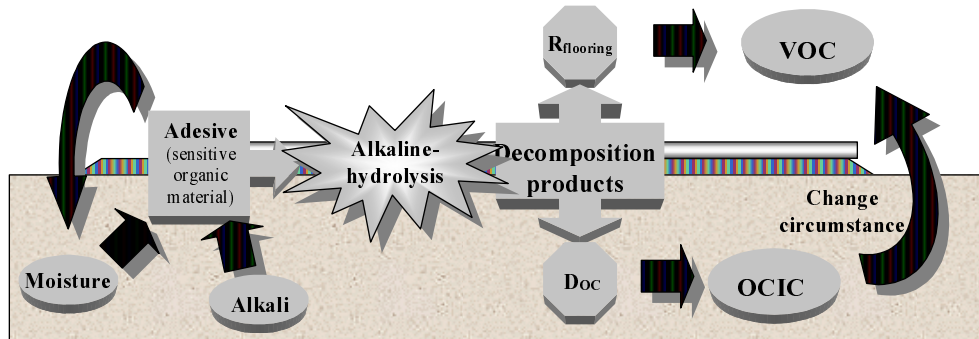


Fig. 6.1 Block diagram of the qualitative model.

Alkaline moisture and acrylate copolymer are two critical components for alkaline decomposition of flooring adhesive. The way moisture distribution in the concrete slab is affected by moisture increment from the adhesive is illustrated at the left hand side of Fig. 6.1.

However, it is not enough for the concrete to be alkaline or moist, both conditions must be satisfied simultaneously, and to a sufficient degree, for the substrate to react with the adhesive. If these conditions are satisfied, decomposition, alkaline hydrolysis of the adhesive, takes place and decomposition products are formed.

These decomposition products, OC, can then be transported away. Depending on the properties of the adjoining materials, they are transported to different extents both upwards and downwards. The quantity that migrates down into the concrete, OCIC, can become bound there and later, when conditions at the surface change, it can migrate upwards again and escape into the air.

In this chapter, three typical cases are examined and qualitatively evaluated. The time scale and extent of the reaction are not dealt with in the qualitative model. These typical cases are bonding of PVC floorings to;

1. Normal structural concrete
2. Self-desiccating concrete
3. Self-desiccating concrete with screed.

6.2 Concrete of high w/c ratio, ca 0.7

Casting up to application of adhesive, Fig. 6.2

Immediately after casting, the moisture level in concrete drops. Drying takes place from the surface. A steeply inclined moisture profile can be formed when moisture is transported upwards through the concrete.

Alkali may be moved with the moisture up towards the surface and increase in concentration as the moisture evaporates. Carbonation of the concrete surface can lower the pH value.

Just before application of adhesive to about one day afterwards, Fig. 6.3

Moisture of adhesive can increase the moisture level at the top of the concrete. However, the critical moisture content is not necessarily exceeded.

Alkali may accompany the moisture of adhesive into the concrete. This transport may be so slight that it has no practical significance.

From one day after application of adhesive to about one month later, Fig. 6.4

Moisture may equalise to the same level in the whole concrete. If the concrete was moist when the flooring was bonded, the moisture level may be above the critical moisture level for alkaline hydrolysis of the adhesive.

The carbonated layer may become alkaline again.

OC may form through hydrolysis of the adhesive. If the concentration of OC just below the flooring is high, transport upwards through the flooring and downwards into the concrete may take place. It may take time for OC to diffuse through the flooring and begin to be emitted into the room air. During all this time, OC may penetrate down into the concrete.

From a month or two after application of adhesive to several years later, Fig. 6.5

Moisture in the concrete can slowly dry out through the flooring. The moisture level can gradually drop below the critical value.

After some time, decomposition may decrease and stop completely if the moisture level is sufficiently low. Concentration below the flooring may decrease when decomposition ceases, since no new OCs are being formed and transport may take place both upwards and downwards. Diffusion through the flooring and emission to the room air may progressively diminish as the concentration below the flooring decreases. Migration down into the concrete may continue, but to a smaller extent as concentration below the flooring decreases.

If concentration below the flooring is lower than that in the concrete, transport may change direction and OCs may be transported up from the concrete and through the flooring into the room air. If moist conditions persist, hydrolysis and emission may continue until a critical component is exhausted.

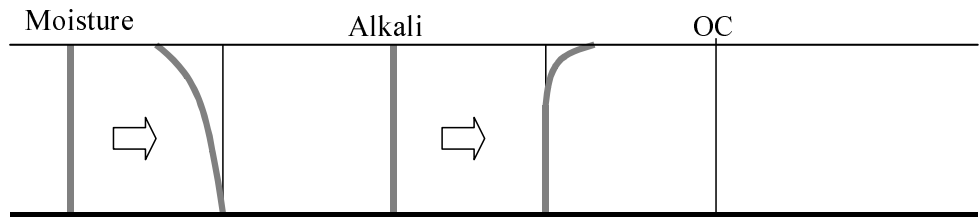


Fig. 6.2 Casting up to application of adhesive.

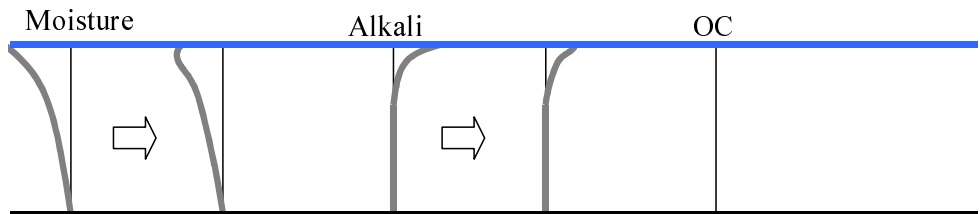


Fig. 6.3 Just before application of adhesive to about one day afterwards.

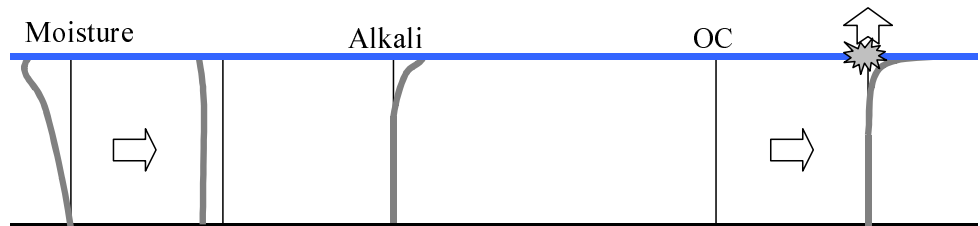


Fig. 6.4 From one day after application of adhesive to about one month later.

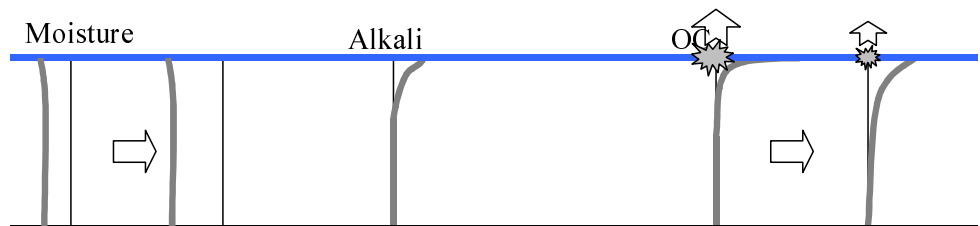


Fig. 6.5 From a month or two after application of adhesive to several years later.

6.3 Self-desiccating concrete

Casting up to application of adhesive, Fig. 6.6

Immediately after casting, the moisture level in concrete drops. Drying may mostly occur through self desiccation. A little water may be transported to the surface where it evaporates, a moisture profile decreasing towards the surface may form.

Alkali may be transported with the moisture up towards the surface and increase in concentration as the moisture evaporates. Some carbonation of the concrete surface may occur, so that the pH value drops.

Just before application of adhesive to about one day afterwards, Fig. 6.7

Moisture of adhesive can increase the moisture level at the top of the concrete. The critical moisture level may be exceeded since the concrete is so impervious that it cannot redistribute moisture.

Alkali may accompany the moisture of adhesive into the concrete. This transport may be so slight that it has no practical significance. Total recarbonation may occur.

OC may form through alkaline hydrolysis of the adhesive. Since the concentration of OC just below the flooring is high, OC may migrate upwards through the flooring and downwards into the concrete.

It may take some time for these OCs to penetrate into the flooring and begin to be emitted into the room air. A little penetration of OC down into the concrete may take place during this time.

From one day after application of adhesive to a month or two later, Fig. 6.8

Moisture level may continue to decrease owing to self desiccation. Moisture increment from the moisture of adhesive, and most of the moisture profile, may have spread out evenly due to drying of the surface. Moisture level at the surface may have dropped below the critical value.

OCs which have formed below the flooring may have penetrated through this and escaped into the room air. Decomposition may have ceased as the moisture level dropped below the critical value. The concentration of OCs below the flooring may decrease when decomposition stops, since transport may take place both upwards and downwards, and there are no new OCs formed.

From a month or two after application of adhesive to a year or two later, Fig. 6.9

Moisture in the concrete may slowly dry out through the flooring. Self desiccation in the concrete may continue, but to a smaller extent than in the beginning.

Penetration through the flooring and emission into the room air may progressively decrease as concentration below the flooring drops. Migration down into the concrete may continue, but to a smaller extent as concentration

below the flooring decreases. If concentration below the flooring is lower than that in the concrete, transport may change direction and OC may be transported upwards from the concrete, through the flooring and into the room air.

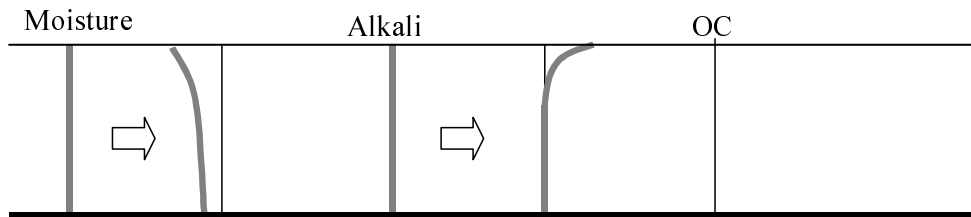


Fig. 6.6 Casting up to application of adhesive.

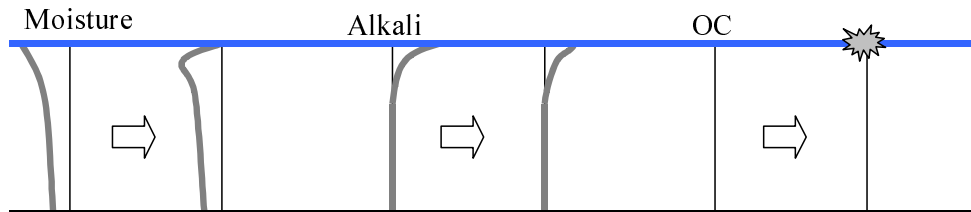


Fig. 6.7 Just before application of adhesive to about a day afterwards.

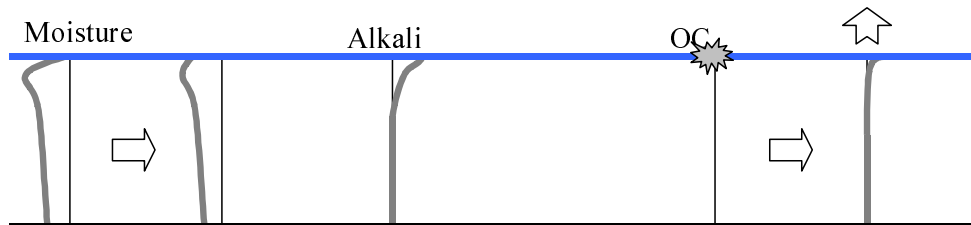


Fig. 6.8 From one day after application of adhesive to a month or two later.

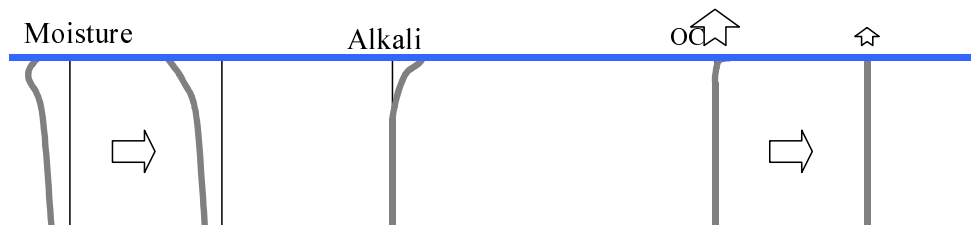


Fig. 6.9 From a month or two after application of adhesive to a year or two later.

6.4 Self-desiccating concrete with screed

Casting up to application of adhesive, Fig. 6.10

Immediately after casting, the moisture level in the concrete drops. Drying may mostly take place through self desiccation. After it is spread, screed may reach a low moisture level in a short time since it is open textured and can rapidly dry out through the surface.

Alkali may be transported with moisture up towards the surface before the screed is spread. Alkali may accompany moisture from the screed down into the concrete. This transport may be so slight that it has no practical significance.

Just before application of adhesive to about one day afterwards, Fig. 6.11

Moisture of adhesive may increase moisture level in the screed. The screed is so open and porous that moisture can be redistributed in the layer without the critical moisture level being exceeded.

Screeds may be low alkaline, which means that their pH value is low, about 11, in the uncarbonated state.

From one day after application of adhesive to a month or two later, Fig. 6.12

Moisture increment in the screed from the moisture of adhesive may spread down into the concrete and also dry out through the flooring. Moisture level in the concrete may continue to decrease owing to self desiccation, but now to a smaller extent.

From a month or two after application of adhesive to a year or two later, Fig. 6.13

Moisture in the screed may slowly dry out through the flooring. Self desiccation in the concrete may almost have ceased.

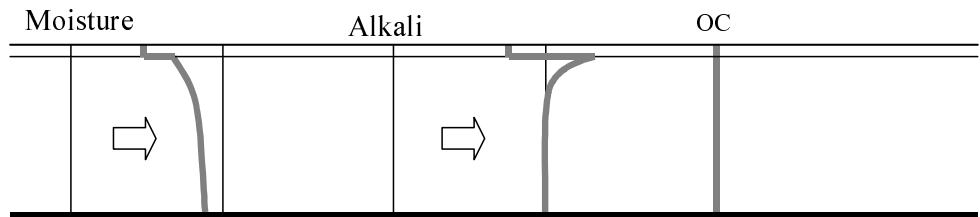


Fig. 6.10 Casting up to application of adhesive.

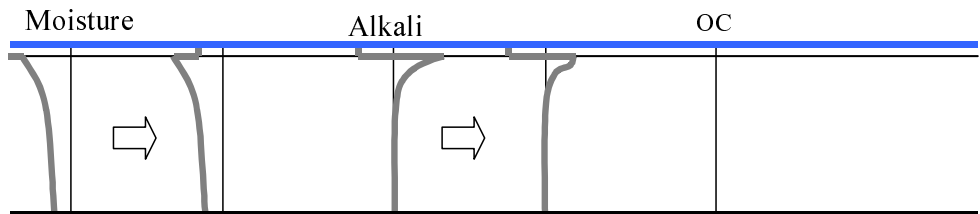


Fig. 6.11 Just before application of adhesive to about a day afterwards.

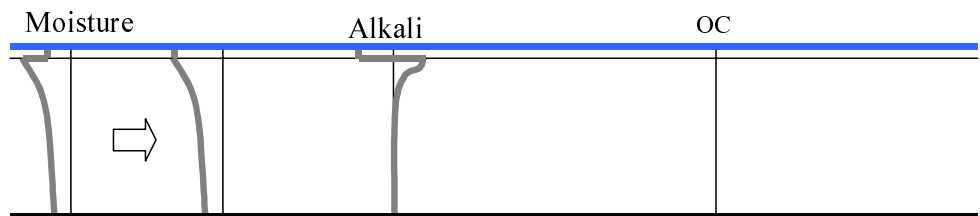


Fig. 6.12 From one day after application of adhesive to a month or two later.

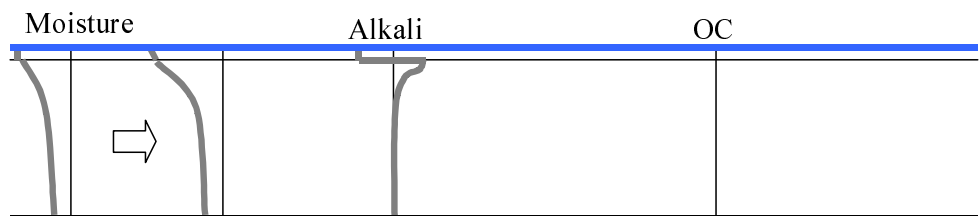


Fig. 6.13 From a month or two after application of adhesive to a year or two later.

7 Quantitative model

The theoretical model described in this chapter focuses on Organic Compounds (OC) which are formed in conjunction with the chemical reaction that can occur when impermeable PVC floor coverings are bonded to moist concrete subfloors with water based acrylate adhesives. The model focuses on the reaction that can form an OC in a material combination, and also on the binding of OC in the floor construction and the transport of OC in the material. Apart from OC, water is also bound and transported in the material. Moisture content is critical in several respects, for instance for the production, binding and transport of OC.

Some aspects relating to the transport and binding of moisture are explained only in outline in this report. The reason is that transport and fixation of moisture in concrete can be assumed to be known in these contexts. Those interested will find references to the literature in the text. Even though moisture is regarded as an area about which a lot is known, there is still appreciable research to be done here.

7.1 Quantity of OC produced in the reaction

The quantity of OC produced (Q) can be described as a function that is governed by many different parameters such as time, RH and pH. It also depends on the materials which are in contact with one another in the studied section, whether these are inert or contain components that may react with one another. The sections which are of interest are primarily the material boundaries where compounds from different materials may meet and undergo a chemical reaction in consequence. The quantity of OC produced (Q) can be expressed as

$$Q = \text{function}(t, RH, pH, \text{materials}) \quad \left[\text{kg}/\text{m}^2 \right] \quad (7.1)$$

The equation for Q can be simplified by fixing certain parameters at a constant value. However, this has the result that the model is not valid in the general case but only under certain conditions. To start with, let us make the simplification that the equation is valid only in the contact zone between adhesive and concrete. As mentioned before, it is mainly the contact zone at material boundaries that is of interest. The reason for studying this contact zone is that it is here that a material which is sensitive to high pH, i.e. the adhesive, meets moist concrete that has a high pH.

According to Meinighaus (2000), decomposition of the adhesive is an alkaline hydrolysis that is catalysed by hydroxide ions. Since hydroxide ions are not consumed the pH – value is only a starting condition for the decomposition associated with material boundaries.

If we take into consideration the experiences from investigations of "sick buildings", we can further simplify the model. According to Schrewelius (2000), a film of adhesive which has lost all its adhesion capacity because of decomposition can still contain some acrylate polymers. In such a case, these can form more decomposition products, OC.

Let us therefore make the simplification that the model is only valid for contact zones with high pH values and that the supply of acrylate polymers from the adhesive does not restrict the decomposition. In that case Q is only a function of the duration of reaction, i.e. the elapsed time (t), and RH.

According to Ramnäs (2000), the rate at which a chemical reaction occurs is determined either by the rate of the reaction itself or the rate of mass transport of the substances that participate in the reaction, up to the site of the reaction. If we bear in mind that hydroxide ions (OH^-) in concrete must be available in the liquid phase at the site of reaction with the adhesive, this can explain an observation made by Kumlin (2000). He noticed that the more moisture there is in the concrete surface, the more extensive the decomposition seems to be. The more moisture there is in the concrete, the more contact zones and transport routes there are for the hydroxide ions. The effect is better contact and faster mass transport, with more extensive decomposition as a result. Let us make the reasonable assumption that the rate of formation of the compounds (q_R) in the reaction is a function of RH in accordance with the above reasoning.

$$q_R = q_R(RH) \quad \left[\text{kg}/\text{m}^2/\text{s} \right] \quad (7.2)$$

If we consider the above plus the observation of Kumlin (2000) that "the longer the concrete surface has been moist, the more extensive the decomposition seems to be", we can develop our reasoning further. It is reasonable to assume that the quantity of OC formed (Q) is governed by the duration of the reaction and that q_R is governed by RH which can, in turn, change over time in accordance with the above.

$$Q(t) = \int_0^t q_R(t) \cdot dt = \int_0^t q_R(RH(t)) \cdot dt \quad \left[\text{kg}/\text{m}^2 \right] \quad (7.3)$$

According to Hedenblad & Nilsson (1987) there is a critical value of humidity (RH_{crit}) for the alkaline hydrolysis in the system with PVC floor coverings bonded to concrete. In that study it was not possible to determine an unambiguous RH_{crit} , but the material combination as a whole must be considered. In the light of this, we can make the simplification that no reaction takes place below the critical limit and that q_R increases as RH exceeds RH_{crit} . For the sake of simplicity we assume a linear increase from RH_{crit} to a maximum value $q_{R,max}$ at 100% RH. See Fig. 7.1. This simplification may not be quite correct since the value of q_R may rapidly increase when some critical parameter changes, and since there is probably a slight decomposition of the adhesive even below RH_{crit} but in practical terms this is negligible in this context.

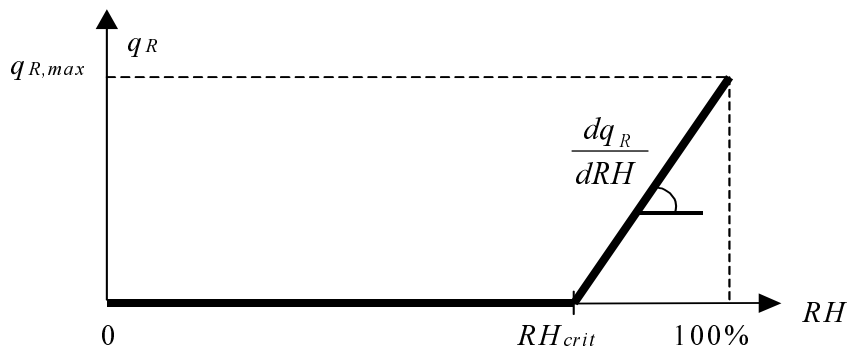


Fig. 7.1. Generalised diagram of rate of reaction q_R over the range 0 – 100% RH.

The equation for the rate of formation is equal to zero over the whole range, except when the actual humidity (RH_{act}) is between RH_{crit} and 1.0 (100% RH).

$$q_R = 0 \quad \left[\text{kg}/\text{m}^2/\text{s} \right] \quad RH_{act} < RH_{crit} \quad (7.4)$$

$$q_R = \frac{dq_R}{dRH} \cdot (RH_{act} - RH_{crit}) \quad \left[\text{kg}/\text{m}^2/\text{s} \right] \quad RH_{act} \geq RH_{crit} \quad (7.5)$$

The differential coefficient of the rate of formation with respect to RH is the same as the slope of the line in Fig. 7.1. In the range between RH_{crit} and 1.0, the differential coefficient can be written as

$$\frac{dq_R}{dRH} = \frac{q_{R,max}}{1 - RH_{crit}} \quad \left[\text{kg}/\text{m}^2/\text{s} \right] \quad (7.6)$$

By substituting equations (7.5) and (7.6) into equation (7.3), we have the following expression for Q when $RH_{act} > RH_{crit}$.

$$Q = \int_{t_1}^{t_2} \frac{q_{R,max}}{1 - RH_{crit}} \cdot (RH_{act}(t) - RH_{crit}) \cdot dt \quad \left[\text{kg}/\text{m}^2 \right] \quad (7.7)$$

The limits in the above equation are the times when RH_{act} passes RH_{crit} . t_1 is the time when RH_{act} passes RH_{crit} with a positive derivative, see Fig. 7.2, and t_2 the time when RH_{act} passes RH_{crit} with a negative derivative. This pair of values (t_1 and t_2) can be repeated in time if the contact zone is rewetted after RH_{act} had dropped below RH_{crit} . This is however something that is very unusual. In the contact zone between adhesive and floor covering, a normal change in humidity may have the form illustrated in Fig. 7.2.

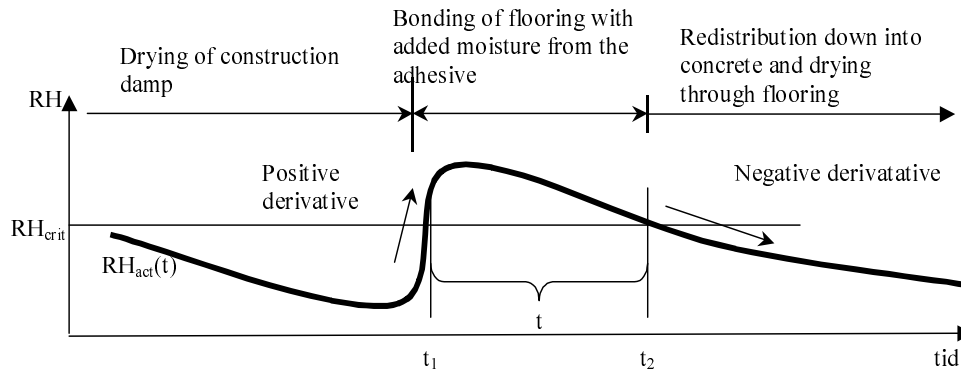


Fig. 7.2. Curve for RH_{act} in the contact zone between adhesive and floor covering.

7.2 Concentration of OC in concrete

The total content (C_{tot}) of organic compounds (OC) in porous moist materials is the sum of OC in the gas phase (C_{air}), OC bound to the cell walls in the pores of the material (C_c), OC dissolved in the pore water of the material (C_w) and OC bound in the structural matrix of the material (C_m), see Fig. 7.3.

$$C_{tot} = C_{air} + C_c + C_w + C_m \quad \left[\text{kg}/\text{m}^3_{\text{material}} \right] \quad (7.8)$$

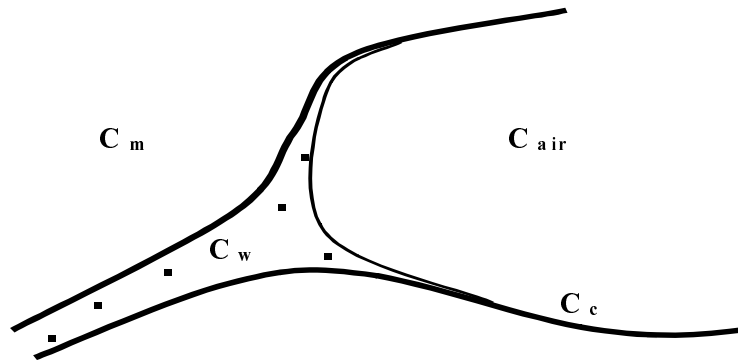


Fig. 7.3. The total quantity of OC (C_{tot}) in a moist pore of the material is the sum of OC in the gas phase (C_{air}), bound on the cell walls (C_c), dissolved in the pore water (C_w) and bound in the matrix (C_m).

The matrix in concrete consists of aggregate, i.e. gravel and sand, and cement gel. The aggregate and the matrix in the cement gel are very impervious inorganic materials which probably have little capacity to adsorb OC. If we assume that this is so, we can ignore C_m .

Already at a moisture level as low as 25-30% RH, on average one layer of water molecules (3.5\AA) is bound on the cell walls in the pores of the material, Ahlgren (1972), Hillerborg (1977) and Xu (1992). When the first layer has been formed, OC must compete for room with water by finding "holes" in the water layer where there is an empty material surface. In normal applications, moisture level in concrete is seldom below 60% RH, which, on average, implies 1.5 molecular layer, and at 80% RH which is a usual value in concrete, two molecular layers will, on average, have been bound to the cell walls. See Fig. 7.4. At high moisture levels, water is also bound by capillary condensation in the narrowest pores. See Fig. 7.5.

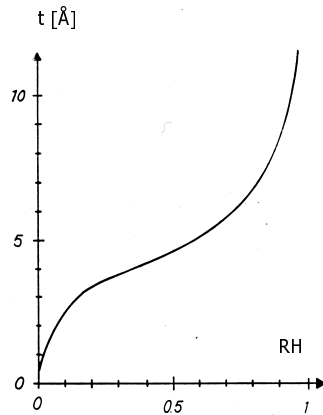


Fig. 7.4 Curve showing mean thickness of adsorbed water layer Hillerborg (1975).

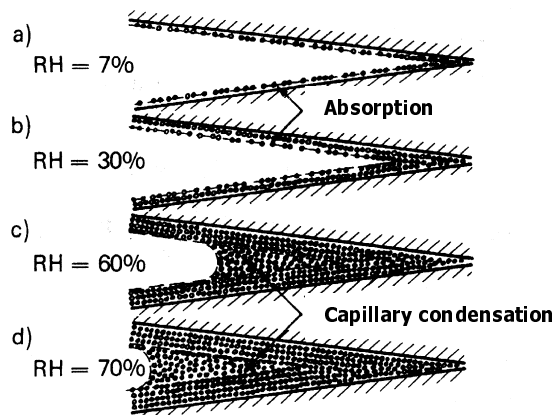


Fig. 7.5 Gradual filling of a pore by adsorption and capillary condensation. Ahlgren (1972).

Since OC must almost always compete for room with water, it might be possible to ignore binding (C_c) to material surfaces. In view of this simplification, the total quantity of OC in concrete can be written

$$C_{tot} = C_{air} + C_w \quad \left[\text{kg}/\text{m}^3_{\text{mort}} \right] \quad (7.9)$$

This assumption will be further discussed in Section 8.1.

According to Henry's law, the mass of gas which is dissolved by a given volume of a liquid at a constant temperature is directly proportional to the partial pressure of the gas (Donald et al 1991). This means that c_w can be written as a function of the solubility (S) in water of OC at a certain partial pressure, prevailing temperature (T), the saturation vapour pressure of OC (c_{sat}) and the concentration of OC in air (c_{air}) above the liquid.

$$c_w = \text{funktion}(S, T, c_{sat}, c_{air}) \quad \left[\text{kg}/\text{m}^3_{\text{water}} \right] \quad (7.10)$$

According to Henry's law, the concentration of OC dissolved in a certain quantity of pore water can be written as

$$c_w = S \cdot \frac{c_{air}}{c_{sat}} \quad \left[\text{kg}/\text{m}^3_{\text{water}} \right] \quad (7.11)$$

Decomposition of adhesive in floor constructions occurs almost always in houses that have been taken into use. The reason is that surfacing materials, among them the floor coverings, are the last to be completed before people move in. We can thus make the simplification that the temperature at the top of the concrete when the chemical reaction takes place and most of the binding of OC occurs, is indoor temperature. Let us assume that temperature is constant at 20°C.

Let us instead study the quantity of a single specific OC per volume of concrete. Concrete contains a certain quantity of water w per unit volume. At constant temperature, 20°C, S and c_{sat} can be treated as constants.

$$C_w = \frac{w}{\rho_w} \cdot S \cdot \frac{c_{air}}{c_{sat}} \quad \left[\text{kg}/\text{m}_{mtrl}^3 \right] \quad (7.12)$$

The quantity of free OC in a certain volume of material (C_{air}) depends on the concentration of OC in the air in the material pores (c_{air}) and the free pore volume (V_a). V_a is that proportion of the pores that are filled not with water but air.

$$C_{air} = c_{air} \cdot \frac{V_a}{V_{mtrl}} \quad \left[\text{kg}/\text{m}_{mtrl}^3 \right] \quad (7.13)$$

In moist porous materials, some of the pore volume is filled with liquid. The free pore volume is then a function of the total pore volume of the material (V_p) and the water content, i.e. the proportion of the volume that the pore liquid occupies.

$$\frac{V_a}{V_{mtrl}} = \frac{V_p}{V_{mtrl}} - \frac{w}{\rho_w} \quad \left[\text{m}_{air}^3 / \text{m}_{mtrl}^3 \right] \quad (7.14)$$

By introducing the expression for porosity, $p = V_p/V_{mtrl}$ the available porosity p_a that is equal to V_a/V_{mtrl} can be written as

$$\frac{V_a}{V_{mtrl}} = p_a = p - \frac{w}{\rho_w} \quad \left[\text{m}_{air}^3 / \text{m}_{mtrl}^3 \right] \quad (7.15)$$

If equations 7.13 and 7.15 are combined, we have an expression for C_{air} :

$$C_{air} = c_{air} \cdot \left(p - \frac{w}{\rho_w} \right) \quad \left[\text{kg}/\text{m}_{mtrl}^3 \right] \quad (7.16)$$

The total quantity C_{tot} in the air and pore water (excluding C_m) can be described by substituting equations 7.12 and 7.16 into equation 7.9:

$$C_{tot} = C_{air} + C_w = c_{air} \cdot \left(p - \frac{w}{\rho_w} \right) + \frac{w}{\rho_w} \cdot S \cdot \frac{c_{air}}{c_{sat}} \quad \left[\text{kg}/\text{m}_{mtrl}^3 \right] \quad (7.17)$$

Since the term c_{air} is a factor of both terms, it can be taken outside the bracket, and equation 7.17 becomes

$$C_{tot} = c_{air} \cdot \left[\left(p - \frac{w}{\rho_w} \right) + \frac{w}{\rho_w} \cdot \frac{S}{c_{sat}} \right] \quad \left[\text{kg}/\text{m}_{mtrl}^3 \right] \quad (7.18)$$

The term for OC in water is much larger than the term for OC in air, see Section 8.1. C_{air} can therefore be ignored, which means that C_{tot} may be equal to C_w .

$$C_{tot} = C_w = c_{air} \cdot \frac{w}{\rho_w} \cdot \frac{S}{c_{sat}} \quad \left[\text{kg}/\text{m}_{mtrl}^3 \right] \quad (7.19)$$

7.3 Transport of OC in concrete

The transport of organic compounds (OC) in porous moist materials is the sum of diffusion in the gas phase (q_{air}), diffusion in the matrix (q_m), convection of OC dissolved in water that is moved along with the mass transport of water (q_{mw}), and diffusion of OC in water (q_w).

$$q_{tot} = q_{air} + q_m + q_{mw} + q_w \quad [kg/(m^2 \cdot s)] \quad (7.20)$$

As we have said before, the matrix in concrete consists of very impervious inorganic materials which may have little capacity to take up and redistribute OC. This means that we can ignore q_m . With this simplification, transport of OC takes place only in the pores of the material. These are at all times wholly or partly filled with water; see Fig. 7.6.

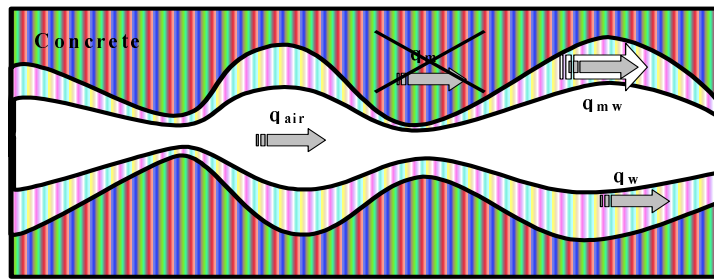


Fig. 7.6 General model for transport of OC in a moist concrete pore.

The magnitude of the transport of OC dissolved in water which is transported in water when this moves along, (q_{mw}), depends on the rate of liquid transport and on the concentration of OC dissolved in water (c_w). According to equation 7.46, transport of water in the pore system in the liquid phase can be described by the water content (w) and the diffusion coefficient for liquid transport.

$$q_{mw} = function(w, D'_w, c_w) \quad [kg/(m^2 \cdot s)] \quad (7.21)$$

Transport of OC in concrete takes place mainly in concrete with an impervious coating, i.e. there is little moisture transport in the liquid phase. The transport of OC with the mass transport of water in motion can therefore be ignored.

The diffusion of OC in pore water (q_w) depends on differences in the concentration of OC in the liquid phase and on the presence of a continuous liquid phase in the pore system. The thickness and continuity of the liquid phase can be described with the help of RH, see Fig. 7.4 and 7.5.

$$q_w = function(RH, c_w) \quad [kg/(m^2 \cdot s)] \quad (7.22)$$

In the model the migration of OC in water is ignored since diffusion of OC in the vapour phase, according to material data taken from CRC (1997), is 10^3 times faster.

Diffusion of OC in the gas phase (q_{air}) is driven by differences in the concentration of OC in air (c_{air}), with the goal of equalising these differences. When the gas is enclosed in a porous material, the rate of diffusion is also influenced by a material-dependent diffusion coefficient (δ_{OC}). According to the conceptual model that is illustrated in Fig. 7.7, δ_{OC} varies with the moisture level.

$$q_{air} = \text{function}(\delta_{OC}, c_{air}) \quad \left[\text{kg}/(\text{m}^2 \cdot \text{s}) \right] \quad (7.23)$$

With the help of Fick's first law diffusion can be described as

$$q_{air} = -\delta_{OC} \cdot \frac{\partial c_{air}}{\partial x} \quad \left[\text{kg}/(\text{m}^2 \cdot \text{s}) \right] \quad (7.24)$$

In numerically describing flow according to equation 7.24, flow takes place between two "midpoints" in cells of size Δx . The driving potential gradient in the flow calculation is $\partial c/\partial x$, i.e. the "slope" of the curve that describes concentration. See Fig. 7.7.

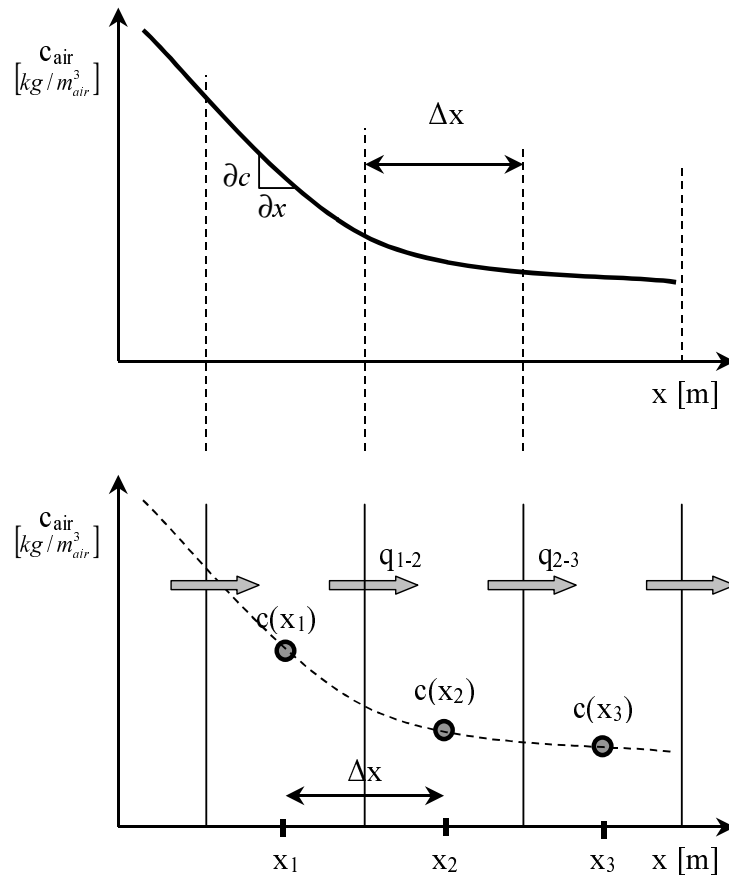


Fig. 7.7. "Real" concentration profile of c_{air} (top), and numerical approximation with distribution of concentration in "points" (bottom).

In a general case, the flow q_{1-2} between points 1 and 2, and the flow q_{2-3} between the points 2 and 3, can be described with the difference in concentration as the driving potential, divided by the distance between the points.

$$q_{1-2} = -\delta_{OC} \frac{c(x_2) - c(x_1)}{\Delta x} \quad [kg/(m^2 \cdot s)] \quad (7.25)$$

$$q_{2-3} = -\delta_{OC} \frac{c(x_3) - c(x_2)}{\Delta x} \quad [kg/(m^2 \cdot s)] \quad (7.26)$$

The flow in the material gives rise to changes in total concentration (C_{tot}) at every point. The change in concentration at a point can be described as the difference in the flow towards and away from the point during a short time (Δt). The "point" has a size (Δx) according to Fig. 7.8.

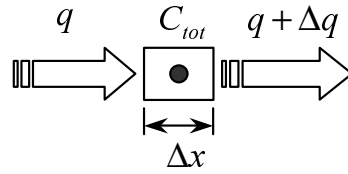


Fig. 7.8. The change in total concentration (ΔC_{tot}) at a point of size (Δx) is described by the flow towards and away from the point during a short time.

During a small time increment the change in concentration in a "cell" is equal to

$$\Delta C_{tot} = \frac{q_{air} - (q_{air} + \Delta q_{air})}{\Delta x} \cdot \Delta t \quad [kg/m^3] \quad (7.27)$$

In the limit when Δx and $\Delta t \rightarrow 0$, the above equation has the following form after it is shortened and rewritten:

$$\frac{\partial C_{tot}}{\partial t} = -\frac{\partial}{\partial x} \cdot q_{air} \quad [kg/(m^3 \cdot s)] \quad (7.28)$$

Through substitution of 7.24 into 7.28, the change in concentration in the cell is described with the concentration difference ∂c_{air} as the driving potential:

$$\frac{\partial C_{tot}}{\partial t} = \frac{\partial}{\partial x} \cdot \delta_{OC} \cdot \frac{\partial c_{air}}{\partial x} \quad [kg/(m^3 \cdot s)] \quad (7.29)$$

In numerically solving the change in a cell according to equation 7.26 it is often assumed that δ is constant and can therefore be moved outside the differentiation.

$$\frac{\partial C_{tot}}{\partial t} = \delta_{OC} \frac{\partial}{\partial x} \cdot \frac{\partial c_{air}}{\partial x} \quad [kg/(m^3 \cdot s)] \quad (7.30)$$

It is sometimes possible to use, in equation 7.29, an effective diffusion coefficient (D_{eff}) that contains the storage capacity (dC_{tot}/dc_{air}), Nilsson (1992).

$$D_{eff} = \frac{\delta_{OC}}{dC_{tot}/dc_{air}} \quad [m^2/s] \quad (7.31)$$

Rewriting Equation 7.30, we get an expression for δ_{OC} :

$$\delta_{OC} = D_{eff} \cdot dC_{tot}/dc_{air} \quad [m^2/s] \quad (7.32)$$

Substituting equation 7.32 into equation 7.29, we have:

$$\frac{\partial C_{tot}}{\partial t} = \frac{\partial}{\partial x} \cdot D_{eff} \cdot \frac{dC_{tot}}{dc_{air}} \cdot \frac{\partial c_{air}}{\partial x} \quad [kg/(m^3_{mtrl} \cdot s)] \quad (7.33)$$

With the simplification that D_{eff} is constant, 7.33 can be rewritten and shortened to Fick's second law. The equation can be rewritten in the following two ways:

$$\frac{\partial c_{air}}{\partial t} = D_{eff} \cdot \frac{\partial^2 c_{air}}{\partial x^2} \quad [kg/(m^3_{air} \cdot s)] \quad (7.34)$$

$$\frac{\partial C_{tot}}{\partial t} = D_{eff} \cdot \frac{\partial^2 C_{tot}}{\partial x^2} \quad [kg/(m^3_{mtrl} \cdot s)] \quad (7.35)$$

The mathematical solution to Fick's second law, in an incremental change in a semi-infinite medium, is the complement to the "error function", Crank (1975):

$$C(x, t) = C_s \cdot \left[1 - erf \left(\frac{x}{2 \cdot \sqrt{D_{eff} \cdot t}} \right) \right] \quad [kg/m^3_{mtrl}] \quad (7.36)$$

C_s is the concentration at the surface. By measuring the states of c_{air} or C_{tot} in structures, D_{eff} can be evaluated if the time during which transport occurred is known. By assuming that the ratio $\partial C_{tot}/\partial c_{air}$ is constant, the value of D_{eff} can be determined.

Equation 7.38 that is needed for this evaluation is plotted in Fig. 7.9 for different values of $D_{eff} \cdot t$. The concentration C_s at the surface of concrete is assumed to be constant.

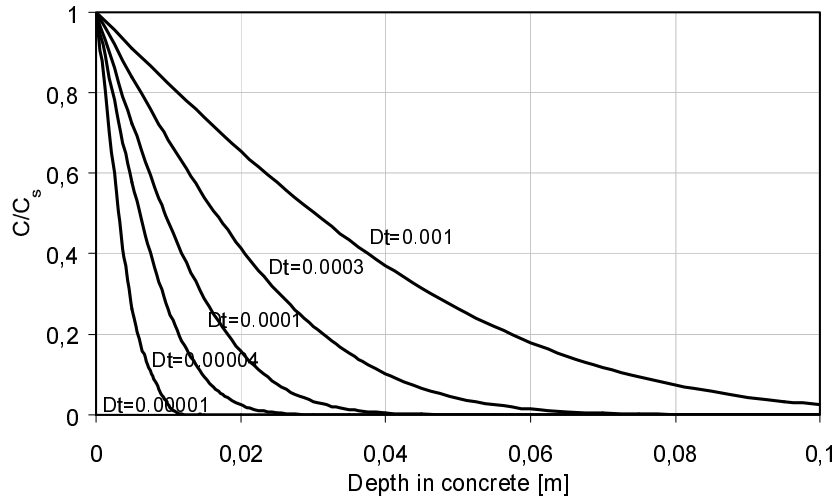


Fig. 7.9. Complement to the error function. The values of $D_{eff} \cdot t$ in equation 7.36 are written alongside each curve.

7.4 Transport of OC through the floor covering

A simplified calculation of OC can be performed if it is assumed that there is only one resistance without storage capacity between two different concentrations. Equation 7.24 can be rewritten so as to apply for a layer between two different concentrations:

$$q_{air} = \delta_{OC} \frac{c_2 - c_1}{\Delta x} \quad \left[\text{kg}/(\text{m}^2 \cdot \text{s}) \right] \quad (7.37)$$

This layer may, for instance, be a floor covering where the thickness is specified, there is little storage capacity, and the concentrations on the two sides are very different. See Fig. 7.10.

q is the flow expressed in SI units or as the emission factor (EF) from the floor covering. EF is, for example, measured with FLEC (Field and Laboratory Emission Cell) and has the unit $\mu\text{g}/(\text{m}^2 \cdot \text{h})$. FLEC is described in Subsection 2.3.3.

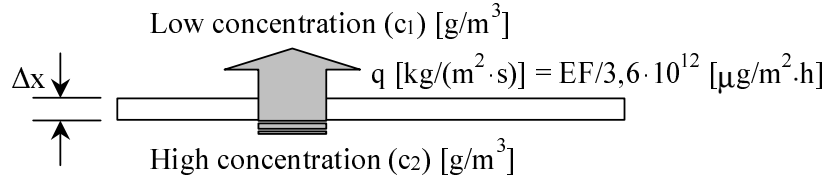


Fig. 7.10. The flow q has the goal of equalising the differences in concentration between the two sides of the floor covering. The storage capacity of the floor covering is ignored.

The flow resistance (R_{fc}) for the floor covering can be defined as

$$R_{fc} = \frac{\Delta x}{\delta_{OC}} \quad \left[\text{s}/\text{m} \right] \quad (7.38)$$

By putting the expression for the flow resistance, equation 7.40, into the rewritten version of Fick's first law, equation 7.37, we have a new equation for the flow:

$$q_{air} = \frac{(c_2 - c_1)}{R_{fc}} \quad \left[\text{kg}/(\text{m}^2 \cdot \text{s}) \right] \quad (7.39)$$

This equation can be rearranged so as to make it better suited for the case when the reaction takes place below a floor covering in a ventilated room. Compared with the concentration below the floor covering (c_2), concentration in the room (c_1) is small. Let us put c_1 equal to the background concentration in the premises (c_0). The equation is then of the form

$$q_{air} = \frac{(c_2 - c_0)}{R_{fc}} \quad \left[\text{kg}/(\text{m}^2 \cdot \text{s}) \right] \quad (7.40)$$

7.5 Moisture fixation in concrete

Every porous material has the capacity to bind (fix) moisture that is taken from the air. The higher the RH of the air, the greater the amount of water that can be bound in the material. Moisture is bound through adsorption on the internal material surfaces and capillary condensation in small pores. These types of binding are discussed in detail by Ahlgren (1972).

The maximum moisture content (w_{max}) of concrete can be estimated with reference to the cement content (CEM), the water/cement ratio (w/c) and the age of the concrete, i.e. the degree of hydration (α), Fagerlund (1982).

$$w_{max} = CEM(w/c - 0,19\alpha) \quad [kg/m^3] \quad (7.41)$$

A special characteristic of concrete compared with other building materials is that the quantity of moisture in the range above the hygroscopic region (98-100% RH) is very small. At 98% RH the pore system in concrete is almost in a state of capillary saturation.

The sorption isotherm describes the relationship between RH in the air and the water content of the material at a given temperature. Owing to hysteresis, the absorption and desorption isotherms for concrete are different. A comparison of Fig. 7.11 and 7.12 will show that the desorption isotherm is at a much higher level than the absorption isotherm. Sorption isotherms and hysteresis are discussed in detail by Ahlgren (1972).

Since it is difficult to deal with hysteresis mathematically, only one isotherm is used in the model.

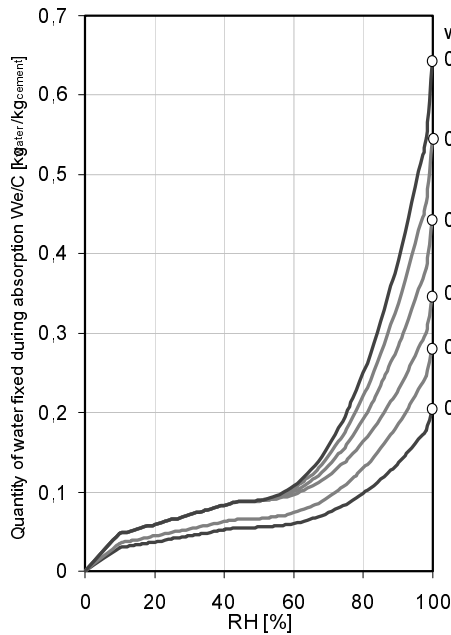


Fig. 7.11. Absorption isotherms for Concrete, from a modify calculation according to Fagerlund (1982). In the figure, w_{max} according to formula 7.41 has been marked with rings.
 w/c 0.3 is $\alpha=0.50$
 w/c 0.4 is $\alpha=0.60$
 w/c 0.50-0.90 is $\alpha=0.80$

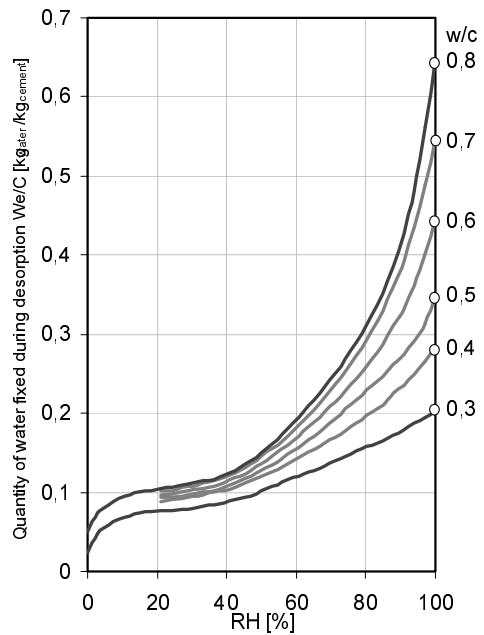
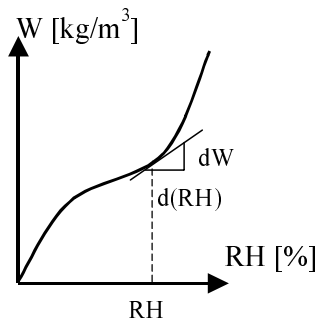


Fig. 7.12. Desorption isotherms for concrete. Nilsson (1980). In the figure w_{max} according to formula 7.41 has been marked with rings.
 w/c 0.3 is $\alpha=0.50$
 w/c 0.4 is $\alpha=0.60$
 w/c 0.50-0.90 is $\alpha=0.80$

In modelling moisture fixation, moisture capacity is an important property of the material. The moisture capacity of a material can be described as the slope of the sorption isotherm at a point; see Fig. 7.13.



$$\frac{dw}{dRH} \quad \left[\frac{\text{kg}}{\text{m}^3} \right] \quad (7.42)$$

Fig. 7.13. The moisture capacity of concrete is equal to the slope of the moisture isotherm. Nilsson (1994).

7.6 Moisture transport in concrete

The transport of moisture in concrete takes place as a combination of a number of different transport mechanisms. According to Nilsson (1994), most transport occurs in the vapour and liquid phases. Fig. 7.14 illustrates the different mechanisms which dominate at different moisture levels in concrete.

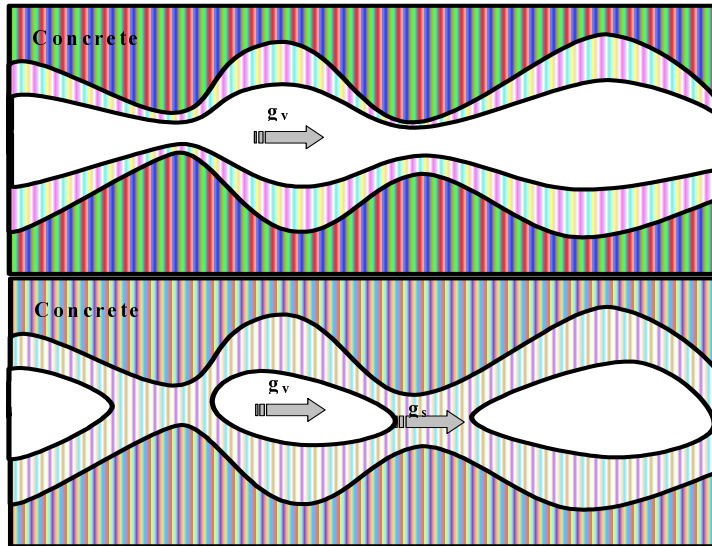


Fig. 7.14. Moisture transport according to betonghandboken. At a low moisture level, transport occurs only through vapour diffusion (g_v). At higher moisture levels, transport occurs as a combination of vapour diffusion and capillary suction (g_s).

When we consider only diffusion of water vapour in the pore system, it is described by Fick's law which states in general terms how differences in concentration are equalised.

$$g_v = -\delta_v \frac{\partial v}{\partial x} \quad [kg/(m^2 \cdot s)] \quad (7.43)$$

When we consider only capillary suction g_s in a pore system filled with liquid, it should, in purely physical terms, be described with the pore water pressure P_w as the driving potential:

$$g_s = -\frac{k_p}{\eta} \cdot \frac{\partial P_w}{\partial x} \quad [kg/(m^2 \cdot s)] \quad (7.44)$$

In order to avoid using the pore water pressure as the driving potential, a liquid diffusivity D'_w can be introduced for liquid transport:

$$D'_w = -\frac{k_p}{\eta} \cdot \frac{1}{dw/dP_w} \quad [m^2/s] \quad (7.45)$$

The equation for capillary suction can then be written with the total water content, i.e. the water content w , as the driving potential:

$$g_s = -D'_w \frac{\partial w}{\partial x} \quad \left[\text{kg}/(\text{m}^2 \cdot \text{s}) \right] \quad (7.46)$$

The total moisture transport is a combination of vapour transport and capillary suction in the pore system:

$$g_w = -\delta_v \frac{\partial v}{\partial x} - \frac{k_p}{\eta} \cdot \frac{\partial P_w}{\partial x} = -\delta_v \frac{\partial v}{\partial x} - D'_w \frac{\partial w}{\partial x} \quad \left[\text{kg}/(\text{m}^2 \cdot \text{s}) \right] \quad (7.47)$$

The pore water pressure is a unique function of the vapour content if the temperature is constant, Ahlgren (1972). This means that the total moisture flow g_w can be described with only one driving potential. The vapour content v or the water content w is usually chosen.

$$g_w = -\delta_{tot} \frac{\partial w}{\partial x} \quad \delta_{tot} = \delta_v + D'_w \frac{1}{v_{sat}} \cdot \frac{dw}{dRH} \quad (7.48)$$

$$g_w = -D_w \frac{\partial w}{\partial x} \quad D_w = \delta_{tot} \left(\frac{v_{sat}}{\frac{dw}{dRH}} \right) \quad (7.49)$$

The water content w at a point in concrete can change, over a certain time Δt , if the moisture flows towards and away from that point are of different magnitude, see Fig. 7.15, and if the cement reaction chemically binds water (w_n). The drying of concrete owing to water being bound by the cement reaction is treated in detail by Norling Mjörnell (1997).

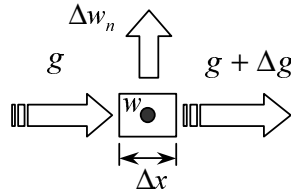


Fig. 7.15. The change in water content at a point of size Δx is described by the flow of moisture towards and away from the point and by the increase in chemically bound water w_n per time Δt .

During a small time increment, the change in water content in a small cell is

$$\Delta w = \frac{g - (g + \Delta g)}{\Delta x} \Delta t - \Delta w_n \quad \left[\text{kg}/(\text{m}^2 \cdot \text{s}) \right] \quad (7.50)$$

In the limit, when both Δx and $\Delta t \rightarrow 0$, the equation can be written

$$\frac{\partial w}{\partial t} = -\frac{\partial g}{\partial x} - \frac{\partial w_n}{\partial t} \quad \left[\text{kg}/(\text{m}^3_{mtrl} \cdot \text{s}) \right] \quad (7.51)$$

7.7 Moisture of adhesive

When the adhesive is applied to the concrete, a certain amount of water may evaporate to the air before the floor covering is laid, see Section 5.2. After the floor covering has been laid, only a small amount of water will be transported up through the floor covering and evaporate to the air.

Most of the water from the adhesive WFA will however be redistributed downwards into the concrete. Flow down into the concrete is determined by the moisture level in the adhesive and in the surface of the concrete, and by the diffusion coefficient of the adhesive (δ_{tot}), equation 7.52.

$$g_w = -\delta_{tot} \frac{\partial v}{\partial x} \quad [kg/(m^2 \cdot s)] \quad (7.52)$$

We can make the simplifying assumption that the water is uniformly distributed in the adhesive. Since the film of adhesive has little thickness, it may be regarded as a flow resistance. The resistance of the adhesive to moisture migration down into the concrete is put at half the total flow resistance of the adhesive layer.

$$g_w = \frac{\Delta v}{Z_{ad}/2} \quad [kg/(m^2 \cdot s)] \quad (7.53)$$

The fixation of moisture in the adhesive is treated in a way similar to that for concrete, with a sorption isotherm; see Section 7.5.

7.8 Moisture transport through the floor covering

Moisture transport through a layer of negligible moisture capacity can be calculated in a simplified way. This simplification is analogous to that made in respect of the transport of OC through impermeable layers of low capacity, see Section 7.4. A PVC floor covering is a surface layer which has large resistance to moisture flow but little moisture capacity.

The water vapour transmission resistance Z_{fc} of the floor covering can be written in a way similar to the flow resistance to OC in equation 7.38.

$$Z_{fc} = \frac{\Delta x}{\delta_{tot}} \quad [s/m] \quad (7.54)$$

Flow through the floor covering is mostly described with the vapour content as the driving potential. Compare equation 7.55 with equation 7.40 which describes the flow of OC through the floor covering.

$$g_v = \frac{\Delta v}{Z_{fc}} \quad [kg/(m^2 \cdot s)] \quad (7.55)$$

7.9 Numerical solution

The equations are solved by using a Forward Finite Difference Method. To get converging solutions a limited time increment is calculated for moisture and OC in every time increment, see equation 7.56. It is usually the moisture flow which decides the required time increment:

$$\Delta t \leq \frac{(\Delta x)^2 \cdot \frac{dw}{dRH}}{2 \cdot \delta \cdot v_{sat}} \quad [s] \quad (7.56)$$

For extreme values, the required time increment can be as short as one minute!

The model calculates the increase in Organic Compounds and the distribution of moisture and Organic Compounds in the following way:

1. Input data for material parameters and environmental conditions are given.
2. Initial conditions for $w(x, t=0)$ and $Q(x, t=0)$ are chosen.
3. A time increment is estimated.
4. The boundary conditions are taken from the climate file containing $T(t)$ and $RH_{act}(t)$ for the air above the surface.
5. With $T(x,t)$, the water content $w(x,t)$ gives the vapour content $v(x,t)$ in each cell from the sorption isotherm.
6. The gradient of vapour contents $v(x,t)$ gives the vapour flows.
7. The flow of moisture to each cell gives a change in moisture content $\Delta w(x,t)$ and a new moisture content $w'(x,t)$.
8. RH in the adhesive gives the amount of newly produced OC and adds it to $Q(adhesive,t)$.
9. The OC content $C_{tot}(x,t)$ gives the OC concentration $c_{air}(x,t)$ in each cell.
10. The gradient of OC concentration $c_{air}(x,t)$ gives the OC flows.
11. The flow of OC to each cell gives a change in OC content $\Delta C_{tot}(x,t)$ and a new OC content $C'_{tot}(x,t)$.
12. With the new moisture and OC distributions a new time increment is estimated.
13. The calculations are repeated from point 4.
14. The calculated results are stored at certain times for display.
15. The calculations continue until a certain calculation time is reached.
16. Calculation results are copied and labelled.

This procedure was run in an Excel Workbook.

8 Quantifying the parameters in the model

The values of many of the parameters in the model in Chapter 7 have been known for some time. This is particularly the case regarding the parameters to do with moisture transport and moisture fixation in concrete. Tables of these parameters have been compiled by e.g. Hedenblad (1996) and Nevander & Elmarsson (1994). These parameters are not discussed further in this study.

The parameters concerning transport and fixation of butanol or some other OC in concrete have not been treated in the literature to the same extent. Two of these parameters, δ_{OC} and R_{fc} , have however been determined by investigations in Chapter 4. In this chapter, another two parameters in the model, binding capacity (dC_{tot}/dc_{air}) and maximum OC produced per unit time ($q_{R,max}$) will be evaluated.

8.1 Evaluation of the storage capacity of concrete for butanol

By far the greatest proportion of OC is bound in concrete, C_{bound} . It is only a small part of the total quantity of OC which is found free in the air filled pores, C_{air} .

When C_{tot} in concrete increases or decreases as a result of e.g. a flow, both the bounded quantity of OC and the free concentration of OC in the air in the pores of the concrete will change. The storage capacity dC_{tot}/dc_{air} is a measure of how a change in the total quantity of OC will affect the free concentration.

Conversely, the total quantity of OC can be calculated from the magnitude of free concentration.

8.1.1 Theoretical evaluation

The foundations for a theoretical evaluation of storage capacity are laid in Chapter 7 where the total quantity, C_{tot} , is described as a function of c_{air} . This expression is valid for the cases where it may be assumed that OC in concrete occurs only in the vapour phase and dissolved in pore water. Equation 7.17 in Chapter 7 expresses this relationship.

$$C_{tot} = C_{air} + C_w = c_{air} \cdot \left(p - \frac{w}{\rho_w} \right) + \frac{w}{\rho_w} \cdot S \cdot \frac{c_{air}}{c_{sat}} \quad \left[\text{kg/m}^3_{\text{concr}} \right] \quad (8.1)$$

The data necessary for solving Equation 8.1 can be found in the literature. According to CRC (1997), for butanol at 20°C S is equal to 0.077 ($\text{kg/m}^3_{\text{water}}$) and c_{sat} equal to $17 \cdot 10^{-3}$ ($\text{kg/m}^3_{\text{air}}$). According to Fagerlund (1994), the porosity of concrete p may be estimated at 0.15.

According to Equation 8.1, the total quantity of OC in a certain quantity of material varies with the moisture content w . For butanol, the relationship between C_{tot} and c_{air} for different values of the moisture content w is plotted in Fig. 8.1.

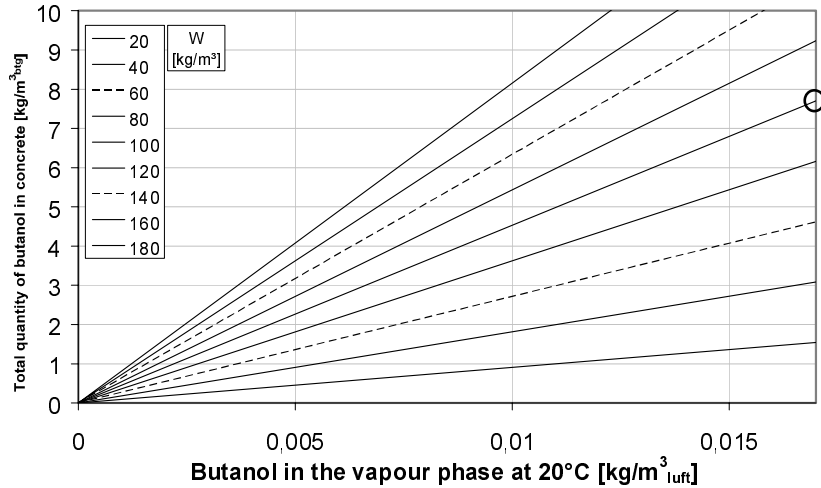


Fig. 8.1 Storage capacity according to bound.0; C_{tot} as a function of c_{air} and w at constant temperature, 20°C.

The storage capacity can be calculated from the slope of the line concerned in Fig. 8.1. For instance, at moisture content $w = 100 \text{ kg/m}^3$ the storage capacity, as given by Equation 8.2, is $0.44 \cdot 10^{-3}$ (-).

$$\frac{dC_{tot}}{dc_{air}} = \frac{\Delta C_{tot}}{\Delta c_{air}} = \frac{7,5}{17 \cdot 10^{-3}} = 0,44 \cdot 10^3 \quad \left[\frac{\text{kg}}{\text{m}^3_{\text{mtrl}}} / \frac{\text{kg}}{\text{m}^3_{\text{air}}} \right] \quad (8.2)$$

8.1.2 Evaluation from measured data

The storage capacity can also be evaluated from measured data for δ_{OC} and D_{eff} . In Section 4.2, the value of δ_{OC} for butanol in concrete was determined as $92,7 \cdot 10^{-9} \text{ (m}^2/\text{s)}$, and in Section 4.3 the value of D_{eff} was determined as $5,80 \cdot 10^{-12} \text{ (m}^2/\text{s)}$. According to Equation 7.31, the storage capacity can be written as the ratio of the diffusion coefficient for OC in the gas phase to the effective diffusion coefficient; see Equation 8.3. The storage capacity, as given by Equation 8.3, is $16,0 \cdot 10^{-3}$ (-).

$$\frac{dC_{tot}}{dc_{air}} = \frac{\delta_{OC}}{D_{eff}} = \frac{92,7 \cdot 10^{-9}}{5,80 \cdot 10^{-12}} = 16,0 \cdot 10^3 \quad \left[\frac{\text{kg}}{\text{m}^3_{\text{mtrl}}} / \frac{\text{kg}}{\text{m}^3_{\text{air}}} \right] \quad (8.3)$$

8.1.3 Appraisal of the evaluation

The results obtained by evaluating the storage capacity in different ways differ by a factor of 36. The reason may be that the result from Equation 8.3 is misleading because the diffusion coefficients δ_{OC} and D_{eff} may have been evaluated from concretes of different properties and moisture levels. According to Section 4.2, diffusion coefficients are highly moisture dependent. In addition, D_{eff} was evaluated from a profile on the assumption that the surface concentration was constant, which may be wrong if we consider the variations, shown in Fig. 8.6, in the flow from the test specimen through the flooring. It is also possible that theoretical evaluation of the storage capacity is incorrect.

Let us call the storage capacity evaluated in Subsection 8.1.1 "Bound,0".

Bound,0

According to Equation 8.1, the total concentration of OC in concrete is the sum of the free concentration C_{air} and the bound concentration C_{bound} . The free concentration can be written as the concentration in the air filled pores multiplied by the available pore volume, as in Equation 8.4.

$$C_{tot} = C_{air} + C_{bound} = c_{air} \cdot \left(p - \frac{w}{\rho_w} \right) + C_{bound} \quad \left[kg/m^3_{mtrl} \right] \quad (8.4)$$

The quantity of bound OC calculated in Equation 8.3 may be too low. The calculation is based on the assumption that OC is only "bound" in proportion to a factor k_0 multiplied by the moisture content of the pores, as set out in Equation 8.5. The value of k_0 can be calculated with reference to Henry's law.

$$C_{bound,0} = \frac{w}{\rho_w} \cdot S \cdot \frac{c_{air}}{c_{sat}} = k_0 \cdot w \cdot c_{air} \quad \left[kg/m^3_{mtrl} \right] \quad (8.5)$$

Bound,1

It is possible that OC is bound in moist concrete in some way different from that described by Equation 8.5. Another possibility is that OC is also bound to wet surfaces in the concrete, as shown in Fig. 8.2.

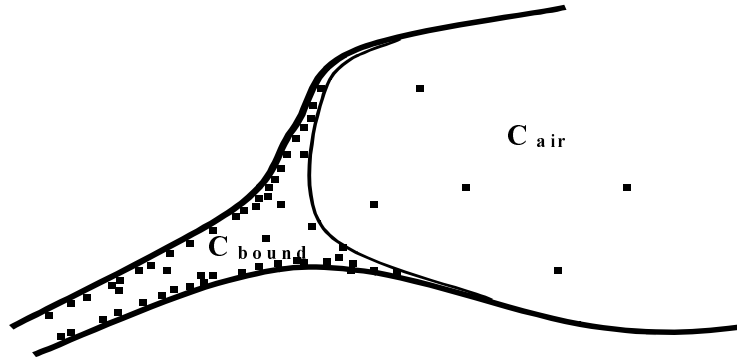


Fig. 8.2 Bound,1 implies that OC can dissolve in liquid and bind to moist surfaces in the concrete. In such a case the binding capacity may be highly moisture dependent.

According to this assumption, OC can also dissolve in the liquid in the pores, and mainly binds to wet surfaces in the concrete pores. This moisture dependence can be described, for instance, by the constant k_1 in Equation 8.6.

$$C_{bound,1} = k_1 \cdot w \cdot c_{air} \quad \left[\frac{\text{kg}}{\text{m}^3_{\text{mtrl}}} \right] \quad (8.6)$$

By assuming that the storage capacity calculated in Equation 8.3 holds for $w = 100 \text{ (kg/m}^3\text{)}$, the value of k_1 is found to be $165 \text{ (m}^3\text{/kg)}$. The storage capacity with $C_{bound,1}$ for different moisture contents is given in Fig. 8.3.

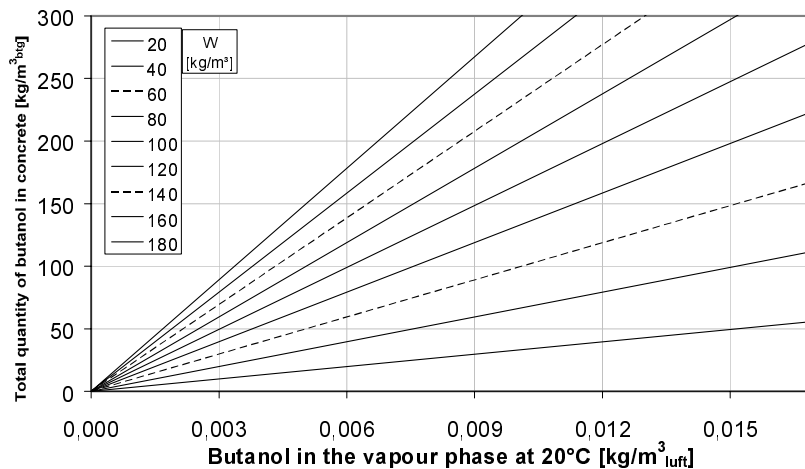


Fig. 8.3 Storage capacity according to bound.1; C_{tot} as a function of c_{air} and w at constant temperature, 20°C . $k_1 = 165 \text{ (m}^3\text{/kg)}$.

The storage capacity for $w = 100 \text{ kg/m}^3$ is now $16.5 \cdot 10^{-3}$.

Bound,2

Binding of OC need not be directly proportional to moisture content. It is possible that OC binds to all surfaces in the concrete, but mainly in the cement gel.

In this case also, the binding capacity is slightly moisture dependent. In Equation 8.7, this moisture dependence is denoted by the constant k_2 . The part of the binding capacity that is not moisture dependent is denoted by the constant b . The value of b should be highly dependent on texture, and perhaps mainly on the specific surface of the concrete.

$$C_{bound,2} = (k_2 \cdot w + b) \cdot c_{air} \quad \left[\frac{kg}{m^3_{mtrl}} \right] \quad (8.7)$$

By assuming that the storage capacity calculated in Equation 8.3 holds for $w = 100 \text{ (kg/m}^3\text{)}$ and that k_2 is equal to $k_0 (= S / \rho_w \cdot c_{sat})$, i.e. $4.53 \text{ (m}^3\text{/kg)}$, the value of b is $16.1 \cdot 10^3 \text{ (-)}$. Storage capacity with $C_{bound,2}$ is now almost independent of the moisture content; see Fig. 8.5. For $w = 100 \text{ kg/m}^3$, the storage capacity is still $16.5 \cdot 10^{-3}$.

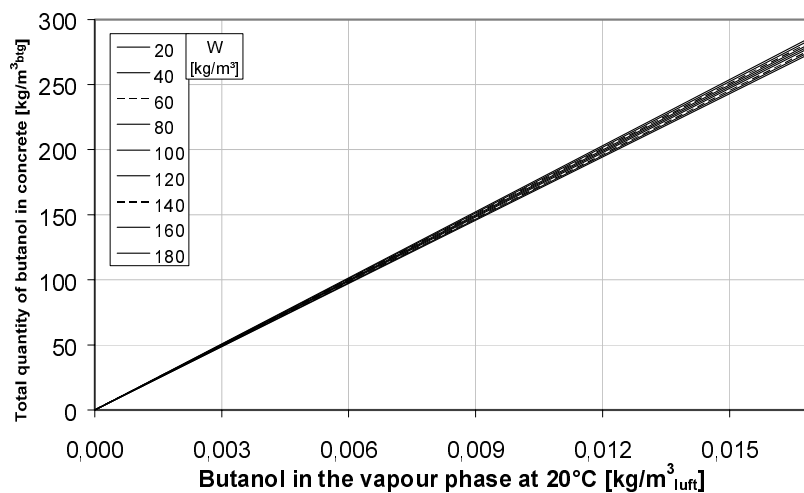


Fig. 8.5 Storage capacity according to bound.2; C_{tot} as a function of c_{air} and w at constant temperature, 20°C . $k_2 = 4.53 \text{ (m}^3\text{/kg)}$ and $b = 16.1 \cdot 10^3 \text{ (-)}$.

8.2 Evaluation of q_R for butanol from experiments

The rate of formation q_R is of critical importance for the incidence of OC in floor constructions of high moisture content. The value of q_R can be determined from experiments in which the moisture status and the total quantity of OC formed are known. The relationship between q_R , moisture status and total quantity of OC formed is given in Equation 7.7.

$$Q = \int_{t_1}^{t_2} \frac{q_{R,\max}}{1 - RH_{crit}} \cdot (RH_{act}(t) - RH_{crit}) \cdot dt \quad \left[\text{kg}/\text{m}^2 \right] \quad (8.8)$$

The total quantity of OC (Q) that has been produced in the material combination can be calculated by drawing up a mass balance. The total quantity of OC produced is equal to the sum of the quantity of OC stored in the concrete and the quantity of OC emitted from the construction, if the quantity that may have been stored in the flooring and the film of adhesive is ignored.

The total quantity of OC bound in the concrete can be evaluated from the experiment described in Section 4.3. In the original study by Wengholt Johnsson (1995) in which the test specimens were used, the emission factor EF and the moisture distribution were also measured. It is thus possible to draw up a mass balance for test specimen NSt2.

8.2.1 Quantity of OC emitted from the sample through the flooring

The emission factor, i.e. the flow, was measured on five occasions in the investigation by Wengholt Johnsson (1995). These measurements, together with the initial value $EF \sim 0$ at the time the flooring was laid, give a good estimate of the total quantity of OC emitted from the test specimen over a period of about 450 days.

The total quantity of OC emitted from the test specimen can be calculated by integrating the flow from the test specimen over the period during which emission proceeds; see Equation 8.9.

$$Q_{emit} = \int_0^t q \cdot dt \quad \left[\text{kg}/\text{m}^2 \right] \quad (8.9)$$

Table 8.1 Summary of the flows measured during emission measurements on NSt2; values of EF ($\mu\text{g}/(\text{m}^2 \cdot \text{h})$) from Wengholt Johnsson (1995).

Days	Butanol	
	EF [$\mu\text{g}/\text{m}^2 \cdot \text{h}$]	q [$\text{kg}/\text{m}^2 \cdot \text{s}$]
0	$\sim 0^*$	$\sim 0^*$
76	2470	$686 \cdot 10^{-12}$
107	1790	$497 \cdot 10^{-12}$
174	940	$261 \cdot 10^{-12}$
230	490	$136 \cdot 10^{-12}$
388	100	$27 \cdot 10^{-12}$

* Initial value, negligible emission when flooring is laid

On day 0, in Table 8.1, the flooring was bonded to the test specimen. The concrete was casted 29 days before day 0. It is assumed that emission of OC caused by decomposition of the flooring starts after the flooring is laid. The emission curve for butanol from NSt2 is plotted in Fig. 8.6.

The reason for the rapid drop in the rate of emission in Fig. 8.6 may be that concentration below the flooring decreased due to cessation of the reaction. It is reasonable to suppose that the reaction ceased since the moisture level at the surface of the concrete dropped below the critical value during the measurement period; see Subsection 8.2.3. This may be due to leakage at the edge of the test specimen, between the flooring and the steel mould.

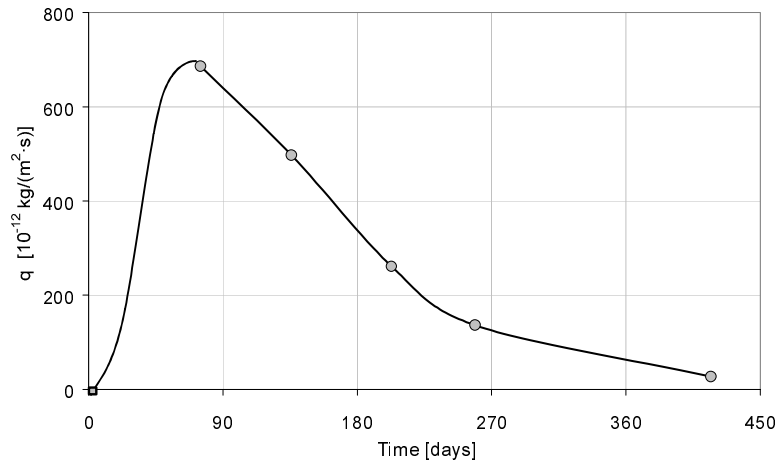


Fig. 8.6 Emission of butanol from test specimen NSt2 as a function of time. Values from Wengholt Johnsson (1995).

The integral in Equation 8.9 above can be determined by calculating the area below the curve. The area is then multiplied by a scale factor to obtain the results in the correct units.

Table 8.2 Total emitted quantity of butanol. Evaluated from Fig. 8.6.

Quantity	Unit	Butanol
Area	$\left[10^{-9} \cdot \frac{\text{kg}}{\text{m}_{\text{mrl}}^2 \cdot \text{s}} \cdot \text{dygn} \right]$	100.5
Q_{emit}	$\left[10^{-3} \cdot \text{kg} / \text{m}_{\text{mrl}}^2 \right]$	8.69

8.2.2 Quantity of OC stored in the concrete

The concentration of free butanol in the concrete, c_{air} in specimen NSt2 (c1.2) is plotted in Fig. 8.7.

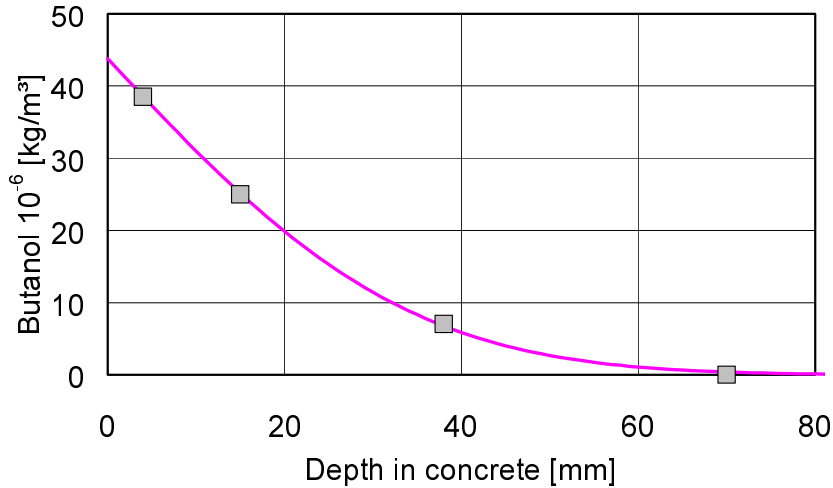


Fig. 8.7 Free concentration c_{air} of butanol in test specimen NSt2 as a function of depth. Values measured about 2 years after the floor had been laid

The total concentration C_{tot} can be calculated from the storage capacity, as shown in Equation 8.10.

$$C_{tot} = c_{air} \cdot \frac{dC_{tot}}{dc_{air}} \quad \left[\text{kg/m}^3_{\text{mtrl}} \right] \quad (8.10)$$

The total quantity of OC in the test specimen is calculated by integrating C_{tot} over the penetration depth

$$Q_{store} = \int_0^L C_{tot} \cdot dx \quad \left[\text{kg/m}^2 \right] \quad (8.11)$$

Table 8.3 Values of c_{air} and C_{tot} calculated from Table 4.7. $C_{tot,0}$ is calculated with the storage capacity according to Equation 8.2, and $C_{tot,1,2}$ according to Equation 8.3.

Depth [10 ⁻³ m]	c_{air} [kg/m ³ _{air}]	$C_{tot,0}$ [kg/m ³ _{mtrl}]	$C_{tot,1,2}$ [kg/m ³ _{mtrl}]
4	$38.5 \cdot 10^{-6}$	$18.2 \cdot 10^{-3}$	$672 \cdot 10^{-3}$
15	$25.0 \cdot 10^{-6}$	$11.8 \cdot 10^{-3}$	$429 \cdot 10^{-3}$
38	$7.0 \cdot 10^{-6}$	$3.3 \cdot 10^{-3}$	$121 \cdot 10^{-3}$
70	0	0	0

The integral in Equation 8.11 above is solved by calculating the area below the curve in Figure 8.7. This area is $978 \cdot 10^{-6}$ (mm · kg/m³_{air}). The area is then multiplied by a scale factor to obtain the results in the correct units.

The results for the storage capacity described in two different ways are set out in Table 8.4.

Table 8.4 Values of Q_{store} for butanol in concrete. Areas.

	Unit	Bound ₀	Bound _{1,2}
Q_{store}	$[10^{-3} \cdot \text{kg} / \text{m}^2_{\text{mtrl}}]$	0.461	16.75

8.2.3 Quantity of OC produced in the reaction

The quantity of OC produced in the construction, Q_{prod} can be described as a function of the maximum rate of formation $q_{R,max}$ if the moisture distribution RH_{act} and the critical moisture level RH_{crit} prevailing during the period are known. The relationship is described in Equation 8.8.

In NSt2, the moisture level at the time the flooring was laid was determined as 95% RH in the measuring tube at depth 0.4d; see Fig. 8.8. Measurement was made by Method No 1 described in Subsection 2.3.1. On day 255 after the flooring had been laid, the moisture level at the concrete surface was measured. For this measurement, pieces of concrete were broken out from an identical test specimen. The pieces were immediately placed in a glass test tube and the moisture level was measured as ca 88% RH. Measurement was performed by Method No 3 described in Subsection 2.3.1.

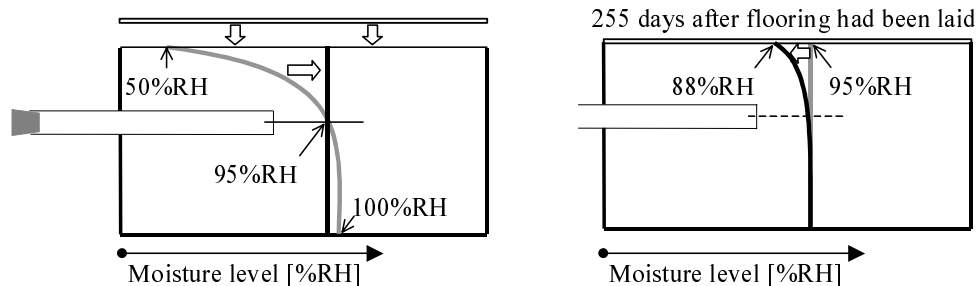


Fig. 8.8 Moisture distribution in test specimen before the flooring is laid, after redistribution of remaining "construction water", and 255 days after the flooring had been laid. Measurements according to Wengholt Johnsson (1995).

According to Nilsson (1979), the moisture level measured at 0.4d, i.e. at 40% of the depth, is equal to the average moisture distribution in the concrete after redistribution. Fig. 8.9 shows the results of calculations of the moisture status at the top of the concrete. The calculations were performed by the forward finite difference method and were based on the RH levels in Fig. 8.8.

During the first 29 days the moisture level drops from 100% to ca 55% RH in the surface of the concrete. After the flooring is laid, the moisture in the concrete is redistributed so that the moisture level at the surface rises. After about 30 days RH_{crit} is exceeded at the surface. Moisture level below the flooring decreases rapidly. The cause may be diffusion of vapour through the flooring and leakage between the flooring and the steel mould.

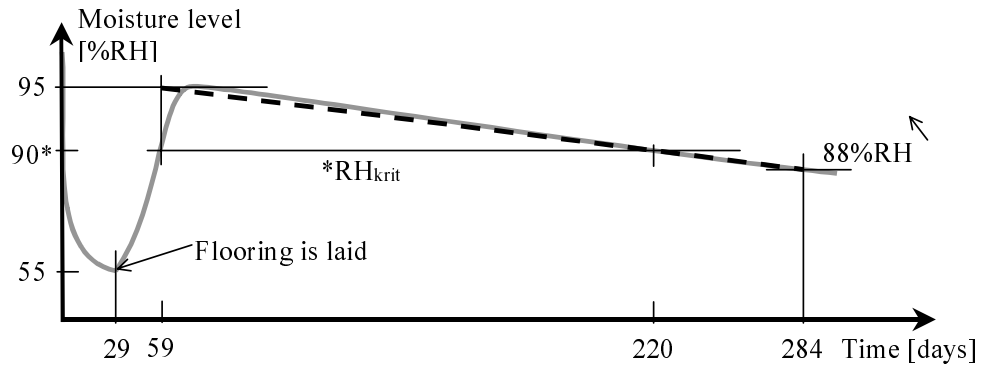


Fig. 8.9 Distribution of moisture in the surface of the test specimen before the flooring is laid, after redistribution and 255 days later. According to Wengholt Johnsson (1995).

The concrete used in NSt2 was B4 as described in Section 2.1. Moisture increment from the adhesive has no major effect on the moisture level because of the high moisture capacity of the concrete. The significance of the moisture of adhesive is examined in depth in Chapter 5.

During the time that RH_{act} is greater than RH_{crit} , the moisture level at the surface of the concrete can be approximated by a straight line. The highest moisture level occurs in the beginning of the period when the remaining construction water has been redistributed. The moisture level thereafter decreases monotonically as shown in Fig. 8.10.

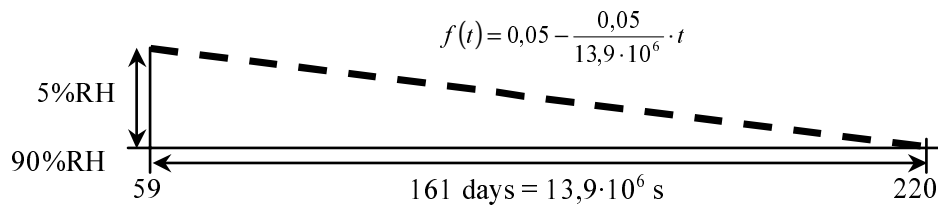


Fig. 8.10 Approximate moisture distribution at the surface of test specimen NSt2 during the time that RH_{act} is greater than RH_{crit} .

If we assign the value 90% RH to RH_{crit} , Equation 8.8 can be simplified to

$$Q_{prod} = \frac{q_{R,max}}{0,1} \cdot \int_{t_1}^{t_2} (RH_{act}(t) - 0,9) \cdot dt \quad [kg/m^2] \quad (8.12)$$

In this special case, the function for $RH(t)$ can be rewritten as the equation for the straight line in Fig. 8.10. $RH(t) = 0,05 - (0,05/13,9 \cdot 10^6) \cdot t$.

$$Q_{prod} = \frac{q_{R,max}}{0,1} \cdot \int_0^{13,9 \cdot 10^6} \left(0,05 - \frac{0,05}{13,9 \cdot 10^6} \cdot t \right) \cdot dt \quad [kg/m^2] \quad (8.13)$$

After integration, we have

$$Q_{prod} = \frac{q_{R,max}}{0,1} \cdot \left[0,05 \cdot t - \frac{0,05}{13,9 \cdot 10^6} \cdot \frac{t^2}{2} \right]_0^{13,9 \cdot 10^6} \quad [kg/m^2] \quad (8.14)$$

After the limits are inserted, the relationship between Q_{prod} and $q_{R,max}$ is

$$Q_{prod} = \frac{q_{R,max}}{0,1} \cdot \frac{0,05}{2} \cdot 13,9 \cdot 10^6 = q_{R,max} \cdot 3,5 \cdot 10^6 \quad [kg/m^2] \quad (8.15)$$

8.2.4 Mass balance

For the mass balance to be correct, the sum of the emitted and stored quantities of OC must be equal to the produced quantity. The rate of formation can be described by using the produced quantity of OC according to Equation 8.16. The quantities formed and the rates of formation are summarised in Table 8.5.

$$Q_{emit} + Q_{store} = Q_{prod} = q_{R,max} \cdot 3,5 \cdot 10^6 \quad [kg/m^2] \quad (8.16)$$

Table 8.5 Quantities formed and rates of formation. Bound,0 is calculated with the storage capacity according to Equation 8.2, and Bound,1,2 according to Equation 8.3.

	Unit	Bound,0	Bound,1,2
Q_{prod}	$[10^6 \cdot kg / m_{mtrl}^2]$	$3,5 \cdot q_{R,max}$	$3,5 \cdot q_{R,max}$
Q_{emit}	$[10^{-3} \cdot kg / m_{mtrl}^2]$	8.69	8.69
Q_{store}	$[10^{-3} \cdot kg / m_{mtrl}^2]$	0.46	16.75
$q_{R,max}$	$[10^{-9} \cdot kg / m_{mtrl}^2]$	2.6	7.3

The maximum rate of formation for butanol, evaluated with bound,0, is calculated by inserting the values in Table 8.5 into Equation 8.16.

$$q_{R,max}^{Bound0} = \frac{Q_{emit} + Q_{store}}{3,5 \cdot 10^6} = \frac{8,69 \cdot 10^{-3} + 0,46 \cdot 10^{-3}}{3,5 \cdot 10^6} = \frac{9,15 \cdot 10^{-3}}{3,5 \cdot 10^6} = 2,6 \cdot 10^{-9} \quad (8.17)$$

The maximum rate of formation for butanol, evaluated with bound,1 or bound,2, is calculated by inserting the values in Table 8.5 into Equation 8.16.

$$q_{R,max}^{Bound1,2} = \frac{Q_{emit} + Q_{store}}{3,5 \cdot 10^6} = \frac{8,69 \cdot 10^{-3} + 16,75 \cdot 10^{-3}}{3,5 \cdot 10^6} = \frac{25,44 \cdot 10^{-3}}{3,5 \cdot 10^6} = 7,3 \cdot 10^{-9} \quad (8.18)$$

8.3 Discussion

The evaluation in this chapter has been made in one case, from one single experiment. Because of this, plus the fact that there is reason to suspect that leakage had occurred in the experiment between the flooring and the steel mould, the results are unreliable.

The binding capacity calculated according to bound,0 appears to be far too small. It implies that only 1/20 of the OC formed, as set out in Table 8.5, penetrates into the concrete. This does not accord with the experiences related by Kumlin (2000). Measurements made after the flooring is replaced show that the value of EF is still quite high, although no reaction is taking place. This phenomenon can be explained by assuming that the value of c_{air} in the concrete is high because Q_{store} is large. With a binding capacity calculated according to bound,1 or bound,2, about two-thirds of the decomposition products have migrated down into the concrete, which may be much more plausible.

There is an ambiguity regarding the value of the surface concentration c_s . In evaluating OCIC, it is assumed to have been constant, $45 \cdot 10^{-6}$ (kg/m^3_{air}), for two years. At the same time, when EF is evaluated, it is assumed to have given rise to a flow through a flooring (of constant resistance). EF is assumed to vary in such a way that c_s decreases from its peak value of $2540 \cdot 10^{-6}$ to $100 \cdot 10^{-6}$ during the first year. The value of c_s may possibly decrease during the second year in such a way that both these assumptions are correct.

The drop in the value of RH in the "adhesive layer", shown in Fig. 8.9, is very rapid. Since this early version of test specimen had no seal around its edge, the rapid drop may be due to leakage between the flooring and the steel mould.

The drop may also be due to an "unknown" error in measurement. It is usual for widely different values of RH to be measured in concrete near places where the adhesive has been hydrolysed. One common explanation for this phenomenon is that the properties of the RH probe are affected by OC. Different RH probes may be affected in different ways.

9 Comparison of measurements and calculations with the model

In this chapter, comparisons are made between some measurements previously described in this study and calculations with the computer model described in Section 7.9.

A comparison is first made with respect to the increase in RH that occurs when moisture of adhesive is adsorbed into the concrete surface. This is described in Section 5.1. Measurements of moisture level, emission from the surface and OCIC, described in Section 8.2, are then compared. Finally, some comparisons are made between the FLEC measurements and the model.

9.1 Material data for the calculations

Material data for calculation of the model were primarily obtained from the literature. Where material data were not available, values were evaluated or assigned.

Generally speaking, material data concerning moisture transport and fixation were taken from the literature, while corresponding values for OC were evaluated in this study or were assumed.

Data according to Hedenblad (1996) apply for old well cured concrete. In the absence of data for young concrete, these data were also used for concretes C1-C4 which, especially in the test with moisture of adhesive, are much younger.

9.1.1 *Material data for the transport and fixation of moisture*

Material data for the transport and fixation of moisture are needed both in calculating adsorption of moisture of adhesive into the concrete surface and in calculating emissions from floor systems. In the latter case this is critical since it is the moisture level in the surface of the concrete that governs the duration of the reaction. For the fixation of OCIC the moisture level in the concrete is also critical.

In the calculations of moisture adsorption, material data for three different grades of concrete, C1, C3 and C4 according to Table 2.1, were used. In calculating EF from the floor system, material data for concrete grade C4 were used. Material data for these are taken from Hedenblad (1996), with the exception of w_{\max} that was evaluated from Fig. 7.12.

Moisture fixation

Moisture fixation in concrete takes place through adsorption into the internal material surfaces and capillary condensation in small pores, in the way described in Section 7.5.

In the model, only one sorption isotherm per concrete is used to describe the relationship between RH and moisture content. The hysteresis effect which occurs when the concrete passes from the dry to the wet state, or vice versa, is

ignored. This simplification may have a very great effect, since a small moisture increment can give rise to a large increase in RH in the cases where the moisture content of the concrete is located on the desorption isotherm. When this occurs, the moisture status, instead of being described by desorption isotherms, Fig. 7.12, changes into being described by absorption isotherms, Fig. 7.11.

In the model simplified sorption isotherms have been used. The isotherms are described by three straight lines which are determined by the origin, w_{max} at 100% RH, and by a further two points where the gradient of the line changes. These points for the sorption isotherms are set out in Table 9.1. Fig. 9.1 shows the simplified isotherms which consist of three straight lines.

The calculations have been simplified by making the sorption isotherms for concretes C1 and C3 equal. In this way, the values from Hedenblad (1996) can be used in all cases.

Table 9.1 Points of gradient change for simplified isotherms for moisture in concrete.

Concrete	C1 / C3	C4
W [kg/m ³]	RH [%]	RH [%]
0	0	0
50	50	65
100	90	90
115	100	–
150	–	100

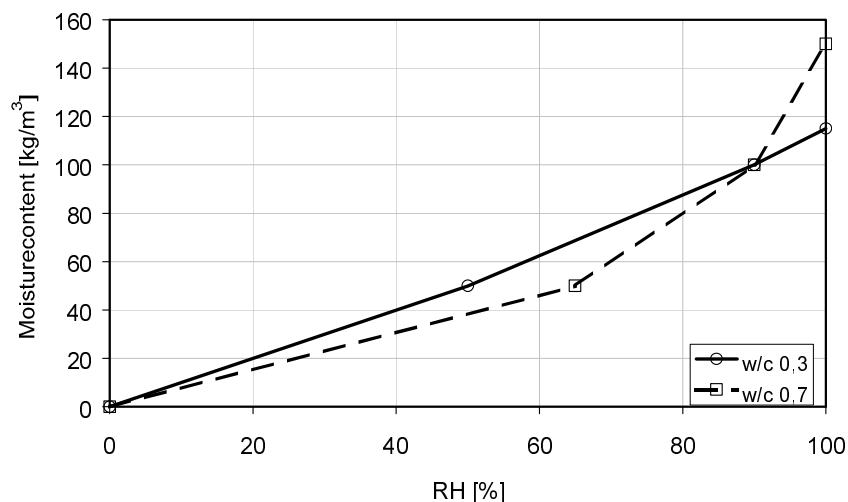


Fig. 9.1 Sorption isotherms for moisture in concrete. The values for C1 and C3 have been put equal. The figure is based on values from Hedenblad (1996).

Corresponding material data for moisture fixation in the adhesive were not found in the literature. In the model the adhesive has been given a simplified sorption isotherm in the same way as the concrete. However, the sorption isotherm for the adhesive consists of only two straight lines. These are determined by the origin, w_{ad} at 100% RH, and by $w_{ad}/8$ at 96% RH.

The maximum value of w_{ad} has been calculated as $80 \cdot 10^{-3}$ kg/m². According to the values in Table 2.4, the water content of a wet adhesive is approximately $400 \cdot 10^{-3}$ kg/m³. And, according to Sjöberg & Wengholt Johnsson (1999), when the adhesive is applied it is spread at a rate of approximately 5 l/m².

Moisture transport

In the model, moisture transport is calculated with the vapour content as the driving potential; see Section 7.6. The diffusion coefficients δ_{tot} , taken from Hedenblad (1996), are set out in Table 9.2. Analogously with fixation of moisture in concrete, material data for concretes C1 and C3 have been put equal.

In the model a simplified curve has been used for the moisture dependence of the diffusion coefficient. Analogously with the simplification of the sorption isotherm above, this curve consists of a number of straight lines. The points of gradient change for these straight lines are given in Table 9.2.

Table 9.2 Points of gradient change for simplified curve showing the moisture dependence of the diffusion coefficient in concrete.

Concrete W [kg/m ³]	C1 / C3 δ_{tot} [m ² /s]	C4 δ_{tot} [m ² /s]
0	$0.13 \cdot 10^{-6}$	$0.17 \cdot 10^{-6}$
70	$0.2 \cdot 10^{-6}$	$0.17 \cdot 10^{-6}$
100	$0.5 \cdot 10^{-6}$	$1.3 \cdot 10^{-6}$
115	$0.7 \cdot 10^{-6}$	–
120	–	$9.0 \cdot 10^{-6}$
150	–	$40.0 \cdot 10^{-6}$

According to Hedenblad (1996), the transmission resistance Z_{fc} of the flooring to moisture is $2 \cdot 10^6$ (s/m) for an impermeable (PVC) flooring, and $0.1-0.2 \cdot 10^6$ (s/m) for an open textured (linoleum) flooring.

Values of the transmission resistance Z_{ad} of films of adhesive to moisture were not found in the literature. In the calculations Z_{ad} was given the value 600 s/m. In view of the fact that moisture transport may occur in the wet adhesive, it was decided to make this value low.

9.1.2 **Material data for the transport, formation and fixation of butanol**

Material data for the transport and fixation of butanol in concrete were not found in the literature. These values, together with the transmission resistances of floorings to butanol, are required for calculations with the model in Section 7.9. The values used in the calculations were either evaluated in this study or assumed.

A total of five different sets of values have been used in calculations in this study; see Table 9.3. Two of the calculation cases, Calc. 1 & 3, are used for the comparisons in this chapter. All the calculation cases are used in the parametric study in Chapter 10. All results from all calculation cases are set out in Appendix No 4.

All the values for transport and fixation of butanol in concrete are constant, i.e. their possible moisture dependence is ignored.

Values of $q_{R,max}$ in Calc.2 – 4, are taken from the evaluation in Table 8.5, but they have been slightly adjusted because of the limitations in the calculation model. Values of δ_{OC} in Calc.4 – 5, are taken from evaluation of measurements in Section 4.2.

"Bound" denotes different ways of describing storage capacity; see Subsection 8.1.3. Factor b is that part of fixation which is not dependent on moisture content in bound,3.

Table 9.3 Values for calculation of transport and fixation of butanol in concrete C4.

Quantity	Unit	Calc.1	Calc.2	Calc.3	Calc.4	Calc.5
$q_{R,max}$	$[10^{-9} \text{ kg}/(\text{m}^2 \cdot \text{s})]$	0.03	0.26	2.6	7.3	7.3
δ_{OC}	$[10^{-9} \text{ m}^2/\text{s}]$	2.5	2.5	2.5	93	93
Bound	–	0	0	0	1	2
S	$[\text{kg}/\text{m}^3]$	0.077	0.077	0.077	2.8	0.077
k_x	$[\text{m}^3/\text{kg}]$	4.53	4.53	4.53	165	4.53
b	$[10^3]$	–	–	–	–	16.1

According to Table 4.3, the transmission resistance R_{fc} of the flooring to butanol is $3.7 \cdot 10^6$ (s/m) for impermeable (PVC) flooring, and $2.9 \cdot 10^6$ (s/m) for open textured (linoleum) flooring. The resistance to moisture transport of the film of adhesive, Z_{ad} , is given the value $0.6 \cdot 10^3$ (s/m).

9.2 Adsorption of moisture of adhesive

In this chapter, the results of three measurements of the adsorption of moisture of adhesive, described in Section 5.1, are compared with calculations. The calculations are made with the model and are based on the material data described above.

In each calculation, the original moisture distribution, before the flooring was bonded, was estimated from the measured values. Its value is given for each case together with the calculated moisture curve.

9.2.1 Calculation of experiment No 1, 300 g moisture of adhesive per m² of concrete C1, w/c ratio 0.32.

In Fig. 9.2, the measured values from the experiment with a large quantity of adhesive are plotted as dots and triangles, and the results of calculations as lines.

The dots show the results of measurements of moisture level before the flooring is bonded. The triangles are values of moisture level measured 133 hours after the flooring was bonded. RH in the concrete had by then reached its maximum value; see Fig. 5.1.

The lower full curve in Fig. 9.2 is the estimated moisture distribution before the flooring is bonded. This moisture distribution is assumed in the calculations to be the initial value. The upper full curve shows the calculated moisture distribution after 133 hours.

On repeated calculations, the value of the diffusion coefficient δ_{tot} in the areas of high moisture increased by about 10 times. The calculation results for this are shown with the dashed line in Fig. 9.2.

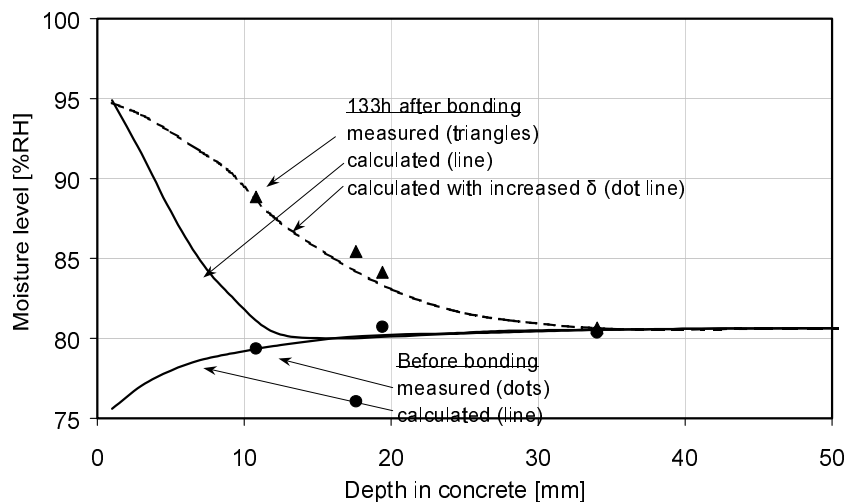


Fig. 9.2 Calculated and measured moisture distribution at different times before and after the PVC flooring was bonded with a large quantity of adhesive to a concrete of low w/c ratio (C1).

The measured and calculated moisture curves are plotted in Fig. 9.3. The measured moisture curve refers to a depth 11 mm below the surface. The calculated moisture curves refer to six different depths, 1, 3, 5, 7, 9 and 12 mm.

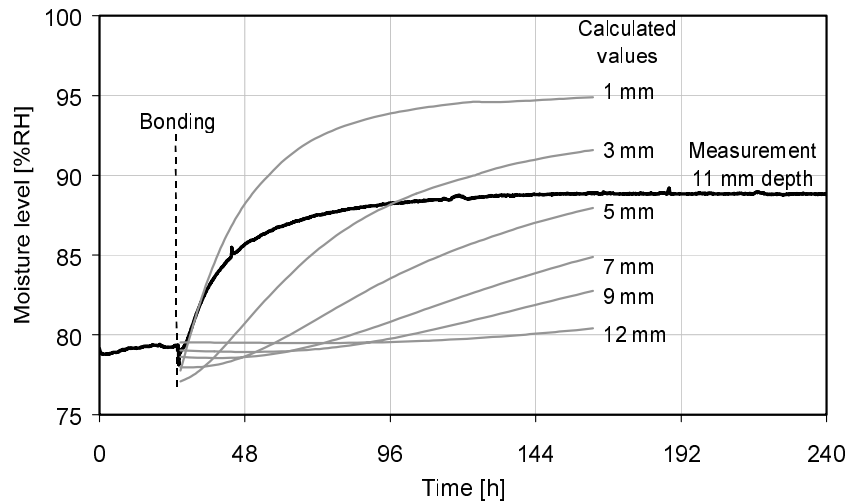


Fig. 9.3 Moisture distribution at different times after the PVC flooring was bonded with a large quantity of adhesive to a concrete of low w/c ratio (C1), compared with moisture level measured at 11 mm depth in the concrete.

9.2.2 Calculation of experiment No 2, 90 g moisture of adhesive per m² of concrete C3, w/c ratio 0.42.

In Fig. 9.4, the measured values from the experiment with a small quantity of adhesive are plotted as dots and triangles, and the results of calculations as lines.

The dots show the results of measurements of moisture level before the flooring is bonded. This moisture distribution is assumed in the calculations to be the initial value. The triangles are values of moisture level measured 58 hours after the flooring was bonded. RH in the concrete had by then reached its maximum value; see Fig. 5.2.

The full curve in Fig. 9.4 is the estimated moisture distribution before the flooring is bonded. The dashed curve shows the calculated moisture distribution after 58 hours.

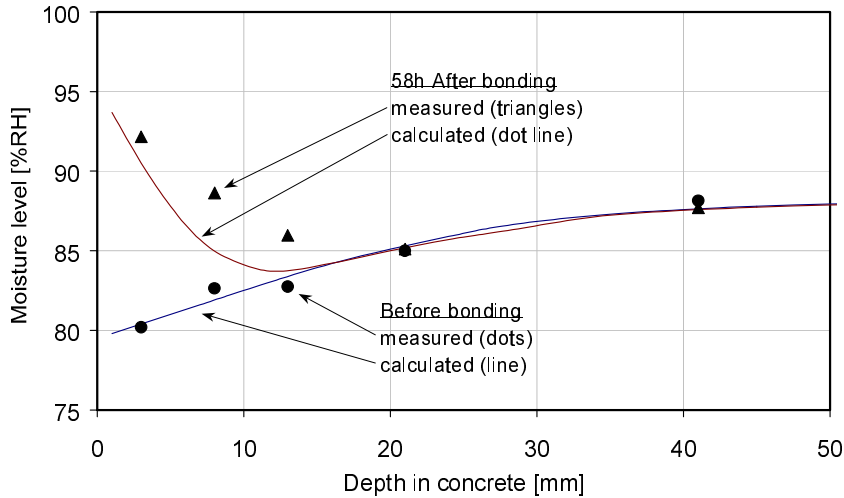


Fig. 9.4 Calculated and measured moisture distribution at different times before and after the PVC flooring was bonded with a small quantity of adhesive to a concrete of low w/c ratio (C3).

The measured and calculated moisture curves are plotted in Fig. 9.5. The measured moisture curve refers to depths 3 and 13 mm below the surface. The calculated moisture curves refer to five different depths, 1, 3, 5, 7 and 9 mm.

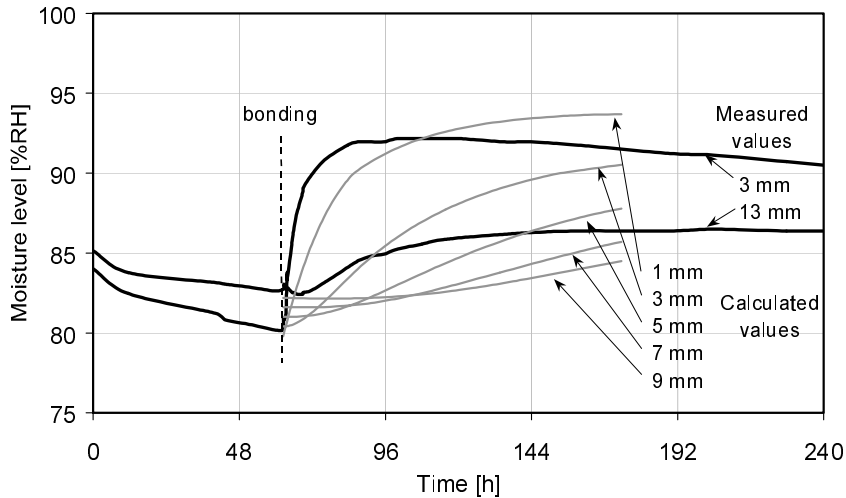


Fig. 9.5 Calculated moisture distribution at different times after the PVC flooring was bonded with a small quantity of adhesive to a concrete of low w/c ratio (C3), compared with moisture level measured at depths of 3 and 11 mm in the concrete.

9.2.3 Calculation of experiment No 3, 230 g moisture of adhesive per m² of concrete C4, w/c ratio 0.66.

In Fig. 9.6, the measured values from the experiment with a large quantity of adhesive on a concrete of high w/c ratio (C4) are plotted as dots and triangles, and the results of calculations as lines.

The dots show the results of measurements of moisture level before the flooring is bonded. This moisture distribution is assumed in the calculations to be the initial value. The triangles are values of moisture level measured 41 hours after the flooring was bonded. RH in the concrete had by then reached its maximum value; see Fig. 5.3.

The full curve in Fig. 9.6 is the estimated moisture distribution before the flooring is bonded. The dashed curve shows the calculated moisture distribution after 41 hours.

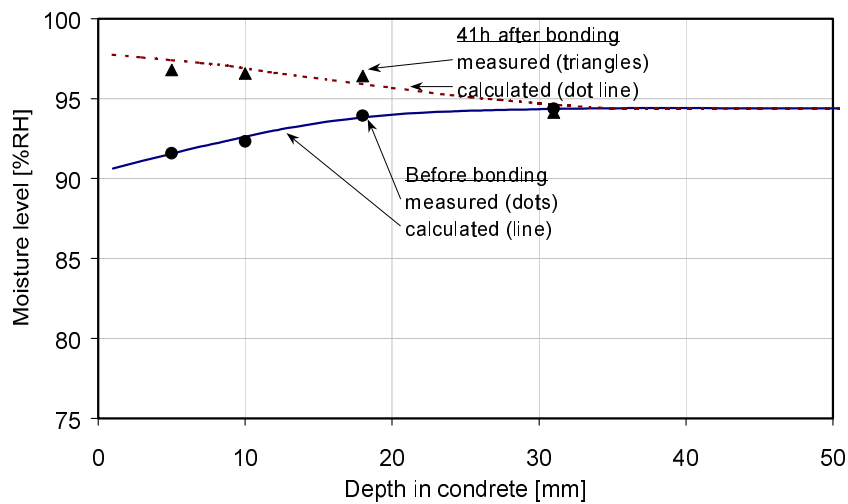


Fig. 9.6 Calculated and measured moisture distribution at different times before and after the PVC flooring was bonded with a large quantity of adhesive to a concrete of high w/c ratio (C4).

The measured and calculated moisture curves are plotted in Fig. 9.7. The measured moisture curve refers to a depth of 5 mm below the surface. The calculated moisture curves refer to four different depths, 5, 9, 12 and 20 mm.

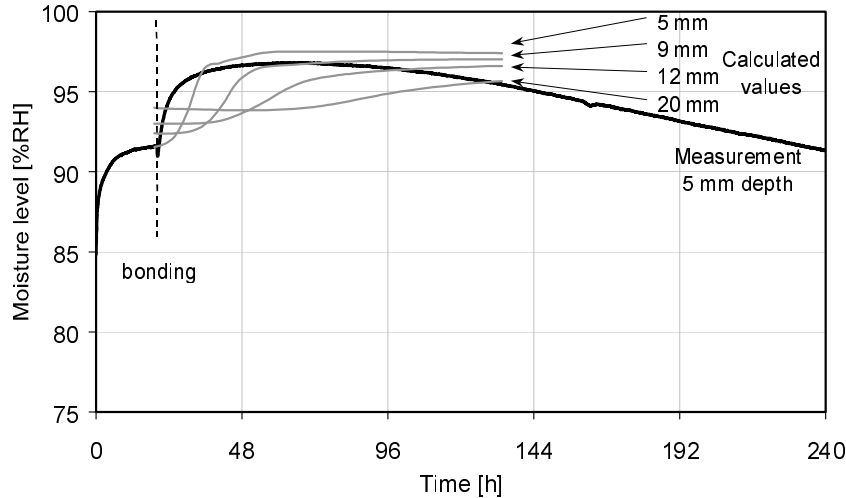


Fig. 9.7 Calculated moisture distribution at different levels at different times after the PVC flooring was bonded with a large quantity of adhesive to a concrete of high w/c ratio (C4), compared with moisture level measured at a depth of 5 mm in the concrete.

9.2.4 Discussion, adsorption of moisture of adhesive

The calculations show that the moisture of adhesive affects the moisture status of the concrete surface, although by not as much as indicated by the measurements.

The measurements show a more rapid rise in the RH level than the calculations. The measurements also show that the increase in moisture level occurs at a greater depth than shown by the calculations.

One important explanation of the difference between calculated and measured moisture curves, mainly the rate of increase, may be hysteresis. The moisture of adhesive wets the drying concrete surface. This wetting actually occurs in accordance with a hysteresis curve that is very flat compared with the desorption and adsorption isotherms in Table 9.1 and Fig. 9.1; what this means is that moisture capacity is much lower than in the calculations, which produces a greater, and more rapid, increase in RH.

Another explanation may be the simplified way of calculating moisture transport, according to which all transport occurs with the vapour content as the driving potential. Calculations may be in better agreement with measurements if transport is divided into two as described in Section 7.4, and is quantified more accurately.

9.3 Comparison with earlier measurements.

In this section, measurements of the moisture curve, emission from the surface and OCIC for test specimen NSt2, PVC flooring bonded to moist concrete of w/c ratio = 0.66 (C4), are compared with calculations with the model. The test specimen and the measurements are described in Section 8.2. Calculations are made with the model and are based on the material data described above.

9.3.1 Moisture curve

The moisture levels measured in test specimen NSt2 form the basis of the assumption in Subsection 8.2.3 concerning a moisture process which may have occurred at the surface of the concrete after the flooring had been bonded. The curve of the moisture process is plotted in Fig. 8.9.

In the calculations, the concrete dried, in a climate at 60% RH and 20°C, to 95% RH at 0.4d. Test specimen NSt2 had dried in a controlled climate room at 50% RH and 20°C. However, during a large proportion of the drying period, NSt2 was covered with plastic; Wengholt Johnsson (1995).

In Fig. 9.8 the moisture curve for NSt2 is compared with the calculated moisture curves. Calculations were made for both an impermeable PVC flooring of $Z_{fc} = 2 \cdot 10^6$ s/m, and for one of lower resistance, $Z_{fc} = 0.1 \cdot 10^6$ s/m. The lower resistance may represent possible leakage between the flooring and the steel mould for the test specimen, or a linoleum flooring.

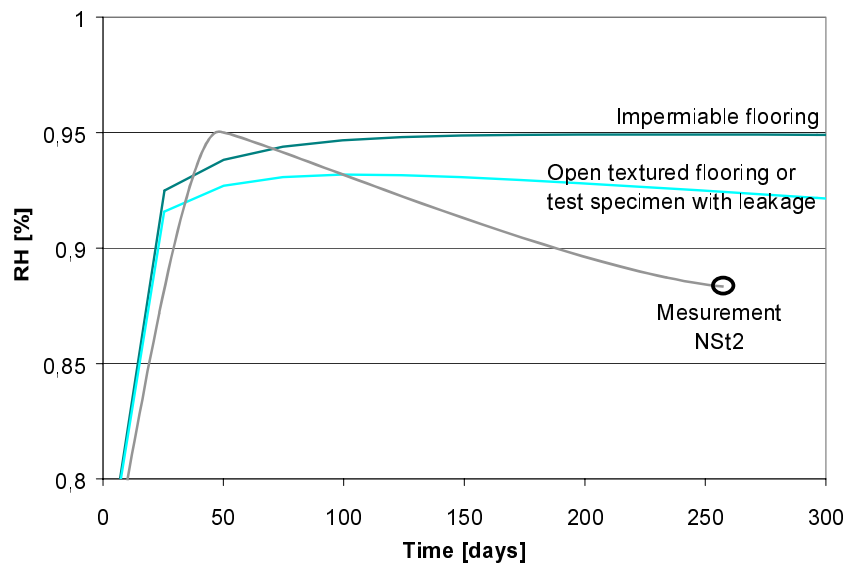


Fig. 9.8 RH at the surface of the concrete, comparison of test specimen NSt2 and values calculated with $Z_{fc} = 2 \cdot 10^6$ and $= 0.1 \cdot 10^6$ s/m.

9.3.2 Emission from the surface

In Fig. 9.9, measurements of emission from NSt2 over 500 days are compared with values calculated with Calc.3; see Table 9.3. The measured values for NSt2 are set out in Table 8.1. Full calculation results for Calc.3 are given in Appendix No 4.

In Fig. 9.9, values of emission from the surface, measured at different times after the flooring had been bonded, are plotted. The dashed curve may represent a least possible emission from NSt2. Prior to the first measurement at 76 days, emission may also have been greater than shown by the dashed curve.

The calculated emissions plotted in Fig. 9.9 apply for floor systems which had dried, at 0.4d, to the moisture levels shown, 91-96% RH, before the flooring was bonded. The calculations represent bonding of a PVC flooring during which the surface of the concrete receives 80 g/m² moisture of adhesive.

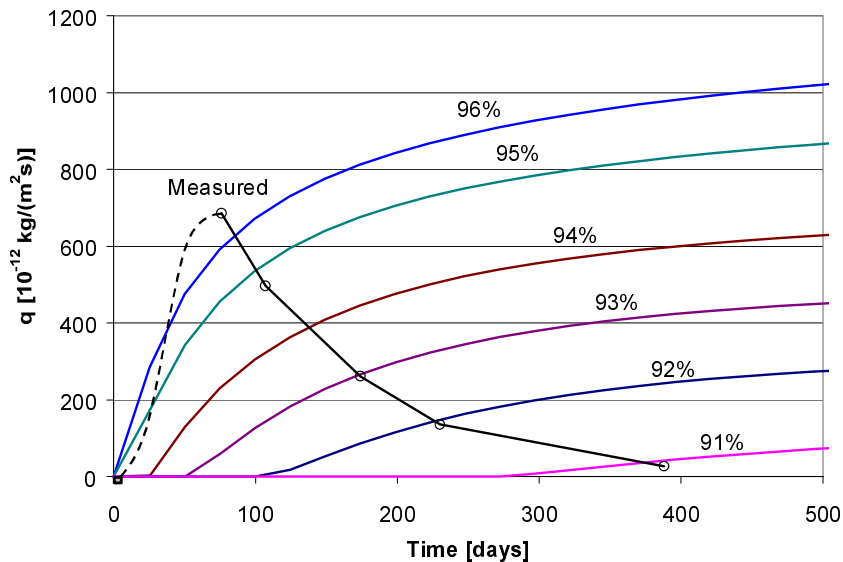


Fig. 9.9 Calculated emission from the surface, comparison with measured values from test specimen Nst2 where the dashed curve may represent a least initial emission. Emission for different moisture levels calculated with Calc.3 in the model.

The total (cumulative) emission from the surface as a function of time is set out in Fig. 9.10. The curves are based on the values in Fig. 9.9.

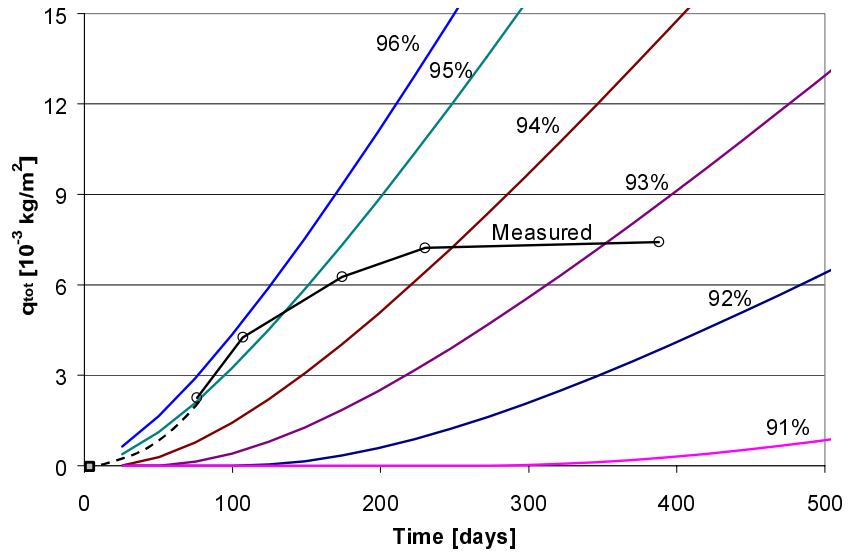


Fig. 9.10 Total emission from the surface, measured from test specimen NSt2 and calculated for different moisture levels with Calc.3.

9.3.3 OCIC

In Fig. 9.11 the measurements of OCIC in NSt2 after ca two years are compared with values calculated with Calc.1. The measured values for NSt2 are set out in Table 8.3. Full calculation results for Calc.1 are given in Appendix No 4.

The rings in Fig. 9.11 are measured values. The calculated profiles for OCIC apply for floor systems which had been dried, at 0.4d, to the moisture levels shown, 91-96% RH, before the flooring was bonded. The calculations represent bonding of a PVC flooring during which the surface of the concrete receives 80 g/m² moisture of adhesive. All profiles refer to the situation ca 2 years after the flooring was bonded.

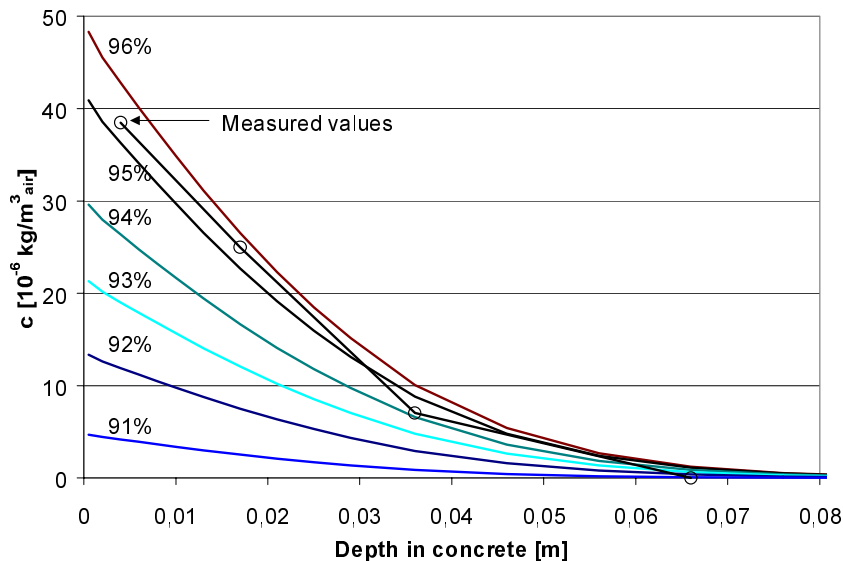


Fig. 9.11 Profile of butanol in the gas phase in concrete, calculated with Calc.1. All profiles refer to the situation ca 2 years after the flooring was bonded. Comparison with values measured in NSt2, represented by rings.

9.3.4 Discussion, previous measurements

Moisture process

The moisture process assumed for NSt2 cannot be recreated in the calculations. The high moisture level in the concrete surface immediately after bonding cannot be obtained when the moisture level must subsequently drop to 88% in ca 200 days.

The explanation may be an error in the assumed moisture process, large uncertainties in the measured results, or something else. What is most likely, however, is that the moisture process which was assumed on the basis of a few calculations was erroneous. The measurements were made at other, different depths, and may be subject to large measurement uncertainties.

It is unreasonable to suppose that the moisture content drops as rapidly as assumed in a test specimen in a steel mould with a "cover" of impermeable PVC flooring, even if there is leakage between the flooring and the steel mould.

Emission from the surface

The shape of the curve in Fig. 9.9 which represents emission measurements on NSt2 does not agree with the calculated curves. Emission from the surface is however about the same as that measured ca 3 months after the flooring had been bonded. After this the calculated values increase, while those measured decrease. The reason for the difference may be that in the calculations the concrete is moist below the flooring and new emissions are produced, while in the test specimen the reaction had ceased. Only the residual substances are being emitted.

The shape of the curve for the measurements has greater similarity to those calculated for an open (linoleum) flooring; see Fig. 9.14. Emission from the surface decreases because the reaction ceases. This happens when the moisture level in the surface of the concrete drops below the critical level.

Reaction in the test specimen may have ceased before the first measurement. In that case it is likely that the emission had been greater earlier, and it had decayed by the time of the first measurement. Decay may then proceed over a long time and it is the mean concentration in the surface which gives rise to the measured penetration profile. However, the simple calculation model used was not able to reproduce this.

OCIC

The penetration profile in the concrete according to Calc.1 agrees with the measured OCIC profile according to Fig. 9.11. However, the surface concentration in calculation case Calc.1 is so low that it cannot give rise to the high emissions which were measured; see Appendix No 4. According to Calc.1, the maximum emission during the first 3 years, when the moisture level in the concrete is 95% RH, is equal to $11 \cdot 10^{-12} \text{ kg}/(\text{m}^2 \cdot \text{s})$. The maximum measured emission from the test specimen is $686 \cdot 10^{-12} \text{ kg}/(\text{m}^2 \cdot \text{s})$. This means that the surface concentration in NSt2 may be more than 60 times as high as in the corresponding calculation which creates the same penetration profile.

In calculation case Calc.3, emission from the surface is about the same as that measured, but the penetration profile does not agree. The free concentration in the concrete surface is approximately 80 times too high; see Appendix No 4.

9.4 Comparison with new measurements

In this section, some of the measurements from the investigation in Sections 5.3 and 5.5 are compared with results calculated with Calc.3.

9.4.1 PVC flooring

Measurements made on specimens d4.2 - .6, d4.9 and d4.14 - .17, with PVC floorings, show an average EF of butanol of ca 1300 $\mu\text{g}/\text{m}^2\cdot\text{h}$ after 70 days, which corresponds to $380\cdot 10^{-12} \text{ kg}/(\text{m}^2\cdot\text{s})$, see Tables 5.9 - 5.11 and Fig. 5.15. After 180 days the average emission was about $150\cdot 10^{-12} \text{ kg}/(\text{m}^2\cdot\text{s})$.

The remaining specimens in investigation d4 are not compared with calculations since they were covered with screed or the surface was allowed to dry for a long time.

The means of the above measurements and calculations of emission from floor systems with bonded PVC floorings are plotted in Fig. 9.12. The calculated emissions refer to floor systems which had dried, at 0.4d, to the moisture levels shown, 91-96% RH, before the flooring was bonded. The calculations represent bonding of a PVC flooring where the concrete surface receives 80 g/m^2 moisture of adhesive.

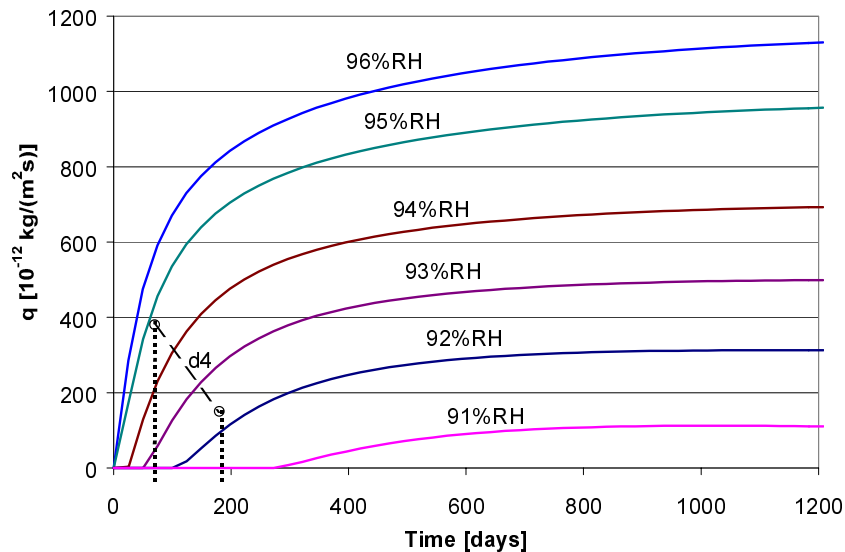


Fig. 9.12 Emission from the surface. The rings represent the means of several measurements in investigation d4. The curves are calculated with Calc.3 for different moisture levels.

Calculations show that the moisture level at the surface of the concrete will be redistributed to the level which prevailed at 0.4d before the flooring was bonded. The moisture level at the surface will then slowly decrease; see Fig. 9.13. This does not agree with the moisture curve assumed for NSt2; see Fig. 9.8. These specimens are similar to NSt2 and may therefore exhibit the same moisture process.

The rate of emission in the measurements also decreases much earlier than in the calculations, which agrees with the presumed drop in RH in the test specimen.

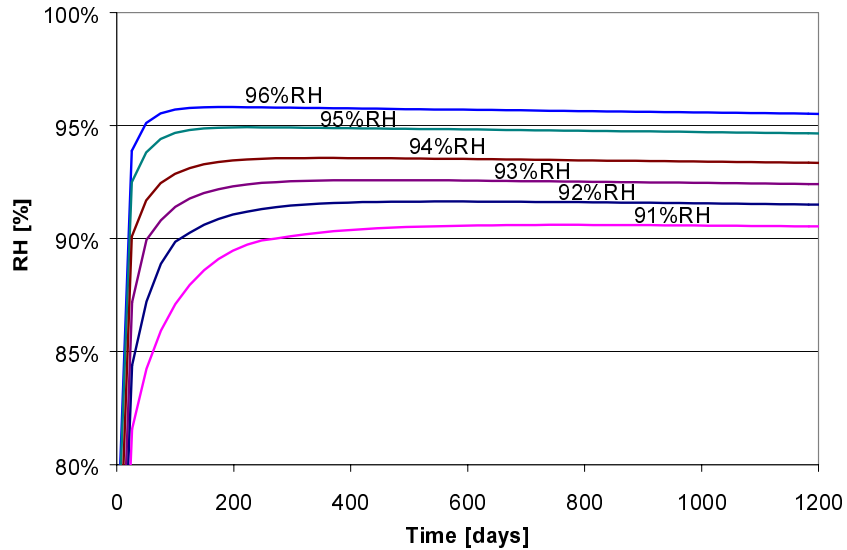


Fig. 9.13 RH at the surface of concrete. The values are calculated with Calc.3 for different moisture levels. It is assumed that Z_{fc} for the PVC flooring is $2 \cdot 10^6$ s/m.

9.4.2 Linoleum flooring

Measurements made on specimen d4.1 with linoleum flooring show no elevated emissions of butanol after 10 or 26 weeks; see Table 5.9. The moisture level measured at the surface before the flooring was laid was ca 72% RH.

Calculated values of emission from floor systems with bonded linoleum flooring are plotted in Fig. 9.14. The calculated emissions refer to floor systems which had dried, at 0.4d, to the moisture levels shown, 94-97% RH, before the flooring was bonded. The calculations represent bonding of linoleum flooring where the concrete surface receives $80/m^2$ moisture of adhesive.

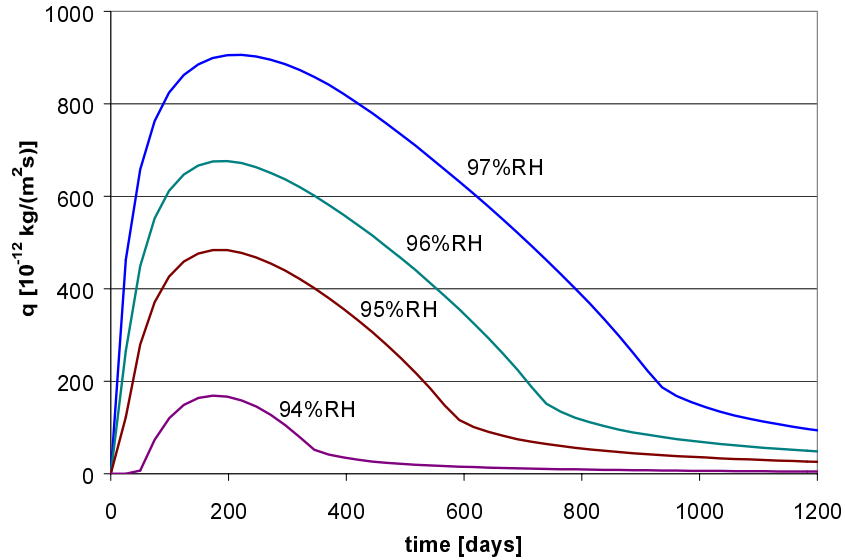


Fig. 9.14 Emission from the surface. The values are calculated with Calc.3 for different moisture levels.

Calculations show that floor systems which have a moisture level below 94% at a depth of $0.4d$ before the flooring is bonded do not exceed the critical moisture level at the surface; see Fig. 9.15. No decomposition products can therefore form, and consequently there is no emission from the surface.

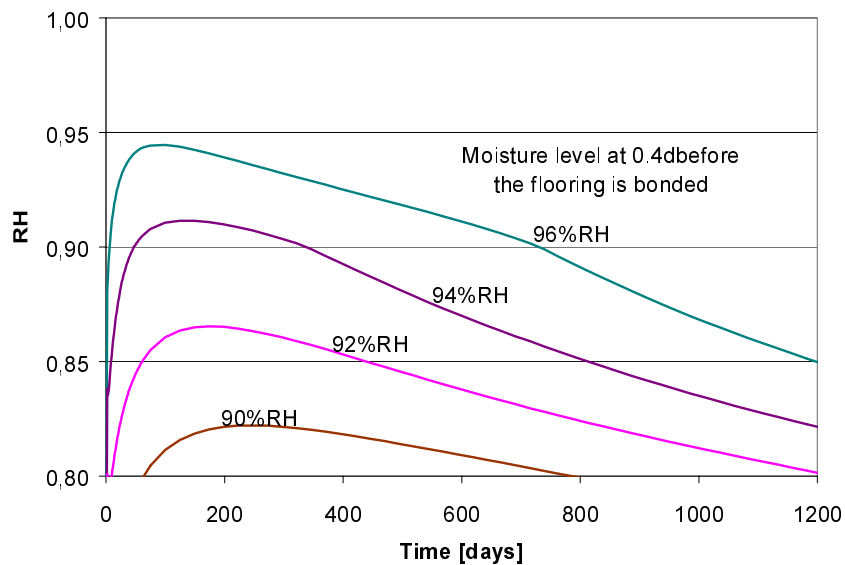


Fig. 9.15 RH at the concrete surface. The values are calculated with Calc.3 for different moisture levels. Z_{fc} for the PVC flooring is equal to $0.1 \cdot 10^6 \text{ s}/\text{m}$.

9.4.3 *Loose laid flooring*

Measurements made on specimens d2.01 and .02 with loose laid PVC flooring show no elevated emissions of butanol; see Table 5.2. This agrees with the model.

The model presupposes that there is adhesive present which can be hydrolysed so that butanol and other decomposition products may be formed. According to the model, mere contact between PVC flooring and a moist alkaline substrate produces no decomposition products.

9.4.4 *Discussion, new measurements*

PVC flooring

In Fig. 9.9 the shape of the curve representing measurements does not agree with the calculated curves. The measured values decrease over time, while the calculated ones increase.

The reason for the difference may be that in the calculation there is moisture below the flooring and new emissions are produced, while in the test specimen the reaction has ceased. Only the remaining substances are being emitted.

Reaction in the test specimen may have ceased before the first measurement because the moisture level at the surface had dropped below the critical value. In such a case it is likely that the emission had been greater before, which agrees with the calculations.

Linoleum flooring

On the assumption that the moisture level at the concrete surface had been lower than 90% the whole time, the measurements on d4.1 may agree with the calculations. According to the calculations, this implies that the moisture level at 0.4d was lower than 94% before the flooring was bonded. Possible leakage of moisture between the flooring and the steel mould might further reduce moisture level at the concrete surface.

Loose laid flooring

According to the model, in loose laying no decomposition products can be formed. The model presupposes that there is adhesive present which can be hydrolysed, so that butanol and other decomposition products may be formed. OC cannot therefore be emitted from the surface or penetrate into the concrete.

The values measured for these floor systems are very low. They may represent primary emissions from the flooring.

Secondary emissions may however occur from a floor system with loose laid flooring if one of the components of the flooring is decomposed by alkaline moisture. It is however not shown that this is the case.

OCIC deposited in the concrete slab may be transported upwards if a flooring is loose laid on a contaminated floor. This is analogous with the results shown in Appendix No 4.

Computer program

The material data used in the calculations were measured on old and well cured concrete, while the measurements were made on fresh concrete in which there was no time for the curing process to be completed. Since the structure of the concrete develops during the curing process, the properties of the materials also change. As a rule, in a fresh concrete of open pore structure, the transport processes take place at a higher rate.

The fact that the assumed moisture distribution in NSt2 could not be recreated in the calculations was a great limitation in comparisons between the model and measurements. It is a limitation not to be able to control the moisture level at the surface of the concrete other than by using different initial values and by assuming different material data in the calculation.

Moisture transport is treated in a simplified manner, with the vapour content as the driving potential. The effect due to hysteresis when the concrete surface is rewetted is ignored. These are two serious simplifications in the model. By improving the model with respect to transport and fixation of moisture, better results can be obtained in calculating the adsorption of moisture of adhesive.

Transport and fixation of butanol in concrete is yet another area which needs closer scrutiny. The assumptions in this study may have been too simple to produce a satisfactory result.

The computer model is written in Excel with Macro in Visual Basic. This means that it is not particularly powerful, and one single calculation may demand several hours of computer capacity.

10 Parametric study with the model

In this chapter the parameters in the model are subjected to analyses. An analysis is made first of all of the maximum acceptable moisture level at the surface when it is drying to different moisture levels in a number of drying climates.

An analysis is then made of some parameters which influence the emission of OC from the surface. The parameters analysed are the rate of formation, $q_{R,max}$, RH at 0.4d at the time the flooring is bonded, and the choice of flooring, whether PVC or linoleum.

This is followed by an analysis of some parameters which influence the transport and fixation of OCIC. The parameters analysed are the method of binding, $Bound_{0.2}$, RH at 0.4d at the time the flooring is bonded, and the choice of flooring, whether PVC or linoleum.

Finally, an analysis is made of emission from the surface and residual OCIC after "remedial treatment with exposure to the air" of a damaged floor. All the results from all calculations are set out in Appendix No 4.

10.1 Highest possible moisture status at the surface

It is the drying climate and the composition of the concrete which determine the available moisture capacity at the surface of the concrete. The diagrams below illustrate the results of calculations with the model in Section 7.9 regarding the highest moisture status that occurs at the surface after the application of 80 g/m² moisture of adhesive.

The term moisture status at the surface denotes the mean level in the topmost 2 mm of the concrete. Obviously, the moisture level in 2 mm of concrete is difficult to measure, but it can be calculated theoretically.

Before the moisture of adhesive is applied to the surface, the concrete has been dried to various moisture levels at the characteristic measurement depth, 0.4d. These moisture levels are set out along the x axis.

The drying climate before the flooring is bonded is represented by different curves in Fig. 10.1 and 10.2. The drying climate was varied between 40 and 70% RH. Any self desiccation of the concrete is disregarded.

The highest moisture level at the surface is read off along the y axis. The dashed line represents the moisture status that will be established after the remaining moisture in the concrete had come to a uniform level following bonding of an impermeable PVC flooring. The quantity of moisture of adhesive is then quite negligible in comparison with the construction water in the concrete.

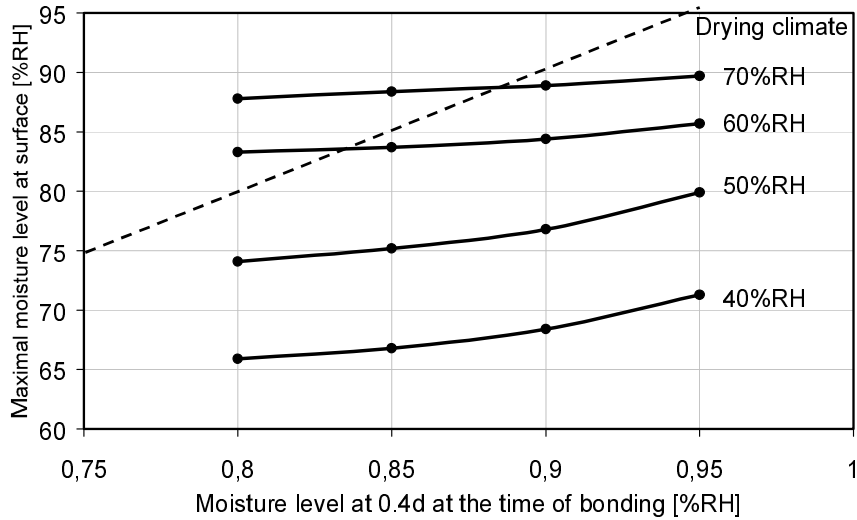


Fig. 10.1 Moisture level including moisture of adhesive at the surface of concrete C1 (w/c ratio=0.32) for different drying climates. The dashed line represents the moisture status that will be established after the remaining moisture in the concrete had come to a uniform level following bonding of an impermeable PVC flooring.

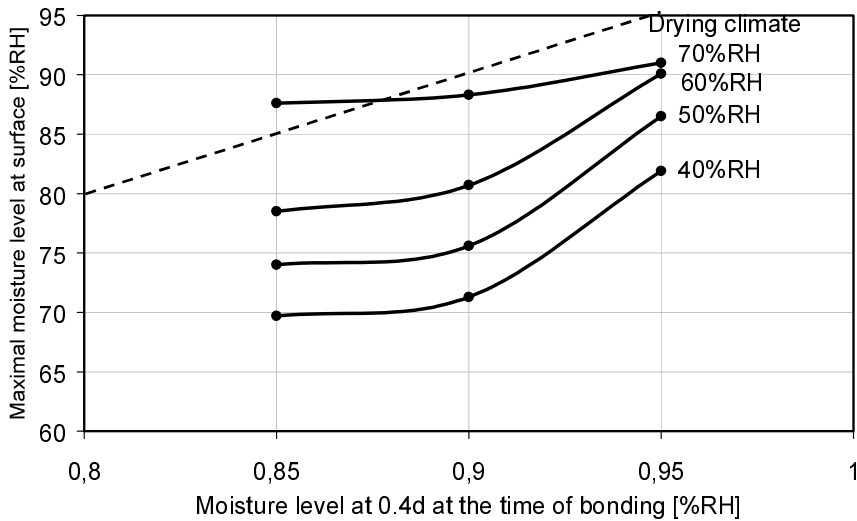


Fig. 10.2 Moisture level including moisture of adhesive at the surface of concrete C4 (w/c ratio=0.66) for different drying climates. The dashed line represents the moisture status that will be established after the remaining moisture in the concrete had come to a uniform level following bonding of an impermeable PVC flooring.

10.1.1 Discussion, highest moisture status

According to the results of calculations which are set out in Fig. 10.1 and 10.2, the concrete surface is able to adsorb the moisture of adhesive if the concrete had been dried in dry drying climates (<60% RH). For normal structural concrete of w/c ratio=0.66, a somewhat more humid drying climate (<70% RH) can be permitted.

The moisture states which will prevail when the moisture of adhesive has temporarily raised the moisture distribution to a level higher than the final one after redistribution, are the triangle shaped area formed over the dashed line in the top left hand corner in Fig. 10.1 and 10.2.

In the calculations illustrated, the moisture of adhesive exerts an influence on the maximum moisture status at the surface only when the concrete is dried to below 90% RH in a drying climate that is 60% RH or more humid.

10.2 Emission of butanol from the surface

Emission of butanol from the surface is influenced by the concentration at the top of the concrete and by the resistance of the flooring.

The influence of concentration at the top of the concrete is analysed with reference to the influence of $q_{R,max}$ of four different values, $0.03 - 7.3 \cdot 10^{-9}$ $\text{kg}/(\text{m}^2 \cdot \text{s})$, and the moisture level at 40% of the depth before the flooring is bonded. The moisture level at 0.4d is varied between 91 and 97% RH.

The influence of the resistance R_{fc} of the flooring is analysed for two values, $2.9 \cdot 10^{-6}$ and $3.7 \cdot 10^{-6}$ s/m . According to the evaluation in Tables 4.3, these are denoted as linoleum flooring and PVC flooring respectively. The resistances Z of these to moisture transport are also completely different, which affects the moisture level at the surface and thus the formation of butanol.

10.2.1 The influence of $q_{R,max}$

The calculated emission of butanol from the surface, as a function of time, is plotted in Fig. 10.3 for four different values of $q_{R,max}$. Note that the y axis has a logarithmic scale. Three of the curves, $q_{R,max} = 0.03$, 0.26 and 2.6 $\text{kg}/(\text{m}^2 \cdot \text{s})$, are calculated with the same values for the transport and fixation of OCIC. The curve denoted $q_{R,max} = 7.3^*$ is calculated with different values; see Table. 9.3.

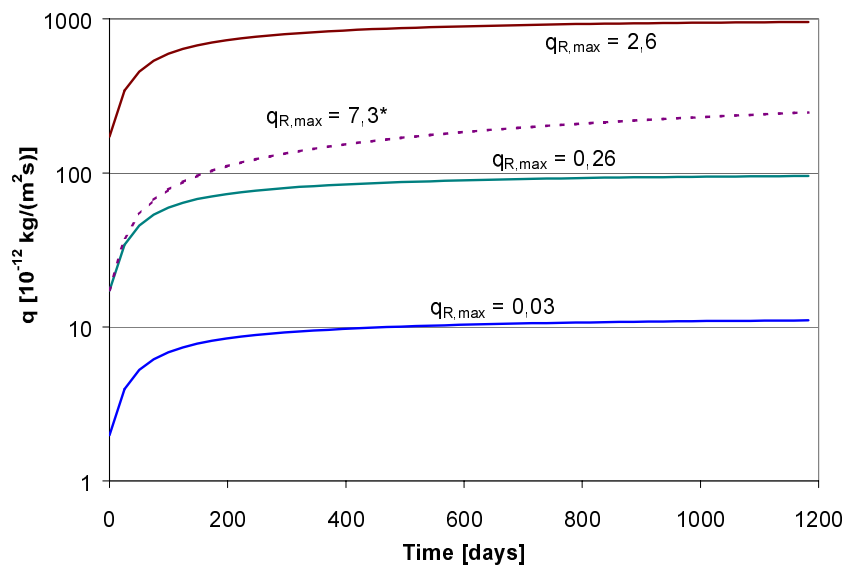


Fig. 10.3 Calculated emission of butanol from the surface of a concrete floor with PVC flooring. Calculated moisture level at 0.4d before the flooring is bonded is 95% RH. All the curves are calculated with the assumption regarding binding Bound.0, except the one denoted * for which Bound.1 is used.

The total calculated emission from the above calculation cases is plotted in Fig. 10.4. The calculations are based on the results set out in Fig. 10.3.

The maximum quantity of butanol that can be formed from the adhesive is $20.8 \cdot 10^{-3} \text{ kg/m}^2$, on the assumption that adhesive is applied at the rate of $5 \text{ m}^2/\text{l}$, the density of adhesive is 1300 kg/m^3 and the adhesive contains 8% butylacrylate; see Subsections 2.1.3 and 3.3.3. The quantity of moisture of adhesive is then $80 \cdot 10^{-3} \text{ kg/m}^2$.

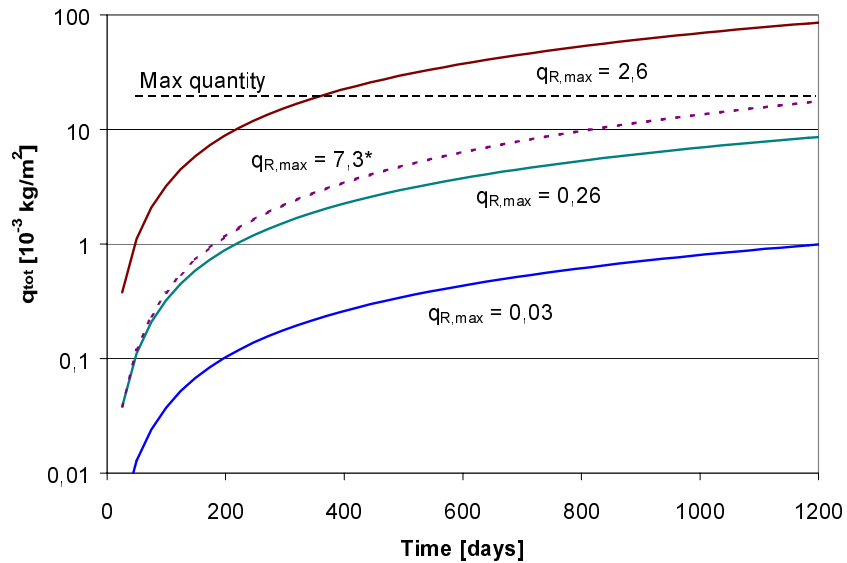


Fig. 10.4 Total calculated emission of butanol from the surface of a concrete floor with PVC flooring. The calculated moisture level at 0.4d before the flooring was bonded was 95% RH. All the curves are calculated with the assumption regarding binding Bound.0, except the one denoted * for which Bound.1 is used.

10.2.2 Influence of RH for floor constructions with PVC flooring

The calculated emission of butanol from the surface, as a function of time, is plotted in Fig. 10.5 for six different values of RH. The moisture levels 91-96% refer to RH at 0.4d before the flooring is bonded. The transmission resistance of the flooring to butanol is $3.7 \cdot 10^{-6} \text{ s/m}$ (PVC flooring). Owing to shortcomings in the calculation model, no calculations could be made for cases with moisture levels exceeding 96% RH.

In the calculations, $q_{R,max} = 2.6 \cdot 10^{-9} \text{ kg}/(\text{m}^2 \cdot \text{s})$. All the parameters are set out in Table 9.3 as Calc.3.

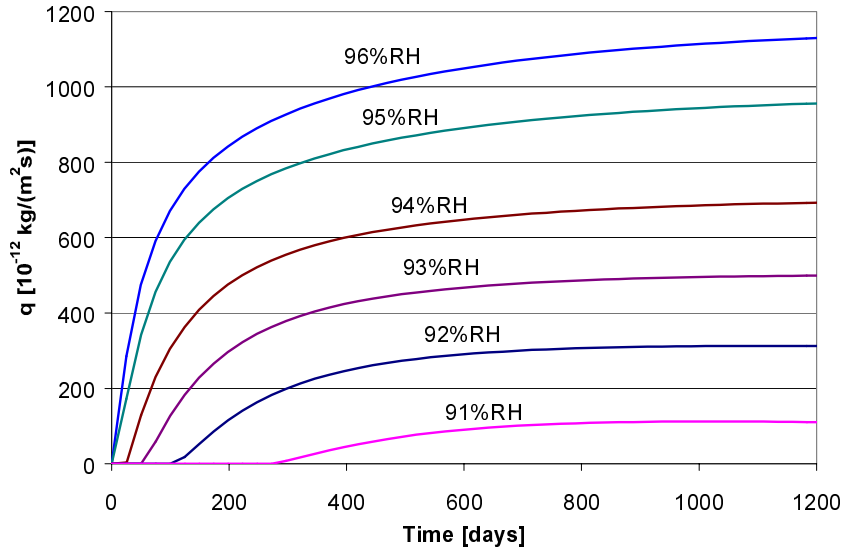


Fig. 10.5 Calculated emission of butanol from the surface of a concrete floor with PVC flooring. The moisture levels refer to 0.4d. Calculated with Calc.3 and $q_{R,max} = 2.6 \cdot 10^{-9} \text{ kg}/(\text{m}^2 \cdot \text{s})$.

The total emission from the above calculation cases is plotted in Fig. 10.6. The calculations are based on the results set out in Fig. 10.5.

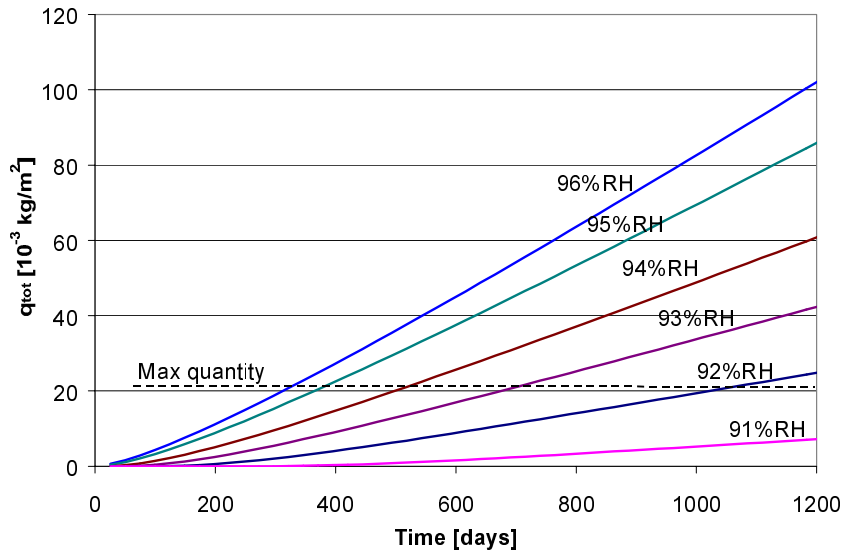


Fig. 10.6 Total calculated emission of butanol from the surface of a concrete floor with PVC flooring. The moisture levels refer to 0.4d. Calculated with Calc.3 and $q_{R,max} = 2.6 \cdot 10^{-9} \text{ kg}/(\text{m}^2 \cdot \text{s})$.

10.2.3 Influence of RH for floor constructions with linoleum flooring

The calculated emission of butanol from the surface, as a function of time, is plotted in Fig. 10.7 for four different values of RH. The moisture levels 94-97% refer to RH at 0.4d before the flooring is bonded. The transmission resistance of the flooring to butanol is $2.9 \cdot 10^{-6}$ s/m (Linoleum flooring) and for moisture it is $0.1 \cdot 10^6$ s/m.

In calculating moisture levels below 94% RH no emissions were obtained from the surface. The explanation is that no reaction had started because RH_{crit} was not exceeded at the surface of the concrete. Owing to shortcomings in the calculation model, no calculations could be made for cases with moisture levels above 97% RH.

In the calculations $q_{R,max} = 2.6 \cdot 10^{-9}$ kg/(m²·s). All parameters are set out in Table 9.3 as Calc.3.

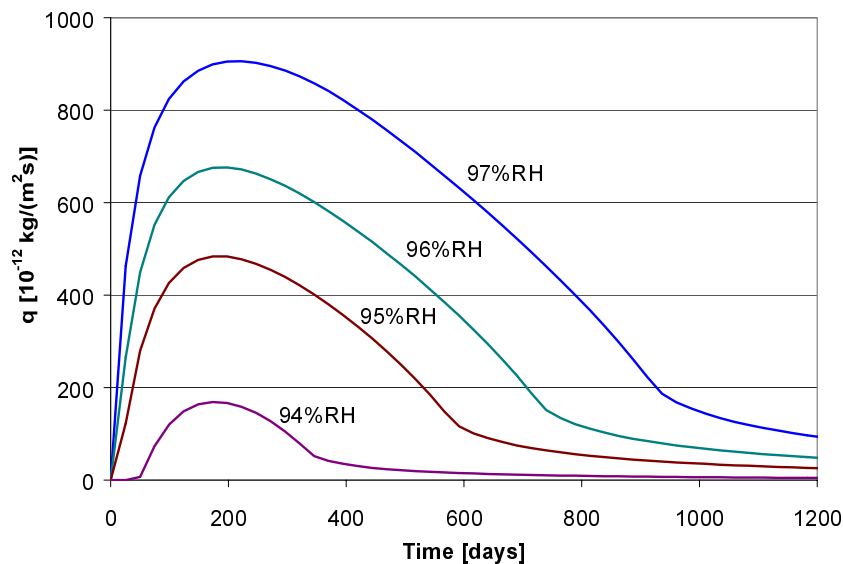


Fig. 10.7 Calculated emission of butanol from the surface of a concrete floor with linoleum flooring. The moisture levels refer to 0.4d. Calculated with Calc.3 and $q_{R,max} = 2.6 \cdot 10^{-9}$ kg/(m²·s).

The total emission from the above calculation cases is plotted in Fig. 10.8. The calculations are based on the results set out in Fig. 10.7.

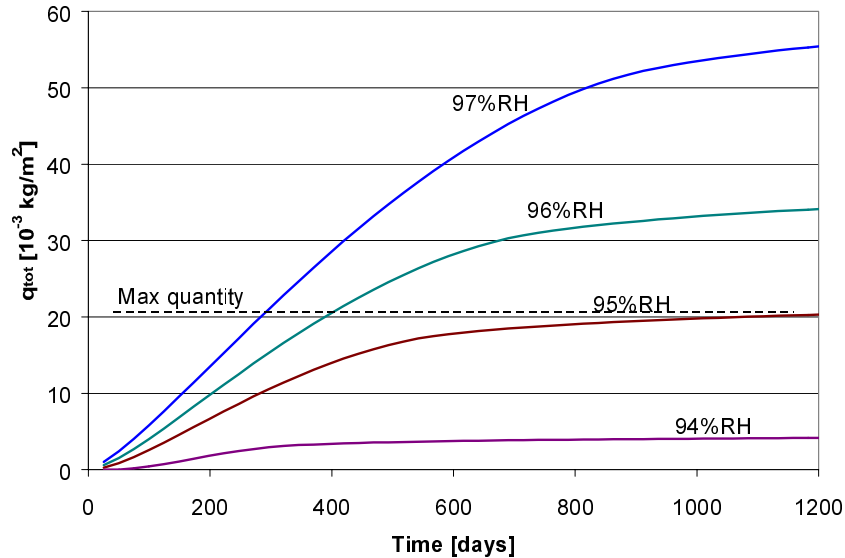


Fig. 10.8 Total calculated emission of butanol from the surface of a concrete floor with linoleum flooring. The moisture levels refer to 0.4d. Calculated with Calc.3 and $q_{R,max}=2.6 \cdot 10^{-9} \text{ kg}/(\text{m}^2 \cdot \text{s})$.

10.2.4 Discussion, emission from the surface

Emission from the surface is primarily governed by the concentration at the top of the concrete and the resistance of the flooring. The surface concentration is largely determined by $q_{R,max}$. This is a parameter whose value must be rigorously verified to enhance the reliability of the model.

The assumption regarding binding also has great influence on emission from the surface. In Fig. 10.3 the curve with $q_{R,max} = 7.3 \text{ kg}/(\text{m}^2 \cdot \text{s})$ has a lower emission than the curve with $q_{R,max} = 2.6 \text{ kg}/(\text{m}^2 \cdot \text{s})$, although it should be the other way round if conditions were otherwise the same. The explanation is that the curve with $q_{R,max} = 7.3 \text{ kg}/(\text{m}^2 \cdot \text{s})$ was calculated with another assumption regarding binding, Bound.1, instead of Bound.0, which means that more OC is bound in the concrete. It is estimated that emission from the surface according to calculations with $q_{R,max} = 7.3 \text{ kg}/(\text{m}^2 \cdot \text{s})$ and Bound.0 would be 10 times higher than with Bound.1.

The transmission resistance of the flooring is also critical for emission. The higher the transmission resistance for OC, the lower is emission (over an extended period) at the same surface concentration. The transmission resistance to moisture is also important since a low resistance enables the concrete to dry out. The consequence of this may be that any reaction that may be taking place ceases after a time and emission from the surface decreases; see Fig. 10.7.

It is likely that the emission processes described in Section 10.2 are approximately the same as from a floor construction with a similar flooring, provided that all other conditions are the same. If the flooring has a different transmission resistance R_{fc} , the rate of emission may however be different.

Equation 7.40 is used to calculate the rate of emission in the new case which has a known transmission resistance.

In the same way, the rate of emission can be calculated from a known surface concentration c_s . However, penetration of OCIC is also influenced by the surface concentration c_s , which means that the above relationship is only approximate.

10.3 Transport and fixation of butanol in concrete

Transport and fixation of butanol in concrete are influenced, among other things, by the concentration of butanol at the top of the concrete, c_s , the diffusion coefficient δ_{oc} and the assumption regarding binding *Bound*.

The influence of concentration at the top of the concrete is analysed with the help of the influence of $q_{R,max}$ at four different levels, $0.03 - 7.3 \cdot 10^{-9} \text{ kg}/(\text{m}^2 \cdot \text{s})$. In the first three calculations, with $q_{R,max} = 0.03 \cdot 10^{-9}$, $0.26 \cdot 10^{-9}$ and $2.6 \cdot 10^{-9} \text{ kg}/(\text{m}^2 \cdot \text{s})$, *Bound.0* was used. In the two calculations with $q_{R,max} = 7.3 \cdot 10^{-9} \text{ kg}/(\text{m}^2 \cdot \text{s})$, *Bound.1* and *Bound.2* were used.

Two different values of the diffusion coefficient were used in the calculations, $\delta_{oc} = 2.5 \cdot 10^{-9}$ and $93 \cdot 10^{-9}$. Finally, three different methods of binding were analysed, *Bound.0*, *Bound.1* and *Bound.2*. See Subsection 8.1.3.

10.3.1 The influence of different assumption regarding binding

The calculated quantity of butanol that is transported down into the concrete as a function of time is plotted in Fig. 10.9 for five different cases. Three of the cases are calculated with the same method of binding, *Bound.0*, but with different surface concentrations. Surface concentration is varied by postulating different values of the rate of formation $q_{R,max}$.

In the cases denoted *Bound.1* and *Bound.2* in Fig. 10.9, the value $q_{R,max} = 2.6 \cdot 10^{-9} \text{ kg}/(\text{m}^2 \cdot \text{s})$ was used. The values of all parameters used in the calculations are set out in Table 9.3. In all calculations, the moisture level before the flooring was bonded was 95% RH.

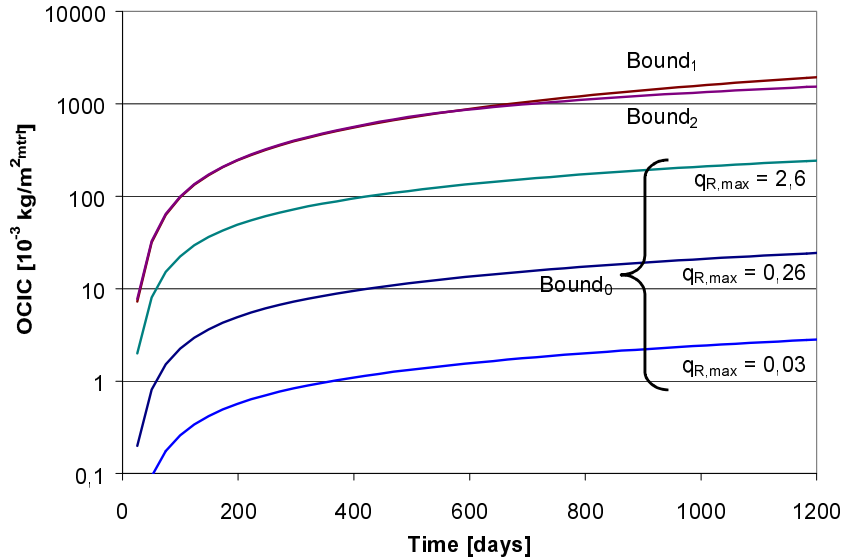


Fig. 10.9 Calculated quantity of butanol transported down into a concrete floor with PVC flooring. Analysis of the effect of different surface concentrations and assumptions regarding binding.

Profiles of butanol in the gas phase which is formed in the concrete after a long time (1200 days) are plotted in Fig. 10.10. The results are based on the same calculations as those for Fig. 10.9.

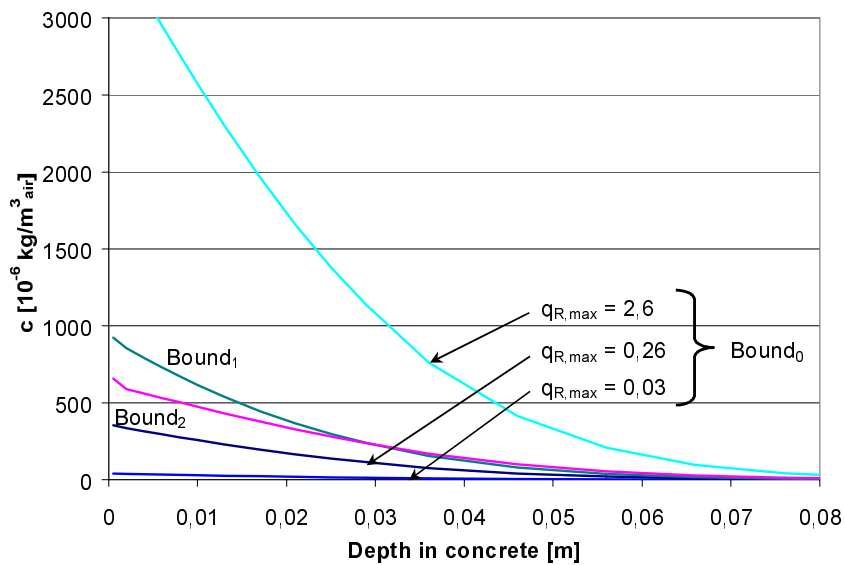


Fig. 10.10 Profiles of butanol in the gas phase in concrete after a long time (1200 days). Analysis of the effect of different rates of formation and assumptions regarding binding.

10.3.2 Influence of RH for PVC flooring

The calculated quantity of butanol that is transported down into the concrete as a function of time is plotted in Fig. 10.11 for six different values of RH. Moisture levels 91-96% refer to RH at 0.4d before the flooring is bonded. The transmission resistance of the flooring to butanol is $3.7 \cdot 10^{-6}$ s/m (PVC flooring). Owing to shortcomings in the calculation model, no calculations could be made for cases with moisture levels above 97% RH.

In the calculations $q_{R,max} = 0.03 \cdot 10^{-9}$ kg/(m²·s). Assumption *Bound.0* regarding binding is used; this gives a small quantity of bound OCIC in the concrete. All parameters are set out in Table 9.3 as Calc.1.

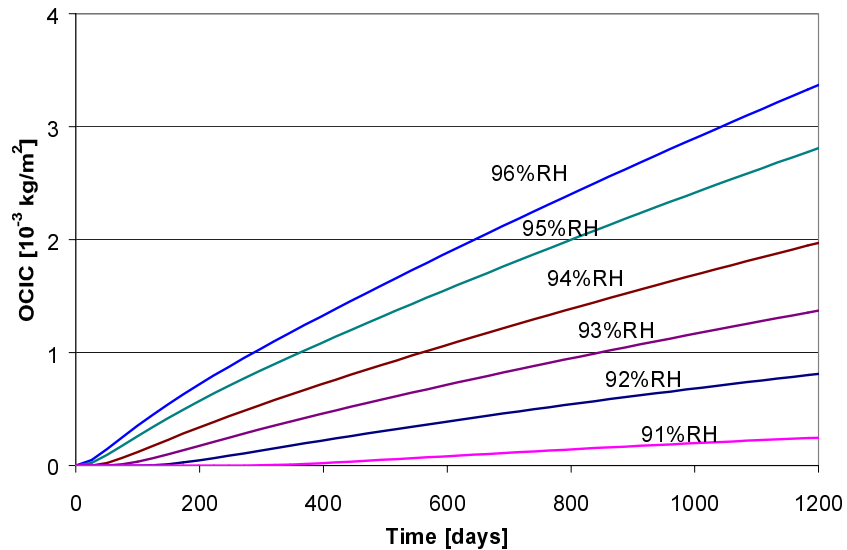


Fig. 10.11 Calculated quantity of butanol that is transported down into a concrete floor with PVC flooring. The moisture levels refer to 0.4d. Calculated with Calc.1 and $q_{R,max} = 0.03 \cdot 10^{-9}$ kg/(m²·s).

Profiles of butanol in the gas phase down in the concrete after a long time (1200 days) are plotted in Fig. 10.12. The results are based on the same calculations as those for Fig. 10.11.

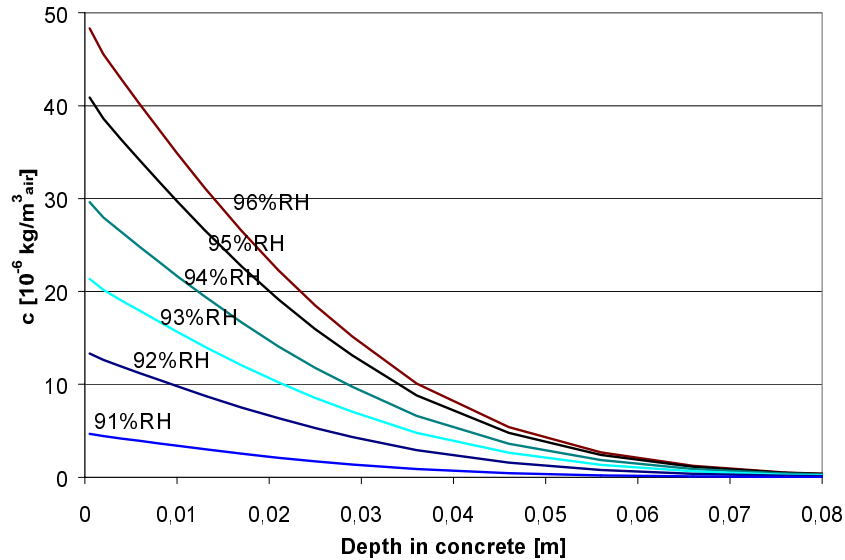


Fig.10.12 Profiles of butanol in the gas phase in a concrete floor with PVC flooring after a long time (1200 days). The moisture levels refer to 0.4d. Calculated with Calc.1 and $q_{R,max} = 0.03 \cdot 10^{-9} \text{ kg}/(\text{m}^2 \cdot \text{s})$.

10.3.3 Influence of RH for linoleum flooring

The calculated quantity of butanol that is transported down into the concrete as a function of time is plotted in Fig. 10.13 for four different values of RH. Moisture levels 94-97% refer to RH at 0.4d before the flooring is bonded. The transmission resistance of the flooring to butanol is $2.9 \cdot 10^6 \text{ s}/\text{m}$ (linoleum flooring).

In the calculations for moisture levels below 94% RH no transport of butanol down into the concrete was obtained. The explanation is that no reaction had started because RH_{crit} was not exceeded at the surface of the concrete. Owing to shortcomings in the calculation model, no calculations could be made for cases with moisture levels above 97% RH.

In the calculations $q_{R,max} = 0.03 \cdot 10^{-9} \text{ kg}/(\text{m}^2 \cdot \text{s})$. Assumption *Bound.0* regarding binding was used; this gives a small quantity of bound OCIC. All parameters are set out in Table 9.3 as Calc.1.

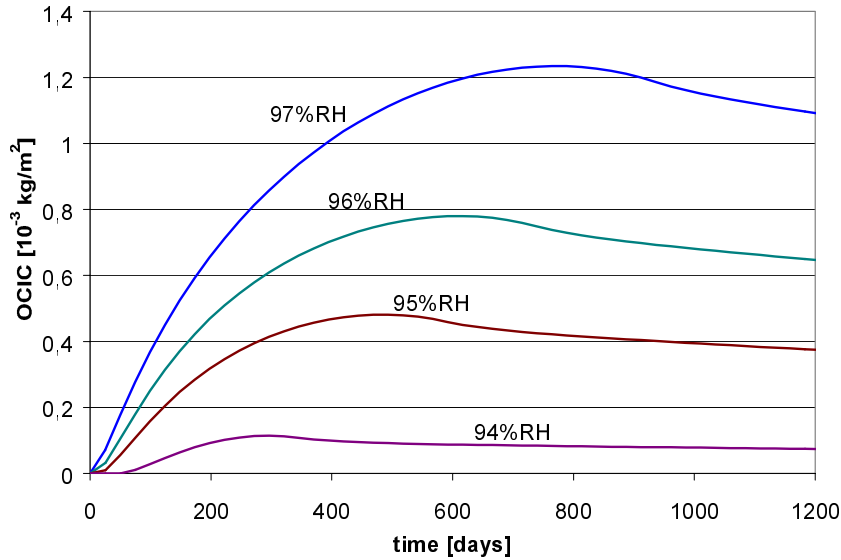


Fig. 10.13 Calculated quantity of butanol that is transported down into a concrete floor with PVC flooring. The moisture levels refer to 0.4d. Calculated with Calc.1 and $q_{R,max} = 0.03 \cdot 10^{-9} \text{ [kg/(m}^2 \cdot \text{s)]}$.

Profiles of butanol in the gas phase, for maximum surface concentration, are plotted in Fig. 10.14. These profiles occur at about the same time as when the quantity of OCIC in the concrete is greatest; see Fig. 10.13. Profiles of butanol after a long time (1200 days) are also plotted. The results are based on the same calculations as those for Fig. 10.13.

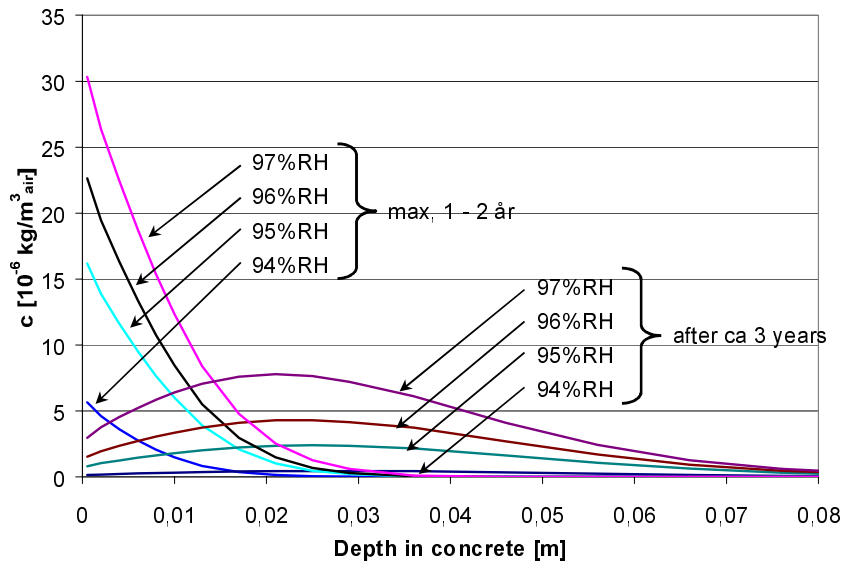


Fig. 10.14 Profiles of butanol in the gas phase in a concrete floor with linoleum flooring, after a long time (1200 days). The moisture levels refer to 0.4d. Calculated with Calc.1 and $q_{R,max} = 0.03 \cdot 10^{-9} \text{ kg/(m}^2 \cdot \text{s)}$.

10.3.4 Discussion, transport and fixation of OCIC

The diffusion coefficient and the binding capacity are critical for the quantity of OCIC that can be found. These are also the parameters whose values must be rigorously verified to enhance the reliability of the model.

In floor constructions where the reaction decreases after a time, OCIC will continue to be emitted from the surface. After the reaction has come to an end, no new OC is formed. Continued emission of VOC from the surface may occur because OCIC is transported upwards through the construction. The rate of emission from the surface decreases when the reaction is over. Continued emission is instrumental in reducing the total quantity of OCIC inside the floor.

10.4 Residual OCIC after exposure to the air

One possible remedial measure when there is high emission from a floor construction is to replace the flooring. Any alkaline hydrolysis will then cease when the adhesive is removed. If the moisture level at the surface of the concrete, inclusive of new moisture of adhesive, exceeds RH_{crit} after the new flooring had been bonded, a new reaction may commence.

When the old flooring is removed, emission from the floor may steeply increase. During the time that the floor construction is exposed to air, the quantity of OCIC in the concrete decreases.

For a floor that has been treated as described above, the calculated moisture level at the surface of the concrete and the emission from the surface are plotted in Fig. 10.15. At 0.4d, the moisture level at time 0, before the PVC flooring is bonded, is 95% RH.

About three years after the flooring was bonded, it is removed. The floor is then left exposed to the air for four months. At the end of this period, a new linoleum flooring is bonded to the concrete.

In the calculations $q_{R,max} = 0.03 \cdot 10^{-9} \text{ kg}/(\text{m}^2 \cdot \text{s})$, $R_{fc} = 3.7 \cdot 10^{-6} \text{ s}/\text{m}$ for PVC flooring and $2.9 \cdot 10^{-6} \text{ s}/\text{m}$ for linoleum flooring. The assumption regarding binding is Bound.0 which gives a small quantity of bound OCIC in the concrete. All parameters are set out as Calc. 1 in Table 9.3.

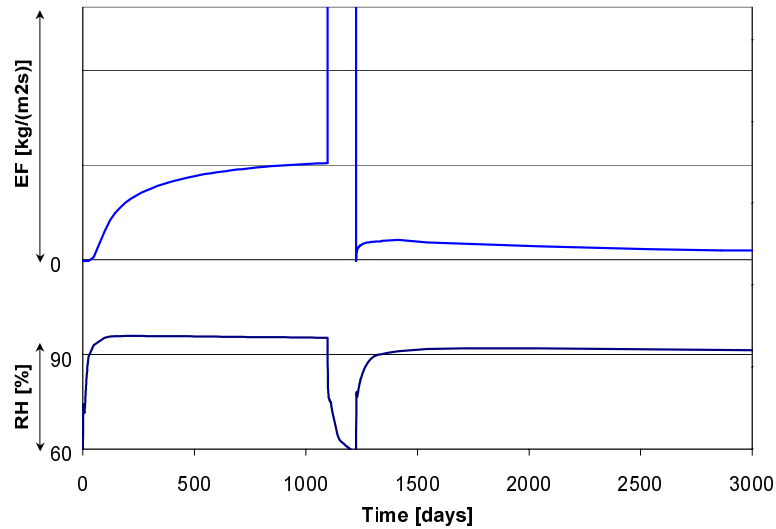


Fig. 10.15 Calculated emission of butanol from the surface, and moisture level at the surface of a floor with PVC flooring which is "exposed to air" at an age of ca 1100-1230 days. A linoleum flooring is then bonded. In the calculations $q_{R,max} = 0.03 \cdot 10^{-9} \text{ kg}/(\text{m}^2 \cdot \text{s})$, Calc.1.

Emission from the surface while it is exposed to the air is plotted in Fig. 10.16. The figure shows the curve, after the flooring had been removed, at a larger scale. The rate of emission is very high in the beginning when the PVC flooring is removed at an age of ca 1100 days. As the quantity of butanol near the surface diminishes, emission of butanol from the surface progressively decreases. When the linoleum flooring is bonded at the age of 1230 days, emission decreases. The change in direction at ca 1140 days may be due to the limitations of the calculation model.

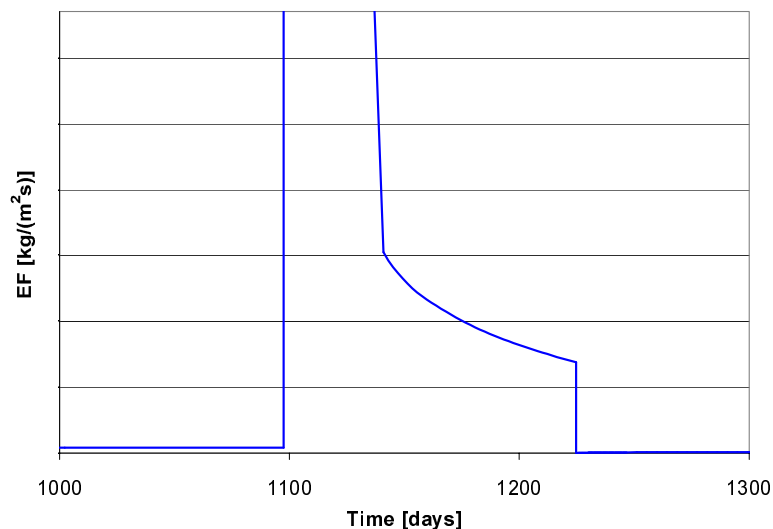


Fig. 10.16 Calculated emission of butanol from the surface while a concrete floor is exposed to the air at an age of ca 1100 – 1230 days. At 1230 days a linoleum flooring is bonded. In the calculations $q_{R,max} = 0.03 \cdot 10^{-9} \text{ kg}/(\text{m}^2 \cdot \text{s})$, Calc.1.

The free concentration of butanol at seven different depths in the concrete, as a function of time, is plotted in Fig. 10.17.

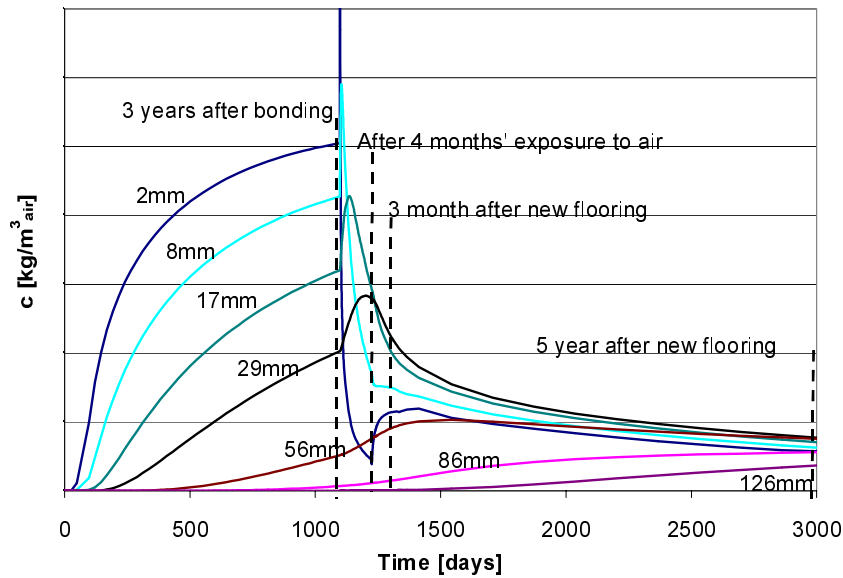


Fig.10.17 Free concentration of butanol at seven different depths in the concrete as a function of time. In the calculations $q_{R,max} = 0.03 \cdot 10^{-9}$ kg/(m²·s), Calc.1.

The profiles of the free concentration of butanol, on four different occasions, are plotted in Fig. 10.18. These occasions are marked in Fig. 10.17. The first is three years after the PVC flooring was bonded, just before it is removed as part of remedial treatment. The next profile in chronological order is after 4 months' exposure to air, just before a new linoleum flooring is bonded to the concrete. The third profile shows the distribution about three months after the linoleum flooring was bonded. The last profile shows what the distribution of the free butanol in the concrete may be like, many years after the reaction had ceased.

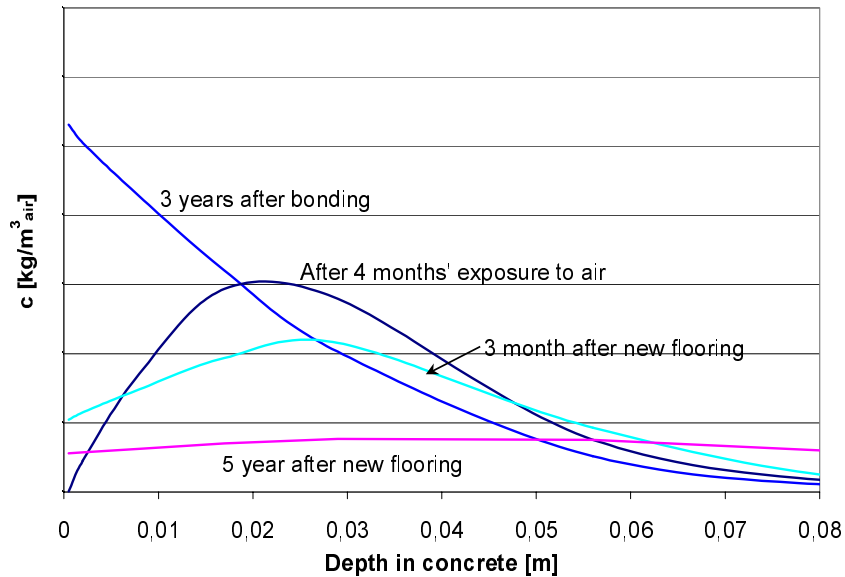


Fig. 10.18 Profiles of free concentration of butanol on four different occasions which are marked in Fig. 10.17. In the calculations $q_{R,max} = 0.03 \cdot 10^{-9}$ kg/(m²·s), Calc.1.

10.4.1 Discussion, residual OCIC after exposure to the air

The results of the calculations, plotted in Fig. 10.15, show that emission from the floor increases when the flooring is removed. As the adhesive is removed and/or the moisture level at the surface decreases, any reaction that may be taking place ceases. The rapid emission when the flooring is removed is instrumental in reducing the total quantity of OCIC at the surface of the concrete.

When the free concentration of OC at the surface of the concrete decreases, it is the transport of the OC in the concrete, up to the surface of the concrete, which determines the rate of emission; see Fig. 10.16. In consequence, decrease of OCIC in the concrete proceeds at the fastest rate in the beginning when the free concentration of OC at the surface of the concrete is high.

In the calculation, emission takes place all the time to room air with negligible concentration. In a real case, concentration in the room air may steeply increase when the flooring is removed. The rate of flow of air in the room must be very high to ensure that concentration in the room remains at a low level.

All calculations have been made on the assumption that OC can be bound only by dissolving in the pore water. If the calculations are instead based on the other two methods of binding, the quantity of OCIC may be much greater. The consequence of this is that emission is higher for a longer period.

11 Discussion and conclusions

11.1 Attainment of the objects

As described in Section 1.3, this study had a number of objects. To a certain extent, all these objects have been attained. They may be summarised as follows.

- Increase knowledge of the interaction in combinations of materials, one of which is concrete, in floor constructions with bonded floorings.
- Create a model, based on an understanding of the physical processes in a floor construction, which can predict the reduction in the service life of the above material combinations.
- Develop methods for non-accelerated measurement of the properties of the construction which are important for these processes.
- Develop knowledge which will help prevent or limit the emission of VOC from the building to indoor air, in both the long and short term.

The project has examined all these points. In Chapter 6 and 7 the processes which give rise to secondary emission are described. All the processes which are not covered in the literature have been quantified. In some cases this was done using methods which are well documented, in other cases methods of measurement developed in this study were used. Some mechanisms, such as the rate of formation of OC below the flooring, could not be measured directly. Values for these were instead evaluated from other measurements with the help of the model.

Both a qualitative and a quantitative model have been developed. The qualitative model which is presented in Chapter 6 comprises all relevant partial processes. The model describes the processes in material combinations for different applications: normal structural concrete, self-desiccating concrete with and without screed. The quantitative model is described in Chapter 7. This model is based on an understanding of the physical processes and quantifiable material parameters. It describes the transport and fixation of essential components of the system, such as moisture and OC.

New methods for non-accelerated measurements have been developed in the study. The aim of these methods is to measure material properties which are used in the quantitative model, and the processes which verify the model. These measurements are described in Chapters 2 – 5. Some of the methods must however be improved since they were found to have large uncertainties.

11.2 The hypothesis

The original hypothesis which is described in Section 1.5 has been found to be largely correct. It has been possible to verify it almost completely in the study.

To begin with, it was demonstrated in the study that significant substances, such as moisture and OC, can migrate into and between the materials and be emitted from the surface of the construction. This is the most important cornerstone of the hypothesis.

Moisture is significant in the sense that it is the moisture level which governs decomposition of the adhesive when it is in contact with the alkaline environment created by the surface of the concrete. An ample supply of moisture in the concrete is a necessary condition for the presence of hydroxide ions and for the establishment of contact between these and the adhesive. The moisture content of the concrete may also influence the sorption isotherm for OCIC. However, this has not been confirmed.

Transport and fixation of OC in the materials is significant for emission from the surface, partly because the transmission resistance of the flooring has a great influence on migration upwards, and partly because it is the transport properties and sorption isotherms which determine the quantity of OC that can penetrate into and be stored in the concrete.

The hypothesis is also correct insofar as there are certain substances in the subfloor, hydroxide ions, which can react with the flooring. It has however been shown that it is primarily the adhesive and not the flooring that decompose.

Alkaline hydrolysis of the adhesive is a catalytic process. The hydroxide ions are not used up in the way posited in the hypothesis. For each hydroxide ion that is "consumed" in the reaction, a new one is formed due to the dissociation of the water. It is the quantity of alkali, i.e. the positive counter-ions to the alkali metals, which is the condition for the commencement of hydrolysis. There is no demand for constant transport towards the surface to "replace the consumed alkali", as posited in the hypothesis.

11.3 The calculation model

The calculation model developed as part of this study has been found to be in reasonable agreement with the measured results. Unfortunately, however, most of the measurements were defective and incomplete, since they are taken from an earlier project. At that time, it was not known what was important to measure and how this should be done.

The weaknesses of the model derive mostly from the fact that all the parameters could not be measured satisfactorily. Examples of two of the parameters which were not measured in the study are the maximum rate of formation and the sorption isotherm for OCIC.

It is also desirable for moisture calculations in the model to be developed so that the hysteresis that occurs when the flooring is bonded can be taken into consideration. The existing model underestimates the increase in RH due to the increment from the moisture of adhesive.

In order that others should be able to use the calculation model, it is necessary to make it more user friendly. It is also desirable to develop it into a freestanding program that makes better use than Excel of the computational capacity of the computer.

11.4 The assumption regarding fixation

One of the great uncertainties in the quantitative model is the assumption regarding fixation. In the study, three different assumptions were made regarding fixation. These are based on assumptions that could not be properly verified. These assumptions have important consequences for the way OC is distributed between emission from the surface and the quantity that is stored in the concrete as OCIC.

No measurements of the sorption isotherm for OCIC were made in the study, and the few values that were found in the literature ignore its dependence on moisture in the concrete. When other investigations refer to sorption isotherms, they often make an outline study of the fixation of a number of compounds to many different materials. One material that is often studied is plasterboard; the idea underlying this choice may be that plasterboard is on the outside of the construction and is in direct contact with compounds in the indoor air. However, plasterboard is usually given a finish, paint or wallpaper, and it is the properties of this material which determine the quantity of OC that can be transported into the material and stored there. The results of such studies cannot be directly used since plasterboard and paper have a pore structure and moisture fixation mechanism different from that of concrete.

The concentration of OC in room air is in most cases negligible in comparison with the total concentration in equilibrium with a material that emits large quantities. In cases where a construction contains a material emitting large quantities, the principal transport to other materials may take place directly into adjoining materials, and not via emission to the room air and then absorption into the materials in the surfaces of the room.

Obviously, this holds on condition that the materials in contact with the emitting material and the surface materials in the room have the structure and the properties which permit adsorption, and that the room has acceptable general ventilation that dilutes the room concentration.

11.5 Maximum quantity of OC which is formed

The assumption that the quantity of OC formed per unit time, i.e. the rate of formation, is directly proportional to the moisture level above RH_{crit} could not be verified satisfactorily.

It is reasonable to assume that the rate of formation is influenced in some way by the moisture level. The simplest relationship, however, would be that there is no reaction at moisture levels below RH_{crit} and that it occurs at maximum rate above this value. This is denoted by line A in Fig. 11.1.

In view of the experiences gained in SBS investigations, presented by Kumlin (2000), it may be more reasonable to assume that the rate of formation increases with the increase in moisture level above RH_{crit} . The simplest curve is then a straight line denoted B in Fig. 11.1 This relationship for the rate of formation is the one used in the calculation model.

The relationship between the rate of formation and RH need not be linear. Fig. 11.1 also gives examples of two possible nonlinear relationships. Curve C is

intermediate between lines A and B. Curve D denotes a function where the rate increases steeply as the moisture level increases above RH_{crit} .

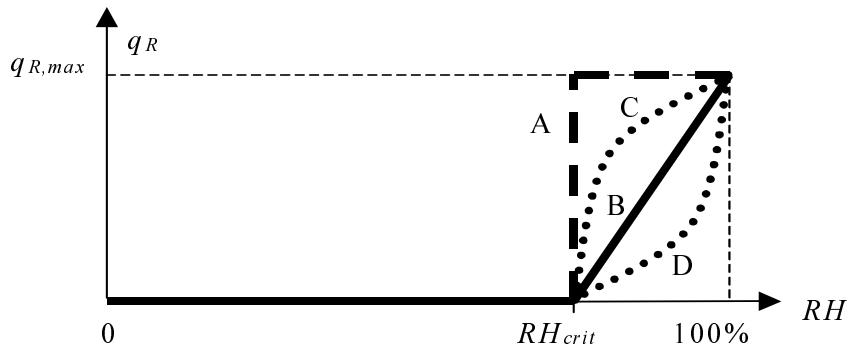


Fig. 11.1 Four possible assumptions regarding rate of formation as a function of moisture level. The assumption represented by line B is the one used in the calculation model.

Even though the relationship between RH and the rate of formation is unknown, a certain amount is known about the reaction through the measurements described in Chapter 3. These measurements show that a higher pH value accelerates the reaction, and also that more decomposition products are formed as the quantity of adhesive increases.

11.6 Emission of VOC from the surface

The calculations presented in Chapter 10 show that the moisture status of the concrete is critical for emission from the surface. Differences in RH by one or two percentage points give rise to markedly different rates of emission.

11.7 OCIC stored in the concrete

The concentration of decomposition products stored in the concrete may be very high after the adhesive had been decomposing for some time. It is difficult at present to make any statement regarding the total concentration of OCIC since it was the free concentration that was measured. Conversion of this into the total quantity would require a verified sorption isotherm.

We know this because in buildings where targeted action was taken to remedy these problems, the complaints of the users were reduced or completely cured. In cases where the action was confined to replacement of the flooring without dealing with OCIC, the complaints of the users often returned after a short time.

The bound quantity is thus much greater than the free concentration in the air and the amount dissolved in the moisture in the pore system.

11.8 Practical application of concentrations in the concrete

It is difficult to establish a safe limiting value for the concentration of OC which has been stored in the concrete. The compounds we have so far studied are trace elements which indicate differences in the construction and cannot with certainty be pinpointed as causing SBS. However, in view of the precautionary principle, it may nevertheless be appropriate to reduce all emissions from the materials in a building. This also applies to emissions from a component damaged by moisture, inclusive of the stored OCIC.

According to the Swedish Internal Climate Institute (1990), new materials can be assigned to material emission classes (MEC). MEC-A denotes low-emitting materials and finishes with a maximum emission factor of $40 \mu\text{g}/(\text{m}^2\cdot\text{h})$ at 20°C and 50% RH. MEC-B are medium-emitting materials and finishes with the maximum limit of $100 \mu\text{g}/(\text{m}^2\cdot\text{h})$, and MEC-C denotes high-emitting materials and finishes without any upper limit to the emission factor.

MEC-A is the class which designers endeavour to use in constructing healthy buildings. Since the emission requirement for this class is $40 \mu\text{g}/(\text{m}^2\cdot\text{h})$, it may be reasonable to stipulate that the emission from composite constructions in the building should also not be permitted to exceed this limit during the service life of the building.

Seifert (1990) writes that "No individual VOC should exceed 50% of the concentration allotted to its class and 10% of the TVOC concentration". According to Seifert's reasoning and the requirement concerning low-emitting building structures, EF for an individual compound must not exceed $4 \mu\text{g}/(\text{m}^2\cdot\text{h})$. In the emission from the decomposition of floor adhesive, the alcohols BuOH and EtHx are the dominant compounds.

For an ordinary PVC flooring which has a transmission resistance $R_{fc} = 3.7 \cdot 10^6$ s/m for butanol, this means that the difference in the concentration of butanol on each side of the flooring must not exceed $4.1 \cdot 10^{-6}$ kg/m³ for the maximum emission of $4 \mu\text{g}/(\text{m}^2\cdot\text{h})$. The corresponding value of the resistance to ethylhexanol is $R_{fc} = 0.38 \cdot 10^6$ s/m, which gives $0.4 \cdot 10^{-6}$ kg/m³ as the maximum difference in concentration on each side of the flooring.

In Table 11.1 values of EF are evaluated for different concentrations of VOC below floorings of different degrees of impermeability. In the table, a dotted line has been drawn at $EF = 4 \mu\text{g}/(\text{m}^2\cdot\text{h})$ and a full line at $40 \mu\text{g}/(\text{m}^2\cdot\text{h})$. These relate to the limits of low-emitting materials according to MEC-A and Seifert's reasoning.

Table 11.1 EF [$\mu\text{g}/(\text{m}^2 \cdot \text{h})$] for different transmission resistances of the flooring to OC and for different surface concentrations of OC. The room concentration of OC is ignored.

$c_s \setminus R_{fc}$		R_{fc} – transmission resistance to OC [s/m]					
		4 000	400	40	4	0.4	0.04
Surface concentration in concrete, c_s	0.11	0.0001	0.001	0.01	0.1	1	10
	1.1	0.001	0.01	0.1	1	10	100
	11	0.01	0.1	1	10	100	1 000
	22	0.02	0.2	2	20	200	2 000
	55	0.05	0.5	5	50	500	5 000
	110	0.1	1	10	100	1 000	10 000
	220	0.2	2	20	200	2 000	20 000
	1 100	1	10	100	1 000	10 000	100 000
	11 000	10	100	1000	10 000	100 000	1 000 000

According to the Swedish Board of Housing, Building and Planning (1994), experiences from the major cities in Sweden show that TVOC contents between 150 and 300 $\mu\text{g}/\text{m}^3$ normally give rise to very few complaints. It is however very uncertain what these values are based on and how they were determined. The Swedish Ventilation Guide for Housing (BFR 1993), however, lays down 200 and 400 $\mu\text{g}/\text{m}^3$ respectively for its best comfort classes.

In view of the precautionary principle, it is advisable to try and limit the occurrence of chemical compounds in room air. Let us assume that 150 $\mu\text{g}/\text{m}^3$ is the maximum concentration that is acceptable for the sake of safety, even though we cannot say that these compounds are harmful for the health of the users. This has been indicated by a full limiting line in Table 11.2 which sets out the contribution of the floor to the concentration in the room for different values of EF and air change rates.

Table 11.2 is based on the room concentration expressed as the sum of emission factors divided by the air change rate and room height; see Equation 11.1.

$$TVOC = \frac{\sum EF [\mu\text{g}/(\text{m}^2 \cdot \text{h})]}{Vent [ach] \cdot \text{room height} [m]} \quad [\mu\text{g} / \text{m}^3] \quad (11.1)$$

It is advisable to limit the contribution that a single source makes to concentration in the room air. If, for instance, it is permissible for 10% of the concentration to derive from a single source, then the maximum contribution of the floor is set at 15 $\mu\text{g}/\text{m}^3$. This is indicated by a dotted line in Table 11.2.

Table 11.2 Contribution to room concentration [$\mu\text{g}/\text{m}^3$] for different emission factors from the floor and for different air change rates. The calculations are based on Equation 11.1. The room height is 2.40 m.

ach \ EF		EF – emission factor from the floor [$\mu\text{g}/(\text{m}^2\cdot\text{h})$]					
		1	10	20	40	100	1 000
Air change rate [ach]	50	0.008	0.083	0.167	0.333	0.833	8.33
	10	0.042	0.417	0.833	1.67	4.17	41.7
	5	0.083	0.833	1.67	3.33	8.33	83.3
	2	0.208	2.08	4.17	8.33	20.8	208
	1	0.417	4.17	8.33	16.7	41.7	417
	0.5	0.833	8.33	16.7	33.3	83.3	833
	0.2	2.08	20.8	41.7	83.3	208	2080

11.9 Conclusions

The secondary emissions from a floor construction comprising a flooring bonded to a concrete slab may derive from a chemical reaction that decomposes the layer of adhesive. No contribution by components in the flooring could be identified in this study.

It is the alkalinity and moisture level at the surface of the concrete, which is in contact with the adhesive, that is critical for the reaction and therefore the future emission from the construction. The reaction is an alkaline hydrolysis in which hydroxide ions catalyse decomposition of acrylate and possibly acetate copolymers which comprise a considerable proportion of the adhesive, ca 25% of the dry weight. Moisture at the surface is determined, inter alia, by the construction water in the concrete and by the moisture increment at the surface, for instance from the moisture of adhesive. The level of construction water can be checked by moisture measurement at the characteristic depth.

The influence of surface moisture decreases when concrete is dried in a dry climate, $RH < 60\%$.

The decomposition products do not only migrate upwards through the flooring to be emitted into the indoor air, they can also migrate down into the concrete and become fixed there. The quantity of organic compounds that is fixed in the concrete (OCIC) constitutes a large proportion of the total quantity of decomposition products. The stored decomposition products may continue to be emitted to the indoor air for a long time after the reaction had ceased. OCIC may be a significant source of volatile organic compounds (VOC) in indoor air after a floor construction damaged by moisture had been renovated, unless special attention is paid to the stored compounds.

These processes can now be quantified with the model developed in this project. It is found that the model can correctly describe many practical applications. The predictions made with the model are however highly dependent on the reliability of the values of the parameters that are available for use as input data. For the materials in use today, data are almost completely nonexistent. Further studies are needed into methods of measurement to obtain these data, and the model must be validated in relation to more accurate laboratory and field measurements.

12 Future research and development

Let us for a time disregard the fact that we do not actually know what causes the SBS, and accept instead the experiences of the Nordic SBS investigators that there is a coupling between secondary emissions from decomposed adhesive and SBS. In such a case our problem becomes tractable, and we can concentrate our resources on learning more about this coupling and also on learning how to reduce these emissions. This can be a practical way of alleviating SBS in many buildings. In order that we may learn how to reduce the secondary emissions, we must focus on understanding the underlying physical relationships. Research based on weak relationships in medical statistics, between illhealth and building technological parameters in general, cannot produce the knowledge needed for this.

The knowledge and the research results that are available today in this area may be sufficient for recommendations on how decomposition can be avoided in new buildings in which existing material combinations are used. If, however, we want to design new floor combinations where special materials are chosen to increase the margin of safety, we need to know more about the underlying mechanisms and the properties of the materials.

When moisture related damage is investigated in a building, a description of the causative relationships often requires a much more thorough knowledge of the material properties, damage mechanisms and critical threshold levels. This knowledge is available today as regards moisture, but it is not quite enough if we want to proceed just a step further and examine the consequential effects of moisture such as emissions and health effects due to decomposition of the adhesive or fungal attack. Often, the SBS investigator will even want to provide a description of the sequence of events on the basis of the condition assessment of the building and the findings of the investigation. It has been found that this demands far more knowledge than that needed at the outset to decide what is the correct procedure.

The relationships and critical levels which govern decomposition of the floor construction have not yet been sufficiently elucidated. We must know more about how different moisture and pH levels affect the mechanism underlying decomposition of the adhesive layer. We do not know at present how temperature influences the process or whether we can prevent it by basing the adhesive on different polymers. We do know, however, that we do not get the same decomposition products.

In order that we may be able to make predictions and record the sequence of events, it is also important that the constituent materials are described in a relevant way. The capacity of OCIC to bind to concrete and also to adhesive and flooring must be measured and verified. These are of great significance for an assessment of how much OC can be stored in the materials and constitute a future emission source. Diffusion coefficients also are important material properties which must be determined in order that these assessments may be made.

The calculation tools which we use today for moisture and its harmful effects must be improved so that relevant tasks may be performed with acceptable accuracy. At present, the tools are designed for researchers rather than for industry. It is often difficult to judge when they can be used, what are the simplifications that are made and therefore how reliable the results are. In order

to solve the problems of industry, it is necessary to develop easy to use tools that are based on accepted and well documented knowledge.

The input data used for these programs often have flaws, and these should also be improved. Material data are often old, development of new material grades and improved methods of measurement has often taken place after the properties of the old materials had been determined. The critical threshold values the calculation results are compared with require further study. As regards the mechanism underlying moisture damage and its consequences, poorly substantiated appraisals which are relevant for old material grades are often made. By elucidating the mechanisms active in the different types of damage, the critical values of the relevant parameters can be determined for each type of damage and each material.

In order that the effects of the intermediate layers in the form of screeds, alkali and moisture barriers which are available in the market today may be reliably evaluated, these must be investigated. We need to chart and understand their material properties and the way they affect the floor system as a whole, so that we may judge whether they confer positive properties on a floor construction.

13 References

- Afshari A. 2000. Determination of VOC Emissions from Surface Coatings by Environmental Test Chamber Measurements. Department of Building Services Engineering, Chalmers University of Technology, Göteborg. Document D46:1999. 152 pages
- Ahlgren L. 1972. Fuktfixering i Porösa Byggnadsmaterial. (Moisture Fixation in Porous Building Materials. In Swedish). Moisture Research Group, Division of Building Materials, Lund Institute of Technology. Report 36. 200 pages.
- Alexandersson J. 1998. Långtidseffekter av alkalisk nedbrytning i golv. (Long term effects of alkaline decomposition in floors. In Swedish). Golv till tak nr 3, 1998.. 3 pages.
- Andersson *et al.* 2001. In *Indoor Air (2001)*. Submitted.
- ASTM 1985 Standard E104-85. Standard Practice for Maintaining Constant Relative Humidity by Means of Aqueous Solutions. American Society for Testing and Materials, USA. 3 pages .
- Atlassi E, Norling K, Radocea A. 1991. Fuktfri betong – en fråga om rätt materialkombination. (Concrete without excess moisture – a matter of the correct material combination. In Swedish). *Betong nr 3*, 1991. Pp 24–26.
- Betonghandboken, 1994. *Betonghandboken, Material, utgåva 2.* (Swedish Handbook of Concrete, Materials. In Swedish). AB Svensk Byggtjänst, Solna. 1127 pages.
- BFR, 1993. Ventilationsguiden, byggherrens guide för bostadsventilation, Nybyggnad. (Ventilation guide, guide on domestic ventilation for clients, New construction. In Swedish). Swedish Council for Building Research, Stockholm. Publication T19:1993. 47 pages.
- Björk F. 1996. Kursmaterial i "Utvecklingsmöjligheter för plaster i byggtillämpningar". (Course literature in "Development opportunities for plastics in building applications. In Swedish). Department of Building Sciences, Royal Institute of Technology KTH
- Björk F, Eriksson C-A., Karlsson S, Khabbaz F. 1999. Alkalisk nedbrytning av golvkomponenter. Två rapporter som behandlar: Kemisk nedbrytning av material i golvbjälklag. Alkalitetsmätning av golvavjämningsmassa utsatt för påskjutande alkalitet. Samt: Alkalisk nedbrytning av golvkomponenter. (Alkaline decomposition of floor components. Two reports dealing with: Chemical decomposition of materials in floors. Measurement of alkalinity in floor screeds exposed to increased alkalinity. And: Alkaline decomposition of floor components. In Swedish). Department of Building Sciences, Royal Institute of Technology KTH, Stockholm. Bulletin No 177. 49 pages.
- Blom P. 1998. Betong i byggnader - en vurdering av konsekvenser for inneklime og helse. (Concrete in buildings – evaluation of its impact on indoor climate and health. In Norwegian). BYGGFORSK, Norwegian Building Research Institute. Project Report No 236-1998. 37 pages.
- Boverket, 1994. Boverkets Byggregler – BBR 94, kurskompendium. (Swedish Board of Housing, Building and Planning, 1994. The Board's Building Regulations – BBR 94, course compendium. In Swedish). Bygginfo, Stockholm. 183 pages.

- Box G, Hunter W, Hunter S. 1978. Statistics for Experimenters. An Introduction to Design, Data Analysis, and Model Building. John Wiley & Sons, USA. 653 pages.
- Crank J. 1975. The Mathematics of diffusion. Clarendon Press, Oxford.
- CRC 2000. Handbook of Chemistry and Physics, 81st edition 2000 - 2001. CRC press, INC., USA. 2400 pages.
- Edenholm K. 1998. Personal communication of measurement results by Krister Edenholm. Analyscentrum, Casco products, Stockholm.
- Fagerlund G. 1982. Fuktmekaniska egenskaper, kapitel 8.6 i Betonghandboken Material. (Moisture mechanics properties, Section 8.6 in Swedish Handbook of Concrete, Materials. In Swedish). AB Svensk Byggtjänst och Cementa AB. Svenskt Tryck AB Stockholm. 619 pages.
- Fritsche M. 1996. Kemisk emission från golvlim på betong – effekt av olika fukt- och alkalispärrar. (Chemical emission from floor adhesive on concrete – the effect of different moisture and alkali barriers. In Swedish). Degree project at Department of Building Materials, Chalmers University of Technology, Göteborg. E-96:1. 44 pages.
- Fritsche M, Sjöberg A, Wengholt Johnsson H. 1997. Kemisk emission från golvsystem av limmad PVC-matta på självtorkande betong – inverkan av limningsteknik, torkförlopp samt cement-, lim- och matttyper. (Chemical emission from floor systems comprising bonded PVC flooring on self-desiccating concrete – the influence of bonding technique, drying process and the types of cement, adhesive and flooring. In Swedish). Department of Building Materials, Chalmers University of Technology, Göteborg. P-97:2. 17 pages.
- GBR, 1999. Mätning av emissionsegenskaper hos sammansatta golvkonstruktioner. (Measurement of the emission characteristics of composite floor constructions. In Swedish). Industry standard, Swedish Flooring Trades Association, Stockholm. 8 pages.
- Gustafsson H., Jonsson B. 1993. Trade Standards for Testing Chemical Emission from Building Materials. Part 1: Measurements of Flooring Materials. Conference Proceeding. Indoor Air '93. Helsinki. Vol 2, 437–442.
- Gustafsson H, Jonsson B, Lundgren B. 1995. Emissionen aus Beschichtungsstoffen – Stand der Technik, Analyse der Emissionen und deren Einfluß auf die Innenraumluft. (Bidragets titel:) Chemical Emission from Paints and Other Surface Materials – Measurements with Field and Laboratory Emission Cell (FLEC) and other climate chambers. Kontakt & studium Band 478, Expert verlag. Sid 95 – 105.
- Gustafsson H. 1996. Golvmaterial på olika typer av fuktiga betonggolv – översikt och kommentarer till undersökningar med inriktning på kemisk nedbrytning och emission. (Flooring materials on different types of moist concrete slabs – overview and comments on investigations concerning chemical decomposition and emission. In Swedish). Swedish Testing and Research Institute, Borås. SP-RAPPORT 1996:25. 27 pages.

- Hedenblad G, Nilsson LO. 1987. Kritiska Fukttillstånd För Några Byggnadsmaterial, Prelimonär Undersökning. (Critical moisture states of some building materials, Preliminary Investigation. In Swedish). Moisture Research Group, Division of Building Materials, Lund Institute of Technology. Rapport TVBM-3028. 47 pages.
- Hedenblad G, Jans M. 1994. Inverkan av alkali på uppmätt RH i betong. (The influence of alkali on RH measured in concrete. In Swedish). Division of Building Materials, Lund Institute of Technology. Rapport TVBM-3057. 26 pages.
- Hedenblad G. 1996. Materialdata för Fuktttransportberäkningar. (Material properties for moisture transport predictions. In Swedish) Swedish Council for Building Research. T19:1996.
- Hedenblad G. 1997. Drying of Construction Water in Concrete, drying times and moisture measurements. Swedish Council for Building Research, Stockholm. T9:1997. 54 pages.
- Hilleborg A. 1975. Kompendium i Byggnadsmateriallära för V3. (Course compendium in Building Materials for V3. In Swedish) Division of Building Materials, Lund Institute of Technology. 151 pages.
- Konieczny H. 1997. Gypsum and Gypsum Based Screeds. Degree project at Department of Building Materials, Chalmers University of Technology, Göteborg. E-97:2. 88 pages.
- Kumlin A. 2000. Personal communication with M.Sc. Anders Kumlin, AK-konsult Indoor Air AB. Stockholm.
- McQuarrie D A., Rock P A., 1991, General Chemistry, third edition. W. H. Freeman and Company, New York. 1991. 1083 pages.
- Meinighaus R. 2000a. Gravimetric Studies on VOC Adsorption By Indoor Materials Under near-Ambient Conditions. Draft, accepted by Indoor G Built Environment.
- Meinighaus R. 2000b. Personal communication with dr Roman Meinighaus, INERS – Institut National de L'environnement Industriel et des Risques, France.
- Nevander LE, Elmarsson B. 1994. Fukthandboken – praktik och teori. (Moisture Manual – practice and theory. In Swedish). AB Svensk Byggtjänst, Stockholm. ISBN 91-7332-716-6. 538 pages.
- Nilsson LO. 1979. Fuktmätning, Del 2 av Byggfukt i betongplatta på mark – torknings- och mätmetoder. (Moisture measurement, Part 2 of Construction water in ground slabs - Drying and measurement methods. In Swedish) Division of Building Materials, Lund Institute of Technology. Report TVBM-3008. 75 pages.
- Nilsson LO. 1980. Hygroscopic Moisture in Concrete – Drying, Measurements & Related Material Properties. Division of Building Materials, Lund Institute of Technology. Report TVBM-1003. 162 pages.
- Nilsson LO. 1984. Fukt i flytspackel. Verksamheten 1981 – 84; (Moisture in self levelling screed. Activity 1981-84. In Swedish). Moisture Research Group at Lund Institute of Technology, Lund. Fuktgruppen informerar 1984:1.

- Nilsson LO. 1987. Temperature effects in relative humidity measurements on concrete – some preliminary studies. Proceedings of Nordic Symposium on Building Physics, Lund. BFR-Rapport D13:1988. 7 pages.
- Nilsson LO. 1992. A Theoretical Study on the Effects of Non-linear Chloride Binding on Chloride Diffusion Measurements in Concrete. Department of Building Materials, Chalmers University of Technology, Göteborg. P-92:13. 40 pages.
- Nilsson LO, Luping T. 1992. Relations Between Different Transport Parameters, section 3 in Performance Criteria for Concrete Durability. E & FN Spon, London. Rilem Report 12. 327 pages
- Nilsson LO. 1994. Fukt och Betong, kapitel 14 i Betonghandboken. (Moisture and Concrete, Section 14 in Swedish Handbook of Concrete. In Swedish). AB Svensk Byggtjänst och Cementa AB. Svenskt Tryck AB Stockholm. 1127 pages.
- Nodling Mjörnell K. 1997. Moisture Conditions in High Performance Concrete – mathematical modelling and measurements. Department of Building Materials, Chalmers University of Technology, Göteborg. P-97:6. 126 pages.
- Nordtest. 1995. Building Materials: Emission of Volatile Compounds – Field and Laboratory Emission Cell (FLEC). Nordtest method NT BUILD 438. Approved 1995-11. 4 pages.
- Ramnäs O. 2000. Personal communication with Ph.D. Olle Ramnäs, Department of Chemical Environmental Science, Chalmers University of Technology, Göteborg.
- RBK. 1999. Manual – Fuktmätning i betong. (Moisture measurement in concrete. In Swedish). Sveriges byggindustrier, Stockholm. 76 pages.
- Salthammer T. 1999. Organic Indoor Air Pollutants. Occurrence, Measurement, Evaluation. WILEY-VCH. Weinheim, Germany. 329 pages.
- Salthammer T, Kephelopoulos S, Villberg K. 2000. WS29 Assessment of Material Emission on IAQ. Workshop summaries, Healthy Buildings 2000, Espoo, Finland. 6 pages.
- Schrewelius K. 1997. Personal information by Kaj Schrewelius, Bona kemi AB, Malmö.
- Schrewelius K. 2000. Personal communication with Kaj Schrewelius.
- Sjöberg A. 1997. En mätmetod för studier av fukttillskottet till betong under nylimnad PVC-matta. (Measuring method for studies of moisture increment to concrete below newly bonded PVC flooring. In Swedish). Department of Building Materials, Chalmers University of Technology, Göteborg. P-97:4. 21 pages.
- Sjöberg A. 1998a. Transportprocesser och reaktioner i belagda betonggolvs – olika faktorer inverkan på emission från golvkonstruktioner. (Transport processes and reactions in concrete floors with finishes – the influence of different factors on emission from floor constructions. In Swedish). Department of Building Materials, Chalmers University of Technology, Göteborg. P-98:13. 193 pages. www.bm.chalmers.se/research/publika/p9813.htm
- Sjöberg A. 1998b. Mätosäkerhet vid fuktmätning i betong med kapacitiva fuktgivare – en bedömning av faktorer som påverkar osäkerheten samt hur de kan minskas. (Uncertainty in measurements of moisture in concrete with

- capacitive moisture sensors – assessment of the factors which influence the uncertainty and the way their effect can be reduced. In Swedish). Department of Building Materials, Chalmers University of Technology, Göteborg. P-98:1. 60 pages. www.bm.chalmers.se/research/publika/p981.htm.
- Sjöberg A. 1998c. Uncertainty in Measurements of Relative Humidity in Concrete. 5th Symposium on Building Physics in the Nordic Countries. Göteborg, Sweden. 24-26 August 1999. 8 pages.
- Sjöberg A, Wengholt Johnsson H. 1999. Fukt- och emissionsförhållanden vid limning av PVC- och linoleummatta på betong. (Moisture and emission conditions in conjunction with bonding of PVC and linoleum floorings to concrete. In Swedish). Department of Building Materials, Chalmers University of Technology. P-99:1.
- Swedish Concrete Association 1997. Betong för sunda golv - fuktdimensionering, materialval och produktion. (Concrete for healthy floors – moisture design, choice of materials and production. In Swedish). Swedish Concrete Association Report Series No 6. Stockholm. 36 pages.
- Swedish Internal Climate Institute (1990). Klassindelade Inneklimatsystem - riktlinjer och specifikationer. (Classification of indoor climate systems – guidelines and specifications. In Swedish). SCANVAC Guideline Series, Report No R1. Stockholm. 63 Pages.
- Tutti K. 1982. Corrosion of Steel in Concrete. Swedish Cement and Concrete Research Institute (CBI). Stockholm. No4.82.
- Wengholt Johnsson H. 1995. Kemisk emission från golvsystem – effekt av olika betongkvalitet och fuktbelastning. (Chemical emission from floor systems – the effect of different concrete grades and moisture loads. In Swedish). Department of Building Materials, Chalmers University of Technology. P-95:4. 58 pages.
- Wengholt Johnsson H. 1998. Golvmaterial på betongunderlag – fältmätningar av torktider och emissioner i kv Gärdsrået, Umeå. (Flooring materials on concrete substrates – field measurements of drying periods and emissions in the Gärdsrået district, Umeå. In Swedish). NCC / SBUF. 27 pages.
- Wolkoff P, Clausen P A, Nielsen P A, Gustafsson H, Jonsson B, Rasmusen E. 1991 Field and Laboratory Emission Cell: FLEC. Conference Proceeding. Healthy Building '91. Washington D.C. Page 160–165.
- Xu A. 1992. Structure of hardened cement - fly ash systems and their related properties. Department of Building Materials, Chalmers University of Technology. P-92:7. 296 pages.

Appendix No 1 – Uncertainty in measuring RH with electrical instruments

The measurement uncertainty for the three methods based on RH measurement with electrical instruments was calculated by applying the recommendations given in Sjöberg (1998b); a summary of this report in English is given in Sjöberg (1998c). The factors which influenced these methods are examined in this appendix.

General

In assessing the total uncertainty, both systematic and random effects are considered. The total measurement uncertainty is calculated as the square root of the sum of the squares of the individual factors, as described later on in this appendix and in Sjöberg (1998b,c).

Systematic and random deviations (factors) can be described by reference to the hit pattern on a target; see Fig. B1.1. The random deviation (spread, precision) is represented by the spread over the hit pattern. Systematic deviation (accuracy, bias) is the difference between the centre of the target and the centre of the hit pattern.

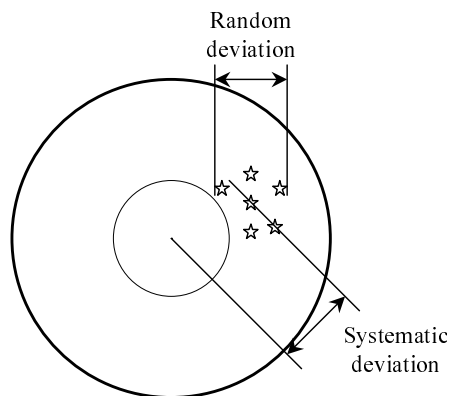


Fig. B1.1 Systematic and random deviation illustrated by the hit pattern on a target.

The systematic and random effects which influence the results in RH measurements mainly derive from only a few sources. For the measurement of relative humidity in materials the four principal sources of error are as follows:

- The measuring instrument, i.e. the factors which arise owing to the properties of the materials the instrument is made of, or owing to the construction of the electronics in the instrument.
- Calibration of the measuring instrument which is carried out to reduce its measurement uncertainty and to correct deviations.
- Handling of the equipment during and between RH measurements.
- Evaluation of the measured values.

These four principal sources and the factors which derive from them and influence the results are described below.

The measuring instrument

Uncertainty in measured values due to the instrument can be compensated for by performing a calibration. The interval between calibrations must be suited to the stability and performance of the instrument to ensure that no major changes can occur in the instrument between calibrations.

According to Vaisala OY, the total uncertainty for the probes used is $\pm 2\%$ RH over the interval 0-90% RH, and $\pm 3\%$ RH over the interval 90-100% RH. The uncertainty in temperature measurements is $\pm 0.3^\circ\text{C}$. There is no information concerning the coverage factors of the values. This uncertainty is considered to be rather large, perhaps unreasonably so in some cases. A more exact evaluation of the instruments used in this study has therefore been made. The sources of uncertainty in RH measurements which can be distinguished in the measuring instrument are as follows:

Systematic factors

- a) Nonlinearity of the RH instrument
- b) Drift of the RH probe, i.e. the value measured by a probe changes over time

Random factors

- c) Hysteresis of the RH probe, i.e. the RH probes have different calibration curves when their moisture content is increasing and decreasing.

Calibration

The object of calibration is to quantify the magnitude of deviations and uncertainties, if any, in the measuring instrument. The correction determined during a calibration is also subject to a measurement uncertainty, and this must be taken into consideration.

Examples of factors which may give rise to uncertainty in calibration are as follows:

Systematic factors

- d) Temperature difference during calibration

Random factors

- e) Random factors associated with salt solutions
- f) Temperature variations during calibration
- g) Other factors during calibration
- h) Total measurement uncertainty of calibration in dual pressure humidity generator

Handling

Factors which arise owing to handling cannot be eliminated by calibration. They can be avoided only by correct handling or, in certain cases, by subsequent correction of the measured values.

The following summary of the factors which arise during handling presupposes that measurement is carried out correctly and that no other factors arise because of faulty handling.

Systematic factors

- i) Moisture measurement at a temperature different from that during calibration
- j) Moisture measurement at a temperature different from that in service
- k) Storage of RH probe in a dry environment
- l) Moisture capacity of RH probe in measurements on extracted samples
- m) Moisture capacity of RH probe in measurements in drilled holes
- n) Temperature difference between sensor and concrete
- o) Recently drilled measuring holes
- p) Difference in alkalinity.

Random factors

- q) Variation in temperature during measurement
- r) Non-uniform extraction of samples
- s) Condensation in test tube during transport of extracted samples
- t) Differences in depths of measuring holes.

Evaluation

There are factors which can influence the results of evaluation, which are not affected by the measurement or the performance of the measuring instrument. The effect of these factors can be taken into consideration by correct and accurate evaluation of the measured data. In many cases it is even possible to correct for the influence of these factors at a later time.

Systematic factors

-

Random factors

- u) Wrong slab thickness.

Method No 1, Measurement with electrical RH probes in cast-in measuring tubes

In this method, RH probe HMP 36 and hand instrument HMI 31 from Vaisala were used. Measurements were made in special tubes which had been mounted in the test specimens before the concrete was poured. The probes were inserted into the tubes one day before the measurement. The RH instruments were calibrated, before and after measurements, in relation to the equilibrium RH above saturated salt solutions.

The factors which contribute to the measurement uncertainty in Method No 1 are discussed and quantified below.

a) Nonlinearity of RH instrument

RH probe HMP 36 from Vaisala which was used in this method was judged to have a nonlinearity of the same order as that described in Hedenblad (1995). The maximum difference between read and "true" RH is 2% RH; the maximum difference occurs at a moisture level of 90% RH. See Fig. B1.2.

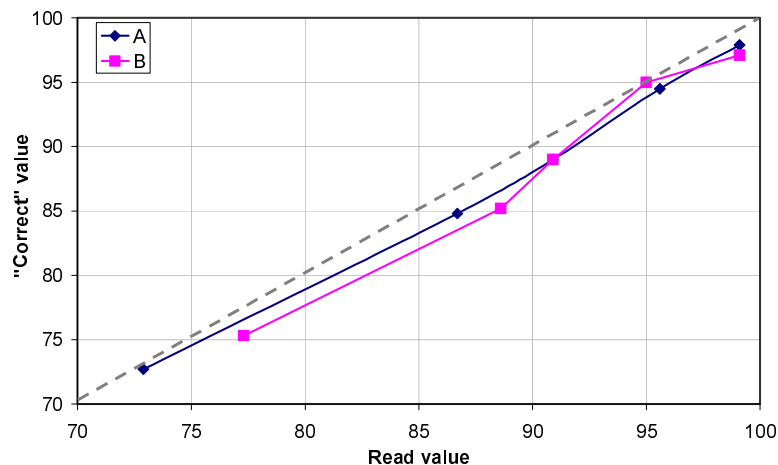


Fig. B1.2 Nonlinearity of RH probe, measured by two different laboratories. According to Hedenblad (1997).

The value of nonlinearity given by Hedenblad (1995) is 2% RH deviation at 90% RH. If we assume that the deviation has normal distribution at 90% confidence level, the standardised measurement uncertainty ($S_a^\#$) is

$$S_a^\# = \frac{2}{1.645} = 1.22\%$$

where 1.645 is the coverage factor for a two-sided confidence interval, with 90% probability of "covering" the true value.

b) Drift of RH probe

The term drift refers to the change over time which occurs in the value read by an RH probe (for the same RH).

In Sjöberg (1998b), 496 measurements made during repeated calibrations of 17 RH probes HMP 36 from Vaisala were statistically evaluated. This evaluation cannot show that there was any systematic drift in these probes.

The standardised measurement uncertainty ($S_b^\#$) in this method can therefore be assumed to be equal to zero:

$$S_b^\# = 0$$

c) Hysteresis of RH probe

The term hysteresis of an RH probe refers to the fact that the RH probe has different calibration curves when its moisture content is increasing and decreasing.

If the temperature has small transient (rapid) variations, deviation due to hysteresis is less than when the temperature is constant. During small transient temperature variations RH varies all the time because the moisture content of the air is constant while its saturation vapour content varies. The moisture content is situated along the hysteresis curves, and the value of RH that is read is between the sorption isotherms for increasing and decreasing moisture content; see Fig. B1.3.

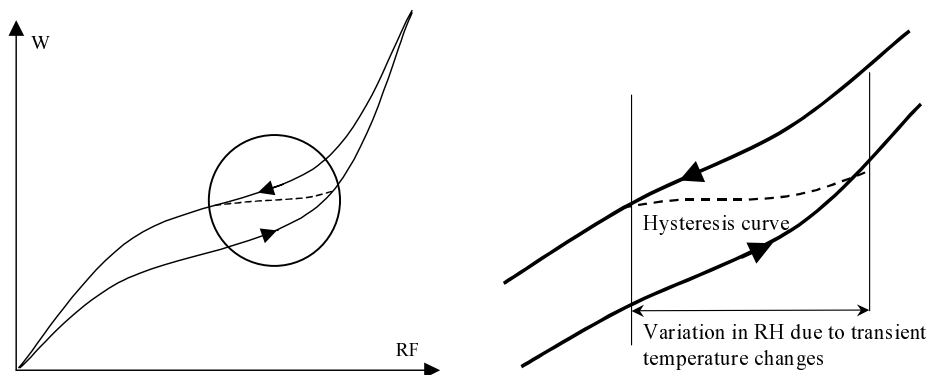


Fig. B1.3 Effect of temperature variations on equilibrium RH owing to hysteresis.

Hedenblad (1995) states, however, that in an investigation made at the Department of Building Materials, University of Lund Institute of Technology, hysteresis of up to 1% was observed on RH probes. If we assume that probability has normal distribution with 90% confidence interval, the coverage factor is 1.645. The standardised measurement uncertainty (S_c) is then

$$S_c = \frac{1}{1.645} = 0.61\%$$

d) Difference in temperature during calibration

The equilibrium RH of salt solutions is temperature dependent. If the temperature of the salt solution is different from the expected temperature, a difference occurs. The equilibrium RH of most salts has some temperature dependence. However, for small temperature differences this factor can be ignored; see Table B1.1

Table B1.1 Differences in equilibrium RH measured above saturated salt solutions due to differences in temperature

Salt	RH (20°C)	%RH / °C	0.1°C	0.5°C	1.0°C
Lithium chloride LiCl	11.3	0,00	0.00	0.00	0.00
Potassium acetate $KC_2H_3O_2$	23.1	-0.09	-0.01	-0.05	-0.09
Magnesium chloride $MgCl_2$	33.1	-0.06	-0.01	-0.03	-0.06
Potassium carbonate K_2CO_3	43.2	0.00	0.00	0.00	0.00
Magnesium nitrate $Mg(NO_3)_2$	54.4	-0.30	-0.03	-0.15	-0.30
Sodium chloride NaCl	75.5	-0.03	0.00	-0.02	-0.03
Potassium chloride KCl	85.1	-0.16	-0.02	-0.08	-0.16
Barium chloride $BaCl_2$	91	-0.17	-0.02	-0.09	-0.17
Potassium nitrate KNO_3	94.6	-0.18	-0.02	-0.09	-0.18
Potassium sulphate K_2SO_4	97.6	-0.06	-0.01	-0.03	-0.06

Of the salts used to calibrate RH probes in this study, potassium nitrate KNO_3 is the one most sensitive to temperature differences. Owing to the uncertainty in the temperature level of the controlled climate room and because of internal heat sources, for instance lighting and the technicians performing the measurements, it is not absolutely certain that the temperature of the salt solution was exactly +20°C. Since the magnitude of this difference is not known, its maximum value was estimated at 1.0°C. It is reasonable to suppose that this temperature difference has normal distribution, and that the probability of the maximum temperature difference (1.0°C) being exceeded is less than 1%. The confidence interval is then 99%, and the coverage factor is 2.576. The standardised uncertainty ($S_d^{\#}$) is

$$S_d^{\#} = \frac{-0.16}{2.576} = -0.06$$

e) Random factors associated with the salt solutions

For ideal conditions, ASTM E104 (1985) states that the uncertainty or accuracy is dependent on the salt used and the temperature of the solution. Table B1.2, from Sjöberg (1998b,c), sets out the uncertainty in the equilibrium RH of saturated salt solutions according to ASTM E104 (1985), and the standardised measurement uncertainty.

Table B1.2 Uncertainty in equilibrium RH of saturated salt solutions, according to ASTM E104 (1985).

Salt	RH (20°C)	Uncertainty	Std. meas. uncertainty
Lithium chloride LiCl	11.3	± 0.3	0.17
Potassium acetate $KC_2H_3O_2$	23.1	± 0.3	0.17
Magnesium chloride $MgCl_2$	33.1	± 0.2	0.12
Potassium carbonate K_2CO_3	43.2	± 0.3	0.17
Magnesium nitrate $Mg(NO_3)_2$	54.4	± 0.2	0.12
Sodium chloride NaCl	75.5	± 0.1	0.06
Potassium chloride KCl	85.1	± 0.3	0.17
Barium chloride $BaCl_2$	91	± 2	1.2
Potassium nitrate KNO_3	94.6	± 0.7	0.40
Potassium sulphate K_2SO_4	97.6	± 0.5	0.29

Of the salts used to calibrate RH probes in this study, potassium nitrate KNO_3 is the one that has the highest measurement uncertainty due to this effect. The standardised measurement uncertainty (S_e) is then

$$S_e = 0.40\%$$

f) Temperature variations during calibration

Transient (rapid) temperature variations in the air that is in equilibrium with the salt solution give rise to deviations from the expected RH value. During these transient temperature variations there is no time for equilibrium between the salt solution and air to be re-established. These transient temperature variations may be caused, for instance, by a door being opened, a light being turned on or a person coming into the room, i.e. events which usually occurred when readings with the RH instrument were made.

The explanation of this phenomenon is that although the air retains its original vapour content during a rapid temperature oscillation, the temperature and thus the saturation vapour content are altered. If the temperature of the air rises, saturation vapour content increases and RH decreases. If the temperature drops, saturation vapour content decreases and RH increases.

The maximum theoretical uncertainties for usual variations and the maximum measured variations are set out in Table B1.3. The magnitude of the uncertainty caused by a certain temperature variation is governed by the temperature and the RH level at which the calibration is performed.

Table B1.3 Maximum theoretical uncertainty in RH owing to transient temperature variations, and the maximum variations measured in concrete. Sjöberg (1998b).

Variation	Uncertainty	Measured variation
±0.1 °C	±0.6 %RH	±0.5 %RH
±0.5 °C	±3.0 %RH	±1.0 %RH
±1.0 °C	±6.0 %RH	-

According to Sjöberg (1998a), temperature variations during measurements in the climatically stable room (CA 12) are approximately ±0.5°C for a moderate occupancy level. According to Sjöberg (1998b), calibration with potassium sulphate K₂SO₄ (97.6% RH) at +20°C produces an uncertainty of 2.93% RH when the temperature variation is ±0.5°C. Let us assume that the temperature has normal distribution and that the probability of the maximum temperature variation being exceeded is less than 1%. The confidence interval is then 99% and the coverage factor is 2.576. The standardised uncertainty (S_f) is

$$S_f = \frac{2.93}{2.576} = 1.14\%$$

where 2.576 is the coverage factor for a two-sided confidence interval, with 99% probability of "covering" the true value.

g) Other factors in calibration

Unless great accuracy and cleanliness are observed in work with salt solutions, it is likely that new factors will arise to influence uncertainty. Since fresh salt solutions prepared in accordance with ASTM (1985) were used, this uncertainty (S_g) can be disregarded.

$$S_g = 0\%.$$

h) Total measurement uncertainty for calibration in dual pressure humidity generator

This type of calibration was not carried out, and the standardised uncertainty (S_h) for this effect need not therefore be considered.

i) Moisture measurement at a temperature different from that during calibration

Calibration and moisture measurements were performed in the same laboratory premises, and the temperature difference at no time exceeded 5°C. The standardised uncertainty (S[#]_i) can therefore be ignored.

$$S^{\#}_i = 0\%.$$

j) Moisture measurement at a temperature different from that in service

The service stage was considered to occur in the same laboratory premises in which moisture measurements were made, since the test specimens at no time left these premises. The standardised uncertainty ($S^{\#}_j$) can therefore be disregarded.

$$S^{\#}_j = 0\%.$$

k) Storage of RH probes in a dry environment

If the RH probes are stored in a drier environment than the one in which measurement are made, the time to establishment of equilibrium increases. The reason is that the RH sensor has dried out and needs time to absorb moisture again.

The RH probes with sensors were stored in a climate of ca 75% RH. The standardised uncertainty ($S^{\#}_k$) can therefore be ignored.

$$S^{\#}_k = 0\%.$$

l) Moisture capacity of RH probe in measurements on extracted samples

This method did not use extracted samples, and the standardised uncertainty ($S^{\#}_l$) for this effect need not therefore be taken into consideration.

m) Moisture capacity of RH probe in measurements in drilled holes

A certain quantity of the moisture in concrete is used up in wetting the RH probe. This gives rise to a systematic factor which makes the measured value too low.

The protective filter is the part of the RH probe that has the highest moisture capacity. Depending on construction, moisture capacity may be assessed as 4-10 mg over the 40-97% RH interval, i.e. if the filter had been exposed to room air, it takes up 4-10 mg moisture from the time it is inserted into the measuring hole until it comes into equilibrium with the moist concrete. According to Nilsson (1979), a sintered bronze filter has a moisture capacity of 4.3 mg/(40% RH;97% RH), and an RH sensor <0.5 mg/(40% RH;97% RH).

For an RH probe of little moisture capacity and for an open texture concrete, the factor is smaller; see Table B1.4. The difference decreases in time if the RH probe is left in place, since moisture is transported to the hole from the concrete. As a rule of thumb, the difference is halved every 5 days; Sjöberg (1998b).

An RH probe of very little moisture capacity does not have much effect on RH in the concrete. By using a guard of minimum moisture capacity, for instance RH probe HMP44 from Vaisala with the "paper filter" removed, moisture capacity can be reduced to less than 1 mg.

Table B1.4 Systematic deviation (% RH) due to the fact that moisture from a hole drilled in concrete, of moisture level of 90% RH, is used to wet the inserted RH probe. Sjöberg (1998b).

Moisture capacity (mg)	Concrete grade (w/c ratio)		
	w/c = 0.4	w/c = 0.5	w/c = 0.7
1	0.7	0.6	0.5
4	2.5	2.3	2.0
10	5.3	4.7	4.2

The moisture capacity of the probes used in this study is about 4 mg. With this method, readings are taken after about one day. The systematic deviation ($S_m^\#$) is then as set out in Table B1.5.

Table B1.5 Systematic deviation $S_m^\#$ (% RH) for different concrete grades.

	Concrete grade (w/c ratio)		
	w/c = 0.4	w/c = 0.5	w/c = 0.7
$S_m^\#$	2.5	2.3	2.0

n) Temperature difference between sensor and concrete

If there is a temperature difference between the RH sensor and the concrete, a systematic error occurs during measurements. If the temperature of the RH sensor is higher than that of the concrete, the measured value is lower than the real RH in the concrete. If the temperature of the RH sensor is lower, the measured value is higher.

In the study, test specimens and measuring equipment were kept in the same climate as the one in which the measurements were made. It is therefore reasonable to suppose that there was no temperature difference between the sensor on the RH probe and the concrete. The standardised uncertainty ($S_n^\#$) can therefore be ignored.

$$S_n^\# = 0\%$$

o) Recently drilled measuring holes

The measuring tubes were cast into the test specimens, not drilled after the concrete had hardened. The standardised uncertainty ($S_o^\#$) for this effect need not therefore be taken into consideration.

p) Difference in alkalinity

RH is influenced by the alkalinity of the concrete. If the quantity of moisture in kg/m^3 is the same for two concrete types which are identical apart from alkalinity, then, according to Hedenblad and Janz (1994), the RH measured in the concrete of lower alkalinity is higher. The pore liquid in the concrete can in

that case be regarded as a salt solution that has a lower RH in equilibrium with air.

Since it is the RH of the air in the pores of the concrete that is measured and this is not converted into moisture content, the effect can be ignored, and the standardised uncertainty $S_p^\#$ is

$$S_p^\# = 0\%$$

q) Variation in temperature during measurements

Concrete is a material that responds slowly to changes in temperature and moisture conditions. Its temperature and moisture content change fairly slowly. It is not likely that large transient temperature variations can arise in concrete. Our own measurements made at the Department of Building Materials, Chalmers University, have shown that the difference can be as much as 1% RH; Sjöberg (1998a).

The largest difference due to this effect that is measured in a test specimen is 1% RH. If it is assumed that the probability function has normal distribution, with 90% confidence level, then the coverage factor is 1.645. The standardised measurement uncertainty (S_q) is

$$S_q = \frac{1\% \text{ RH}}{1.645} = 0.61$$

r) Non-uniform extraction of samples

In this method measurements were made not on extracted samples, but in cast-in measuring tubes. The standardised measurement uncertainty (S_r) for this effect need not therefore be taken into consideration.

s) Condensation in test tube during transport of extracted samples

In this method measurements were made not on extracted samples, but in cast-in measuring tubes. The standardised measurement uncertainty (S_s) for this effect need not therefore be taken into consideration.

t) Differences in the depths of measuring holes

Drill holes were not always precisely the depth they were supposed to be. This difference is important, for instance when RH is measured at the characteristic depth when concrete slabs are drying out, and the value is compared with a critical limiting value. If the hole is drilled too deep, the measured value will be on the safe side, while if it is too shallow, the value measured will be lower than that at the characteristic depth.

The value measured in the measuring tubes which are cast into test specimen No 3 (the pot) is a mean over a depth which is equal to the inside diameter of the tube. See Fig. B1.4. The placing of the measuring tubes was improved in test specimen No 4 (the bucket). There they are fixed into the base, and the depth of measurement is determined by the distance between the top of the tube and the surface. See Fig. 2.12.

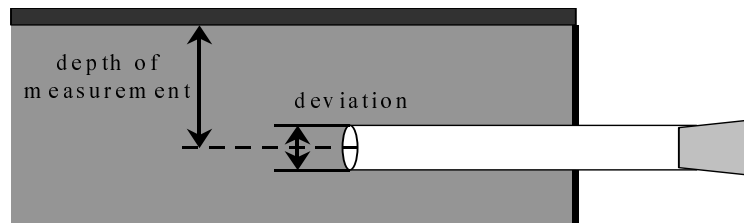


Fig. B1.4 Determination of depth of measurement.

The positions of the measuring tubes are determined and well documented in this study. This effect can therefore be ignored, and the standardised uncertainty (S_t) is

$$S_t = 0\%$$

u) Wrong slab thickness

It is sometimes found that the actual thickness of the slab is different from that given. The reason may be that the person giving the information has mixed up different figures, or his memory is at fault. The reason may also be that for some reason the slab was not cast to the thickness specified on the drawing. Whatever the reason, evaluation of the maximum moisture content after the residual construction water had been redistributed will be in error if the thickness of the slab is not correct. After an impermeable finish has been applied, the level of moisture in the whole slab will be that which prevailed at the characteristic depth before redistribution took place.

Since the thicknesses of the test specimens and the positions of the measuring tubes are determined and documented, this effect can be disregarded, and the standardised uncertainty (S_u) is

$$S_u = 0\%$$

Total measurement uncertainty in Method No 1

For the calculation of the total uncertainty in this method, the 21 standardised measurement uncertainties $S_a \dots S_u$ are combined. The factors which influence uncertainty may be assumed to have normal distribution, and there is little probability that all factors act fully in concert. There is also very little probability that all factors cancel out, i.e. act completely in opposition. According to Lindskog (1994), a suitable "statistical compromise" is to sum the factors as shown by C in Fig. B1.5.

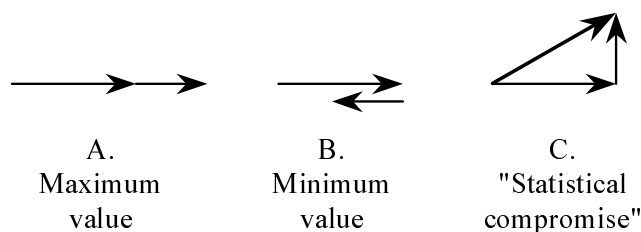


Fig. B1.5 The figure illustrates three possible ways of combining measurement uncertainties. A and B produce too high or too low values, while C provides a suitable statistical compromise, according to Lindskog (1994).

The combined standardised measurement uncertainty ("statistical compromise") can be calculated as

$$S_{\text{tot}} = \sqrt{S_a^2 + S_b^2 + S_c^2 + \dots + S_s^2 + S_t^2 + S_u^2}$$

where

- S_{tot} = combined standardised measurement uncertainty
- $S_a \dots S_u$ = standardised measurement uncertainty for factor a ... u

The combined standardised measurement uncertainty has a standardised coverage factor of 1.0, and its confidence interval is equal to 68.27.

The factors which contribute to the total measurement uncertainty for Method No 1 are summarised in Table B1.6.

Table B1.6 Summary of factors and their magnitudes, Method No 1.

	name	w/c ratio		
		0.4	0.5	0.7
a	nonlinearity	1.22	1.22	1.22
b	drift	0	0	0
c	hysteresis	0.61	0.61	0.61
d	ΔT , calibration	-0.06	-0.06	-0.06
e	salt	0.40	0.40	0.40
f	ΔT^* , calibration	1.14	1.14	1.14
g	calibration	0	0	0
h	dual pressure humidity generator	–	–	–
i	ΔT calibration/measurement	0	0	0
j	ΔT measurement/service	0	0	0
k	storage in the dry	0	0	0
l	moisture capacity, samples	–	–	–
m	moisture capacity, drilled holes	2.50	2.30	2.00
n	ΔT sensor/concrete	0	0	0
o	recently drilled holes	–	–	–
p	alkalinity	0	0	0
q	ΔT^* , measurement	0.61	0.61	0.61
r	non-uniform extraction of samples	–	–	–
s	condensation	–	–	–
t	deviations, depth of measurement	0	0	0
u	wrong slab thickness	0	0	0
a-u	Sum	3.15	3.00	2.77

* transient temperature variations

Method No 2, Measurement with electrical RH probes left inside cast-in measuring tubes

In this method, RH probe HMP 44 from Vaisala and datalogger Mitec AT40, and RH probe HMP 36 and hand instrument HMI 31 from Vaisala were used. Measurements were made in special tubes which had been mounted inside the test specimens before the concrete was cast. The probes remained inside the tubes during the entire measurement period which varied between 11 and 45 days for different measurements. The RH instruments were calibrated before and after measurements in relation to the equilibrium RH above saturated salt solutions.

The factors which contribute to the measurement uncertainty in Method No 2 are discussed and quantified below. In the absence of better data, factor a) for RH probe HMP 44 is judged to be the same as for HMP 36; these have already been discussed in Method No 1. Factors c-e, g-i, k-s are also judged to be the same as in Method No 1.

b) Drift of the RH probe

It is reported that the standardised measurement uncertainty ($S_b^{\#}$) of RH probe HMP44 from Vaisala is very high, but this has not been verified. According to information that has not been documented, it may be as much as several % RH per month.

Let us assume that the drift is normally distributed and that the probability that the maximum drift between calibrations will exceed 3% RH is less than 5%. The confidence interval is then 95% and the coverage factor is 1.96. The standardised uncertainty ($S_b^{\#}$) is

$$S_b^{\#} = \frac{3}{1.96} = 1.53\%$$

f) Temperature variations during calibration

Probes HMP44 are calibrated in an insulated aluminium block. The method is described in detail in Sjöberg (1998a). The transient temperature variations in the block are approximately $\pm 0.1^{\circ}\text{C}$ since it had been kept in a room of stable temperature.

According to Sjöberg (1998b,c), calibration with potassium sulphate K_2SO_4 (97.6% RH) at $+20^{\circ}\text{C}$ gives an uncertainty of 0.58% RH when the temperature variation is $\pm 0.1^{\circ}\text{C}$. Let us assume that the temperature has normal distribution and that the probability of the maximum temperature variation being exceeded is less than 1%. The confidence interval is then 99% and the coverage factor is 2.576. The standardised uncertainty (S_f) is

$$S_f = \frac{0.58}{2.576} = 0.23\%$$

m) Moisture capacity of RH probe in measurements in drilled holes

A certain quantity of moisture in the concrete is used to wet the probe. This systematic factor makes the measured value too low. The deviation decreases in time if the RH probe is left in the hole, since moisture is transported to the hole from the concrete. As a rule of thumb, the deviation set out in Table B1.5 may be said to decrease by half every 5 days.

Since in this method the probes are left inside the measuring tubes, this effect is greatest at the beginning of the measurements and is small at the end. On average, measurements lasted 18 days. The middle of the measurement period thus occurred, on average, after 9 days when, according to the rule of thumb, the effect had been halved almost twice.

The moisture capacity of the probes used in the study is about 4 mg. Measurements are made over a long period, and it may be assumed that the effect is, on average, reduced by half twice. The systematic deviation ($S_m^{\#}$) is then as set out in Table B1.7.

Table B1.7 Systematic deviation ($S_m^{\#}$) for different concrete grades.

	Concrete grade (w/c ratio)		
	w/c = 0.4	w/c = 0.5	w/c = 0.7
$S_m^{\#}$	0.63	0.58	0.50

t) Deviations in the depths of the measuring holes

The positions of the measuring tubes were subsequently determined with a dial gauge. The accuracy of measurement is estimated to be better than ± 0.5 mm. Sjöberg (1998b,c) describes that a usual moisture gradient is 3% RH/cm.

Let us assume that there is very little probability that the error in measuring the positions of the tubes exceeded 0.5 mm, which means that the error in RH is $\pm 0.15\%$ ($0.05 \text{ cm} \cdot 3\% \text{ RH/cm}$). Let us also assume that the confidence interval is 99%, which makes the coverage factor 2.576. If the error in measurement is assumed to be normally distributed, the standardised measurement uncertainty (S_t) is

$$S_t = \frac{0.15}{2.576} = 0.06\%$$

Total measurement uncertainty in using Method No 2

The factors which contribute to the total uncertainty for Method No 2 are set out in Table B1.8.

Table B1.8 Summary of factors and their magnitudes, Method No 2.

	name	w/c ratio		
		0.4	0.5	0.7
a	nonlinearity	1.22	1.22	1.22
b	drift	1.53	1.53	1.53
c	hysteresis	0.61	0.61	0.61
d	ΔT , calibration	-0.06	-0.06	-0.06
e	salt	0.40	0.40	0.40
f	ΔT^* , calibration	0.23	0.23	0.23
g	calibration	0	0	0
h	dual pressure humidity generator	–	–	–
i	ΔT calibration/measurement	0	0	0
j	ΔT measurement/service	0	0	0
k	storage in the dry	0	0	0
l	moisture capacity, samples	–	–	–
m	moisture capacity, drilled holes	0.63	0.58	0.50
n	ΔT sensor/concrete	0	0	0
o	recently drilled holes	–	–	–
p	alkalinity	0	0	0
q	ΔT^* , measurement	0.61	0.61	0.61
r	non-uniform extraction of samples	–	–	–
s	condensation	–	–	–
t	deviations, depth of measurement	0.06	0.06	0.06
u	wrong slab thickness	0	0	0
a-u	Sum	2.28	2.26	2.24

* transient temperature variations

No consideration has been given in this estimate to the difference in moisture level which may arise between the concrete precisely above the tube and the rest of the concrete at the same distance from the surface. This difference is probably greater when the distance between the tube and the surface is smaller.

Method No 3, Measurement with electrical RH probes on pieces of concrete placed in test tubes

In this method, RH probe HMP 36 and hand instrument HMI 31 from Vaisala were used. Measurements were made in test tubes into which pieces of concrete from the test specimen had been placed. The probes were inserted into the tube one day prior to the measurement. The RH instruments were calibrated before and after measurements in relation to the equilibrium RH above saturated salt solutions.

The factors which contribute to the measurement uncertainty in Method No 3 are discussed and quantified below. Factors a-k, m-q, and u, are judged to be the same as in Method No 1.

l) Moisture capacity of RH probe in measurements on extracted samples

A certain quantity of the moisture in the samples is used in wetting the RH probe. Note that this systematic factor makes the measured value too low, and that the factor decreases as the size of the piece of concrete used increases.

The pieces of concrete used in the study weighed at least 20 grammes. According to Sjöberg (1998b), the standardised systematic deviation ($S^{\#}_i$) over the 80-90% RH interval is as set out in Table B1.9.

Table B1.9 Systematic deviation ($S^{\#}_i$) over the 80-90% RH interval for different concrete grades.

	Concrete grade (w/c ratio)		
	w/c = 0.4	w/c = 0.5	w/c = 0.7
$S^{\#}_i$	0.24	0.24	0.20

r) Non-uniform extraction of samples

When pieces of concrete are taken from the test specimens, they must represent the concrete at the depth of measurement. If the pieces are irregular in shape or if the distribution of the coarse aggregate is not uniform, their centre of gravity may be displaced so that it is not at the calculated depth of measurement; see Fig. B1.6. In a 100 mm thick slab of normal structural concrete, RH at the characteristic depth may vary by ca 2-3% RH/cm.

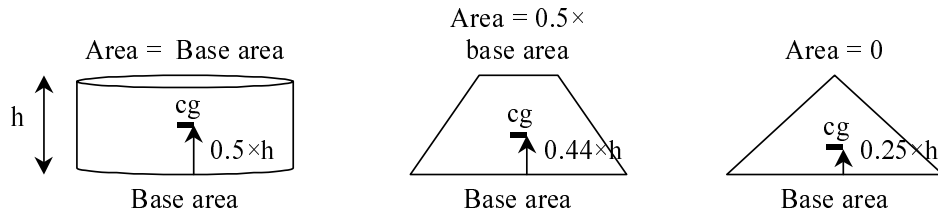


Fig. B1.6 Systematic deviation of "centre of gravity" in circular test pieces because of their shapes.

The pieces in the study are about 1 cm high. Let us assume that the shapes of the pieces are as in the centre illustration in Fig. B1.6, but with the larger area at the top. The measured value in this case is too low since the centre of gravity of the piece is above the depth of measurement. The RH gradient is assumed to be about 3% RH/cm. The random deviation will then be $[(0.5-0.44) \times 3] = 0.18\%$ RH.

It is further reasonable to assume that the position of the centre of gravity in cement paste is normally distributed if a large number of samples are taken, and that the confidence interval for the above assessment is 68%. The coverage factor is then equal to 1, and the standardised measurement uncertainty (S_r) is

$$S_r = \frac{0.18}{1} = 0.18\%$$

s) Condensation in test tube during transport of extracted samples

Test tubes with the pieces of concrete were at no time exposed to large temperature variations. The standardised uncertainty (S_s) for this effect can be ignored.

$$S_s = 0\%$$

t) Differences in depths of measuring holes

In this method there is an effect due to the depth at which the pieces are taken. It is estimated that accuracy in this study is ± 5 mm. According to Sjöberg (1998b), a usual moisture gradient is 3% RH/cm.

Let us assume that there is very little probability that the error in measuring the position where the pieces were taken was more than 5 mm, and that this gives rise to an error of $\pm 1.5\%$ RH

($0.5 \text{ cm} \cdot 3\% \text{ RH/cm}$). Let us also assume that the confidence interval is 99%, which makes the coverage factor 2.576. If the error in measurement is assumed to have normal distribution, the standardised measurement uncertainty (S_t) is

$$S_t = \frac{1.5}{2.576} = 0.58\%$$

Total measurement uncertainty in Method No 3

The factors which contribute to the total uncertainty in Method No 3 are summarised in Table B1.10.

Table B1.10 Summary of factors and their magnitudes, Method No 3.

name		w/c ratio		
		0.4	0.5	0.7
a	nonlinearity	1.22	1.22	1.22
b	drift	0	0	0
c	hysteresis	0.61	0.61	0.61
d	ΔT , calibration	-0.06	-0.06	-0.06
e	salt	0.40	0.40	0.40
f	ΔT^* , calibration	1.14	1.14	1.14
g	calibration	0	0	0
h	dual pressure humidity generator	–	–	–
i	ΔT calibration/measurement	0	0	0
j	ΔT measurement/service	0	0	0
k	storage in the dry	0	0	0
l	moisture capacity, samples	0.24	0.24	0.24
m	moisture capacity, drilled holes	-	-	-
n	ΔT sensor/concrete	0	0	0
o	recently drilled holes	–	–	–
p	alkalinity	0	0	0
q	ΔT^* , measurement	0.61	0.61	0.61
r	non-uniform extraction of samples	0.18	0.18	0.18
s	condensation	–	–	–
t	deviations, depth of measurement	0.58	0.58	0.58
u	wrong slab thickness	0	0	0
a-u	Sum	2.03	2.03	2.03

* transient temperature variations

Appendix No 2 Uncertainty in measuring organic compounds

General

In the literature there are studies which evaluate, among other things, the uncertainty in measuring emissions with FLEC-GC-FID/MS (Field and Laboratory Emission Cell – Gas Chromatography – Flame Ionisation Detector / Mass Spectrometry). Four of these investigations, one of which is our own, and experiences communicated by tekn. dr. Ramnäs, form the basis for the assessment of the total standardised measurement uncertainty in this study. See Table A2.1.

Table A2.1 Uncertainty in measuring organic compounds with FLEC – GC. Coverage factor are 1.

Author	Uncertainty	Type
Gustafsson and Jonsson (1993)	±16%	Reproducibility
Wengholt Johnsson (1995)	±19%	Reproducibility
Gustafsson et al (1995)	±15%	Reproducibility
Sjöberg (1998a)	±10%*	Repeatability

*>20 hours' conditioning period

The total standardised measurement uncertainty for this method is judged to be less than ±20%. According to Ramnäs (2000), analysis of the TENAX tube in GC-FID accounts for only a small proportion of this (<±3%). Most of the total uncertainty is probably attributable to variations in the objects of measurement, sampling, handling of the TENAX tube or possibly some other factor which is dealt with later on in this appendix.

Some previous investigations

Gustafsson and Jonsson (1993) describe a study in which twin analyses were made parallel with sampling. 35 different materials were measured on two occasions. In these 70 sampling events, two TENAX tubes were used in parallel. The evaluated total standardised measurement uncertainty from these "twin analyses" was 16%.

Wengholt Johnsson (1995) used twin specimens to evaluate the total measurement uncertainty in the test method. A large number of identical "twin" specimens, comprising bonded PVC flooring on concrete, were cast and conditioned in the same way. At the time of sampling, one TENAX tube was taken from each specimen of the twin. The standardised measurement uncertainty for the whole method, evaluated from 30 pairs of analyses, was 19%.

Gustafsson et al (1995) describe a study in which emission measurements were made on the same material in two laboratories. Measurements of primary emissions from a PVC flooring were made on three occasions, 1, 14 and 28 days after production. The total standardised measurement uncertainty for this investigation was 15%.

Sjöberg (1998a) measured the concentration of exhaust air from FLEC after different conditioning periods, without moving the FLEC in between. This investigation is described later in this appendix.

Contributions due to different factors

The total uncertainty in the studies which is set out in Table A2.1 can be divided into four principal contributory components. The contributions by these principal components vary a lot in the different studies. These components are the contribution due to the GC analysis of the TENAX tube (I), the contribution due to sampling with FLEC including the handling of the TENAX tube (II), the contribution due to differences between laboratories (III), and the contribution due to the difference between twin specimens (IV).

These principal components can, in turn, be broken down into subsidiary components which make up the contribution by the principal component. One example is that sampling with FLEC can be broken down into the contribution due to variations in conditioning period, the variation in flow through the TENAX tube, the compounds left in the TENAX tube, etc. The more a method is examined in depth, the greater the number of contributions that can be identified and later quantified.

Table A2.2 Four principal components that contribute to the total uncertainty in measuring with FLEC.

	Component	Contribution
I	GC analys of TENAX tube	±3 %
II	Sampling with FLEC	±9.5 %
III	Different laboratories	±11 %
IV	Twin specimens	±16 %

The contribution due to the GC analysis of the TENAX tube (I) can, according to Ramnäs (2000), be estimated at ca ±3%. This is a recognised estimate of the uncertainty of analysis with GC.

The contribution due to sampling with FLEC (II) including the handling of the TENAX tube can be estimated according to Sjöberg (1998a), as described later in this appendix. All measurements were made in the same laboratory with the same equipment and by the same person. Measurements in one series were in addition made on the same test specimen. In these measurements, it is therefore only components (I) and (II) which contribute to the total measurement uncertainty. According to Box et al (1978), contributions to the total measurement uncertainty can be combined by adding the squares.

$$(\text{Total std. uncertainty})^2 = (\text{contribution No 1})^2 + (\text{contribution No 2})^2 \dots + (\text{contribution No n})^2$$

If the total measurement uncertainty is ±10% in this case, then contribution (II) is equal to $\sqrt{10^2 - 3^2} = 9.5\%$.

The contribution due to the difference between laboratories (III) can be estimated according to Gustafsson et al (1995). In this investigation, a material was split up and sent under controlled conditions to different laboratories for measurement. In these measurements it can therefore be assumed that components (I), (II) and (III) together contribute to the total measurement uncertainty. With the help of earlier estimates, the contribution due to (III) can be calculated as $\sqrt{15^2 - 3^2 - 9.5^2} = 11\%$.

The contribution due to the difference between twin specimens (IV) can be estimated according to Wengholt Johnsson (1995). All measurements were made at the same laboratory, with the same equipment and by the same person. Measurements were made on pairs of twin samples which had been made and handled in exactly the same way by the same person. In these measurements it can therefore be assumed that components (I), (II) and (IV) together contribute to the total measurement uncertainty. With the help of earlier estimates, the contribution due to (IV) can be calculated as $\sqrt{19^2 - 3^2 - 9.5^2} = 16\%$.

Experimental study of measurement uncertainty in sampling with FLEC

In the study an investigation was made of the influence due to the period of conditioning the surface with FLEC, i.e. the time during which the surface was "flushed" with air before sampling commenced. From the results it is possible to evaluate the contribution that this parameter makes to the total measurement uncertainty in sampling with FLEC.

Sampling was performed with the measurement cell FLEC (Field and Laboratory Emission Cell) and a TENAX tube as absorber. In the subsequent analysis GC – FID was used. The entire measurement procedure is described in Subsection 2.3.3. The arrangement for sampling is shown in Fig. A2.1.

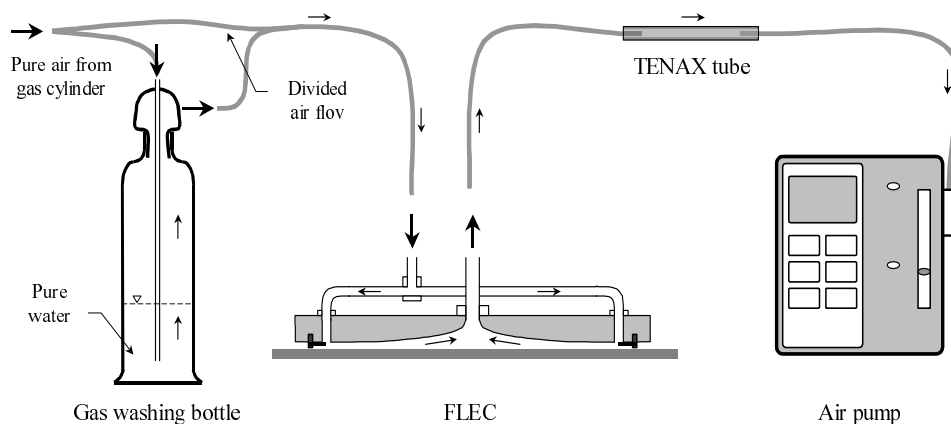


Fig. A2.1 Arrangement for sampling with FLEC.

In the investigation the total uncertainty was determined experimentally by making a number of measurements on the same test specimen. The quantities and distributions of OC in the TENAX tubes may alter if they are left for a long time before the analysis. The risk increases if they are stored warm. In order to minimise the "waiting time" for the TENAX tubes, the GC analysis was completed before the next sampling was performed.

A total of 64 emission measurements were made in 12 "measurement series". The term measurement series refers to the measurements which were made on a test specimen after different conditioning periods (without moving the FLEC). On average, each series consisted of five measurements, one of which was made after a conditioning period of about 24 hours.

The measurement after 24 hours' conditioning has been used as the reference in comparing the measurement series. The values measured in each series were divided by the value obtained after 24 hours. The quotient is called the relative emission factor. The relationship between conditioning period and relative emission factor is plotted in Fig. A2.2.

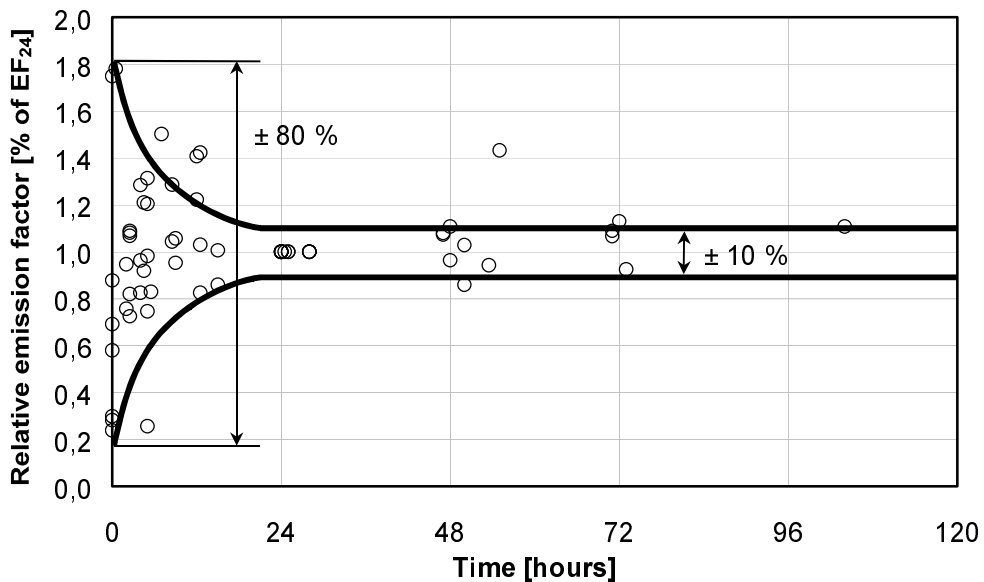


Fig. A2.2 Relative emission factor (EF/EF_{24}) as a function of the conditioning period, and the approximate interval for the total standardised measurement uncertainty.

The confidence interval with a standard deviation is shown in the figure by full lines. The lines delineate the outer limits of the interval within which the measured value will be located with 68% probability. If it is assumed that the value measured after 24 hours is the "true" value, there is 68% probability that a value which is measured after 1 hour will be located within the "true" value $\pm 80\%$. Measurements made after a conditioning period of 20 hours or more have a repeatability (uncertainty) of $\pm 10\%$.

Field tests on the significance of the conditioning period

Edenholm (1998) made comparative measurements in the field to study the influence of the conditioning period. Sampling was performed with room air through FLEC after conditioning periods of 1 and 24 hours. The subsequent analysis was made with GC – FID / MS as described in Subsection 2.3.2.

The object of measurement was a newly constructed flat in Stockholm, with flooring of linoleum (1) and PVC (2 & 3). The results of three measurements, after the readings had been adjusted to allow for contaminants in the room air, are set out in Table A2.3.

Table A2.3 Field measurements with FLEC – GC. Comparison of results after conditioning periods of 1 and 24 hours with FLEC.

Experiment	1 hour	24 hours	Relationship
1	>2000*	>2000*	uncertain
2	180	115	1.6
3	125	125	1.0

* larger than the measurement range of the instrument

The field measurements do not indicate that there is an unambiguous relationship between emissions after conditioning periods of 1 and 24 hours. Differences varied between measurements, and the relationships between the results in the three measurement series were different.

Discussion

It has been found that it is difficult to measure the emission from floor combinations with great accuracy using FLEC. There are many factors, not only sampling, which influence the results. However, the use of FLEC – GC provides a useful technique for assessing the order of magnitude of emissions from surfaces.

The greatest contribution to the total measurement uncertainty in measuring emissions from material combinations derives from differences between the specimens in twin tests. In the test specimens in this investigation, a chemical reaction was created; the conditions governing this have not been fully clarified. To some extent, the breakdown products from this reaction will be fixed in the material but will also be emitted from the surface. Today, we have only begun to research into what governs this fixation and transport. In view of this, it is not unreasonable to find that the difference between emissions from two test specimens is 16% when we proceed as well as we can.

It is recognised that there is a variation in analytical results between laboratories. In this case, this difference gave rise to a measurement uncertainty of 9.5%. It may be reasonable to believe that the difference is of the same magnitude irrespective of the purpose of the emission measurements. This may be something to bear in mind when emission factors for different materials are compared.

Appendix No 3 Vapour content at saturation for some OC

The diagrams are based on values of vapour content at saturation at different temperatures, taken from CRC (2000).

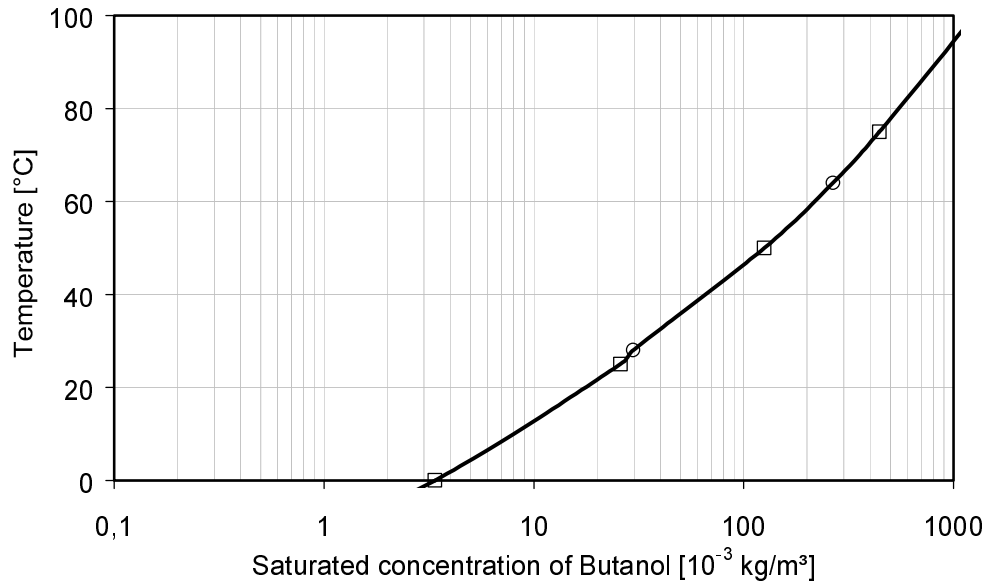


Fig. A3.1 Vapour concentration of *n*-butanol at saturation as a function of temperature.

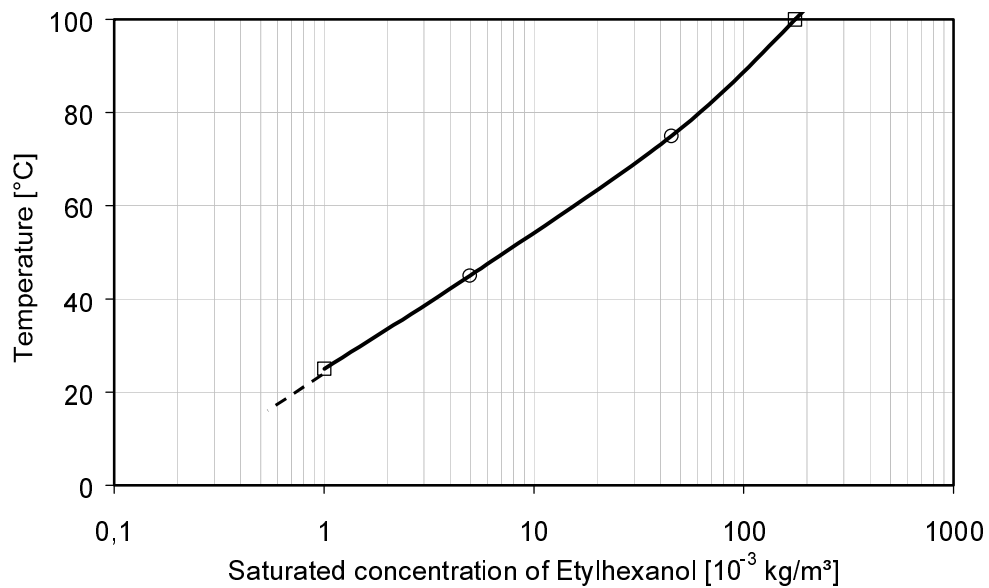


Fig. A3.2 Vapour concentration of 2-ethylhexanol at saturation as a function of temperature

Appendix No 4 Results from all calculations

In this appendix, the results of 10 calculations made in Excel with the calculation model described in Chapter 7 are summarised. The calculation results are compared in Chapter 9 with the measured values for butanol. In Chapter 10, the effect on the calculation results due to variations in some of the parameters in the model are studied.

The calculations are made with 5 different combinations of parameters for the formation, fixation and transport of butanol in concrete. These combinations of parameters are called Calc.1 – 5; see Table B4.1.

For each parameter combination, calculations were made with two different floorings, PVC and linoleum. In the calculations, the floorings are treated as transmission resistances for moisture and OC, with no storage capacity whatever. See Table B4.2.

Table B4.1 Values for calculation of transport and fixation of butanol in Concrete C4.

Quantity	Unit	Calc.1	Calc.2	Calc.3	Calc.4	Calc.5
$q_{R,max}$	$[10^{-9} \text{ kg}/(\text{m}^2 \cdot \text{s})]$	0.03	0.26	2.6	7.3	7.3
D_{OC}	$[10^{-9} \text{ m}^2/\text{s}]$	2.5	2.5	2.5	93	93
Bound	–	b_0	b_0	b_0	b_1	b_2
S	–	0.077	0.077	0.077	2.8	0.077
b	$[10^3]$	–	–	–	–	16.1

Table B4.2 Transmission resistance for moisture and OC – PVC and linoleum flooring.

Quantity	Unit	PVC	Linoleum
Z_{fi}	$[10^6 \text{ s}/\text{m}]$	2	0.1
R_{fi}	$[10^6 \text{ s}/\text{m}]$	3.7	2.9

A4.1 Calculation No 1, results with PVC flooring

Calculations made with maximum rate of formation $q_{R,max} = 0.03 \cdot 10^{-9}$ [kg/m²·s]. The diffusion coefficient of concrete for OC in the gas phase, $D_{OC} = 2.5 \cdot 10^{-9}$ [m²/s]. Fixation assumption according to Equation 8.5, $C_{bound,0} = k_0 \cdot w \cdot c_{air}$, where $k_0 = 0.077$ [m³/kg].

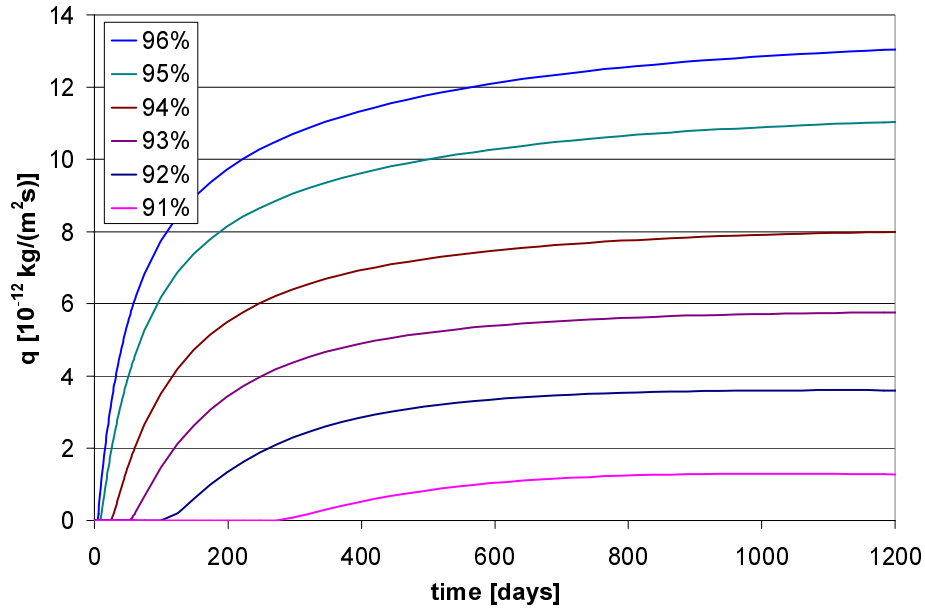


Fig. A4.1 Emission from surface, results from Calc.1 with PVC flooring.

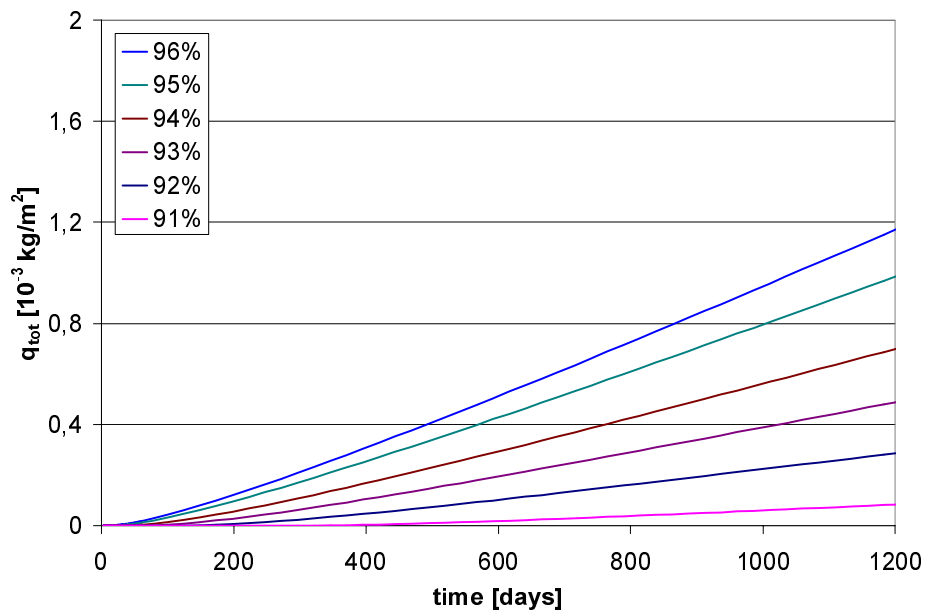


Fig. A4.2 Curves of total emission from Calc.1 with PVC flooring.

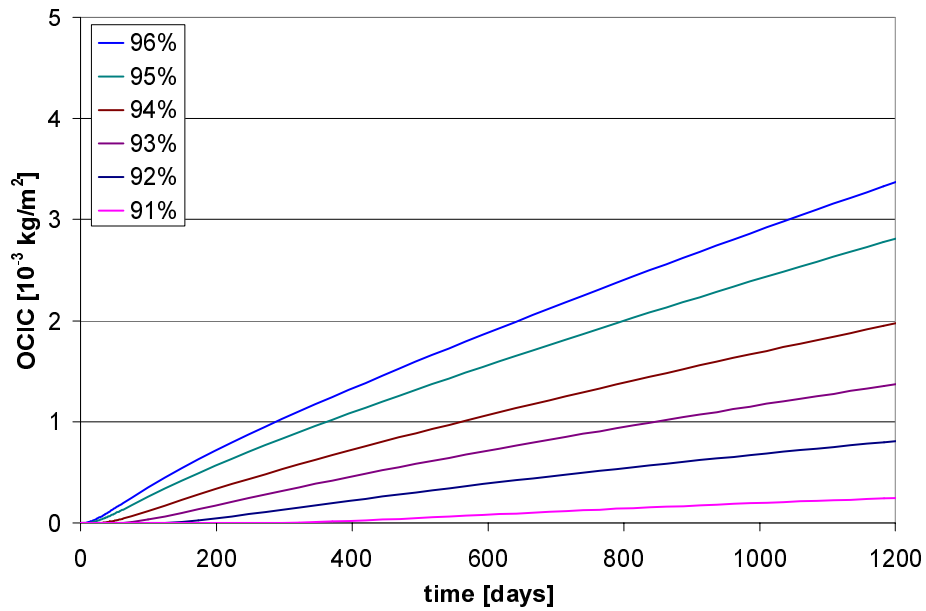


Fig. A4.3 OCIC as a function of time in Calc.1 with PVC flooring.

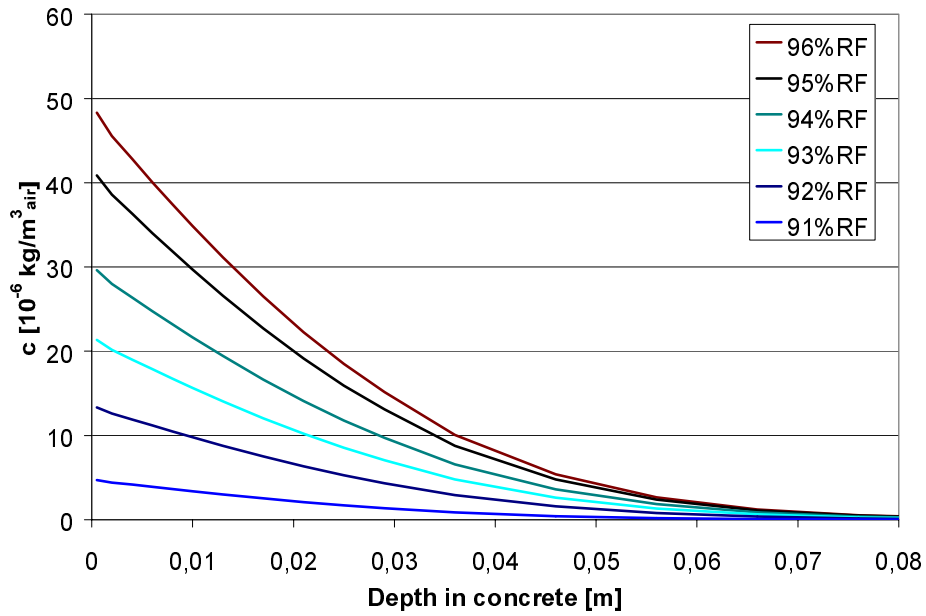


Fig. A4.4 Profile of OCIC after a long time in Calc.1 with PVC flooring.

A4.2 Calc.2, results with PVC flooring

Calculations made with maximum rate of formation $q_{R,max} = 0.26 \cdot 10^{-9}$ [kg/m²·s]. The diffusion coefficient of concrete for OC in the gas phase, $D_{OC} = 2.5 \cdot 10^{-9}$ [m²/s]. Fixation assumption according to Equation 8.5, $C_{bound,0} = k_0 \cdot w \cdot c_{air}$, where $k_0 = 0.077$ [m³/kg].

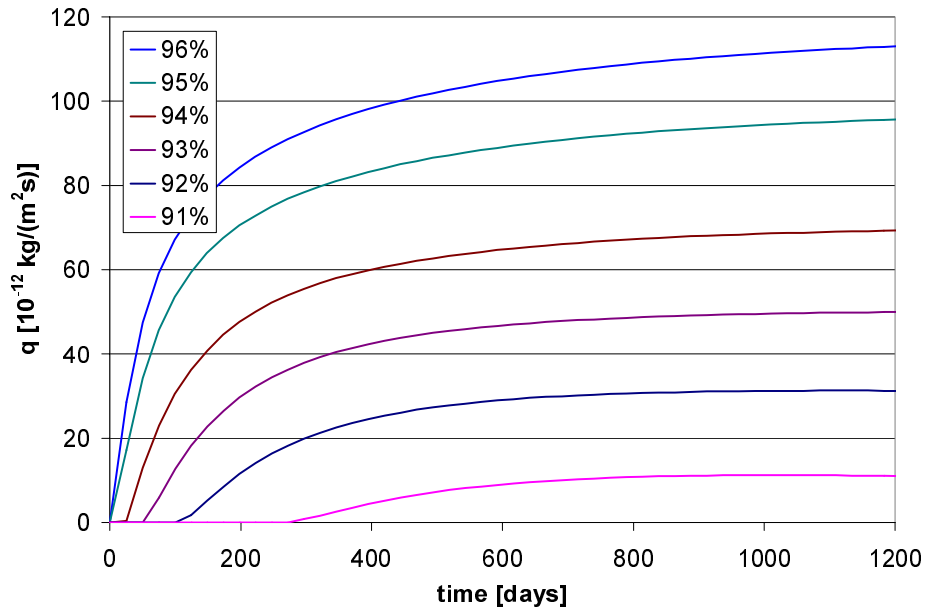


Fig. A4.5 Emission from surface, results from Calc.2 with PVC flooring.

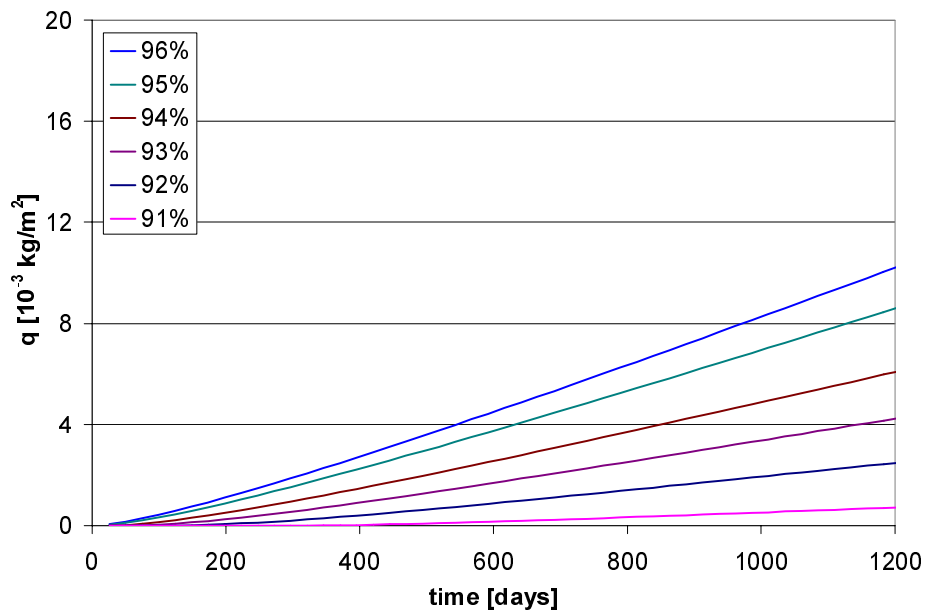


Fig. A4.6 Curves of total emission from Calc.2 with PVC flooring.

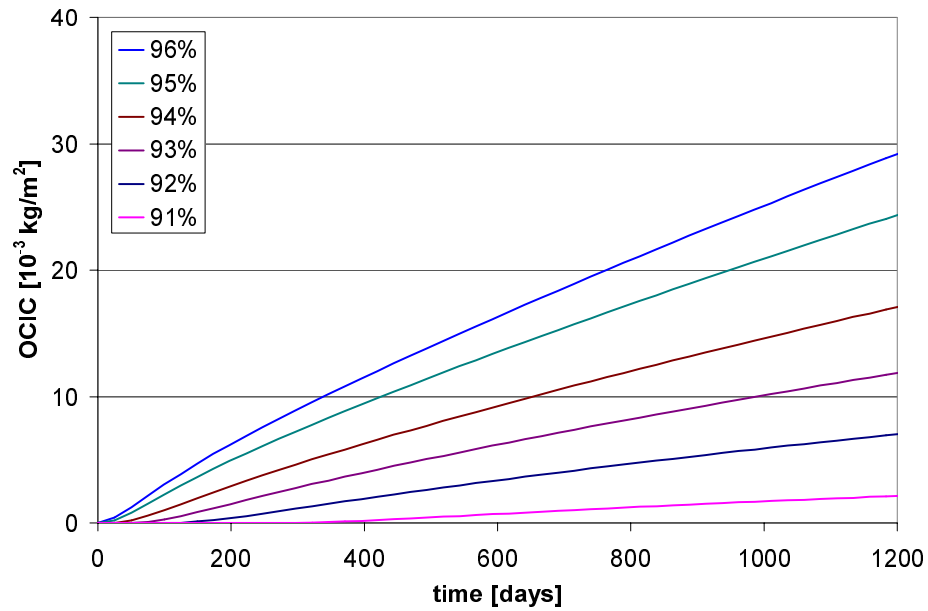


Fig. A4.7 OCIC as a function of time in Calc.2 with PVC flooring.

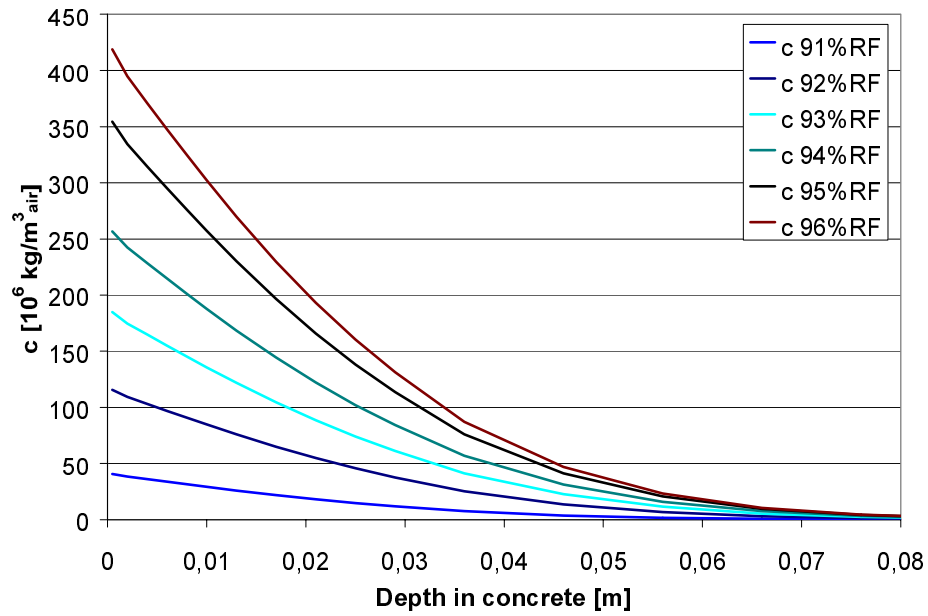


Fig. A4.8 Profile of OCIC after a long time in Calc.2 with PVC flooring.

A4.3 Calc.3, results with PVC flooring

Calculations made with maximum rate of formation $q_{R,max} = 2.6 \cdot 10^{-9}$ [kg/m²·s]. The diffusion coefficient of concrete for OC in the gas phase, $D_{OC} = 2.5 \cdot 10^{-9}$ [m²/s]. Fixation assumption according to Equation 8.5, $C_{bound,0} = k_0 \cdot w \cdot c_{air}$, where $k_0 = 0.077$ [m³/kg].

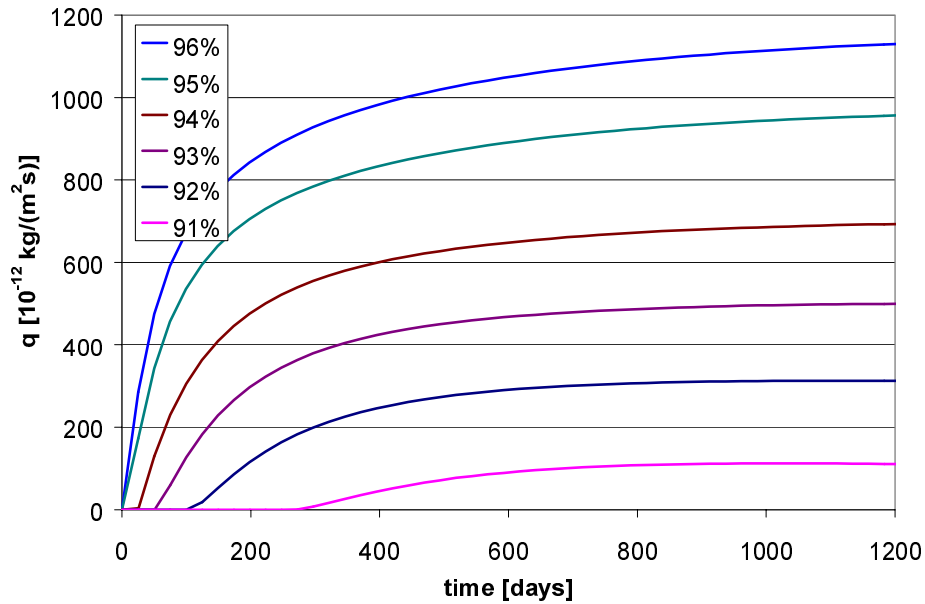


Fig. A4.9 Emission from surface, results from Calc.3 with PVC flooring.

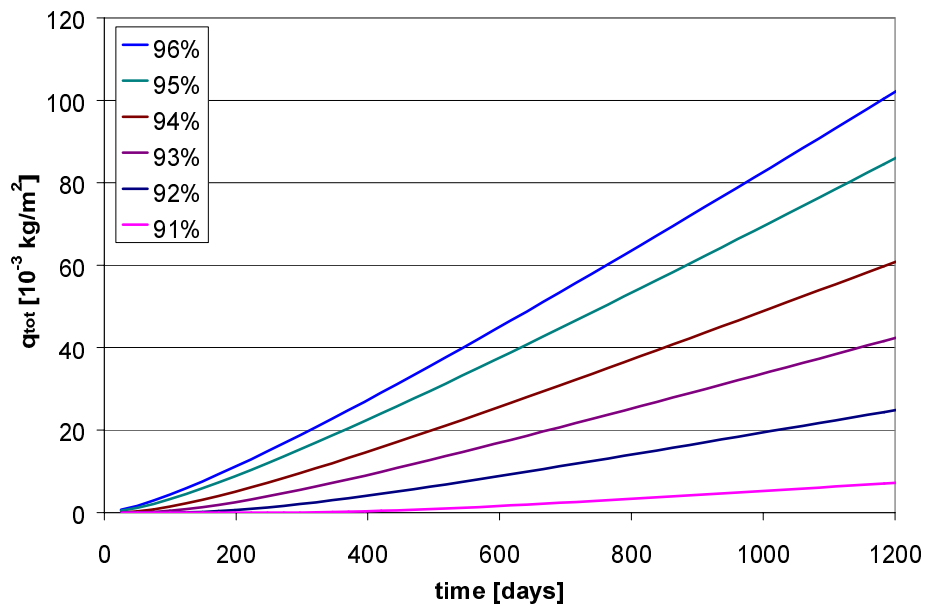


Fig. A4.10 Curves of total emission from Calc.3 with PVC flooring.

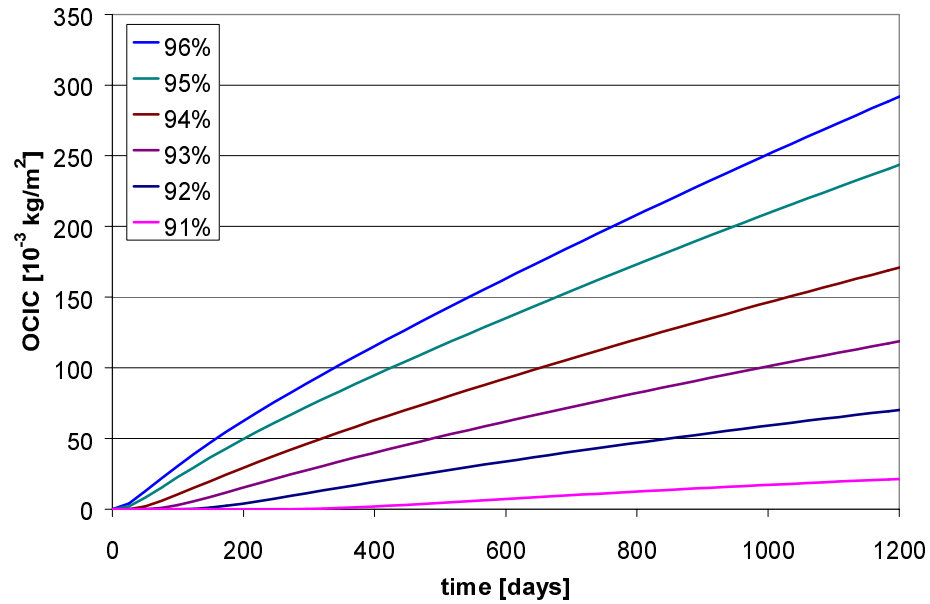


Fig. A4.11 OCIC as a function of time in Calc.3 with PVC flooring.

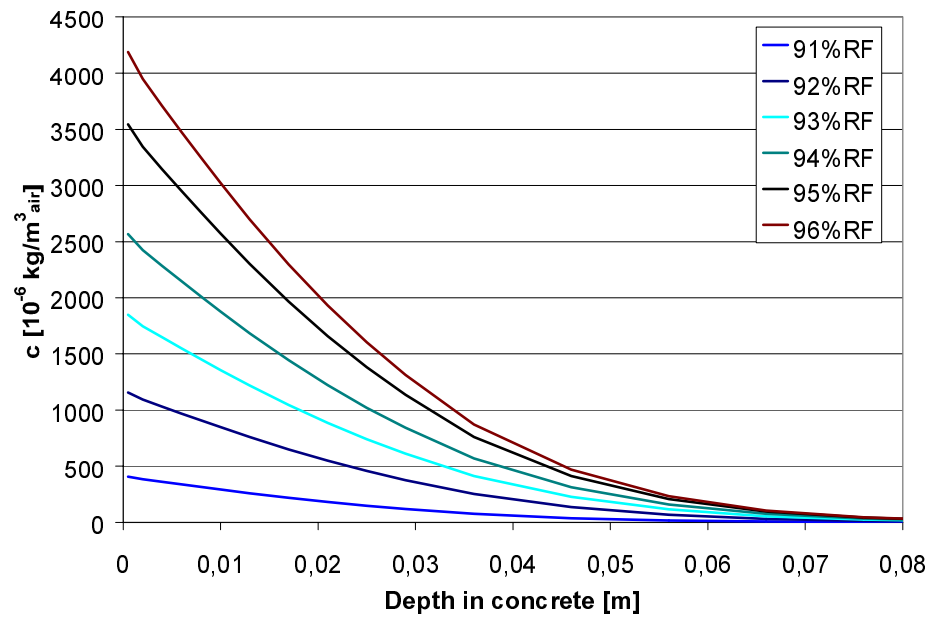


Fig. A4.12 Profile of OCIC after a long time in Calc.3 with PVC flooring.

A4.4 Calc.4, results with PVC flooring

Calculations made with maximum rate of formation $q_{R,max} = 7.3 \cdot 10^{-9}$ [kg/m²·s]. The diffusion coefficient of concrete for OC in the gas phase, $D_{OC} = 9.3 \cdot 10^{-8}$ [m²/s]. Fixation assumption according to Equation 8.6, $C_{bound,0} = k_1 \cdot w \cdot c_{air,t}$, where $k_1 = 2.8$ [m³/kg].

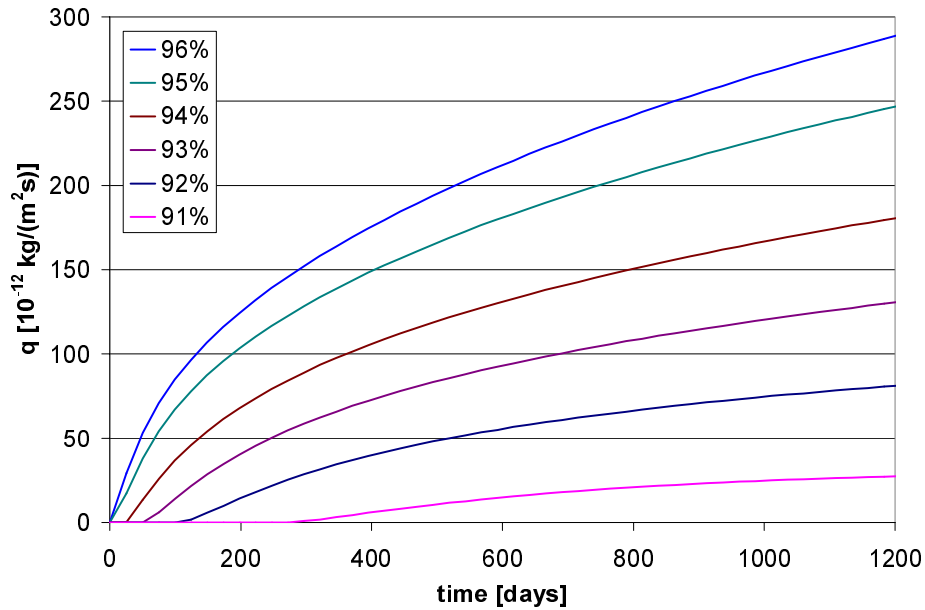


Fig. A4.13 Emission from surface, results from Calc.4 with PVC flooring.

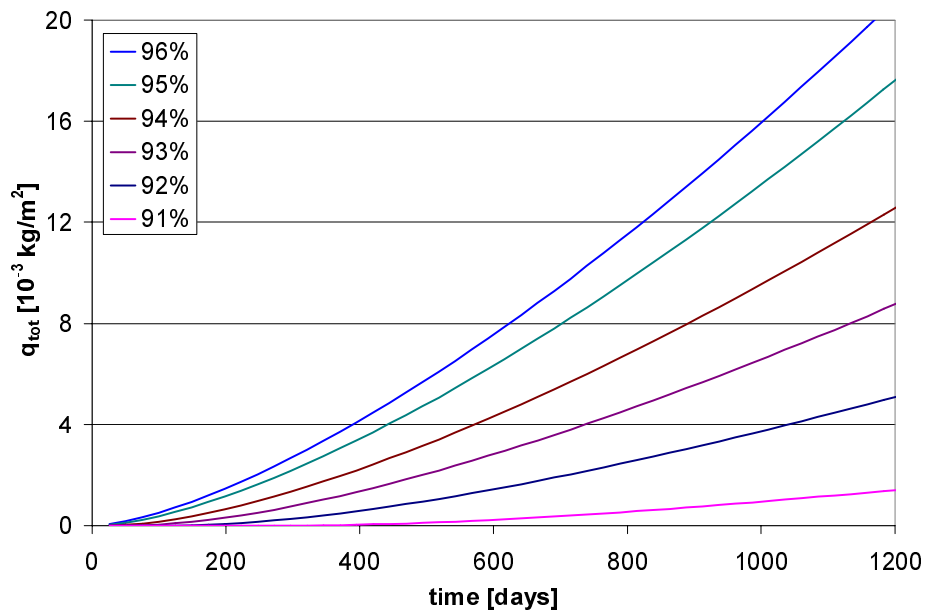


Fig. A4.14 Curves of total emission from Calc.4 with PVC flooring.

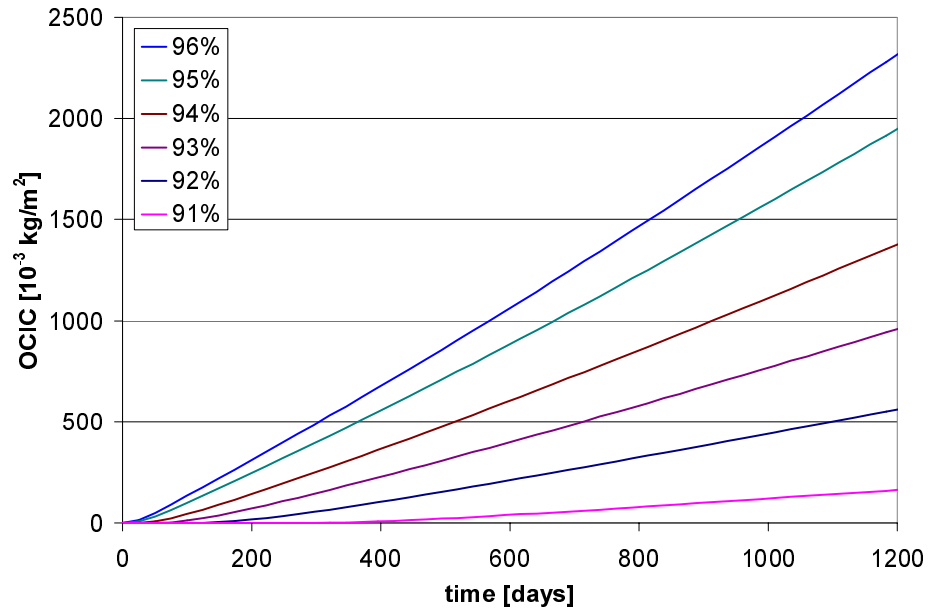


Fig. A4.15 OCIC as a function of time in Calc.4 with PVC flooring.

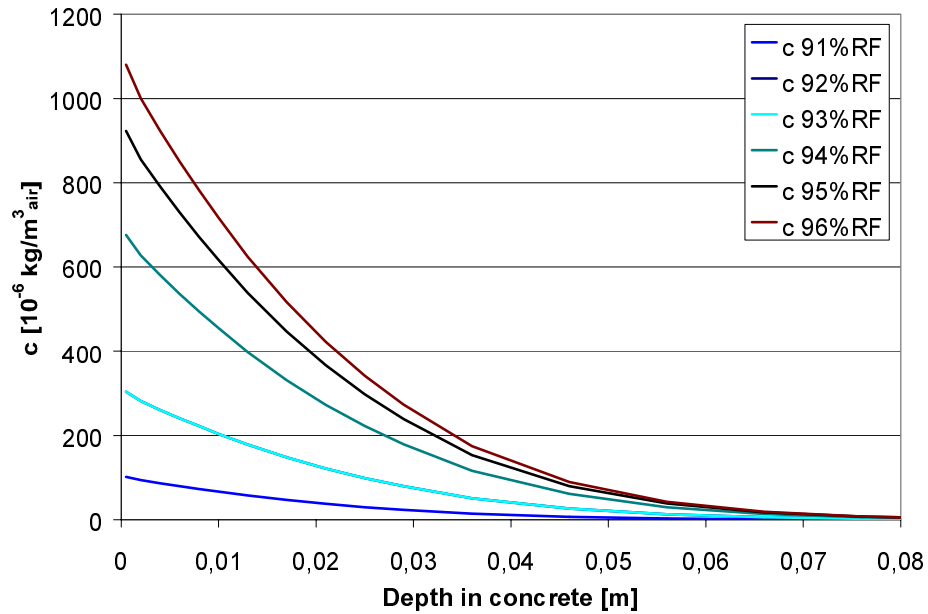


Fig. A4.16 Profile of OCIC after a long time in Calc.4 with PVC flooring.

A4.5 Calc.5, results with PVC flooring

Calculations made with maximum rate of formation $q_{R,max} = 7.3 \cdot 10^{-9}$ [kg/m²·s]. The diffusion coefficient of concrete for OC in the gas phase, $D_{OC} = 9.3 \cdot 10^{-8}$ [m²/s]. Fixation assumption according to Equation 8.7, $C_{bound,0} = (k_2 \cdot w + b) \cdot c_{air,t}$, where $k_2 = 0.077$ [m³/kg] and $b = 16100$ [-].

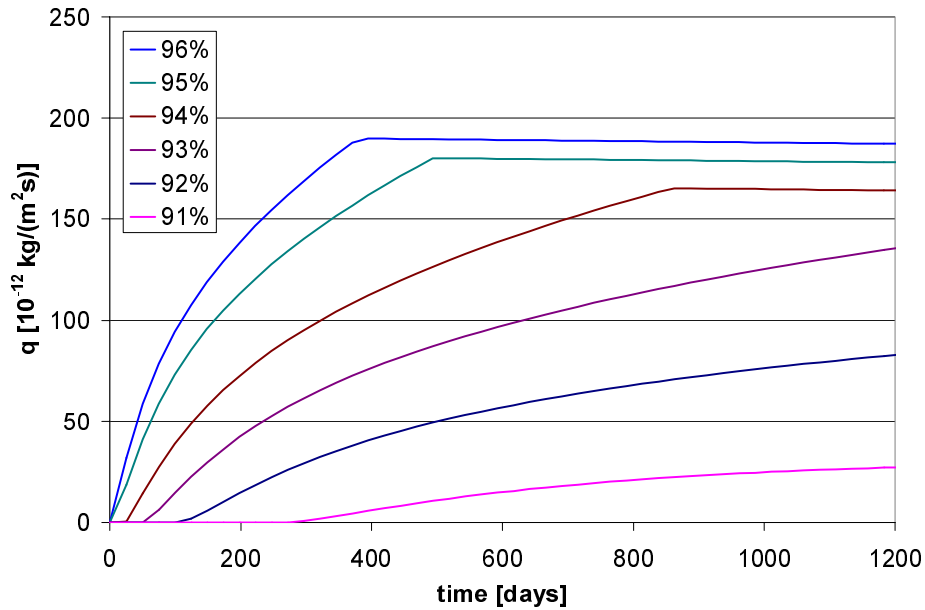


Fig. A4.17 Emission from surface, results from Calc.5 with PVC flooring.

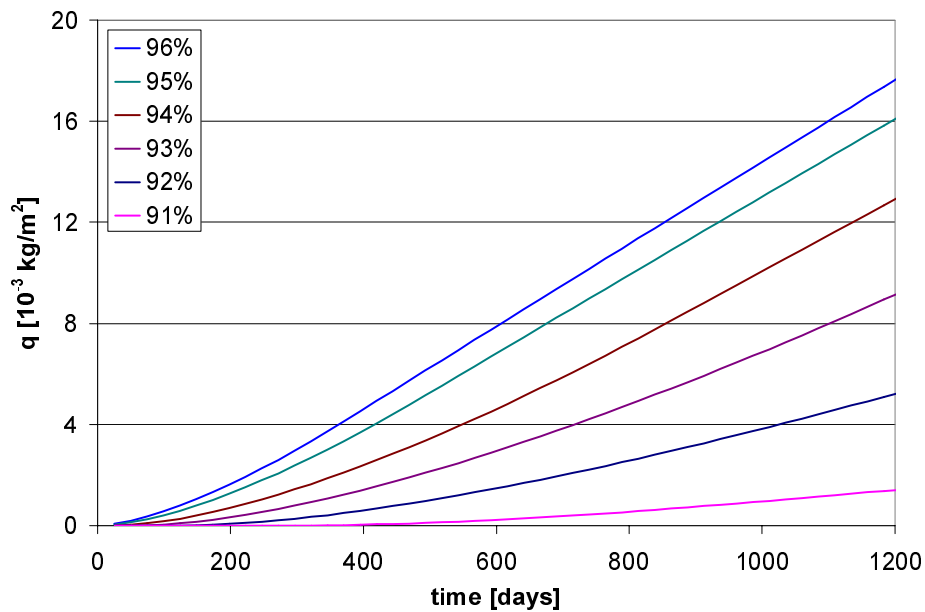


Fig. A4.18 Curves of total emission from Calc.5 with PVC flooring.

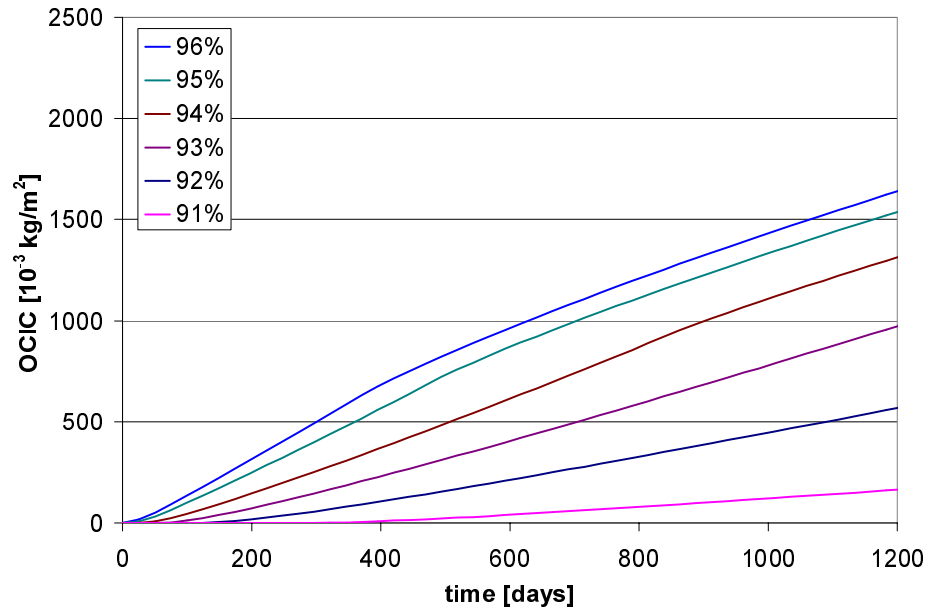


Fig. A4.19 OCIC as a function of time in Calc.5 with PVC flooring.

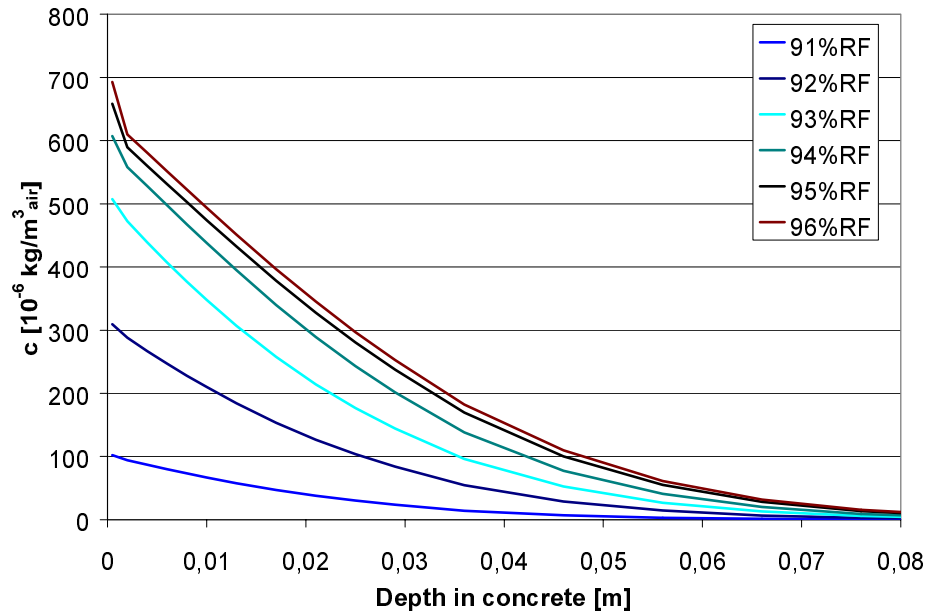


Fig. A4.20 Profile of OCIC after a long time in Calc.5 with PVC flooring.

A4.6 Calc.1, results with linoleum flooring

Calculations made with maximum rate of formation $q_{R,max} = 0.03 \cdot 10^{-9}$ [kg/m²·s]. The diffusion coefficient of concrete for OC in the gas phase, $D_{OC} = 2.5 \cdot 10^{-9}$ [m²/s]. Fixation assumption according to Equation 8.5, $C_{bound,0} = k_0 \cdot w \cdot c_{air}$, where $k_0 = 0.077$ [m³/kg].

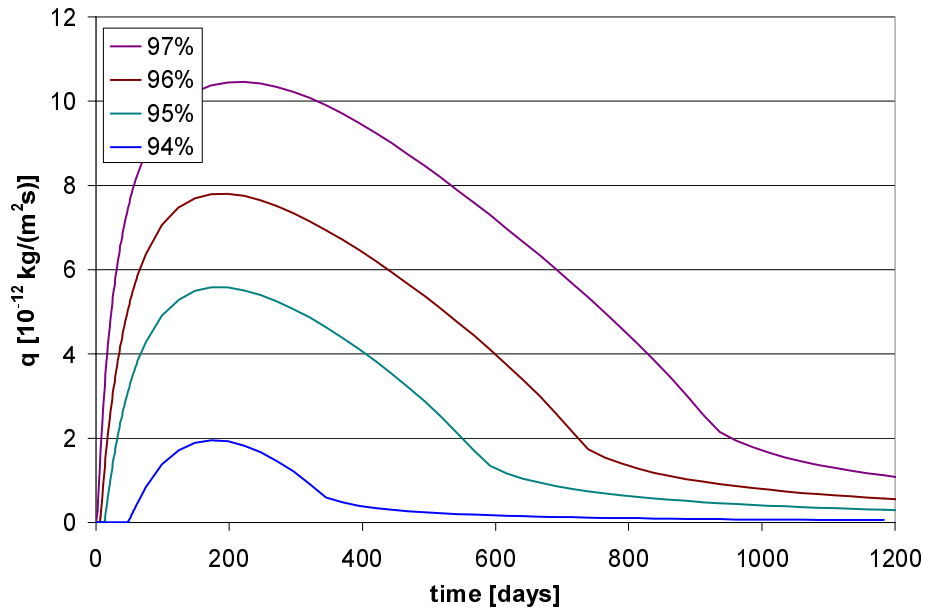


Fig. A4.21 Emission from surface, results of Calc.1 with linoleum flooring.

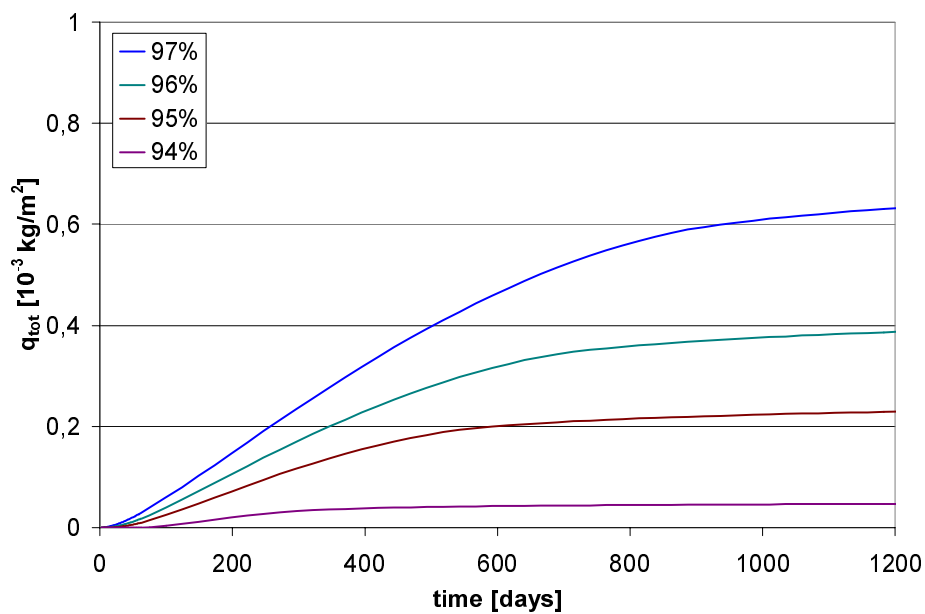


Fig. A4.22 Curves of total emission from Calc.1 with linoleum flooring.

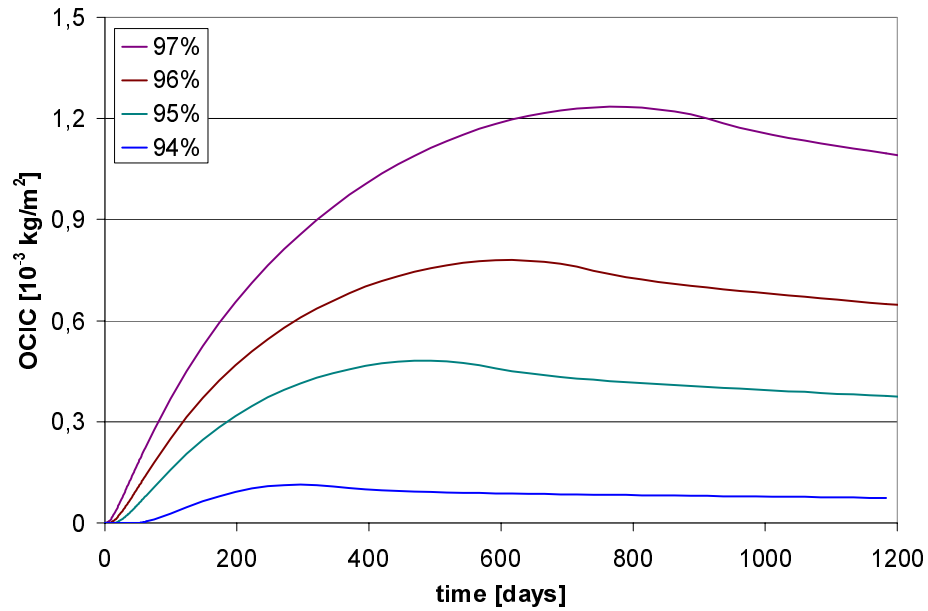


Fig. A4.23 OCIC as a function of time in Calc.1 with linoleum flooring.

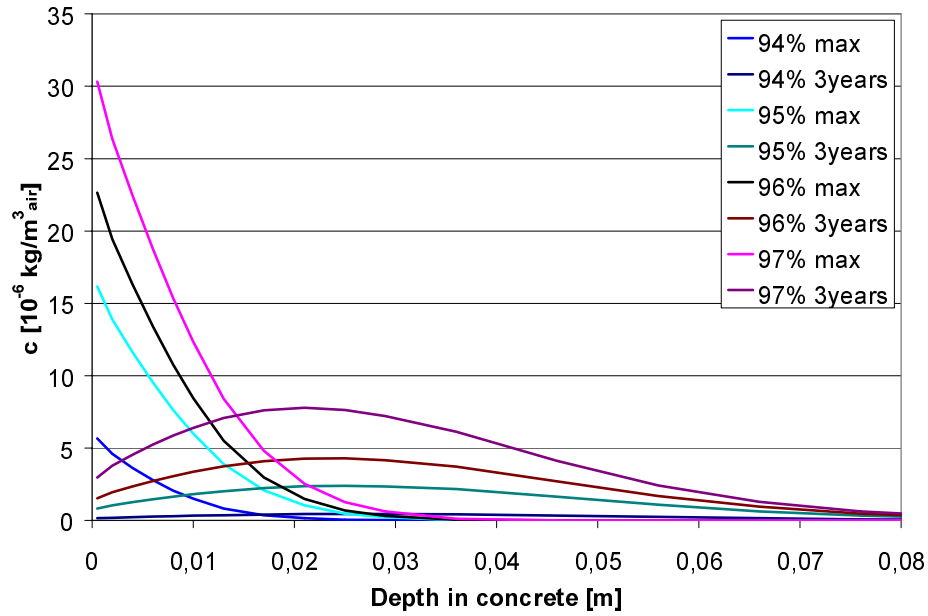


Fig. A4.24 Profile of OCIC at max c_s and after a long time in Calc.1 with linoleum flooring.

A4.7 Calc.2, results with linoleum flooring

Calculations made with maximum rate of formation $q_{R,max} = 0.26 \cdot 10^{-9}$ [kg/m²·s]. The diffusion coefficient of concrete for OC in the gas phase, $D_{OC} = 2.5 \cdot 10^{-9}$ [m²/s]. Fixation assumption according to Equation 8.5, $C_{bound,0} = k_0 \cdot w \cdot c_{air,t}$, where $k_0 = 0.077$ [m³/kg].

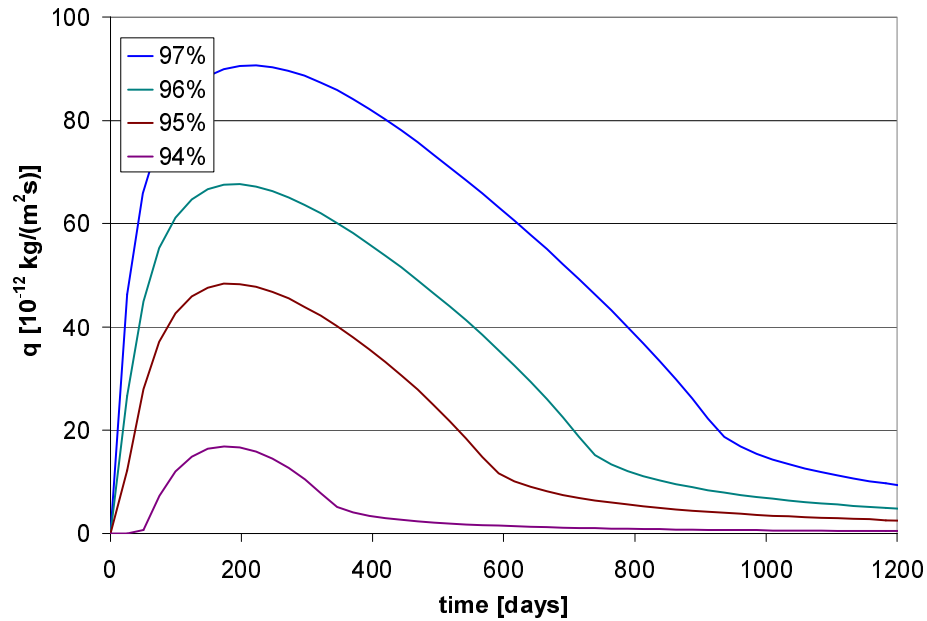


Fig. A4.25 Emission from surface, results from Calc.2 with linoleum flooring.

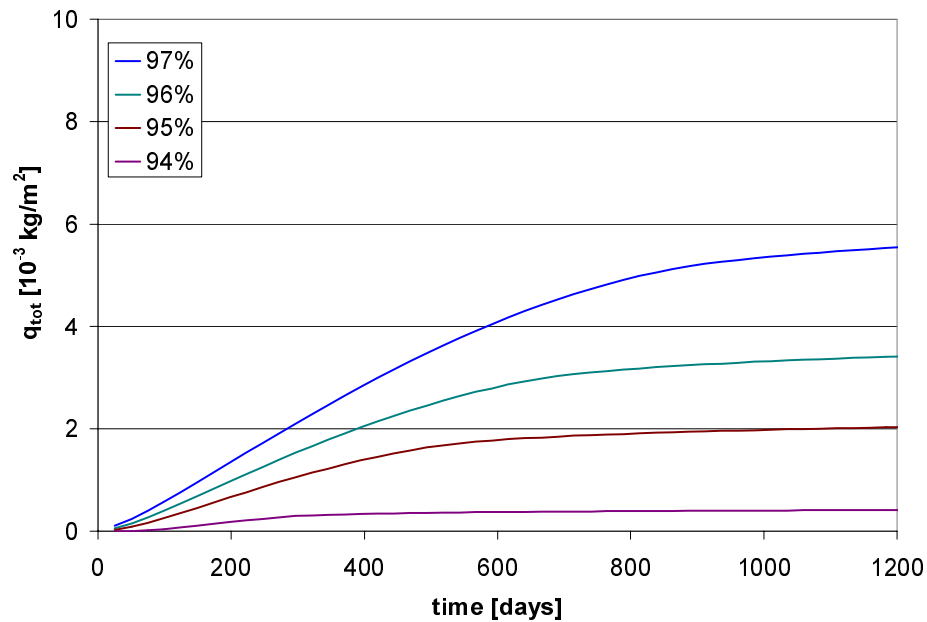


Fig. A4.26 Curves of total emission from Calc.2 with linoleum flooring.

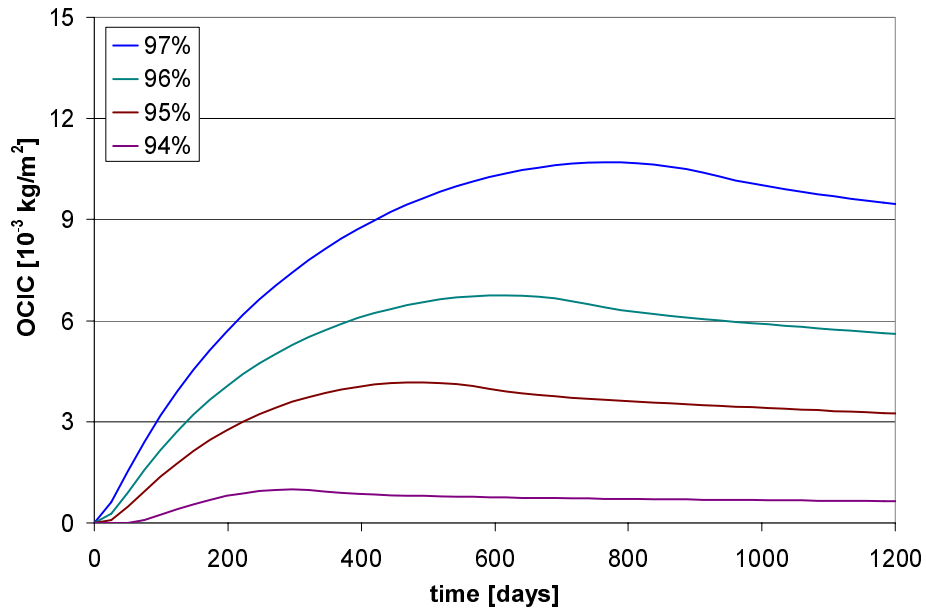


Fig. A4.27 OCIC as a function of time in Calc.2 with linoleum flooring.

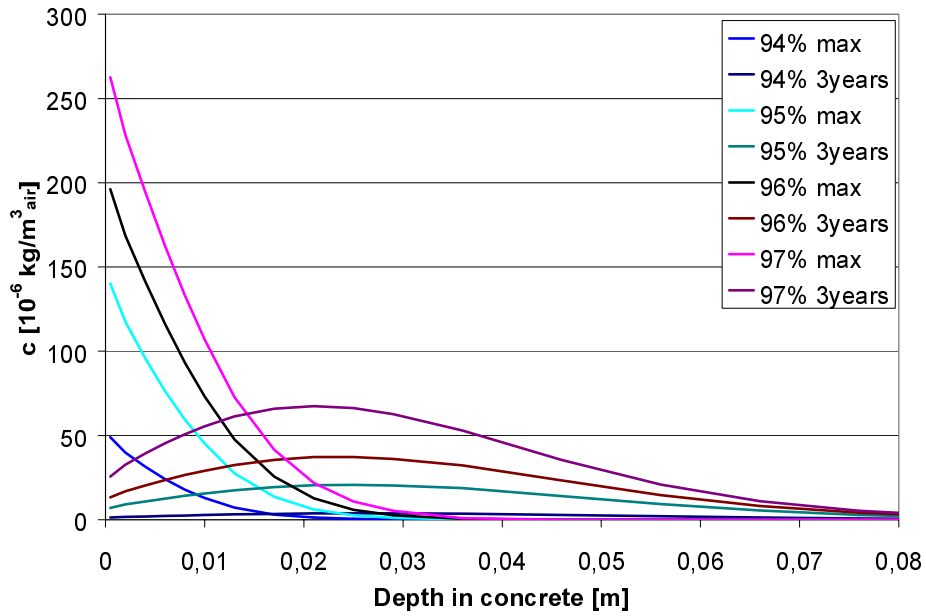


Fig. A4.28 Profile of OCIC at max c_s and after a long time in Calc.2 with linoleum flooring.

A4.8 Calc.3, results with linoleum flooring

Calculations made with maximum rate of formation $q_{R,max} = 2.6 \cdot 10^{-9}$ [kg/m²·s]. The diffusion coefficient of concrete for OC in the gas phase, $D_{OC} = 2.5 \cdot 10^{-9}$ [m²/s]. Fixation assumption according to Equation 8.5, $C_{bound,0} = k_0 \cdot w \cdot c_{air}$, where $k_0 = 0.077$ [m³/kg].

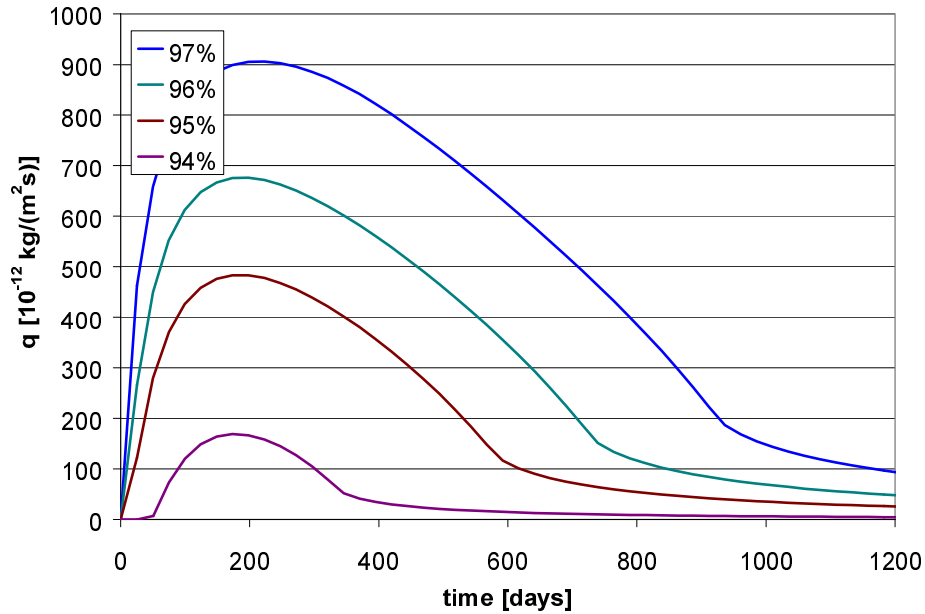


Fig. A4.29 Emission from surface, results from Calc.3 with linoleum flooring.

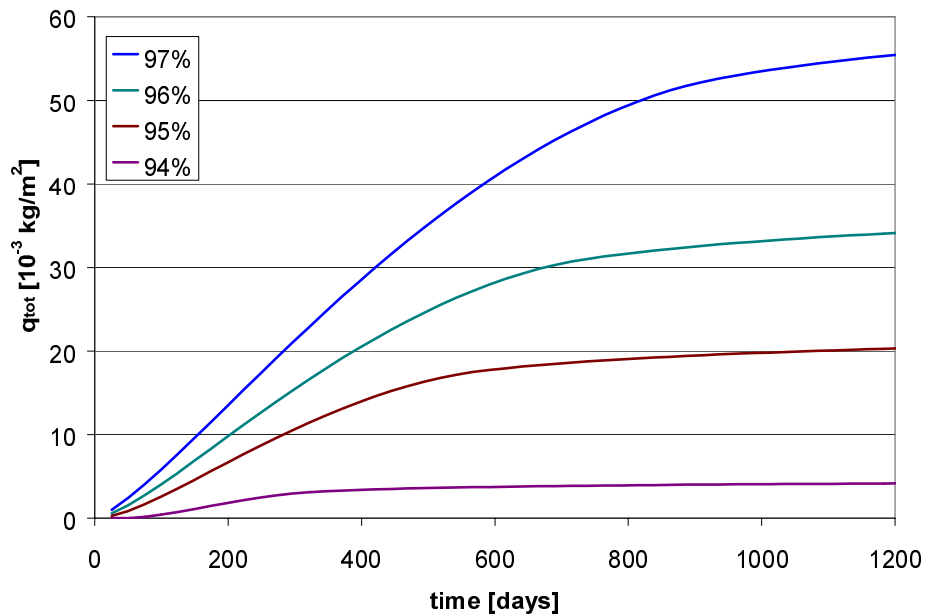


Fig. A4.30 Curves of total emission from Calc.3 with linoleum flooring.

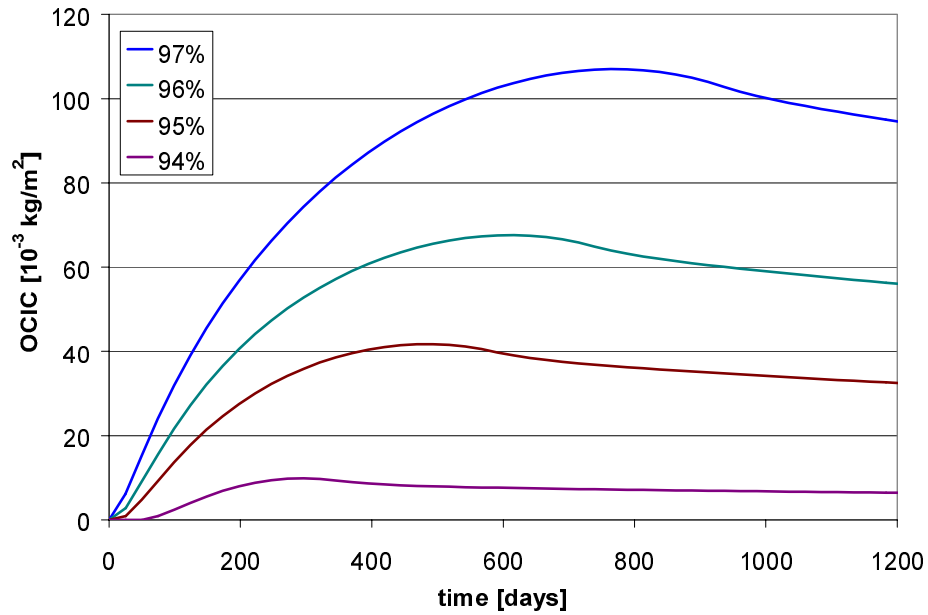


Fig. A4.31 OCIC as a function of time in Calc.3 with linoleum flooring.

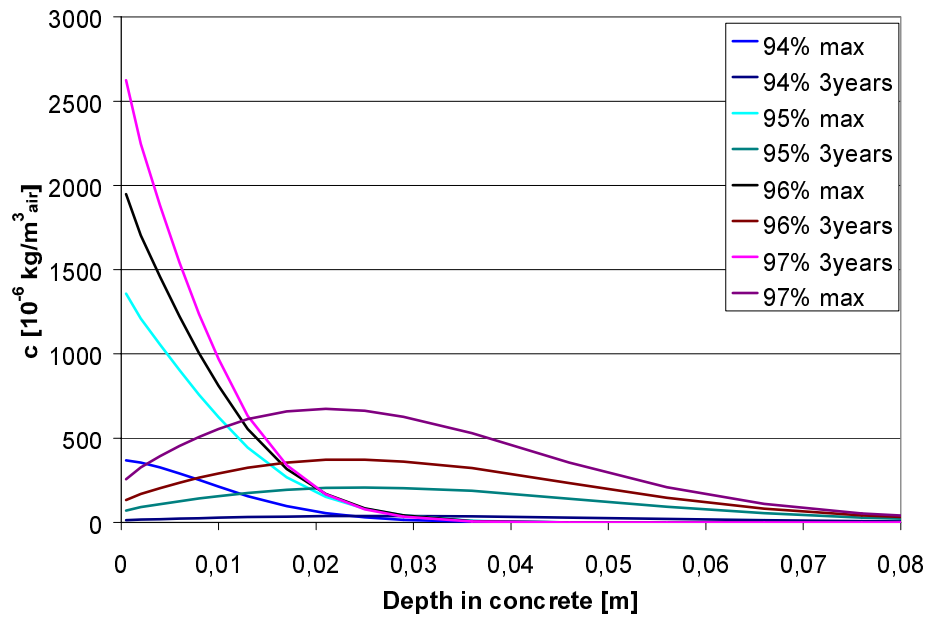


Fig. A4.32 Profile of OCIC at max c_s and after a long time in Calc.3 with linoleum flooring.

A4.9 Calc.4, results with linoleum flooring

Calculations made with maximum rate of formation $q_{R,max} = 7.3 \cdot 10^{-9}$ [kg/m²·s]. The diffusion coefficient of concrete for OC in the gas phase, $D_{OC} = 9.3 \cdot 10^{-8}$ [m²/s]. Fixation assumption according to Equation 8.6, $C_{bound,0} = k_1 \cdot w \cdot c_{air,t}$, where $k_1 = 2.8$ [m³/kg].

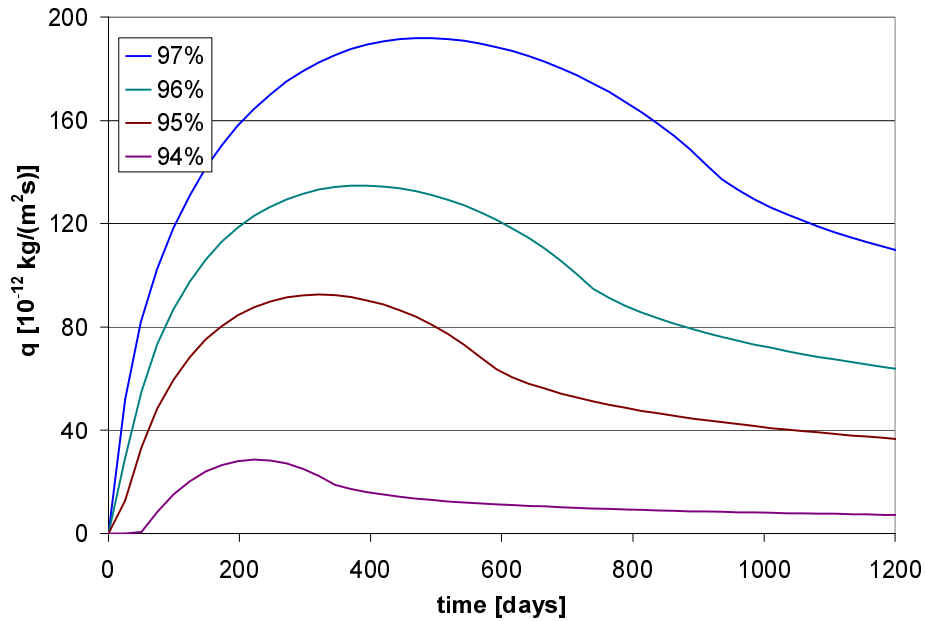


Fig. A4.33 Emission from surface, results from Calc.4 with linoleum flooring.

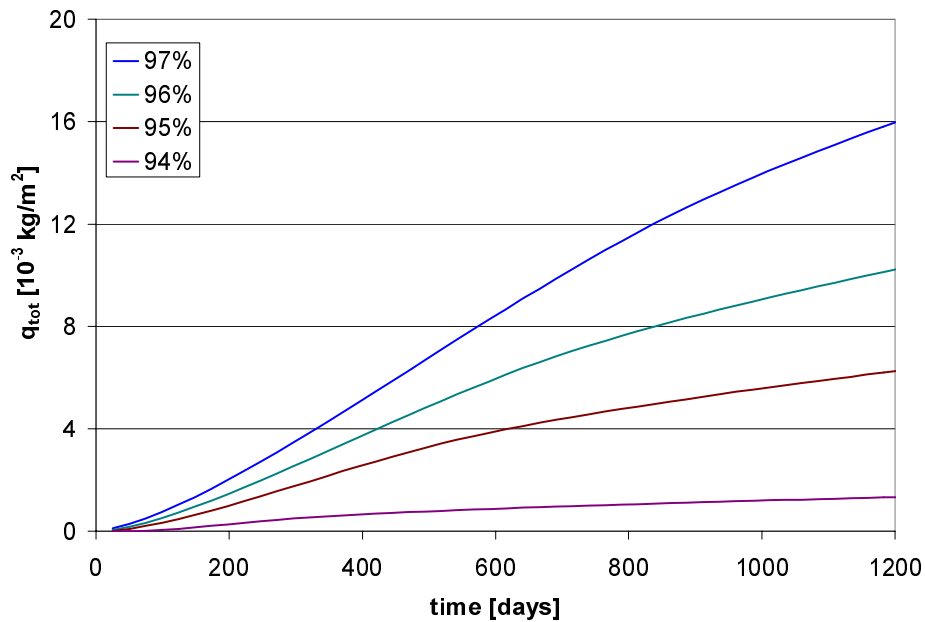


Fig. A4.34 Curves of total emission from Calc.4 with linoleum flooring.

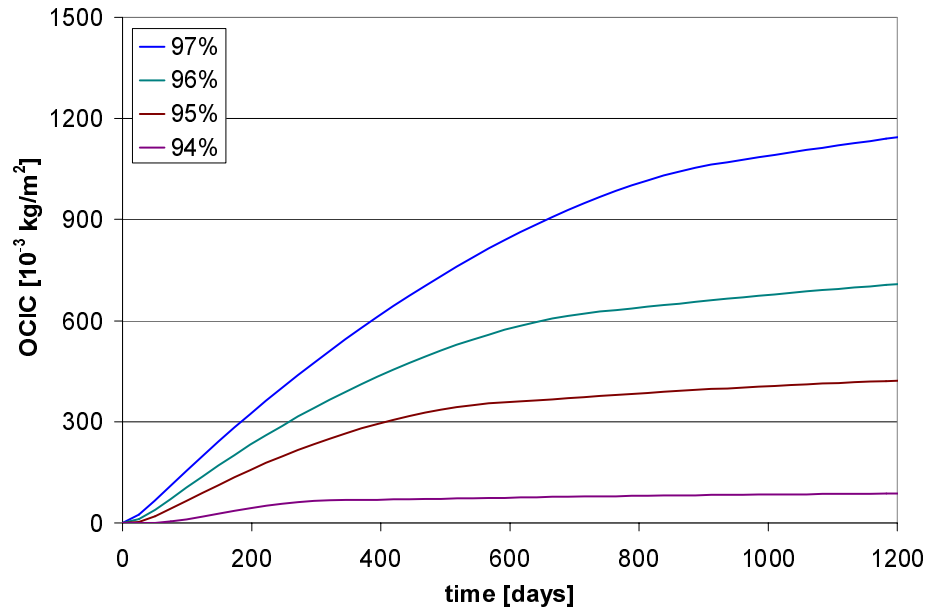


Fig. A4.35 OCIC as a function of time in Calc.4 with linoleum flooring.

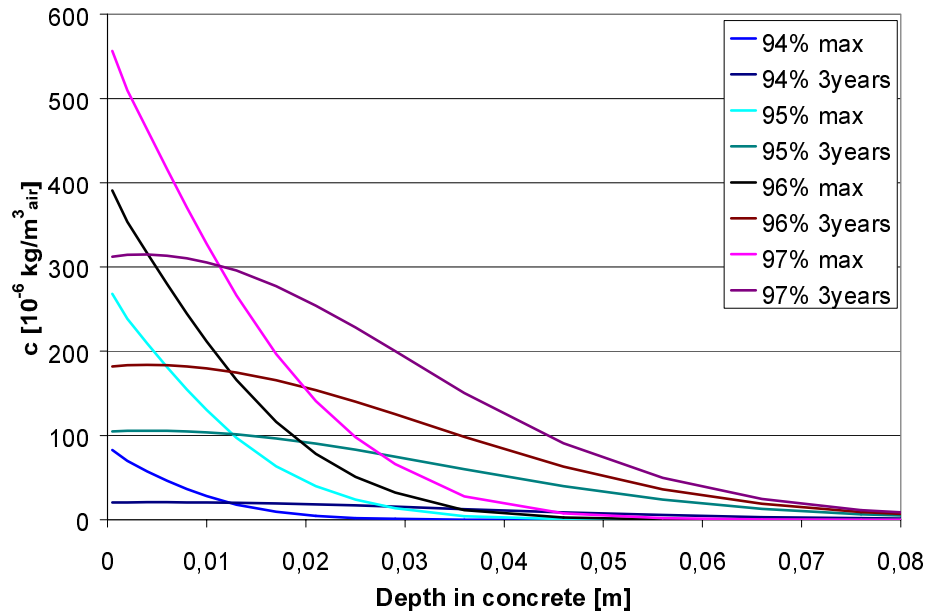


Fig. A4.36 Profile of OCIC at max c_s and after a long time in Calc.4 with linoleum flooring.

A4.10 Calc.5, results with linoleum flooring

Calculations made with maximum rate of formation $q_{R,max} = 7.3 \cdot 10^{-9}$ [kg/m²·s]. The diffusion coefficient of concrete for OC in the gas phase, $D_{OC} = 9.3 \cdot 10^{-8}$ [m²/s]. Fixation assumption according to Equation 8.7, $C_{bound,0} = (k_2 \cdot w + b) \cdot c_{air,t}$, where $k_2 = 0.077$ [m³/kg] and $b = 16100$ [-].

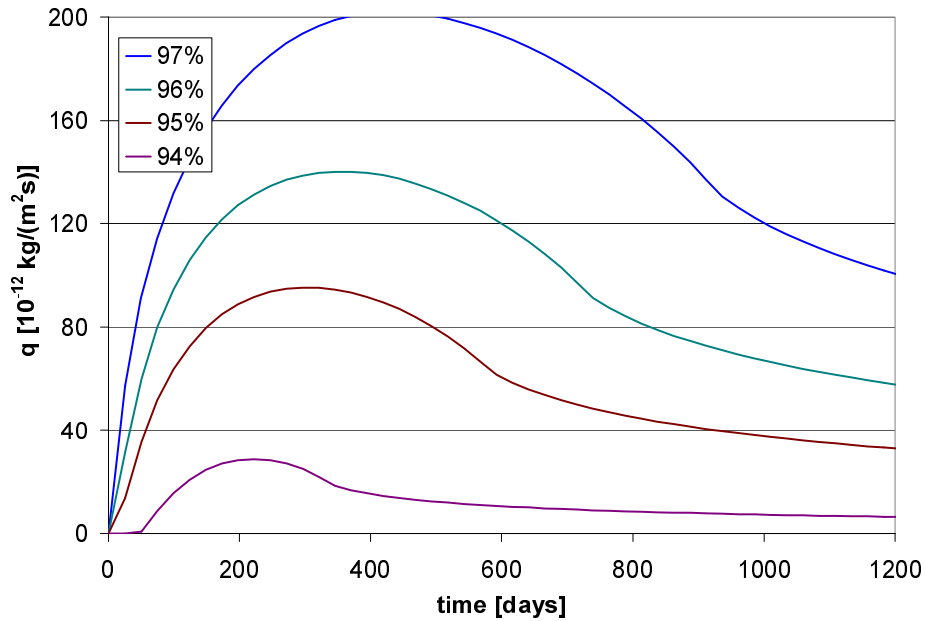


Fig. A4.37 Emission from surface, results from Calc.5 with linoleum flooring.

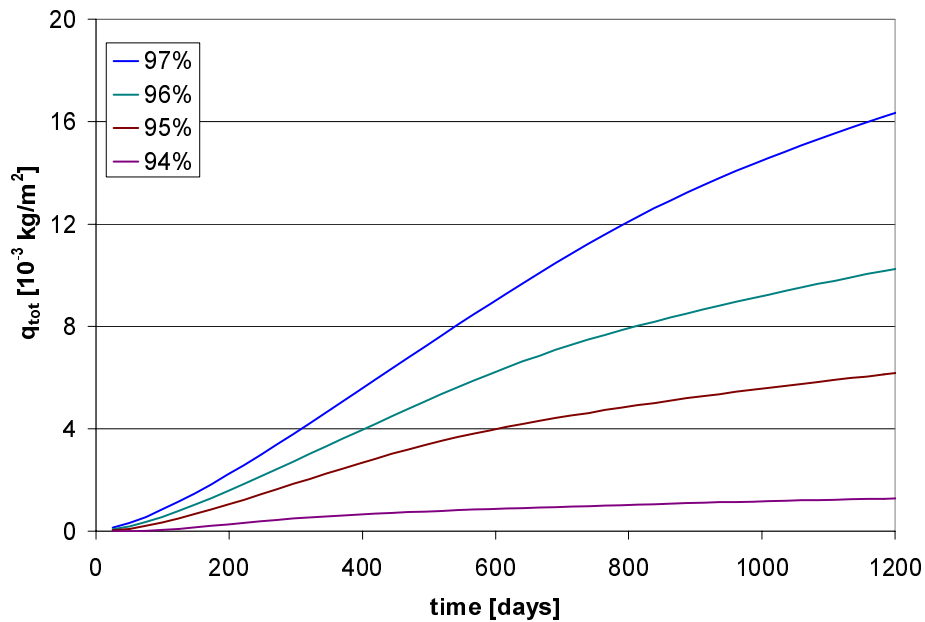


Fig. A4.38 Curves of total emission from Calc.5 with linoleum flooring.

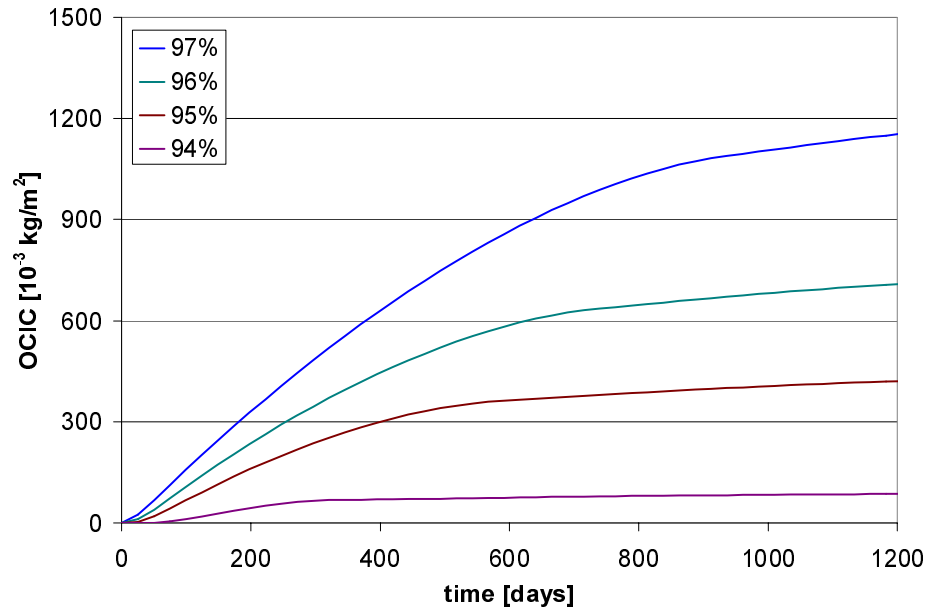


Fig. A4.39 OCIC as a function of time in Calc.5 with linoleum flooring.

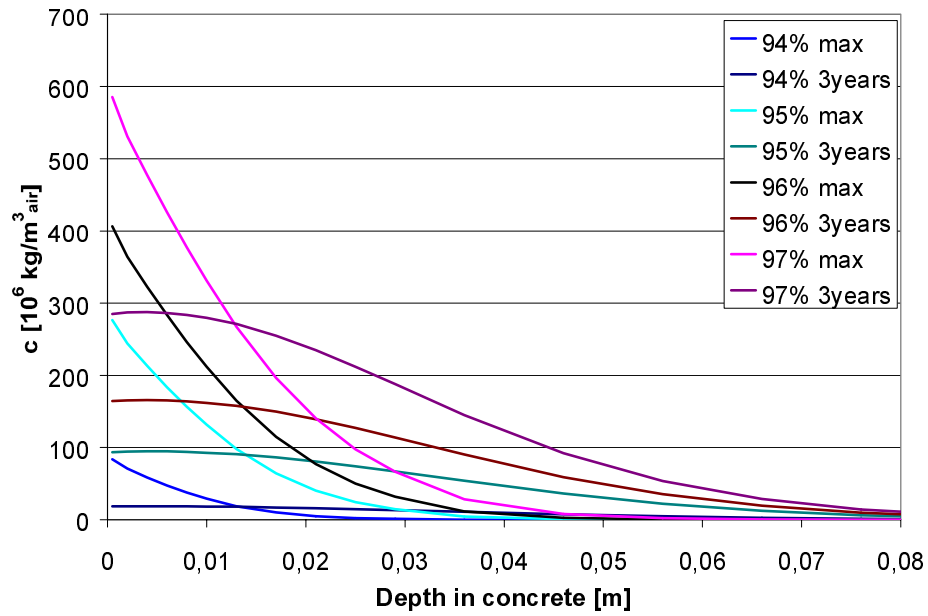


Fig. A4.40 Profile of OCIC at max c_s and after a long time in Calc.5 with linoleum flooring.